83-2780

Behavior of Concrete Block Masonry Walls Subjected to Repeated Cyclic Displacements

U.S. Department of Commerce
National Bureau of Standards
Washington, D.C. 20234

October 1983

Sponsored by

Bureau of Mines
Department of the Interior

NBSIR 83-2780

BEHAVIOR OF CONCRETE BLOCK MASONRY WALLS SUBJECTED TO REPEATED CYCLIC DISPLACEMENTS

Kyle Woodward
Frank Rankin

U.S. Department of Commerce
National Bureau of Standards
Washington, D.C. 20234

October 1983

Sponsored by
Bureau of Mines
Department of the Interior

U.S. DEPARTMENT OF COMMERCE, Malcolm Baldrige, *Secretary*
NATIONAL BUREAU OF STANDARDS, Ernest Ambler, *Director*

ABSTRACT

An experimental investigation into the behavior of unreinforced, ungrouted concrete block masonry walls subjected to repeated in-plane lateral cyclic displacements indicated a pronounced effect of loading history on the wall performance, but only at load/displacements nearing the load capacity failure point. A total of 15 walls were tested of which 10 were 64 in. x 64 in. planar walls and 5 were 64 in. high corner walls having equal leg lengths of 48 in. The primary parameter varied in the investigation was loading history. The cyclic tests included fully reversed displacement patterns and reversed displacement patterns superimposed on static displacement offsets. Monotonic tests at both slow and rapid strain rates were done. The cyclic tests included at least 100,000 repetitions.

TABLE OF CONTENTS

TABLE OF CONTENTS

LIST OF TABLES

LIST OF FIGURES

LIST OF FIGURES

LIST OF FIGURES

LIST OF FIGURES

LIST OF FIGURES

LIST OF FIGURES

LIST OF FIGURES

LIST OF FIGURES

LIST OF FIGURES

ACKNOWLEDGMENTS

The investigation reported herein was conducted for and sponsored by the Bureau of Mines, Department of the Interior. The assistance of the following Bureau of Mines personnel during the actual testing is gratefully acknowledged: Mark Stagg, Dave Siskind, Dan Vick, Michael Stevens, and G. Robert Vanderbos.

The National Concrete Masonry Association provided both the concrete block and an experienced mason to fabricate the walls. Their contributions are gratefully acknowledged.

Special thanks go to Mark Stagg, William Kovacs, and Spencer Wu for their diligent review of this report.

1. INTRODUCTION

Blasting in mines and quarries present potential problems when they are adjacent to residential developments. Blasting generates ground motions which radiate from the blast source some distance determined by a number of parameters such as blast size, soil and rock type and layering. The ground motion can induce vibrations in a residential dwelling. The characteristics of the vibration (frequency, acceleration, velocity, and amplitude) may range between levels such that no vibration is perceived by people and no damage occurs to the residence structure to levels which cause distress to people and damage to structures. It is clearly necessary that only blasting which minimizes or eliminates undesirable effects on adjacent people and their dwellings be permitted. However, such an outcome is only possible if rational, effective criteria are available by which blasts may be designed.

The Bureau of Mines has been extensively investigating the problem of blast-induced ground motion damage to residential structures with the final goal being blast designs which minimize damage to residences. As part of their investigation the Bureau of Mines required detailed information on the fatigue characteristics of concrete block masonry walls. Such walls, usually unreinforced and ungrouted, are commonly used to form the basement walls and provide support to the dwelling superstructure.

The experimental research program described herein was carried out under contract to the Bureau of Mines by the Structures Division, Center for Building Technology, National Bureau of Standards. The research program involved the testing of 10 planar walls and 5 corner walls. The focus of the research was on the fatigue characteristics of the walls when subjected to in-plane lateral forces. In addition, however, the walls were also tested to obtain their maximum lateral load capacities.

1.1 SCOPE

The purpose of this report is to document the experimental investigation as prescribed by the sponsor. The emphasis has been placed on details of the test program and its results rather than interpretations. The reader will find sufficient information by which independent interpretations may be developed.

Chapter 2 is a description of the test apparatus and to a limited extent procedure. The Tri-directional Test Facility is described and its salient features are discussed as they apply to this investigation.

The material properties for both mortar and concrete block are presented in chapter 3 and the test specimens are described in chapter 4 including geometry, materials, and construction.

A more detailed description of test procedures is presented in chapter 5. The method of wall placement and testing are explained. The instrumentation used to measure wall behavior are also described.

A description of each wall test is presented in chapter 6. The loading histories are described and the pertinent acquired load, displacement, and strain data are presented.

Chapter 7 includes the interpretation of the acquired data emphasizing the points of interest to the sponsor.

The summary and conclusions are presented in chapter 8.

2. TEST SETUP

The test setup (figure 2.1) is the Tri-directional Test Facility (TTF), a permanent loading apparatus designed to test building components using three-dimensional loading histories. In this chapter, the general characteristics of the TTF and the specific manner in which it was used for this investigation are described.

2.1 TRI-DIRECTIONAL TEST FACILITY (TTF)

The TTF is a computer controlled loading apparatus which can apply forces/displacements in all six degrees of freedom at one end of a specimen. The other end of the specimen is fixed. The six degrees of freedom are the translations and rotations in and about three orthogonal axes (x, y, z). The application of such actions are accomplished by seven closed-loop, servo-controlled hydraulic actuators which receive their instructions by means of computer generated commands. Referring to figure 2.1 it is possible to observe the major components of the TTF. The reaction system is composed of the structural tie down floor and two vertical buttresses. The load distribution system is the two x-shaped crossheads, one at the bottom and the other at the top of the test specimen. The load application system is made up of the seven hydraulic actuators of which four are visible in the figure. The control system is not visible in the figure, but includes the servo-control electronics, the data acquisition equipment, and a mini-computer. The general concept of the facility is simple though its operation is complex. The test specimen is fitted between two very stiff members (crossheads), one of which is fixed in place, while the other is free to move in any direction. The movement of the free crosshead is dictated by the actions of the hydraulic actuators.

A schematic of the crosshead and actuator arrangement is shown in figure 2.2. The load capacity of each actuator is also shown in figure 2.2.

2.1.1 Reaction System

The loads transmitted by the lower crosshead are resisted directly by the structural tie down floor. The reaction of the horizontal hydraulic actuators is provided by the two buttresses which also transmit the forces to the tie down floor (figure 2.2).

The lower crosshead is attached to the tie down floor by means of post-tensioned high strength bolts. The lateral (or shear) forces are resisted by means of positive stops rather than friction. The overturning forces are resisted by tension in the tie down bolts. The upper crosshead has no reactive capacity other than that provided by action of the hydraulic actuators. The vertical actuators are attached to both crossheads, but only use the lower crosshead for reaction. The horizontal actuators transmit forces both to the lower crosshead by means of the test specimen and to the vertical buttresses.

The structural tie down floor is a 6 ft thick heavily reinforced concrete slab. The tie down floor has vertical embedded receptacles for attaching objects to the floor by means of high-strength bolts. In addition, the embedded receptacles include provisions for including shear sleeves concentric with the bolts. The shear sleeves bear directly against embedded steel plates so that shear is not resisted by the bolts. The vertical buttresses are monolithically cast reinforced concrete. The buttresses are post-tensioned both vertically and horizontally. The vertical post-tensioning provides the shear and overturning capacity by being attached to the tie down floor by means of rock anchors placed in the floor. The buttresses include mounting locations on the face near the crossheads by which the hydraulic actuators may be attached. The attachment method permits continuously variable height adjustment to accomodate leveling of the horizontal actuators at any practical height above the floor.

2.1.2 Load Distribution System

The load distribution system includes the two steel crossheads and the attached reinforced concrete footings. The primary function of the steel crossheads is to transmit the concentrated actions of the hydraulic actuators as more uniformly distributed forces. The crossheads are purposely designed to be extremely stiff to limit the compliance of the loading members. The crossheads are heavily stiffened pairs of 21 in. deep wide flange shapes welded along their adjoining flanges to produce a box shape. The resulting width of the loading surface is about 26 in. The reinforced concrete footings are additions solely for the testing of concrete masonry components. The top footing is 18 in. deep and the bottom footing is 21 in. deep. Each footing is attached to the crosshead by 40 post-tensioned 1-1/2 in. diameter high-strength bolts. The footings provide a transitory medium between the steel crosshead and the masonry walls and reduce the severe discontinuity in material properties. In addition, as discussed later, the footings permitted a simple method of attaching the walls to the crossheads, namely, epoxy mortar.

2.1.3 Load Application System

As illustrated in figure 2.2 there are seven hydraulic actuators to control the action of the upper crosshead. The hydraulic actuators are servo-controlled which simply means that the action of each actuator is electrically controlled so that the actual response of the actuator is at all times equal to the response commanded of the actuator. The commands are in the form of an applied analog signal generated either locally or by the computer. The action required of each actuator is quite complicated for simultaneous multi-directional movements or when the overall geometry changes due to actuator movements are large.

The hydraulic actuators are displacement controlled which means that the variable which is used in the command-response loop is the displacement of the actuator's retractable piston. Such control ensures that specimen instability cannot occur during a test since at any moment the location of the upper crosshead is fixed by the relative lengths of actuators. The force seen by each actuator can vary, but the displacement is controlled. The end fittings of each actuator are swivels which permit sufficient rotation in all directions to accommodate crosshead movements without introducing bending into the actuators. Such fittings are required since otherwise the $\pm$ 6 in. travel of the actuator pistons (exception: the single horizontal 220 kip actuator has $\pm$3 in.

travel) could produce geometry changes sufficient to introduce substantial extraneous bending forces in the hydraulic actuators. Each hydraulic actuator has an internal, integrally mounted linear variable differential transformer (LVDT) to measure piston movement and a load sensing transducer mounted in line with the piston. The resulting information permit the global forces and displacements imposed by the upper crosshead to be measured.

2.1.4 Control System

The control system coordinates the actions of the TTF. Through the control system the operator interacts with the hydraulic actuators to control loading, acquires test data, and manipulates the test data to display the acquired information in the most meaningful form. The major parts of the control system are the servocontrollers, the data acquisition equipment, the computer, and a variety of computer peripherals such as printers, plotters, and video terminals.

The computer connects all the parts of the system to each other. The computer acquires the data on the test environment through a high-speed analog-to-digital converter. The computer instructs the hydraulic actuators through the servo-controllers by issuing analog commands to the controllers which then actually perform the analog loop function. The computer receives instructions from the operator and transmits responses to the operator by means of the peripherals.

Specially developed software enable the computer to understand instructions submitted by the operator, sense the test environment, manipulate the upper crosshead, and display the condition of the test specimens on a real-time basis. In addition, to the real-time capabilities there are post-test data analysis and presentation software to further refine the manner in which data is displayed.

2.2 USE OF THE TRI-DIRECTIONAL TEST FACILITY

In the previous section, the general capabilities and features of the TTF were described. The actual use of the TTF for the investigation reported herein varied considerably from the intended use of the TTF. In this section, the differences and actual techniques are described. The TTF is directed to slow loading rate tests due to the available computing power and hydraulic flow rate. The requirement of high rate cyclic loadings imposed by this investigation precluded the use of computer controlled loading. The computer directed data acquisition and display functions were retained, but in a modified form.

2.2.1 Load Application Technique

The single direction and very small magnitude of displacement application permitted the walls to be tested without computer control and only a minor loss of response capability. The small displacement magnitudes meant that geometry corrections of the applied actions were not required as long as the position of the crosshead was centered and leveled on the masonry wall.

Great care was taken to assure these conditions and the set up procedure did involve computer controlled crosshead movement. The procedure for a test began with the application of an axial (vertical or z axis) compressive load to the wall. This presented some difficulty since the vertical actuators had to be displacement controlled in order to achieve the desired condition of rotational fixity. The compressive load was introduced by gradually applying a uniform vertical displacement to the wall until the desired load level was attained. The vertical actuators were computer controlled for this action. Upon reaching the proper load the displacement was then maintained by the servo-controllers without further direction by the computer. The application of the in-plane (x axis, figure 2.2) lateral displacement was done by the single 220 kip actuator and its movements were also controlled by a servo-controller. However, the varying commands were produced by a frequncy generator having many different wave forms (e.g., sine wave and ramp) and not by the computer. The out-of-plane horizontal hydraulic actuators were locked against displacement during a test.

2.2.2 Data Acquisition and Display

Because of the high sampling rate required to properly assess wall performance only selected portions of the data could be displayed on a real-time basis. The remainder of the acquired data could be displayed only after a test. The sheer volume of data taken required large amounts of time for preparation to display and then display. As an example, one of the tests produced close to 8 million data points. Needless to say, the most efficient form of data display was plotting which is used extensively for that reason in this report.

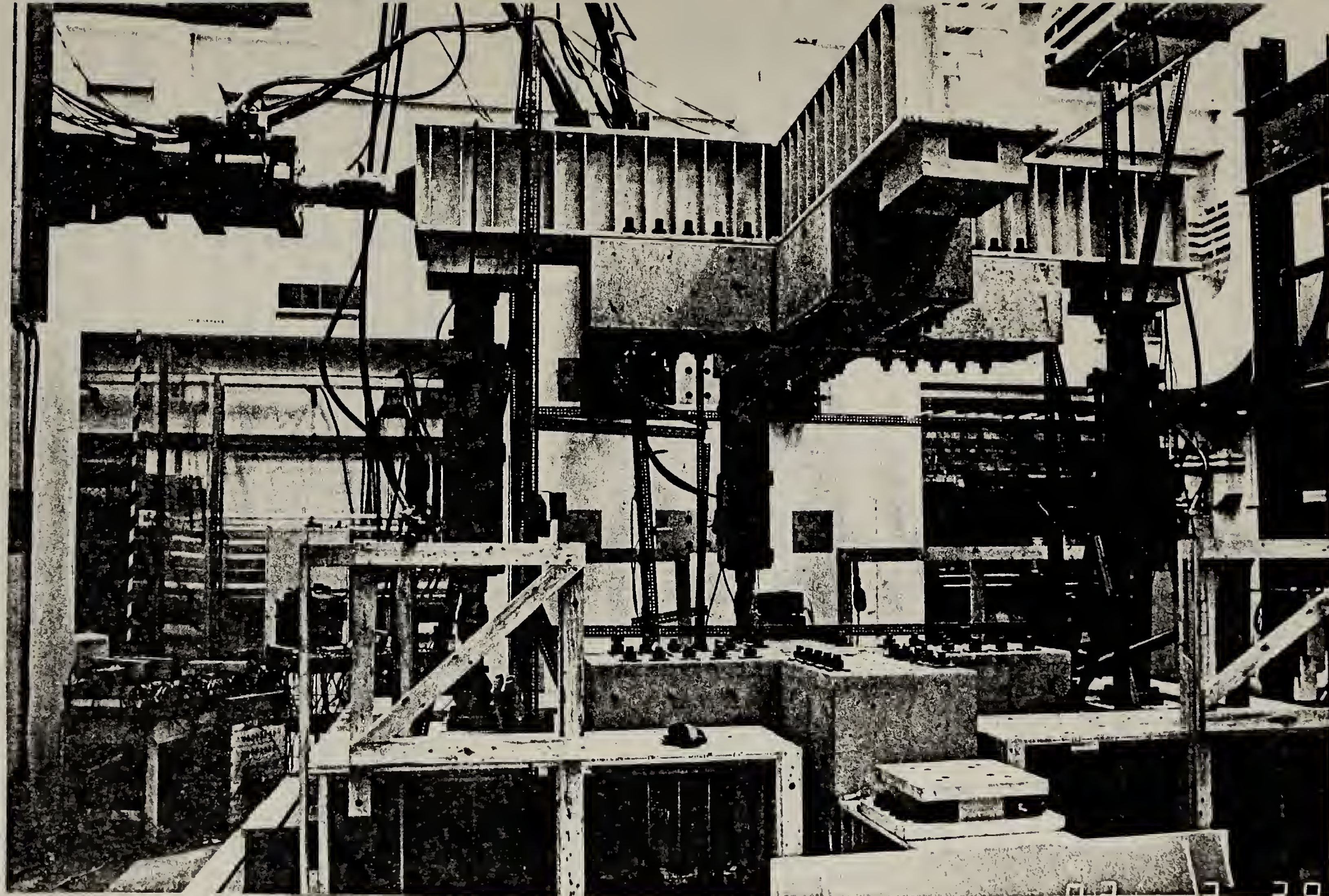

Figure 2.1. Overall view of test setup (looking to the north)

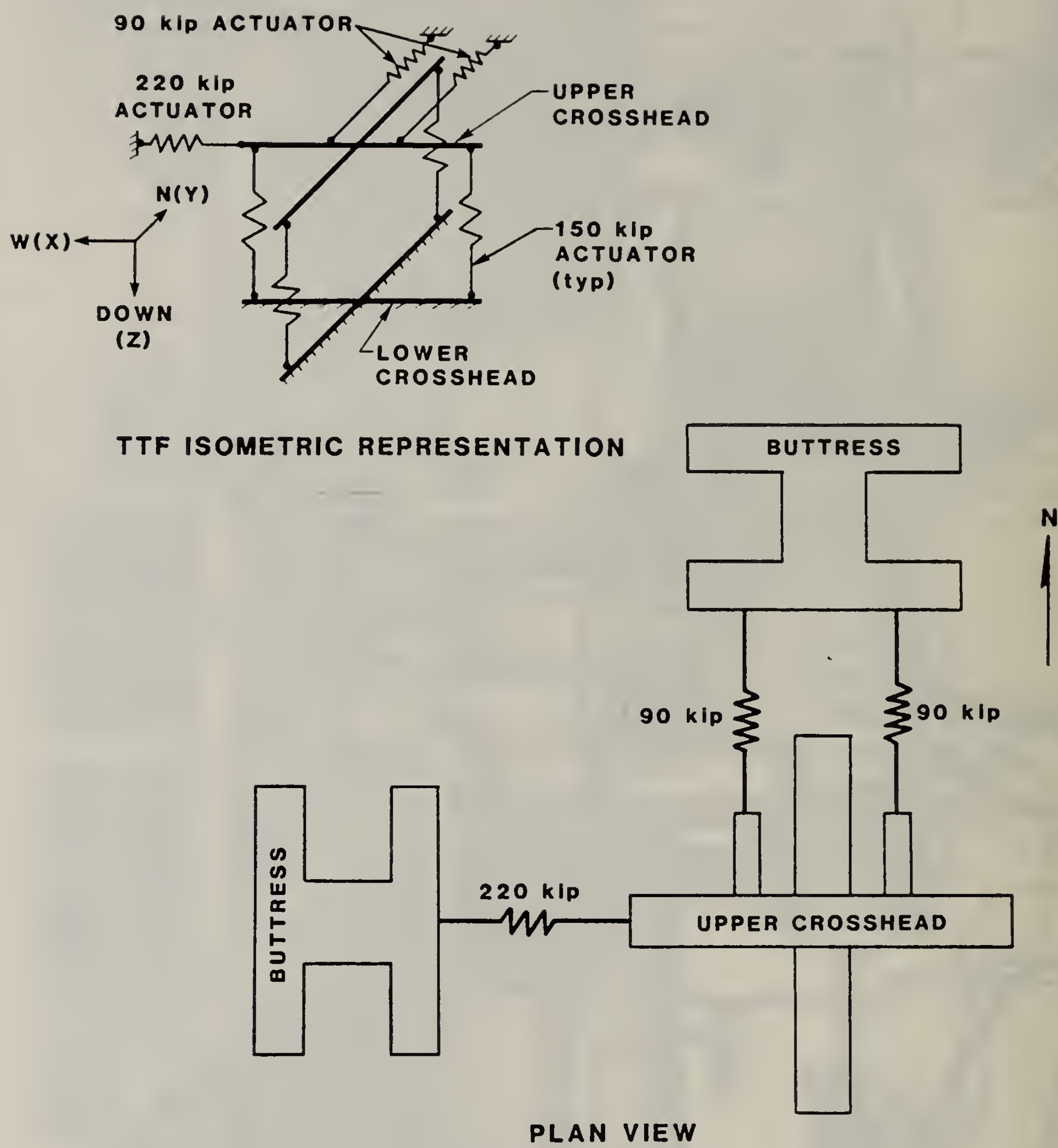

Figure 2.2 Schematic of crosshead, buttress, and actuator arrangement

3. MATERIALS

All materials used in the wall panel construction and associated prisms were commercially available and were representative of those commonly used in building construction.

3.1 CONCRETE MASONRY UNITS

Two types of concrete masonry units were used in the construction of the wall panels and prisms:

1. 8 in. x 8 in. x 16 in., 2 core hollow stretcher block
2. 8 in. x 8 in. x 16 in., 2 core hollow kerfed corner block with a steel sash groove in one end.

These units are illustrated in figure 3.1

The half block at the end of alternate courses of the wall panels were made by sawing the kerfed corner block in half through the kerf, using the square end and discarding the end containing the steel sash groove.

All the concrete masonry units for this testing program were manufacturered the same day using mixture proportions that would produce units with ultimate strength over the gross area of 1,000 psi. The mixture proportions were:

1950 lbs lightweight expanded shale aggregate

1250 lbs sand

200 lbs portland cement

190 lbs NewCem

NewCem is the proprietary name for a very finely ground water granulated blast furnace slag manufacturered by Atlantic Cement Co., Inc. It meets the requirements of ASTM C989-82, grade 120 and when blended within the range of 25 to 65 percent with portland cement, meets the requirements of ASTM C595 Standard Specifications for Blended Hydraulic Cements. This mixture produced 118.2 units with 3.3 pounds of cementitious materials per unit. The block machine was set for 1.75 second feed, 1.25 second finish with a 0.25 second delay. The dimensions and physical characteristics of these units are given in table 3.1.

3.2 MORTAR

One type of mortar was used throughout this testing program in fabricating the wall panels, prisms, and mortar cubes. The mortar was a portland cement-lime mortar that was proportioned within the limits of a type N mortar according to the specifications of ASTM C270-80a. The materials used in the mortar were:

1. Sand - a natural bank sand that was dug locally with its primary end use being masonry mortar. Sieve analyses were performed according to ASTM C144-81 and the results appear in table 3.2. The fineness modulus was 1.57.

2. Portland cement - a commercially available, bagged, 94 lbs per bag, Type I portland cement meeting the specifications of ASTM C150.

3. Lime - a commercially available, bagged, 50 lbs per bag, hydrated lime, Type S, meeting the specifications of ASTM C270.

These materials were proportioned 1:1:5 with 1 part by volume of cement, 1 part by volume of lime, 5 parts by volume of sand. The parts were mixed in a typical mortar mixer (fixed horizontal drum with rotating blades) for a period of not less than 3 minutes after all cement, lime, sand, and most of the water was added. Finally, small amounts of water were added to produce mortar of a consistency acceptable to the mason.

Immediately upon leaving the mixer, the time was recorded, a sample was taken for determining the initial flow rate, and the air content of the mortar was taken (air content was not always measured because it did not vary significantly during the course of construction). A set of three, 2 in. x 2 in. mortar cubes was made at this time, also. After the mason built the wall specimen and three prisms, a second set of three, 2 in. x 2 in. mortar cubes was made. The finish time was then recorded. Thus, each batch of mortar produced a wall specimen, three prisms and two sets of three 2 in. x 2 in. mortar cubes. Retempering of the mortar was permitted once per batch.

Table 3.1 Dimensions and Properties of Concrete Masonry Units

	Hollow Stretcher	Hollow Corner/Sash Groove
Width (in.)	7.66	7.64
Height (in.)	7.55	7.58
Length (in.)	15.66	15.67
Minimum Face Shell Thickness (in.)	1.34	1.32
Gross Area (in.^{2})	120.0	119.7
Net Solid Area (%)	49.6	55.2
Gross Compressive Strength (psi)	1310	1440
Density (lb/ft^3)	98.2	98.2
Absorption (lb/ft^3)	14.4	14.3

Table 3.2 Masonry Sand Sieve Analysis*

Screen Size Number	Cumulative Percent Retained
4	0.1
8	0.6
16	2.0
30	11.0
50	56.9
100	86.6
100+	....
Total	157.2 ÷ 100 = 1.57 Fineness Modulus

* Average results of three samples of masonry sand taken during construction of walls P1 - P10 and C1 - C5.

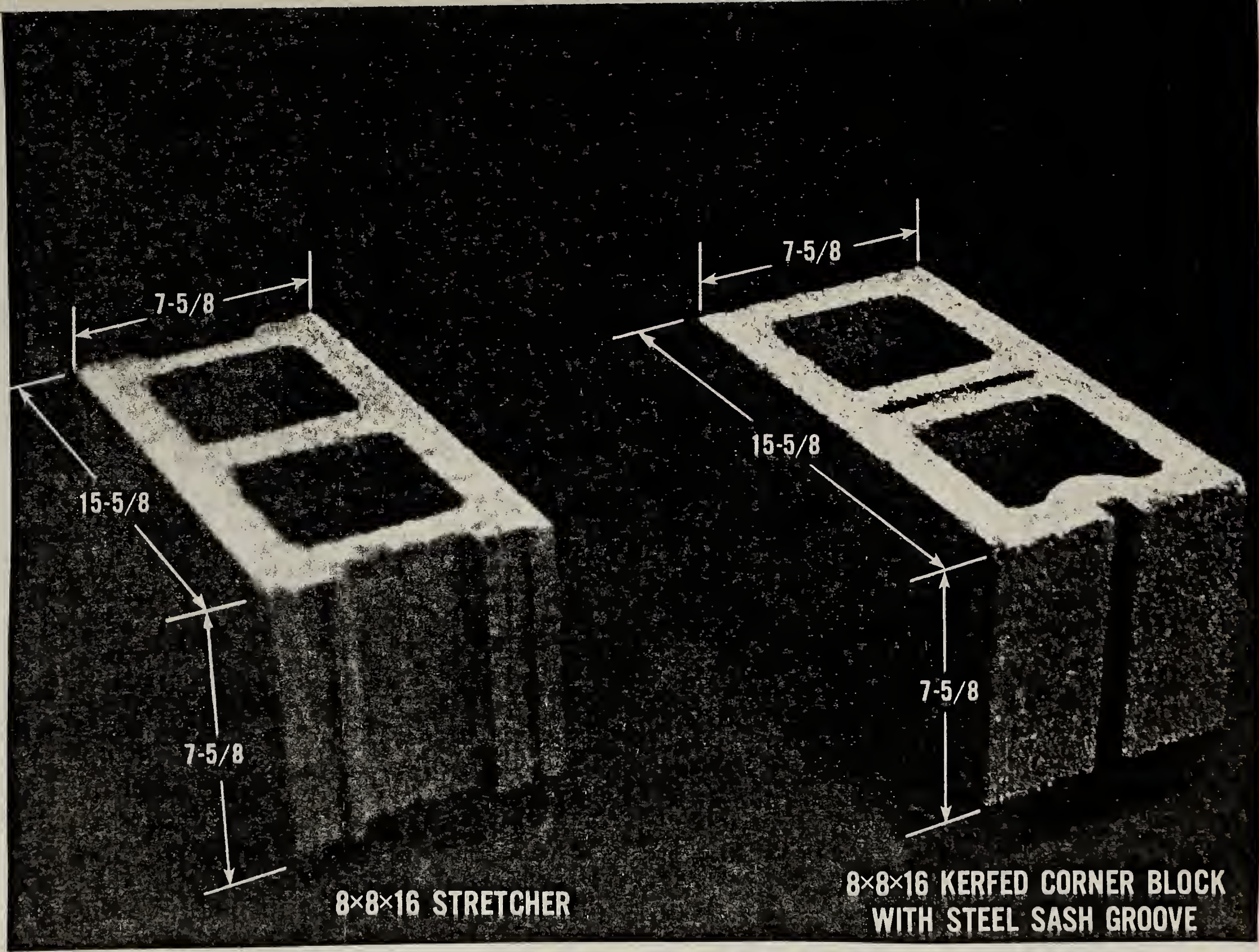

Figure 3.1 Concrete masonry units

4. TEST SPECIMENS

A detailed description of the wall and prism specimens and the methods of fabrication are presented in this section.

4.1 DESCRIPTION OF WALLS AND PRISMS

Two styles of walls were built for testing in this program. The first style was a planar wall 64 inches long and 64 inches tall. The second was a corner wall with each leg of the 90° corner being 48 inches long and the height being 64 inches. These were nominal dimensions. The prisms (figure 4.1) were nominally 16 inches long by 24 inches high (this was accomplished by laying three blocks in a vertical stack.)

4.2 FABRICATION OF WALLS AND PRISMS

The specimens previously described were fabricated by an experienced mason using techniques representative of good workmanship. They were built of materials that had been stored in the laboratory environment for at least 30 days. After fabrication the specimens were air-cured until they were tested. All fabrication and curing took place in a controlled-environment laboratory that was maintained at 73°F ± 3°F with 50 percent ± 5 percent relative humidity. The block in these walls were laid in a running bond[1] with the mortar joints on both sides of the walls cut flush and not tooled. The bottom course of block in the planar walls was laid dry on the laboratory floor using small wooden wedges for shimming any block that did not sit steadily on the floor. The bottom course of block in the corner walls was laid dry on a channel-iron base that was welded to form a flat base with a 90° included angle. (Because of level imperfections in the floor surface, it was easier to level the channel-iron base with wood wedges than to level the block individually, although individual block unsteadiness was still corrected on an as-needed basis with wooden wedges.)

In the planar walls, the first unit laid was a kerfed corner block at the end of the course without head joint mortar. Head joints were subsequently formed by buttering one end of the next block to be laid in that course just before placing it in the wall. In this way, all head joints were "shoved" and there were no closure units or "slushed" head joints. The end block on each course was alternately a kerfed corner and a half corner. All blocks were laid in mortar using face shell bedding only with the exception of the outside edges at the end of each course where mortar was applied to the end cross web. Stretcher blocks were used in the wall interior. Each course was leveled by the mason, using a 4 foot level. The end blocks were plumbed and then all intermediate blocks were brought into horizontal alignment using the level as a straightedge.

---

[1] Units in successive courses are laid half-over (overlapping 50 percent) with head joints in alternate courses in vertical alignment.

In the construction of the corner walls, the first block laid on each course was the kerfed corner block that formed the corner of the two intersecting legs of the wall. Successive units were buttered and shoved into place to complete the course on both legs. The mason then leveled the top of the block on both legs, plumbed the corner block and the two end blocks and then brought the intermediate block into horizontal alignment using the level as a straightedge. This was done on each course.

In the construction of the prisms, three stretcher blocks were laid by stacking them vertically using face shell bedding only. The mason used his level to maintain the levelness of each block and the plumbness of the prism. Three prisms were constructed as companions to each wall specimen using mortar from the same batch that the wall was built from.

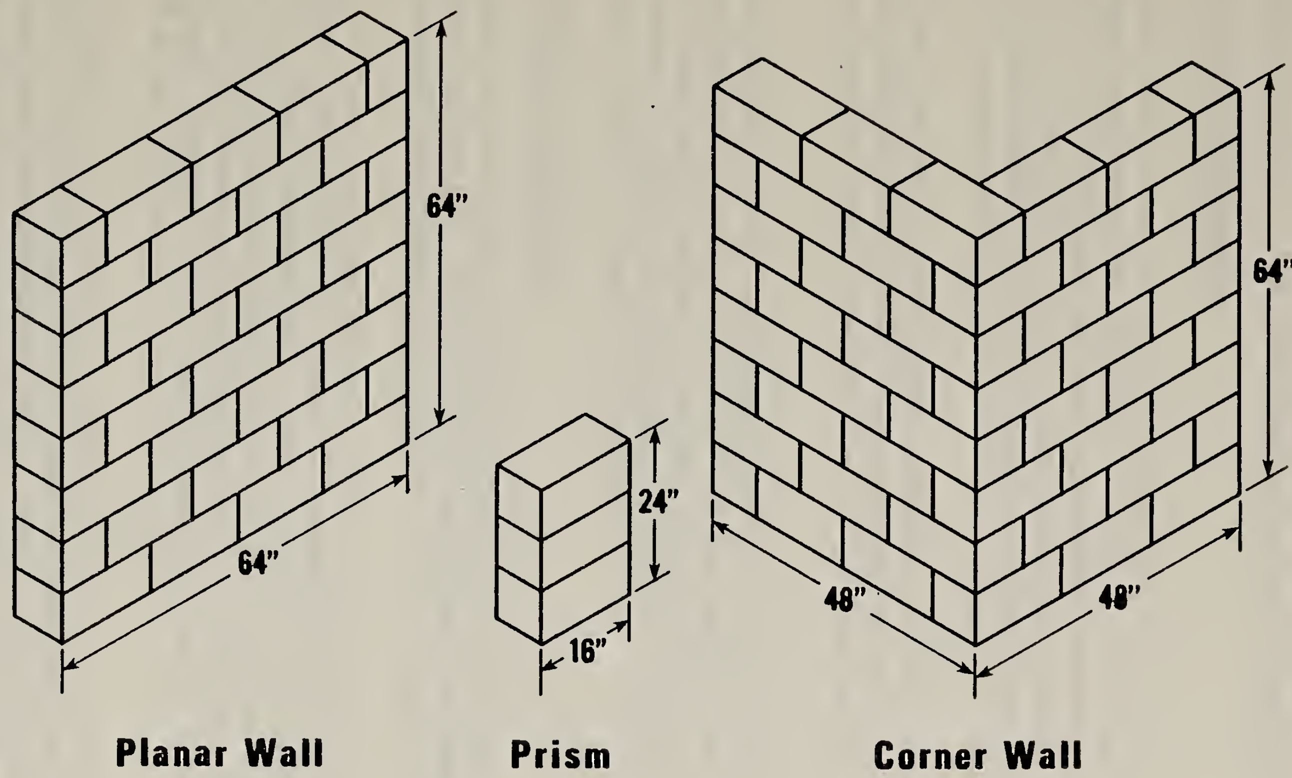

Figure 4.1 Typical walls and prisms

5. TEST PROCEDURES

Testing as well as the methods of handling, positioning, bonding the specimens to the testing facility, and instrumentation are discussed in this section.

5.1 PRISM TESTING PROCEDURES

High strength plaster was used for capping the prisms. In order to get a plane surface, the prism was placed on a thin layer of wet plaster that had been spread on a plate glass surface, carefully checking that the prism was perpendicular to the glass. After that surface hardened, the process was repeated on the opposite end of the prism. These plane surfaces allowed the prisms to be placed directly into the testing machine with uniform bearing.

The prisms were tested in accordance with ASTM C140-75 in a testing machine capable of 400,000 pounds force in compression or tension. A spherically seated upper bearing block covering the entire bearing surface of the prism was used.

The load was applied at any convenient rate for the first 30,000 to 40,000 pounds force while the balance of the load was applied at a rate of 40,000 pounds per minute until failure occurred. This event took place between 1 and 2 minutes later. Maximum load was then recorded. Average prism strengths based on gross area are given in table 5.1.

5.2 WALL TESTING PROCEDURES

The techniques for handling and positioning the planar walls were quite different than those used for the corner walls but the bonding of the specimens, the typical instrumentation, and the testing was similar.

The planar walls were gripped with a fixture that clamped the walls longitudinally. This device is shown diagramatically in figure 5.1 and in use in figure 5.2. Four pick-up points were provided with two on each side of the wall. These points were located symmetrically on either side of the longitudinal center line of two channel-irons that bolted to the structural steel tube (ST 6 x 12) that provided the clamping force on the wall. Slotted holes were provided for minor differences in wall lengths.

A 'C' hook (figure 5.3) similar to a crane pallet lifter was used to lift the walls. A pair of turnbuckles was attached to each of the two forks of the lifter and each pair straddled the wall. These four turnbuckles permitted the walls to be easily aligned such that the walls were level and plumb. The 'C' hook lifting a planar wall is pictured in figure 5.2. The twin vertical legs of the 'C' hook allowed it to straddle the south leg of the upper crosshead as the wall moved northward to the east-west centerline of the testing facility.

Positioning of the planar walls was accomplished with the aid of two mechanical stops that held the walls in proper horizontal position. Vertical positioning (for level and plumb) was accomplished by using small wooden wedges under the edges of the walls.

After making certain the wall could be installed on the centerline, plumb and level, the crane was used to move the wall several feet off the centerline to make placement of the bonding material easier. A mixture of epoxy having additives that gave it non-sag characteristics with clean, dry sand was used as an epoxy mortar. While no cubes were made or tested, manufacturer's literature suggested that the compressive strength would be in excess of 10,000 psi and the modulus of elasticity would be 1.24×10^6 psi. Face shell bedding of the wall specimen was used as the wall was placed within the stops, lowered into the epoxy mortar and then wedged into a plumb and level position. To complete the installation, the upper footing and crosshead was lowered onto a layer of face shell bedded epoxy mortar on the top of the wall. A compressive vertical load of 500 to 1500 pounds force was applied to seat the upper footing securely in the epoxy mortar. The hydraulic rams that applied this load have a no-flow characteristic that prevents movement (i.e., loading) when the servo-controllers are turned off. Thus, when the proper preload was sensed, the hydraulics and the servo-controllers were shutoff and the epoxy mortar was allowed to cure under a controlled load. The initial set took place within 1 hour and no tests were done until it had hardened at least 16 hours.

The corner walls presented unique handling and testing problems. The clamping forces on the lower courses of the wall necessary to provide enough grip for handling without applying any torque to the corner was accomplished by using two interwoven boxes - one box clamped on each leg of the wall. The vertical lifting force was applied through a sling around the intersections of the interior struts, top and bottom, of the two clamped boxes, see figure 5.4. Since the center of gravity of the corner wall held in the pick-up device was on a line bisecting the angle of the corner wall approximately 11 inches from the inside corner, the overhead crane could pick up the assembly and install it directly into the test facility with the sling just clear of the upper crosshead. Again, two plywood positioning fixtures were used to locate and position the corner wall as it was lowered into the epoxy mortar. The processes of mortaring, plumbing, and leveling were essentially the same as described for the planar walls.

The initial plan was to apply the racking load to the corner wall horizontally along a line that bisected the corner angle. After the first test, it was decided that this loading did not produce the type of failure that was of interest at this time, the decision was made to load transversely along the axis of one leg of the corner wall.

5.3 INSTRUMENTATION

The typical instrumentation for the planar walls is shown in figure 5.5. LVDTs (linear variable differential transformers) measured displacement in the plane of the wall and were mounted in a vertical array at each end of the wall. The strain measuring devices, mounted on one face of the wall only, were strain amplifying devices utilizing strain gages mounted on a flexible leaf spring, see figure 5.6. Load and position information was also taken from the load cells and LVDTs in the hydraulic actuators that controlled loading and positioning of the upper crosshead during the testing. Typical instrumentation for the corner walls is shown in figure 5.7.

Table 5.1 Average Mortar and Prism Data

Wall ID	Average Maximum Cube Stress* PSI	Average Maximum Prism Stress** PSI
P1	2400	747
P2	2300	658
P3	2240	653
P4	2230	625
P5	2430	664
P6	2360	715
P7	3480	632
P8	2290	664
P9	2460	736
P10	2320	710
C1	1370	688
C2	1410	649
C3	1310	736
C4	1370	710
C5	1120	736

* Calculated by averaging the strengths of at least three cubes.

** Stress computed on the basis of gross area of the block. Each average is based on strengths from three prism tests.

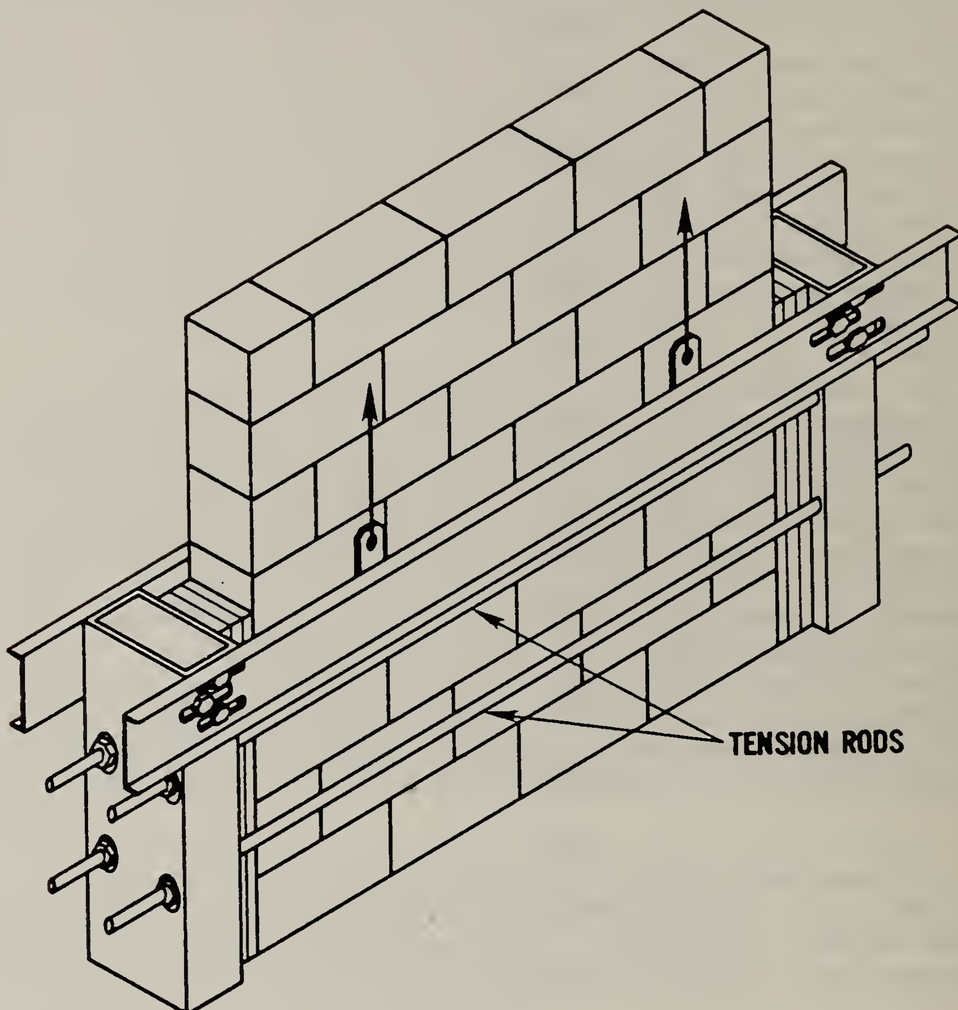

Figure 5.1 Planar wall lifting rig

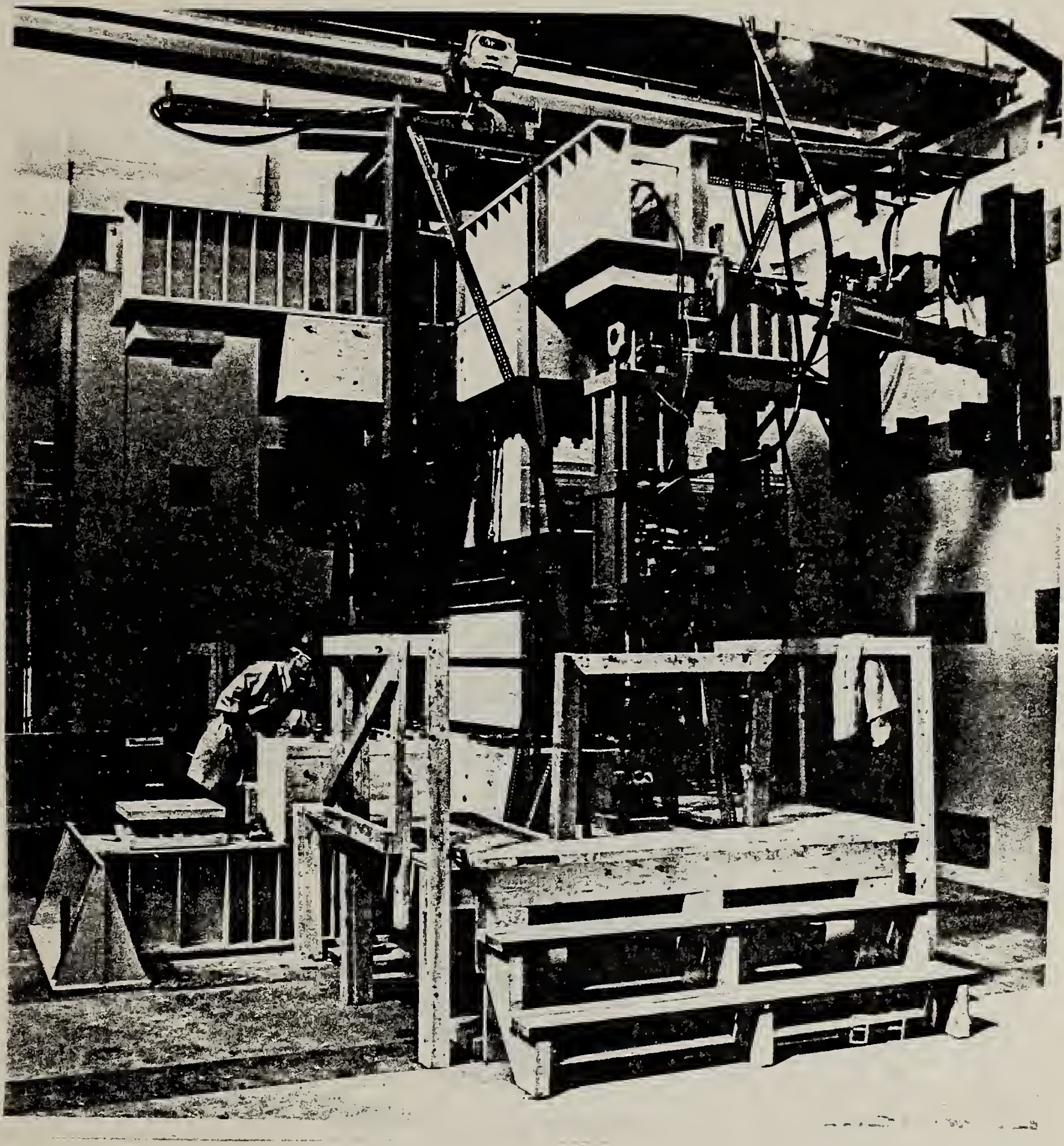

Figure 5.2 View of typical wall placement (looking to the west)

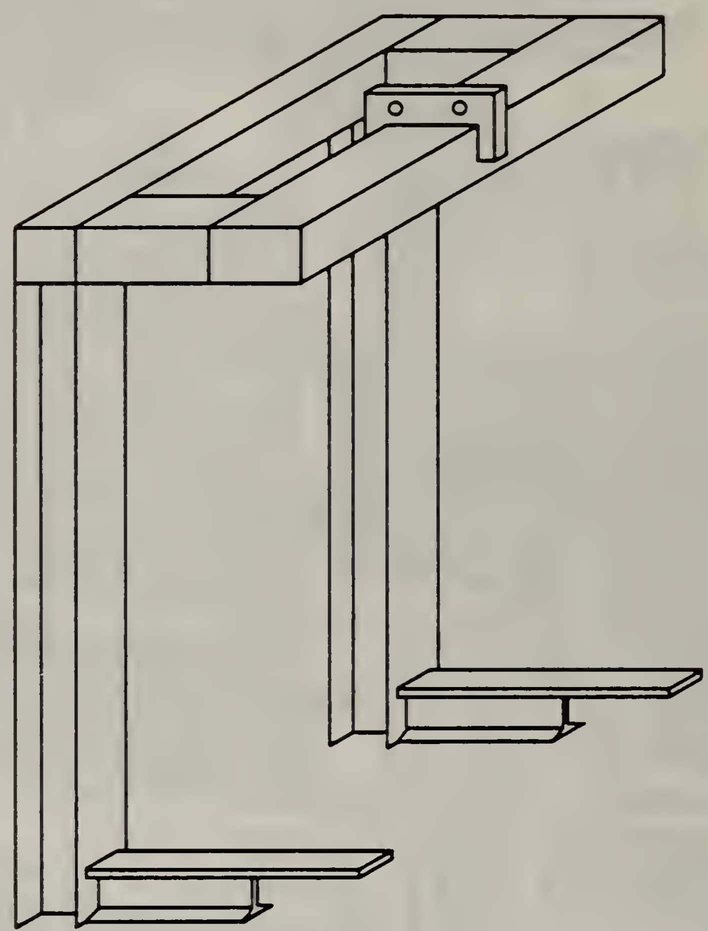

Figure 5.3   C-hook

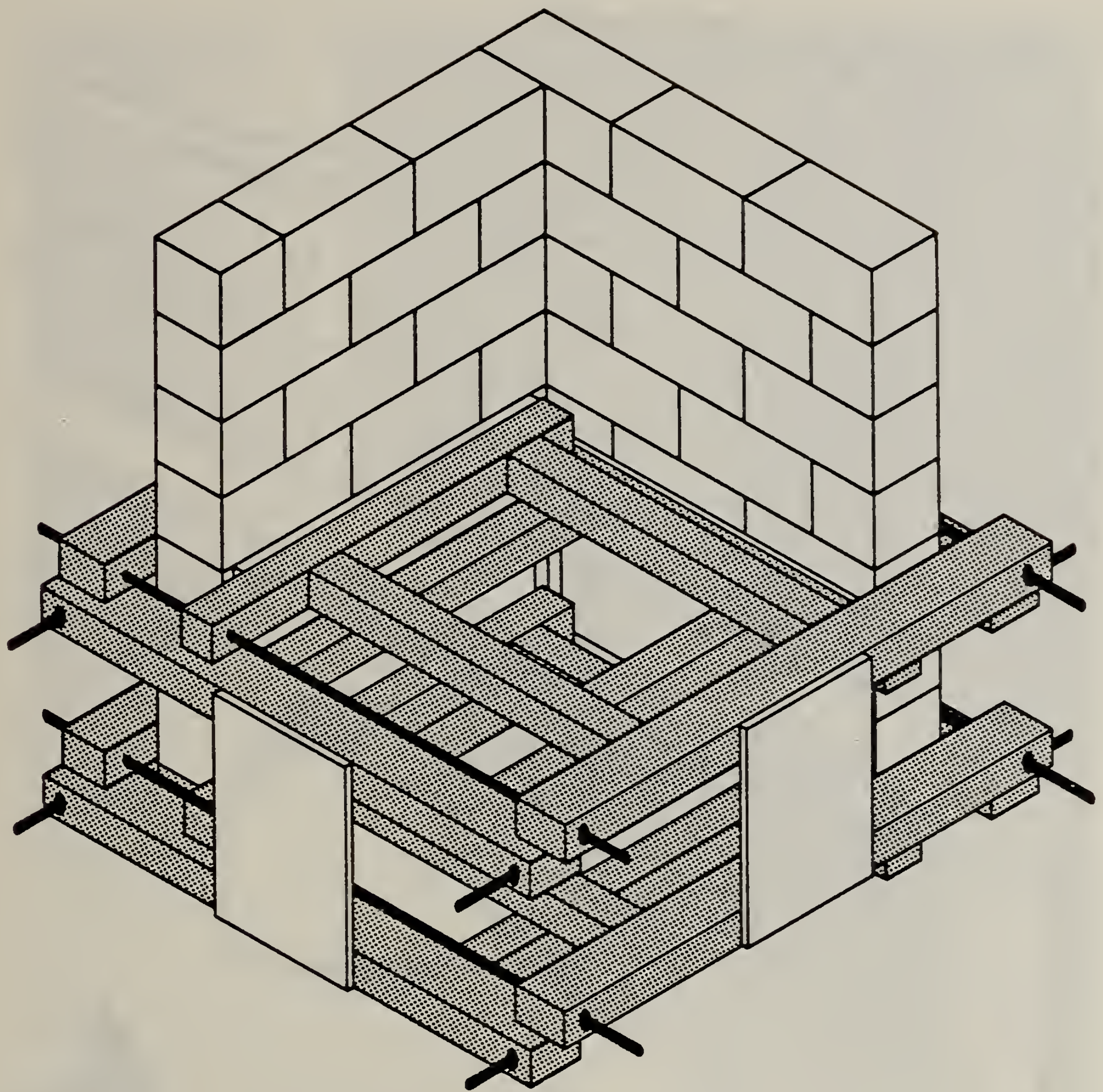

Figure 5.4 Corner wall pickup

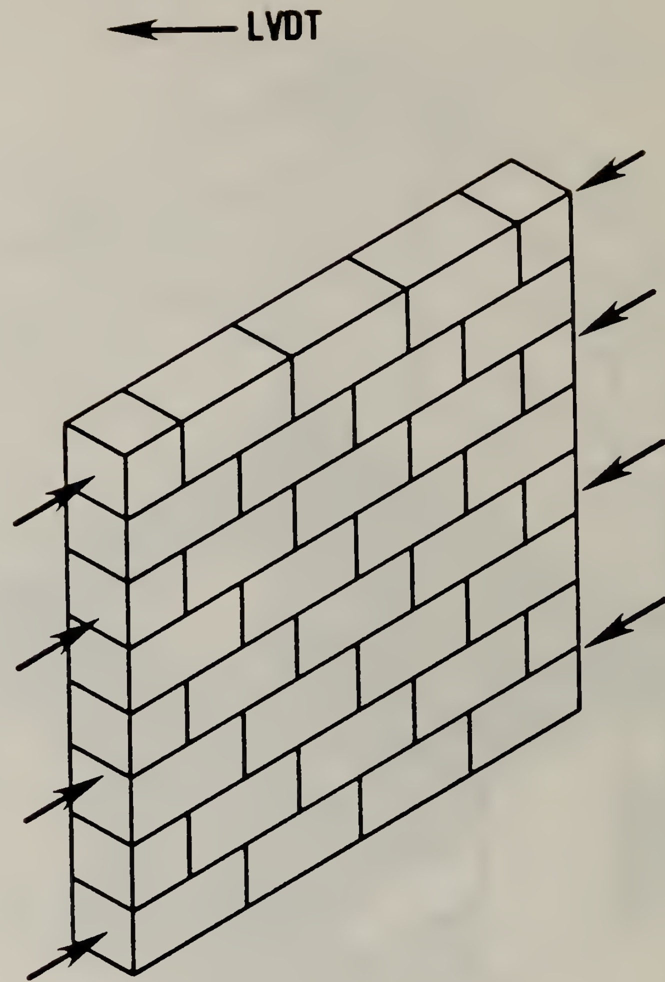

Figure 5.5 Typical planar wall instrumentation

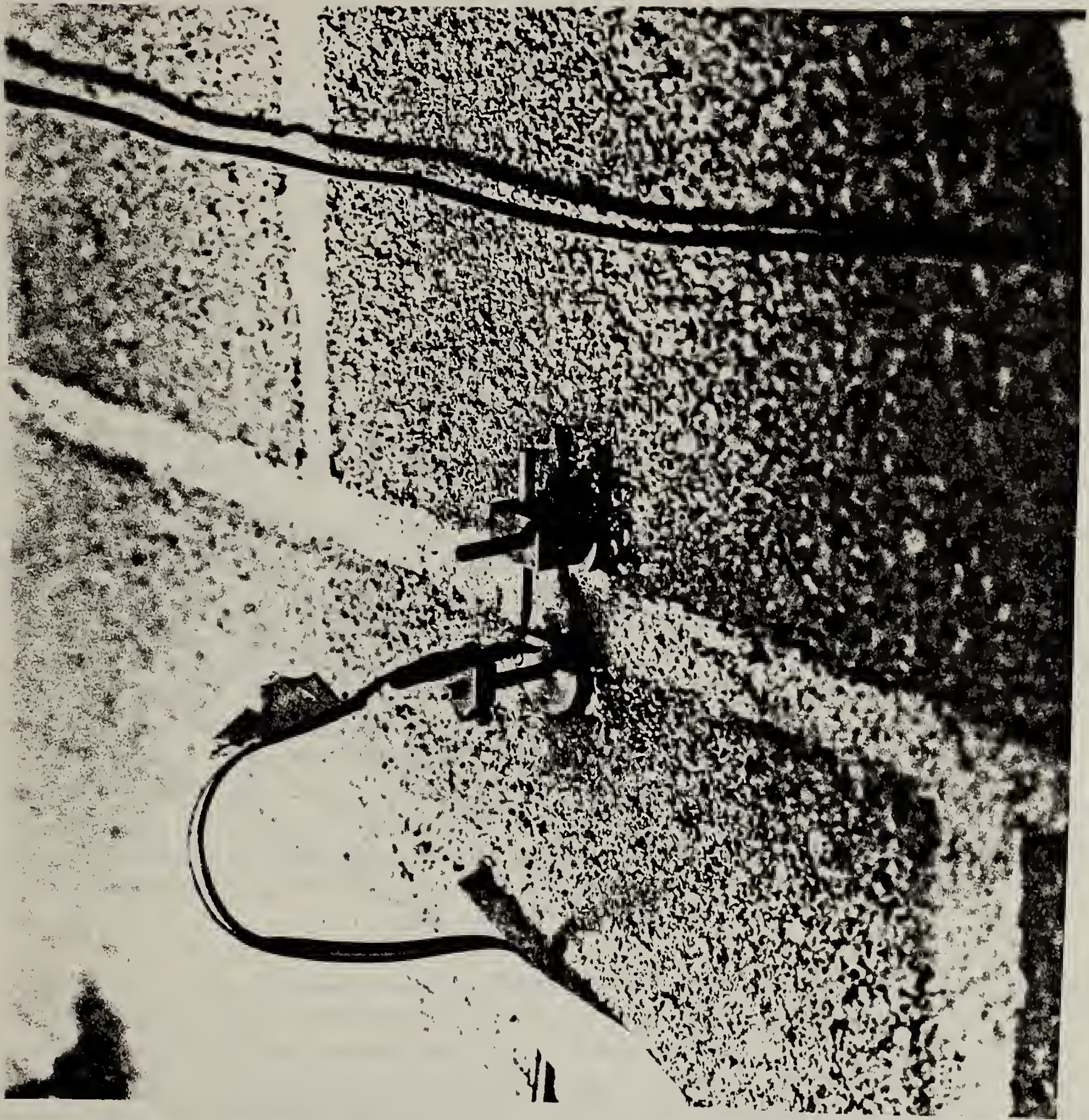

Figure 5.6 Strain measuring device

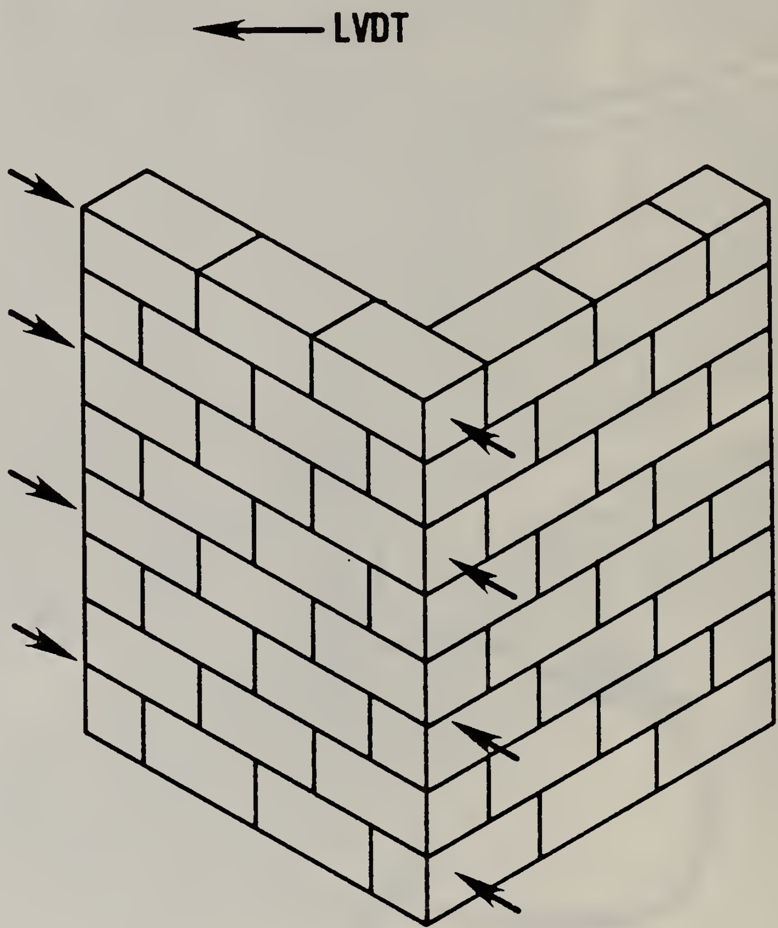

Figure 5.7   Corner wall instrumentation

6. TESTING PROGRAM

A total of 15 wall specimens, 10 planar, and 5 corner were fabricated and tested. A description of typical planar and corner walls is presented in chapter 4. The central purpose of the investigation was to determine the damage susceptibility of concrete block masonry walls when subjected to repeated cyclic loadings. Damage in this investigation included visual cracking as well as load carrying capacity reduction. The primary parameter in the investigation was loading history. This chapter describes the testing program as it was actually performed and includes a general discussion of loading histories, a general overview of the type of information presented for each wall test, and lastly a section for each wall describing the test loading history and resulting data. Data analysis, interpretation, and conclusions are presented in chapters 7 and 8.

6.1 LOADING HISTORIES

A loading history describes the magnitude, rate, direction, and duration of applied loads during a test. The term load is used as a general notation for any imposed action. In fact, the wall specimens were actually subjected to controlled displacements rather than controlled forces.

Except for one test, the directions of loading were the same for each test. There was a vertical displacement imposed on the wall to produce vertical compression in the wall. This is termed precompression in the following discussion. The vertical displacement was not intentionally varied after the desired precompression level was achieved. The main part of each test was the action of an imposed lateral displacement. The lateral displacement (figure 6.1) was directed along the length of the planar wall and along the length of one leg of the corner wall. One corner wall was subjected to approximately equal displacements along each leg resulting in a diagonal displacement path.

There was a limited examination of the effect of loading rate on behavior using one wall, but essentially rate was not a parameter studied in this investigation.

The principal variable in the loading history was magnitude and duration of displacement. The actual variations used in the test program reflected the exploratory nature of the investigation. The results of each test influenced the loading history selected for the next test. Thus, except for two wall tests there were no replicates, instead, each test was used to define limiting conditions. Such a program precludes detailed investigation of parameters, but it enables a much broader examination of the problem to be made with a limited number of tests.

The initial loading history choices were selected based on the assumption that the walls would be susceptible to damage and that the measured strains across mortar joints at cracking would be comparable to the strains observed in field tests conducted by the Bureau of Mines on actual residential dwellings. Two basic loading histories were selected. The first was simple monotonic loading and the second was cyclic using fully reversed displacement levels about the initial undisplaced position. However, testing indicated that the fully reversed cyclic displacements reaching the strain observed in the field did not cause visible damage. As a result, a third loading history was adopted which was termed cyclic with prestrain. This loading history involved the initial application of a lateral displacement which caused a preselected level of measured strain. Cycling of the displacement then began about this offset displacement. The cyclic displacement amplitude (disregarding the offset component) was kept the same in the tests and was $\pm$ 0.003 in. The value of $\pm$ 0.003 in. of displacement was established by the sponsor. The value was obtained from a simple analysis of a basement wall assumed stationary at its base and subjected to a ground particle velocity of 0.1 in/sec. The motion was assumed to be sinusoidal with a frequency of 6.5 Hz. The first set of cycles in each test was continued for at least 100,000 cycles. Further cycles at larger displacements were also done, but the number of cycles varied depending on the observed effect of such cycling.

6.2 TEST DATA DESCRIPTION

Four types of measurements were taken during the tests: 1) loads imposed by each hydraulic actuator, 2) displacements of the wall profile relative to a fixed reference, 3) the hydraulic actuator piston displacements, and 4) strains on a wall side surface. The instrumentation itself was described in chapter 3 and will not be discussed here. In the interest of simplicity, only the most relevant data is presented in this chapter, the redundant, uninformative, and extraneous data has been omitted for clarity. A consistent form of data presentation has been adopted to ease discussion and aid future comparisons. In the sections which follow, the different data presentation forms are described.

6.2.1 Load Versus Displacement Curves

Two different load-displacement curves are presented. The first is the lateral load (the in-plane lateral load, or expressed another way, the lateral load measured in the east-west direction [figure 6.1]) versus the displacement of the east-west hydraulic actuator piston. The second load-displacement curve is the lateral load versus the in-plane displacement of the upper course of the wall. The two curves are different because the displacements are different. The first curve (load versus piston displacement) is very reliable because both measurements are relatively immune to extraneous events. However, the piston displacement is not a good measure of the actual wall displacement since the piston displacement is affected by the total test system compliance. The second curve (load versus wall displacement) more accurately reflects the wall behavior, but its displacement measurement is affected by such things as local wall distortions (such as splitting), accidental bumping, and a non-rigid connection to the wall. Each curve serves a useful purpose, the load versus wall displacement gives a good indication of wall stiffness and behavior up to the onset of major cracking while the load versus piston displacement gives a reliable, complete history for cross-test comparisons.

6.2.2 Strain Histories

Each of the wall test descriptions includes a sketch of the wall with the approximate location of each strain measuring device. A typical sketch showing mounting locations is figure 6.8. The mounting devices are represented by a dumbbell shaped symbol and an associated reference number. The number is a position number and has no purpose other than for identification. In this report, the strain measuring locations are referred to by the acronym SML followed by a position number. The orientation of the dumbbell symbol denotes the direction of measurement with the cross bar of the dumbbell lying parallel to the direction of measurement. Only vertical and horizontal orientations were used on the walls. With few exceptions the strains were measured across head (vertical) and bed (horizontal) mortar joints. A strain measuring device placed across a bed joint is shown in figure 5.6. The strain values were computed by dividing the measured displacement of each device by the initial measured gage length. For strains measured across mortar joints the gage length was taken to be the nominal thickness of the mortar joint (0.51 in.).

The presentation of the strain histories takes one of two forms depending on the loading history of the test. For the non-cyclic test the strains are plotted versus the piston-displacement. The cyclic tests were not done to provide strain versus displacement histories, but rather to observe strain versus repetition histories. Therefore, for cyclic tests strains are plotted as a function of a relative index of test duration. The index of test duration has no direct relation to any physical unit of measure such as time. The index is a non-dimensional guide which identifies common points in the test for purposes of comparison of data within a test. For the cyclic tests the piston-displacement and lateral load are also plotted against the same index so that the strains can be related to displacements and loads if necessary. As a general rule only data from horizontal SMLs which measured tensile strains are presented. All of the strains are plotted using the same scale and limits for ease in comparison. The limits of $\pm$ 2000 microstrain were chosen as a reasonable compromise between the range in which changes become pronounced and the peak values that the strains could achieve.

6.2.3 Crack Patterns

Sketches of the crack patterns are presented. One sketch indicates the cracks observed on the wall prior to testing. The other sketch shows only the cracks which formed at what is termed load capacity failure.

The pre-test crack inspection was done only on the instrumented side of the wall. In general, the cracks marked in this observation were anything which might be assumed to be a crack during the test.

The method in presenting the cracks was to sketch the crack path. In general, any crack which parallels a mortar joint was a crack at the block-mortar interface. The crack line is drawn on the side of the joint which exhibited the interface crack. The failure crack patterns are shown only on one side of the wall (instrumented side) because with the exception of local spalling the crack patterns were identical on either side.

6.3 TEST DESCRIPTIONS

The wall test descriptions are presented in the sequence in which they were tested. The first three wall tests were used as shakedown tests to verify the suitability of the general testing procedure.

6.3.1 Wall P10

Equipment malfunctions occurred during the test of wall P10. The first malfunction caused an out-of-plane bending to be applied to the wall. The wall exhibited a crack along the tension side face shell at the first mortar bed joint down from the top of the wall. In order to continue the test the bending moment was removed and a compressive axial load of about 13 kips (55 psi net area stress) was applied to close the crack and prevent slip along the crack. The loading history consisted of a single-cycle in which the east direction peak displacement was large, but not sufficient to cause diagonal cracking. The displacement to the west, however, caused diagonal cracking. The test was then terminated because of a malfunction in the data acquisition equipment.

There was no pre-test inspection for cracking and no strain measuring equipment was mounted on the wall. The load versus deflection curves are shown in figures 6.2 and 6.3. The post-test wall condition is shown in figure 6.4.

6.3.2 Wall P7

An unusually large number of problems occurred during this test which limited the usefulness of the data. For this reason data from this test is omitted except for a picture of the post-test cracking pattern (figure 6.5).

6.3.3 Wall P9

The purpose of this test was to observe the effect of displacement rate on wall behavior. The limitations of the equipment imposed a maximum displacement rate of 0.75 in/sec. The test for rate effect was composed of two half-cycle loadings to a displacement approximately one-half of that which caused diagonal cracking in the previous tests. The first loading was done such that the displacement was reached at an equivalent cyclic frequency of 0.003 Hz while the second loading had an equivalent frequency of 3 Hz.

This test suffered an equipment malfunction which affected the test procedure. The malfunction caused an in-plane moment to be applied to the wall which caused bed joint cracking of both face shells at the first joint down from the top of the wall. The moment was removed and a vertical compressive load of 18 kips (75 psi stress on the net area) was applied to the wall to close the crack and prevent slip along the existing crack.

Subsequent to the first two loadings, the displacement was increased at the maximum rate until load capacity failure occurred -- load capacity reduction with increasing displacement. Diagonal cracking occurred near the failure point. The test was continued using cycles with increasing displacement limits.

The load-displacement relationships are shown in figures 6.6 and 6.7. The general loading history can be observed in these figures. The strain measuring locations are shown in figure 6.8 while the strain histories are presented in figures 6.9 and 6.10. The load-displacement curve using the wall displacement is truncated to show only the test up to diagonal cracking because damage to the wall occurred in the region of the instrument making post-crack measurements unreliable. The strain histories only show the loading part of each of the first three loading increments (prior to diagonal cracking). The unloading portion of the histories are omitted for clarity. The crack observations are shown in figure 6.11 and 6.12.

6.3.4 Wall P6

The test of wall P6 was the first cyclic test performed in the series. The general loading history was cyclic fully reversed about the original undisplaced position. An axial compressive load of 4 kips (15 psi on the net area) was applied to the wall as precompression. The displacement varied sinusoidally with a frequency ranging between 2 and 4 Hz depending on the cyclic displacement amplitude. The maximum rate of loading was a constant, so that the frequency of loading varied with the required cyclic displacement. The cyclic displacement limits at each stage were selected somewhat arbitrarily to produce a desired cyclic tensile strain at a minimum of one SML. The first stage was based on achieving a tensile strain of 50 microstrain.

There were three stages during the test which had 100,000 cycles of the displacement sine wave. The first stage had displacement limits of -0.002 and 0.001 in measured at the top course of the wall. In further discussions, all displacements will be wall displacements at the top course. The second stage cycling had displacement limits of -0.003 and 0.005 in while the third stage had displacement limits of -0.010 and 0.011 in. After the third stage cycling was completed, the cyclic displacement amplitude was gradually increased while cycling until diagonal cracking and load capacity failure occurred. This last stage involved about 10,000 cycles. The load-displacement curves are shown in figures 6.13 and 6.14. The large number of cycles tend to overlap and cause the solid appearance of the curves. The strain measuring locations are shown in figure 6.15. The pertinent strain histories are shown in figures 6.16 through 6.21. For convenience in relating the strains to loading the piston displacement and lateral load are similarly plotted in figures 6.22 and 6.23. The crack observations are shown in figures 6.24 and 6.25.

6.3.5 Wall P8

The loading history for this test was a series of ramp functions. Each ramp started from the zero displacement condition and the displacement increased linearly to a maximum value at which point the displacement was returned to zero. The increase was done at a slow rate, but the return to zero was done at the maximum velocity. Each ramp had an incrementally larger displacement limit. The precompression axial load was about 5 kips for a net area stress of 20 psi. The load-displacement curves are presented in figures 6.26 and 6.27. The curves do not show the release portion of each ramp (except for the last) for clarity. The strain measuring locations are shown in figure 6.28 and the strain histories as functions of piston displacement are shown in figures 6.29 through 6.38. Again, the release portion of each ramp are not shown for clarity. Each ramp can be identified by its limiting displacement and is differentiated by different line types. The reader will note that the line types each occur twice due to a limited number of line types available. The crack observations are presented in figures 6.39 and 6.40.

6.3.6 Wall P4

The displacement was applied at a higher velocity than intended and the data acquisition equipment sampled at too slow a rate to adequately describe the test. The data for this test are omitted from discussion and only the crack observations (figures 6.41 and 6.42) are presented.

6.3.7 Wall P2

The loading history for this test was a series of ramp functions similar to those described for wall P8 (section 6.4.5). The precompression axial load was approximately 14 kips for a net area compressive stress of 60 psi. The second ramp reached the failure condition of the wall which was not expected based on the test of wall P8. A third ramp clearly demonstrated that the wall had indeed reached a failure condition. After the third ramp, the axial compressive load was increased to 23 kips (100 psi net area compressive stress) and several more ramps were applied.

The load-displacement curves are shown in figures 6.43 and 6.44. The curve for the wall displacement is terminated at the third ramp peak because the measurements after that point were severely affected by wall cracking and spalling in the measurement region. The strain measuring locations are shown in figure 6.45 and the pertinent strain histories are shown in figures 6.46 through 6.53. Only the data for the first three ramps are shown and the release portion of each ramp is not shown for clarity. Each ramp can be identified on the basis of its peak displacement and the line type. The crack observations are presented in figures 6.54 and 6.55.

6.3.8 Wall P5

The loading history was cyclic with prestrain. The prestrain was introduced by monotonically increasing the lateral displacement until a pre-selected value of strain at one of the SMLs was reached. For this test the prestrain level was selected to be 1400 microstrain in tension at any one of the horizontal SMLs. Vertical SMLs were predominantly influenced by flexural effects and so were considered not to be suitable indicators for shear prestrain. Prior to applying the prestrain, a 14 kip vertical precompression was applied to the wall. The resulting net area compressive stress was approximately 60 psi.

The 1400 microstrain value was first reached at SML 10 at a lateral displacement of 0.043 in as measured at the top course of the wall. The load deflection curves are presented in figures 6.56 and 6.57. The cyclic displacement amplitude was $\pm$ 0.003 in. initially, but was increased to $\pm$ 0.006 in. in an effort to increase the cyclic strain amplitude. During cycling, the lateral load capacity decreased until a stable level was reached at about 70 percent of the level before cycling. Also during cycling a diagonal crack formed and after 25,000 cycles the cycling was stopped and the displacement returned to zero. The displacement was then gradually increased until the load displacement-curve showed a sharp descending branch and the crack widths became excessive. This action of returning to zero displacement and then applying the displacement was then repeated twice.

The strain measuring locations are shown in figure 6.58 and the pertinent strain histories are presented in figures 6.59 through 6.65. The piston displacements and lateral load are shown in figures 6.66 and 6.67 as an aid in studying the strain histories. The crack observations are presented in figures 6.68 and 6.69.

6.3.9 Wall P3

The loading history for this test was cyclic with prestrain. The prestrain was selected to be 300 microstrain in tension at any one of the horizontal SMLs. The axial precompression was 14 kips for a net area compressive axial stress of about 60 psi. The prestrain was first reached at SML 10 at a displacement of 0.007 in. measured at the top course of the wall. The first stage of cycling was done at a frequency of 5 Hz and a cyclic displacement amplitude of $\pm$ 0.003 in. The value of $\pm$ 0.003 in. was selected on the basis of achieving a cyclic strain amplitude of $\pm$ 50 microstrain at SML 10. After 100,000 cycles were done at the first stage the displacement was increased without cycling until 600 microstrain in tension was achieved at SML 10. Cycling was again initiated with the same frequency and the same cyclic displacement amplitude. The cyclic displacement amplitude was kept constant for comparative purposes. Cycling was continued at the second stage for 100,000 cycles. Subsequently, displacements were increased, but not the cyclic displacement amplitudes to reach 1650, 2350, and 3800 microstrains (tension) at SML 10. Only 10,000 cycles were done at each of these three strain levels. The final part of the test was a continuous increase in displacement (with cycling) until a diagonal crack formed. With the formation of the crack the displacement was increased without cycling.

The load-displacement curves are presented in figures 6.70 and 6.71. The strain measurement locations are shown in figure 6.72 and the useful strain histories are shown in figures 6.73 through 6.79. The piston displacement and lateral load are plotted like the strain histories for comparison in figures 6.80 and 6.81. The crack observations are presented in figures 6.82 and 6.83.

6.3.10 Wall P1

The loading history was cyclic with prestrain. The axial precompression load was 14 kips resulting in a net area compressive stress of about 60 psi. The first 100,000 cycles were done about a displacement of 0.036 in. measured at the top course of the wall. The maximum horizontal tensile strain was 35 microstrain at SML 3. The cyclic displacement amplitude was $\pm$ 0.003 in. and the frequency was 6.5 Hz.

After the first 100,000 cycles the displacement was increased without cycling until the tensile strain at SML 13 reached 690 microstrain. The corresponding displacement was 0.044 in. Cycling was begun again at the same frequency and cyclic displacement amplitude. The lateral load slowly decreased with cycling until about cycle 840. At this point a diagonal crack formed and the lateral load dropped much more rapidly as cycling continued. The lateral load capacity stabilized after about 11,000 cycles. After completing 15,000 cycles the cycling was stopped and the displacement was increased without cycling to fully develop the wall crack pattern.

The load-displacement curves are shown in figures 6.84 and 6.85. The strain measurement locations are presented in figure 6.86 and the pertinent strain histories are shown in figures 6.87 through 6.93. The piston displacement and lateral load are similarly presented in figures 6.94 and 6.95. The crack observations are shown in figures 6.96 and 6.97.

6.3.11 Wall C5

The loading history was a simple half-cycle to a displacement which failed the corner wall. The displacement, however, was directed along the diagonal or z-axis of the corner wall as described in figure 6.1. The axial precompression was 16 kips which produced a net area stress of about 50 psi.

The load-displacement curves are shown in figures 6.98 and 6.99. Each figure shows two curves. One curve is the east-west component of load versus the east-west component of displacement and is the solid line. The other curve is dashed and is the north-south load component versus the north-south displacement component. The strain measurement locations are shown in figure 6.100. The strain histories are shown in figures 6.101 through 6.113. The displacements shown depend on which face the SML is mounted. Those SMLs mounted on the east-west leg of the wall have their strains plotted against the east-west component of the piston displacement. The SMLs mounted on the north-south leg of the wall have their strains plotted against the north-south component of the piston displacement. The crack observations are shown in figures 6.114 and 6.115.

6.3.12 Wall C4

The load history was a half-cycle to a maximum displacement which failed the corner wall. The displacement was directed only along the east-west leg of the wall (figure 6.1). The axial precompression load was 16 kips which produced a net area stress of about 50 psi.

The load-displacement curves are shown in figures 6.116 and 6.117. The strain measurement locations are presented in figure 6.118 and the pertinent strain histories in figures 6.119 through 6.129. The crack observations are shown in figures 6.130 and 6.131.

6.3.13 Wall C3

The loading history was a half-cycle to a maximum displacement which failed the corner wall. The displacement was directed only along the east-west leg of the wall (figure 6.1). The axial precompression load was 16 kips which produced a net area stress of about 50 psi. The load-displacement curves are shown in figures 6.132 and 6.133. The strain measurement locations are presented in figure 6.134 and the pertinent strain histories in figure 6.135 through 6.145. The crack observations are shown in figures 6.146 and 6.147.

6.3.14 Wall C2

The loading history for this test was cyclic with prestrain. The displacement was directed only along the east-west leg of the wall (figure 6.1). The axial precompression load was 16 kips which produced a net area stress of about 50 psi.

The first prestrain level was selected to be 300 microstrain in tension at any one of the horizontal SMLs. The resulting displacement was 0.002 in measured at the top course of the wall. The strain level was reached at SML 12 first. The cyclic frequency was 6.5 Hz and the cyclic displacement amplitude was ± 0.003 in. After 100,000 cycles the strain at SML 12 was quite high, but no other SMLs reported significant tensile strains. Upon examination of the wall it was concluded that SML 12 was unduly affected by a local flaw. Therefore, it was decided to ignore the data from SML 12 for determining prestrain levels. The second prestrain level was selected to again be 300 microstrain in tension, but at some other SML. The level was reached at SML 5 at a displacement of 0.016 in. Another 100,000 cycles were performed at 6.5 Hz and a cyclic displacement amplitude of ± 0.003 in. Again, very little change was observed except for SML 5. The final stage of the test was an attempt to have all of the SMLs along a diagonal show tension before initiating cycling. However, failure of the wall occurred very quickly just before the last SML along the diagonal went into tension.

The load-displacement curves are shown in figures 6.148 and 6.149. The strain measurement locations are shown in figure 6.150. The pertinent strain histories are shown in figures 6.151 through 6.159. The piston displacement and lateral load are similarly plotted in figures 6.160 and 6.161. The crack observations are presented in figures 6.162 and 6.163.

6.3.15 Wall C1

The loading history for this test was cyclic with prestrain. The displacement was directed only along the east-west leg of the corner wall (figure 6.1). The axial precompression load was 16 kips which produced a net area stress of about 50 psi.

The first 100,000 cycles were done about a displacement of 0.034 in. measured at the top course of the wall. This displacement level corresponded to the point at which the first SML (SML 9) in the expected diagonal cracking region reached 300 microstrain (tension). The cyclic frequency was 6.5 Hz and the cyclic displacement amplitude was ± 0.003 in. After the first 100,000 cycles were completed the displacement was increased to 0.060 in. which resulted in a strain of 1200 microstrain (tension) at SML 9. Another 100,000 cycles were performed at the same cyclic frequency and displacement amplitude. Upon completion of the second group of 100,000 cycles the displacement was incrementally increased and at each step at least 10,000 cycles were performed. This continued until a diagonal crack formed. The displacement was then increased without cycling until the lateral load capacity dropped. The initial diagonal cracking did not penetrate the block at each corner of the diagonal, but when the maximum lateral load capacity was reached the diagonal crack split these end blocks. The load-displacement curves are shown in figures 6.164 and 6.165. The strain measurement locations are shown in figure 6.166. The strain histories and similarly plotted piston movement and lateral load are shown in figures 6.167 through 6.175.

The crack observations are shown in figures 6.176, 6.177, and 6.178. It was observed that while no diagonal cracking was observed during the first 100,000 cycles some cracking along the mortar joints did occur. The cracking, however, was not along the same path that the final failure crack followed. The first cracking which seemed to be part of the failure crack occurred during the incrementally increased displacements after the second 100,000 cycles and formed in the blocks (figure 6.177).

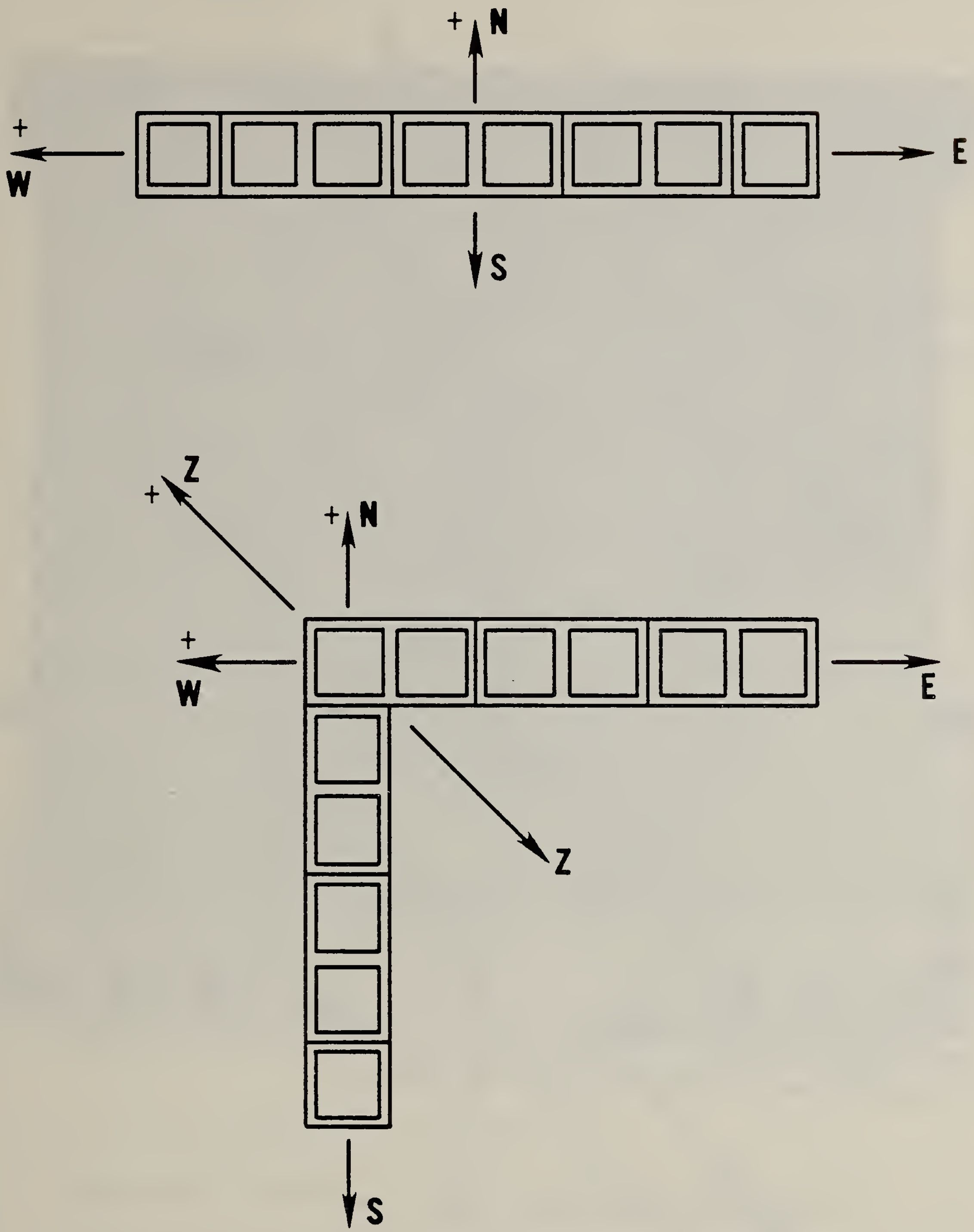

Figure 6.1. Wall displacement directions

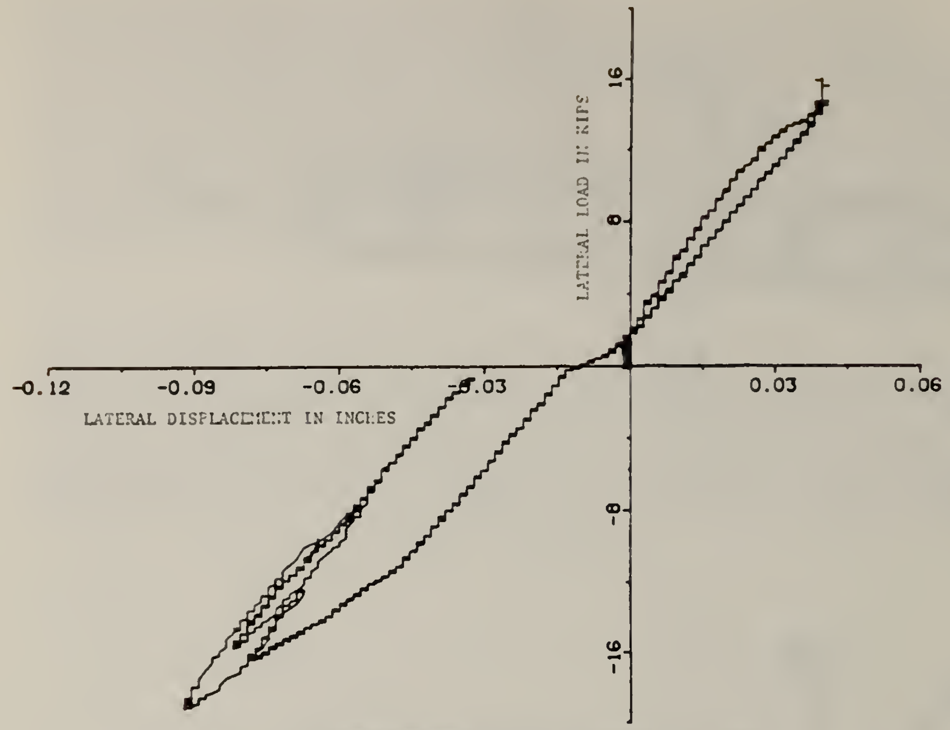

Figure 6.2. Lateral load versus piston displacement for wall P10

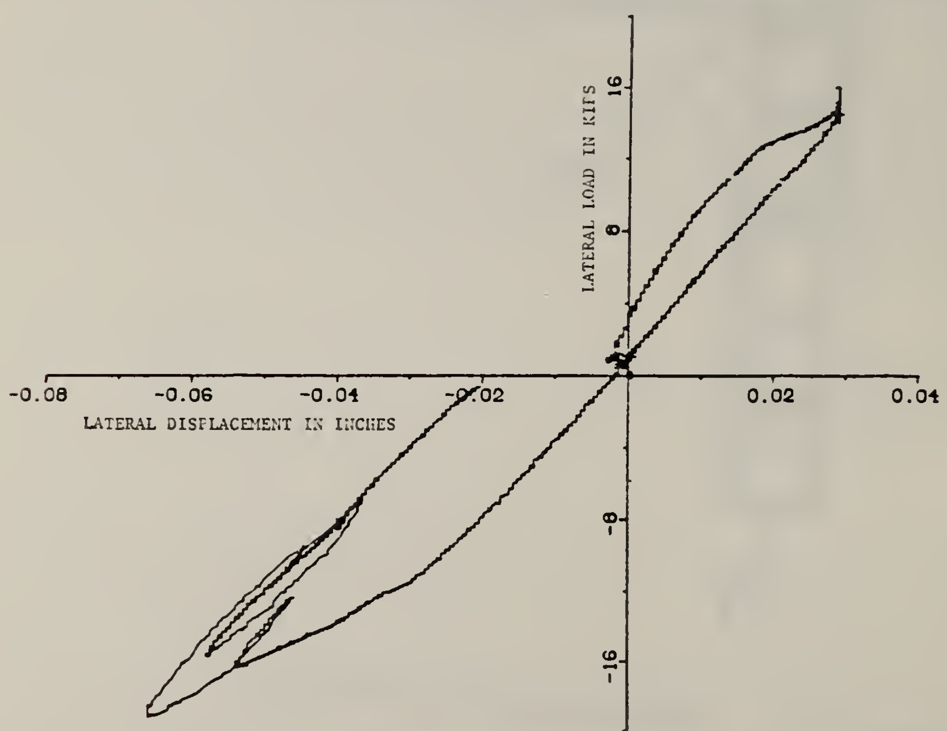

Figure 6.3. Lateral load versus wall displacement for wall P10

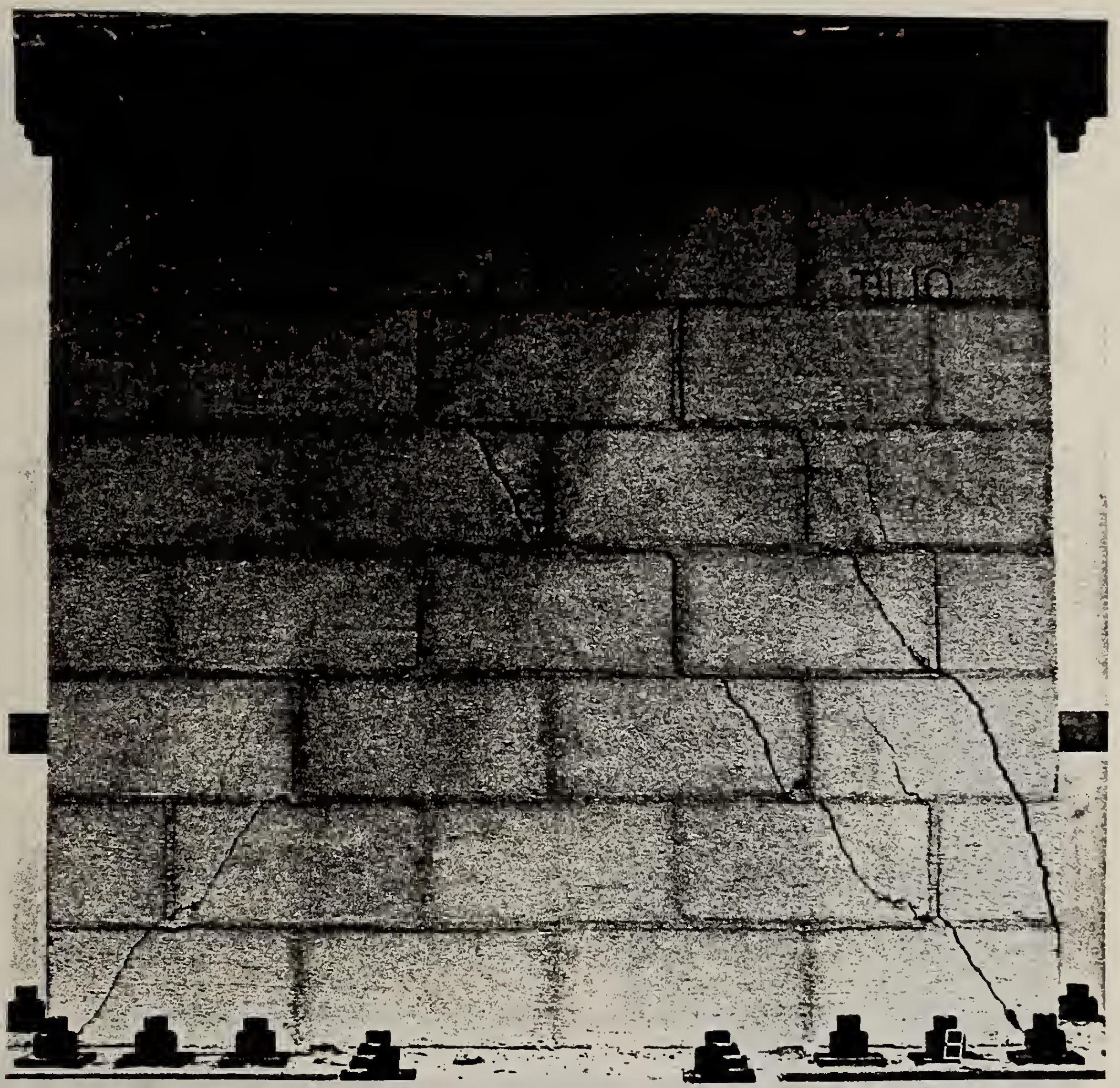

Looking to the north.

Figure 6.4. Post-test crack observations for wall P10

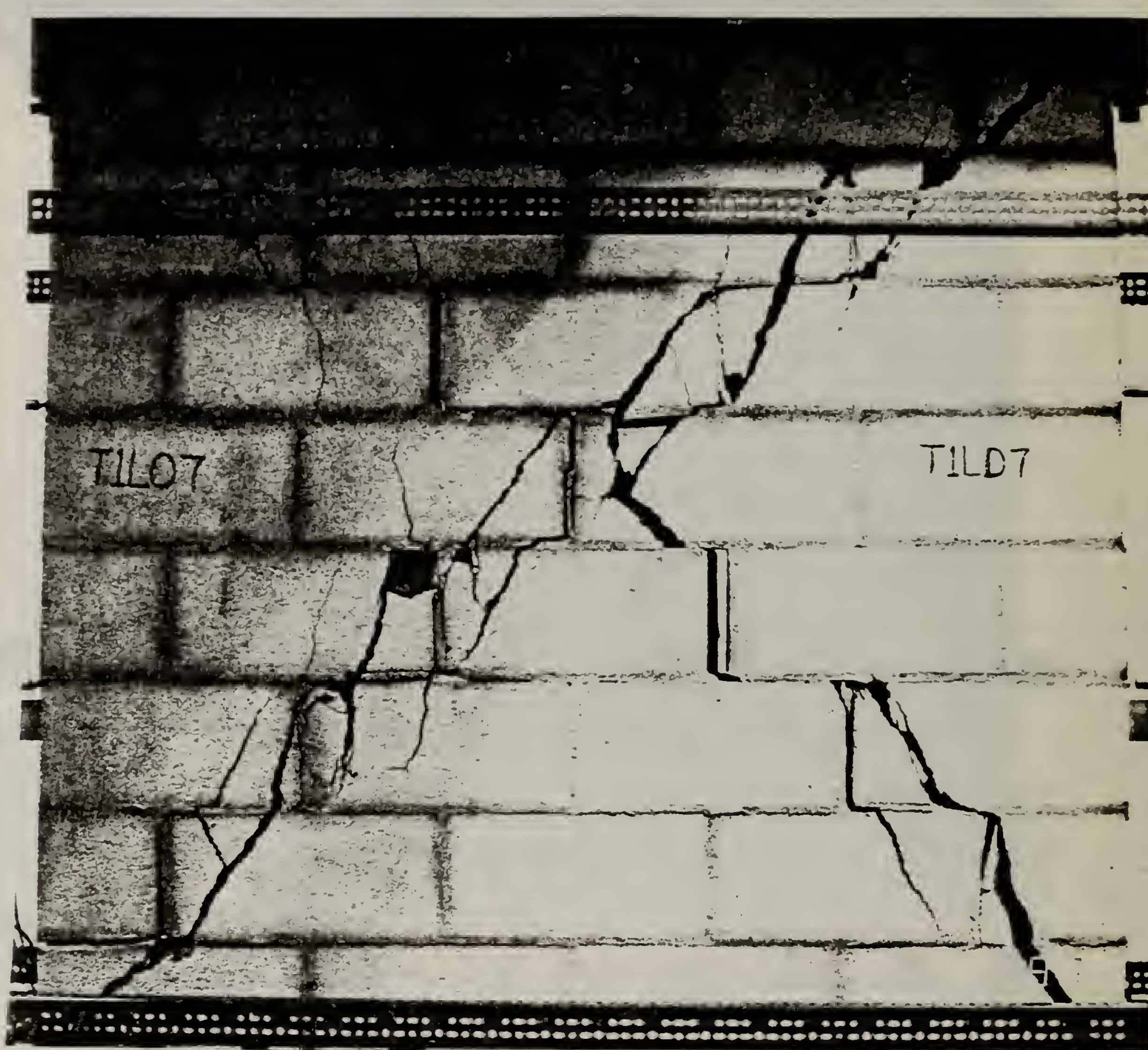

Looking to the north.

Figure 6.5. Post-test crack observations for wall P7

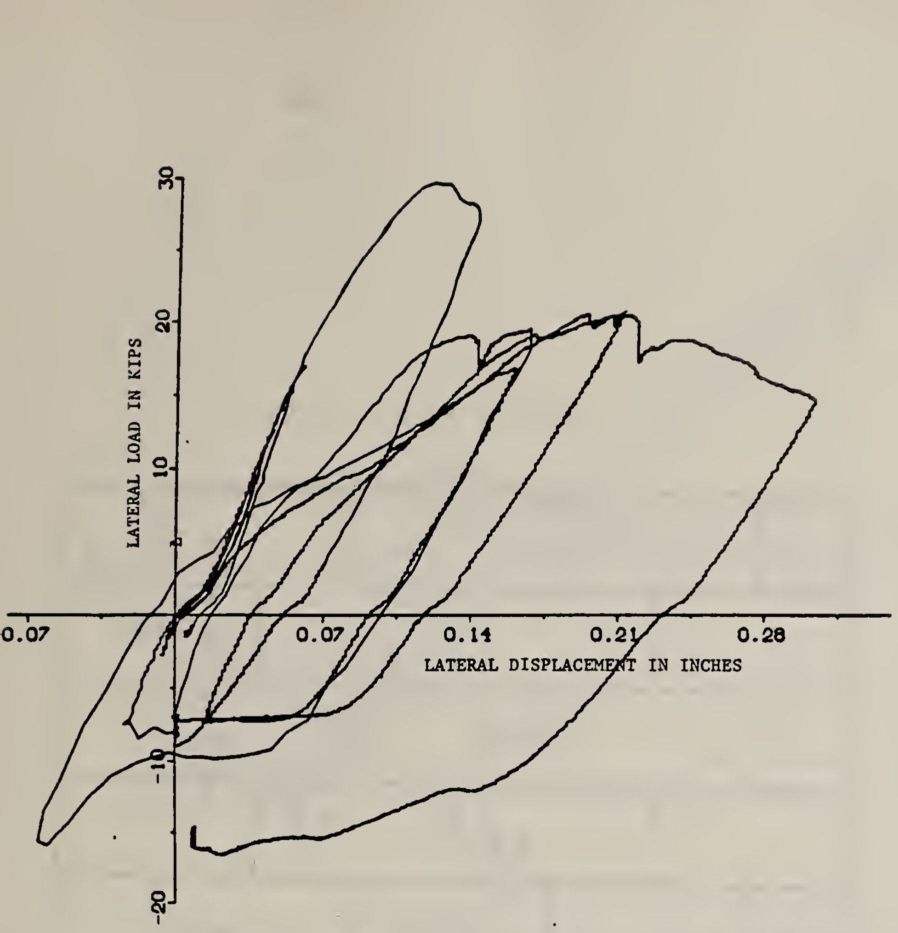

Figure 6.6. Lateral load versus piston displacement for wall P9

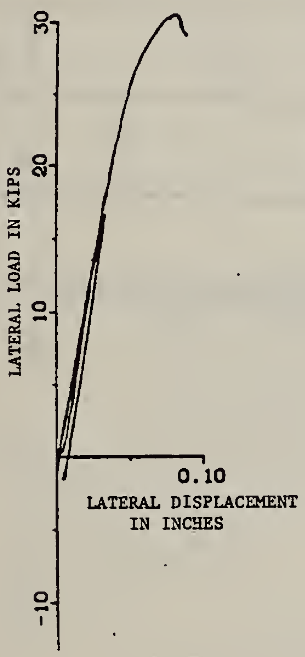

Figure 6.7. Lateral load versus wall displacement for wall P9

Looking to the north.

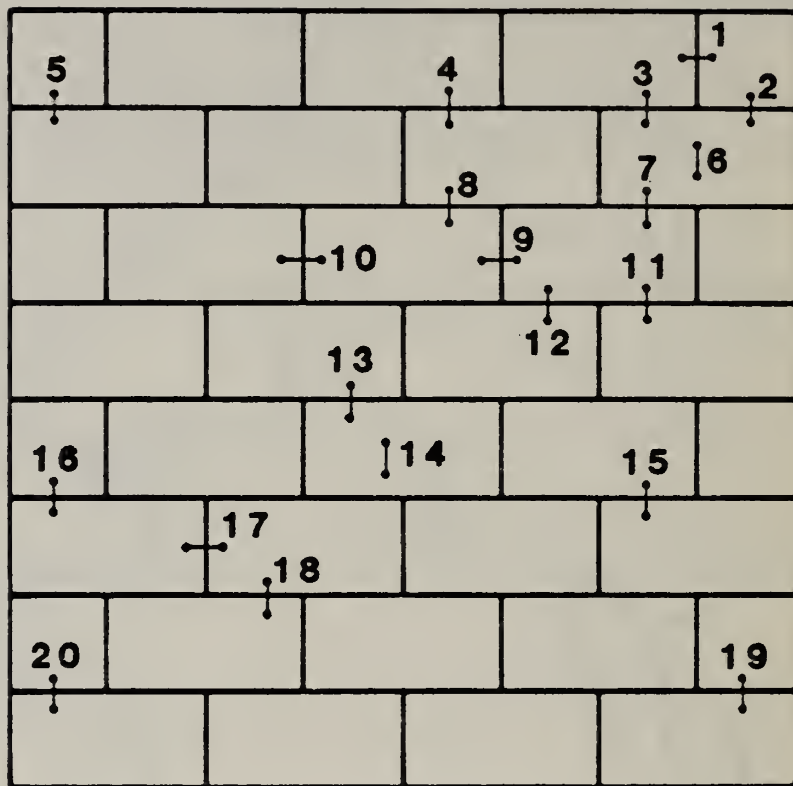

Figure 6.8. Strain measuring locations for wall P9

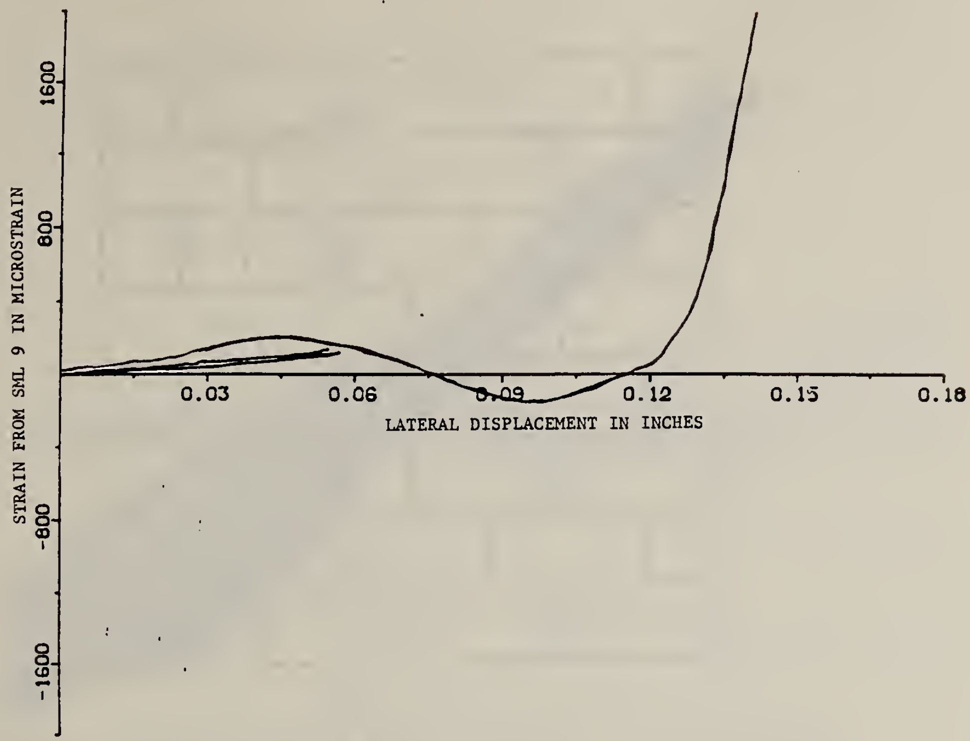

Figure 6.9. Strain history of SML 9 for wall P9

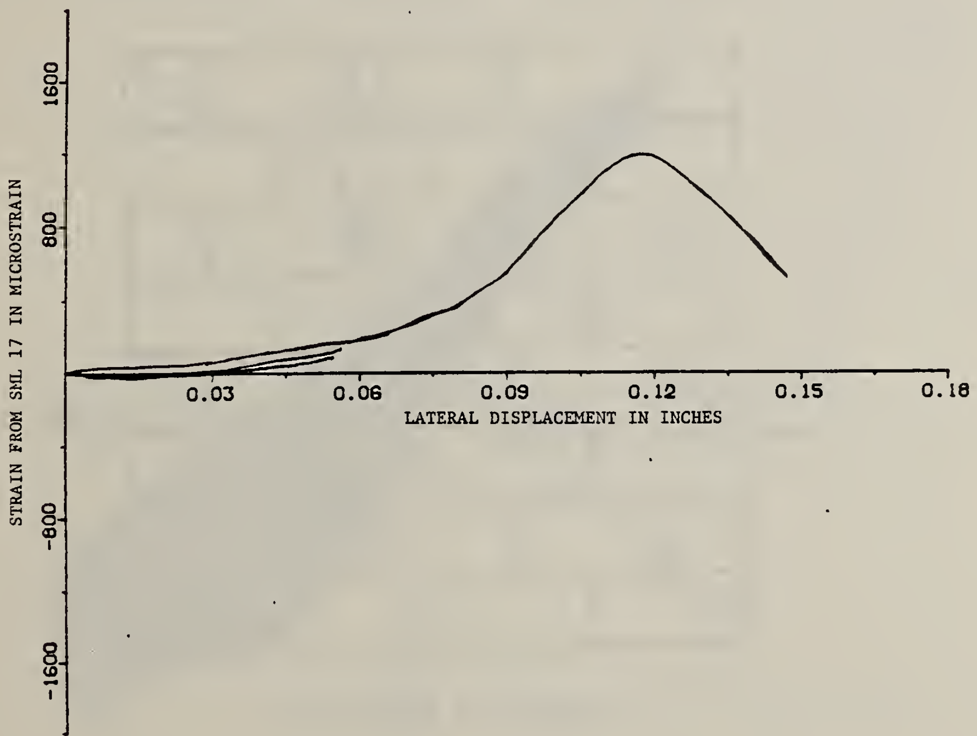

Figure 6.10. Strain history of SML 17 for wall P9

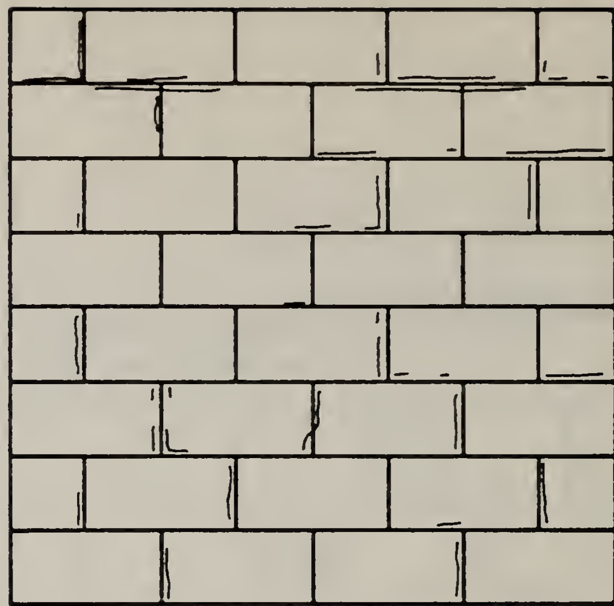

Figure 6.11. Pre-test crack observations for wall P9

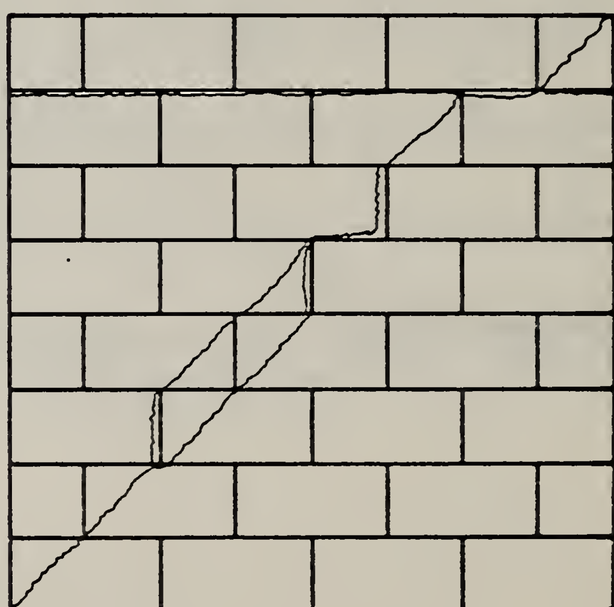

Looking to the north.

Figure 6.12. Post-test crack observations for wall P9

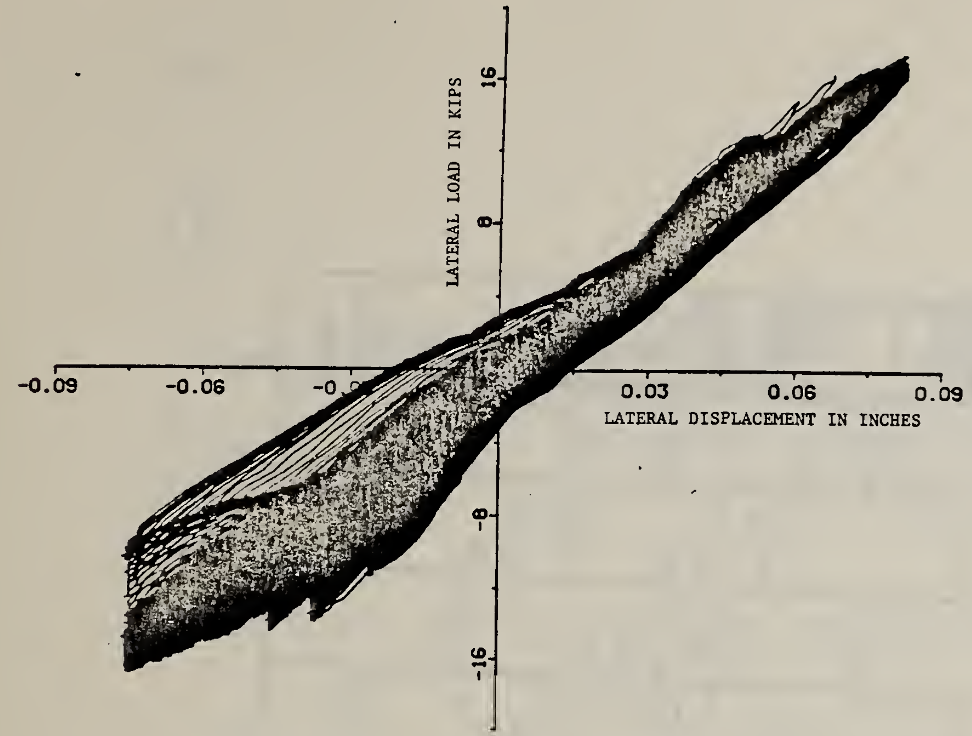

Figure 6.13. Lateral load versus piston displacement for wall P6

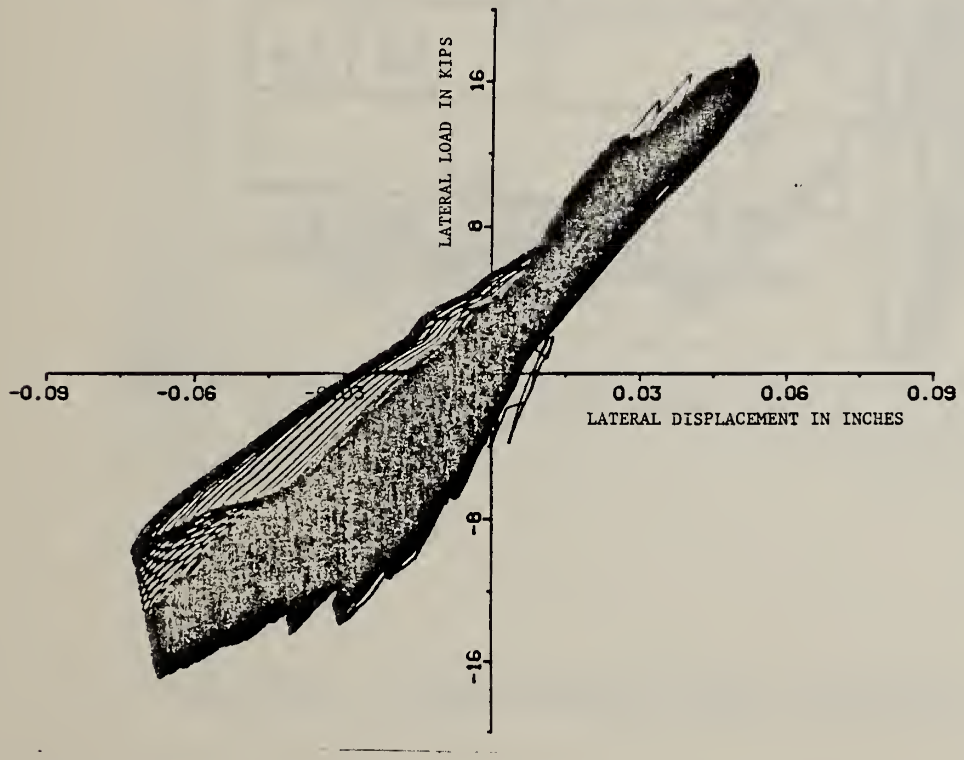

Figure 6.14. Lateral load versus wall displacement for wall P6

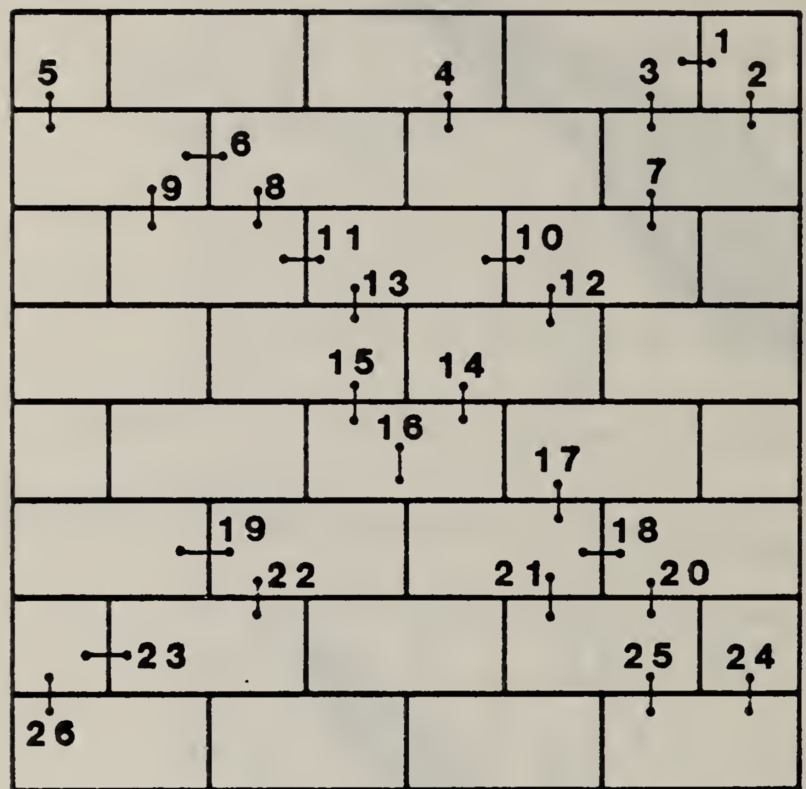

Looking to the north.

Figure 6.15. Strain measuring locations for wall P6

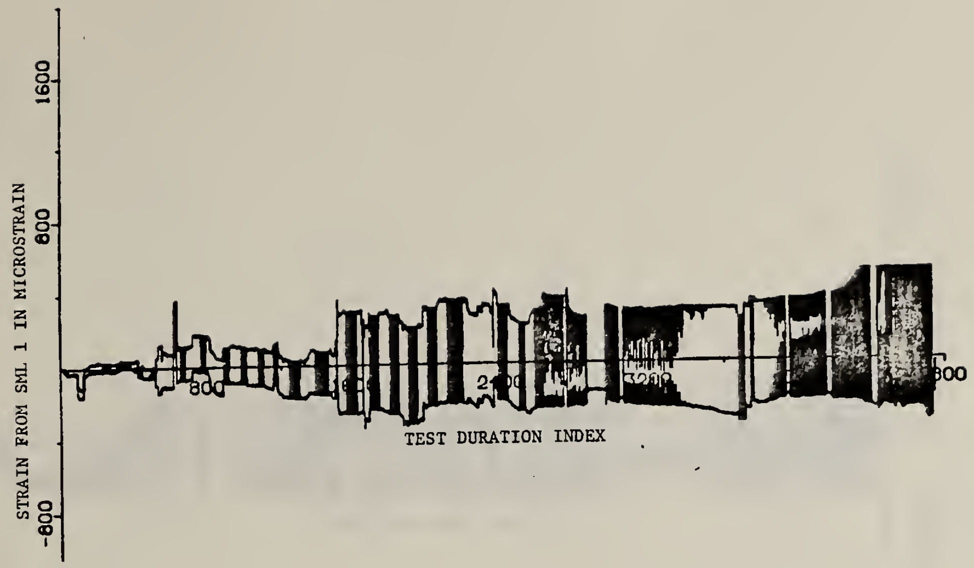

Figure 6.16. Strain history of SML 1 for wall P6

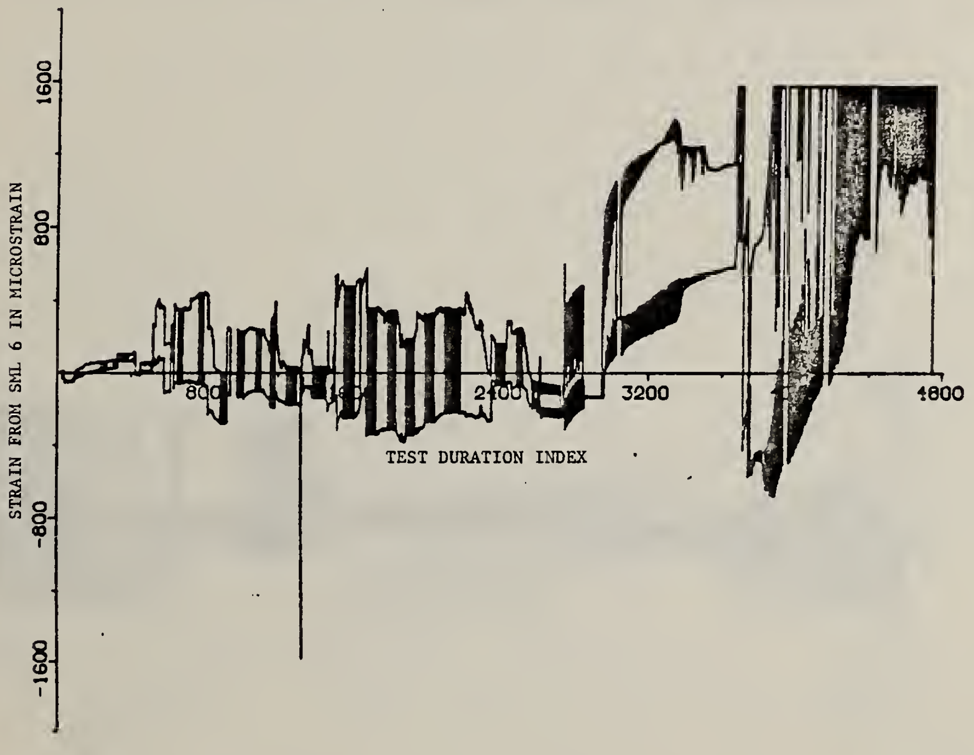

Figure 6.17. Strain history of SML 6 for wall P6

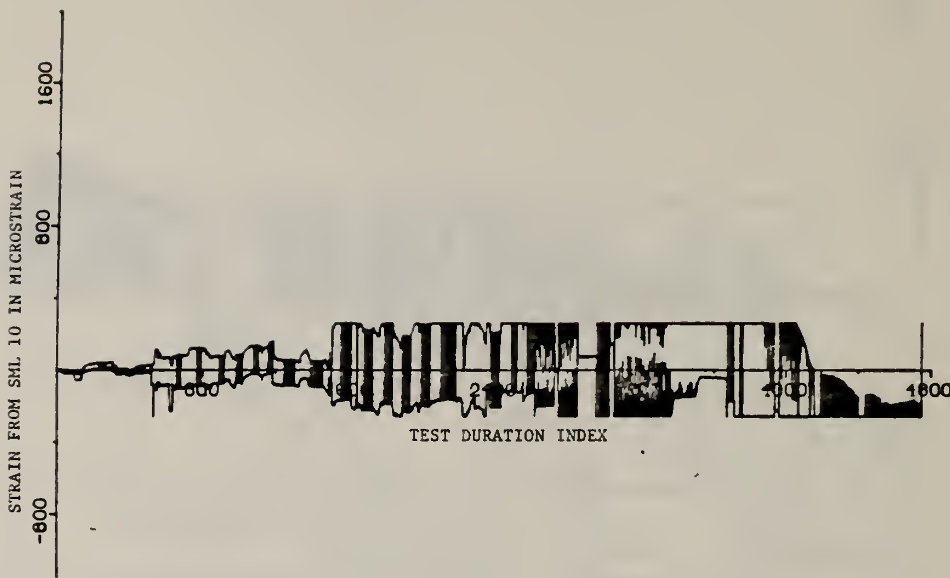

Figure 6.18. Strain history of SML 10 for wall P6

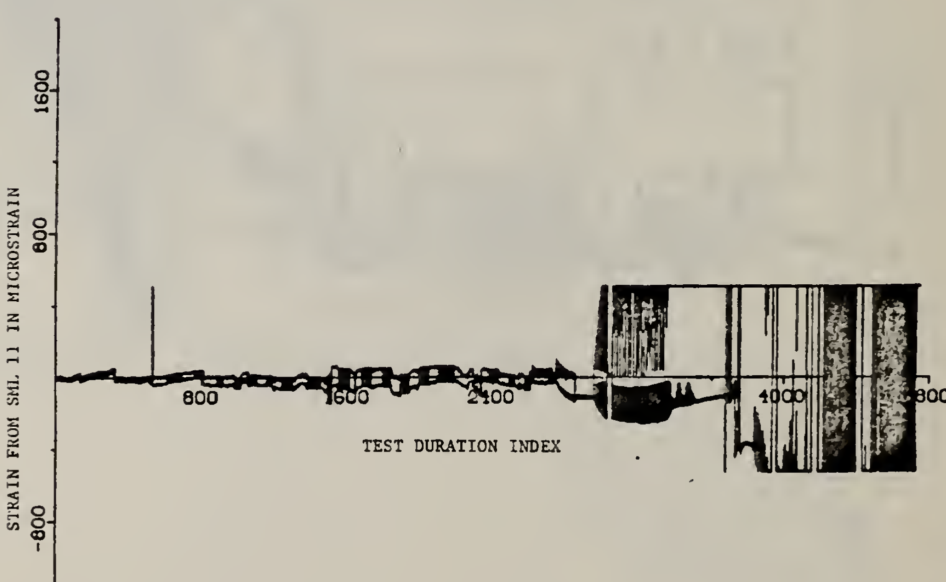

Figure 6.19. Strain history of SML 11 for wall P6

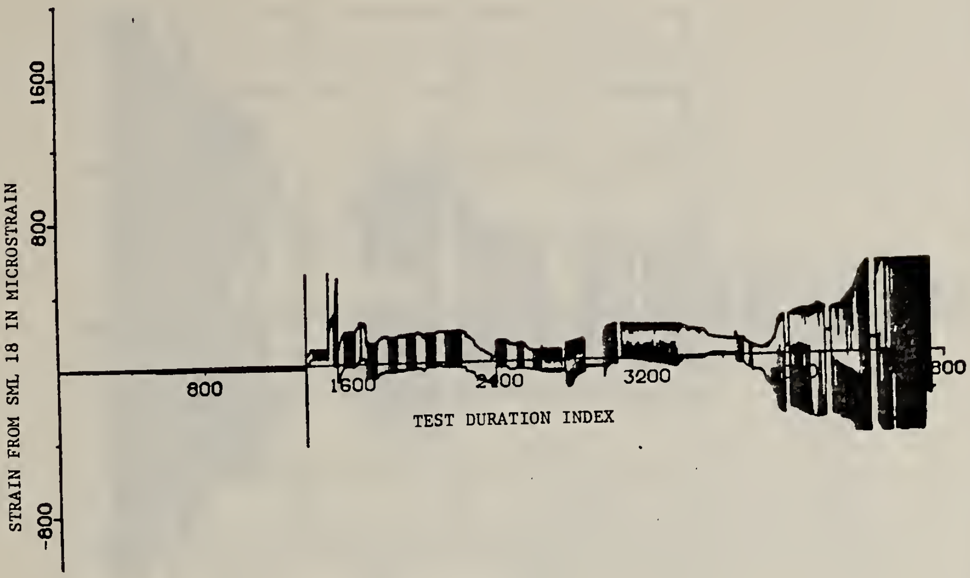

Figure 6.20. Strain history of SML 18 for wall P6

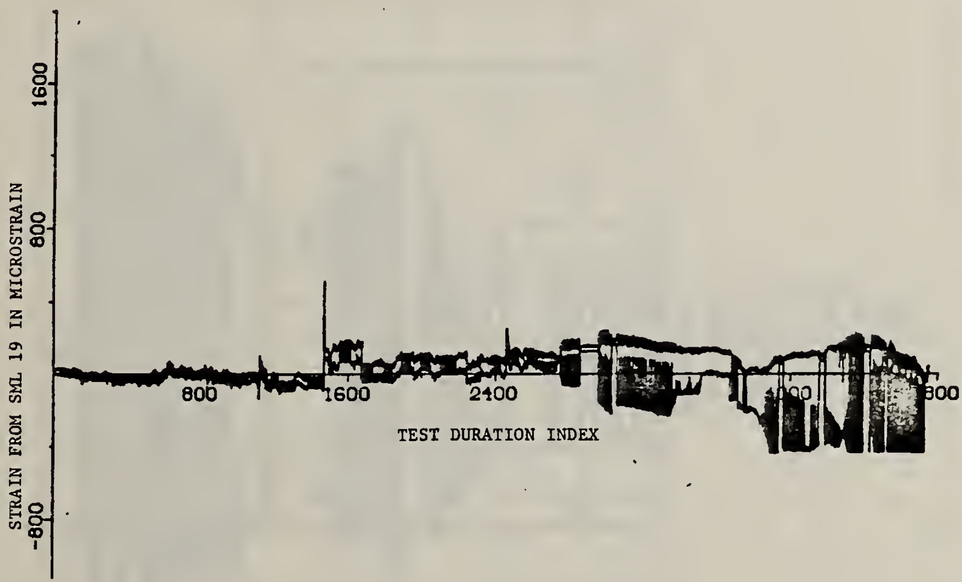

Figure 6.21. Strain history of SML 19 for wall P6

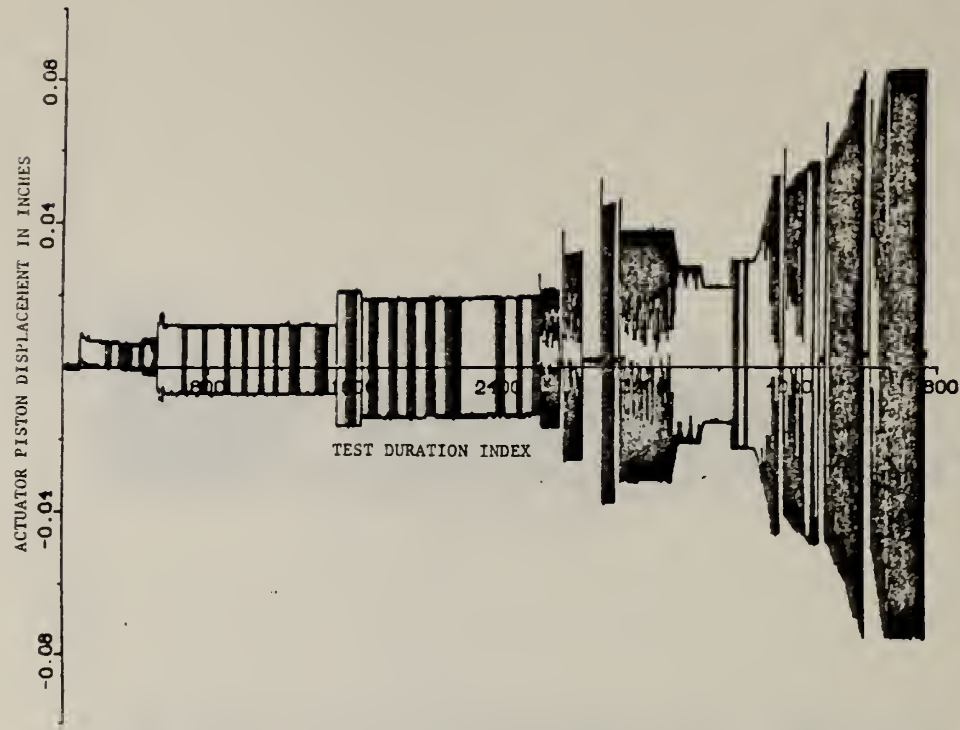

Figure 6.22. Piston displacement history for wall P6

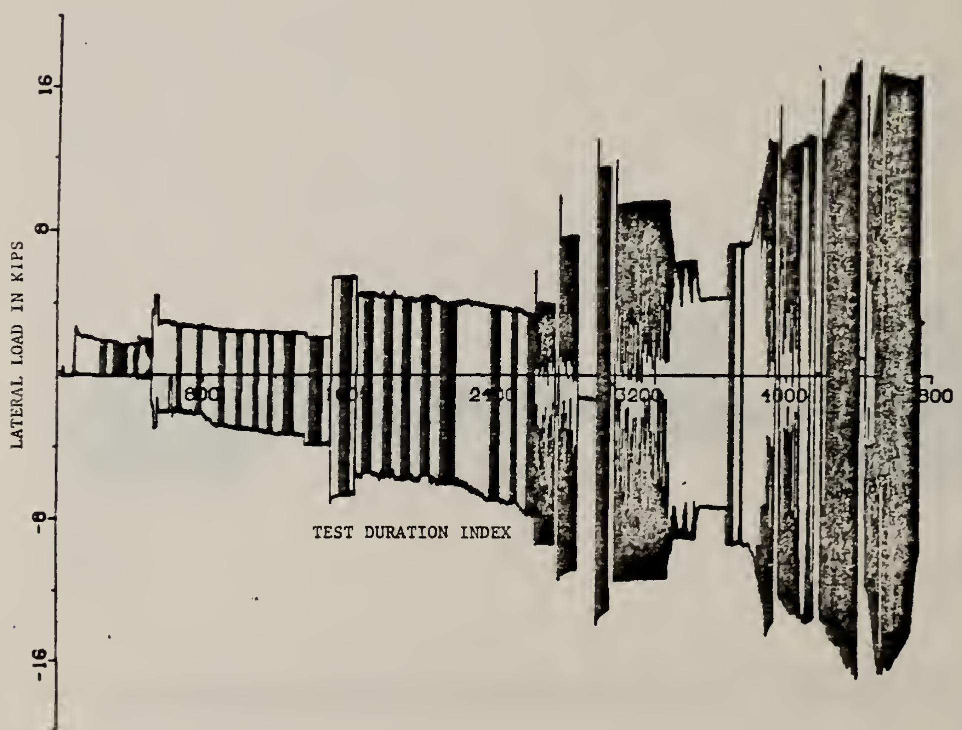

Figure 6.23. Lateral load history for wall P6

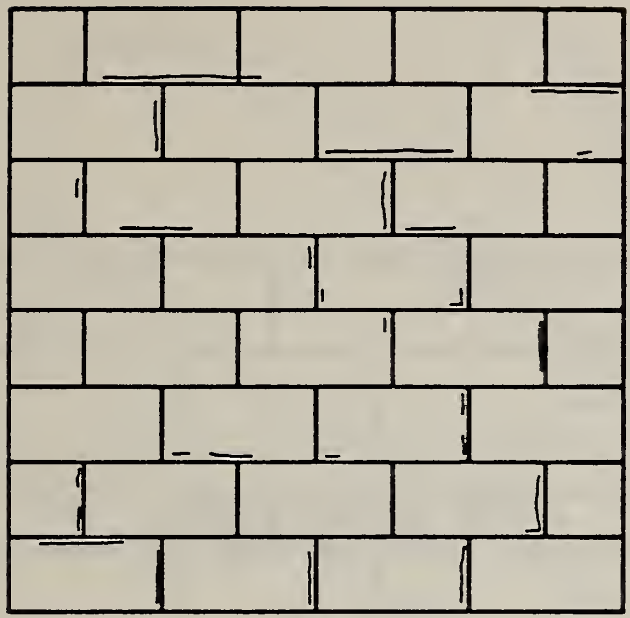

Figure 6.24. Pre-test crack observations for wall P6

Looking to the north.

Figure 6.25. Post-test crack observations for wall P6

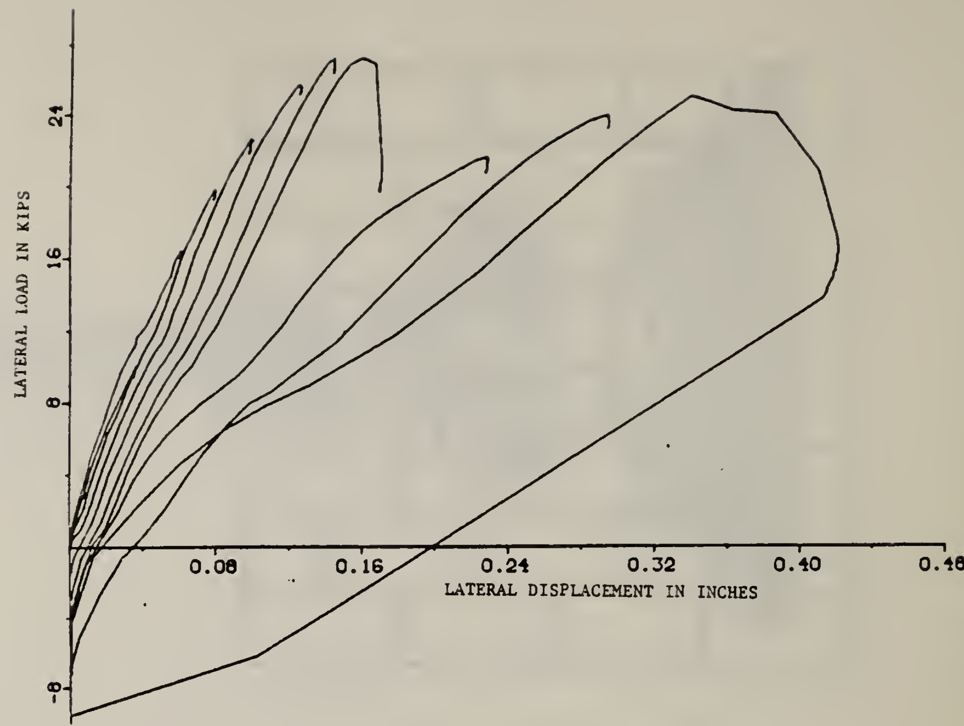

Figure 6.26. Lateral load versus piston displacement for wall P8

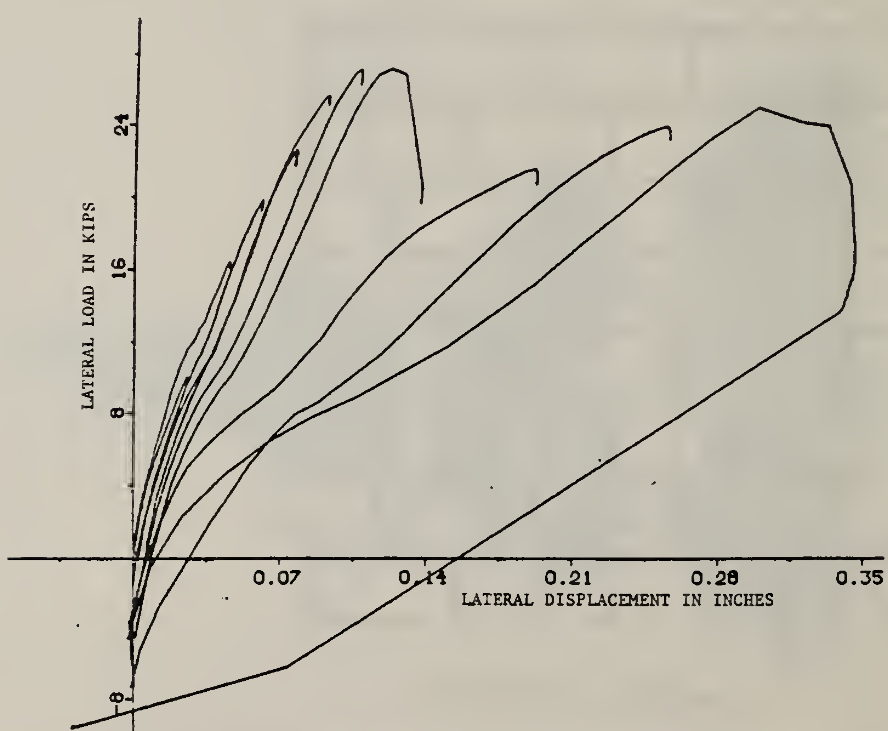

Figure 6.27. Lateral load versus wall displacement for wall P8

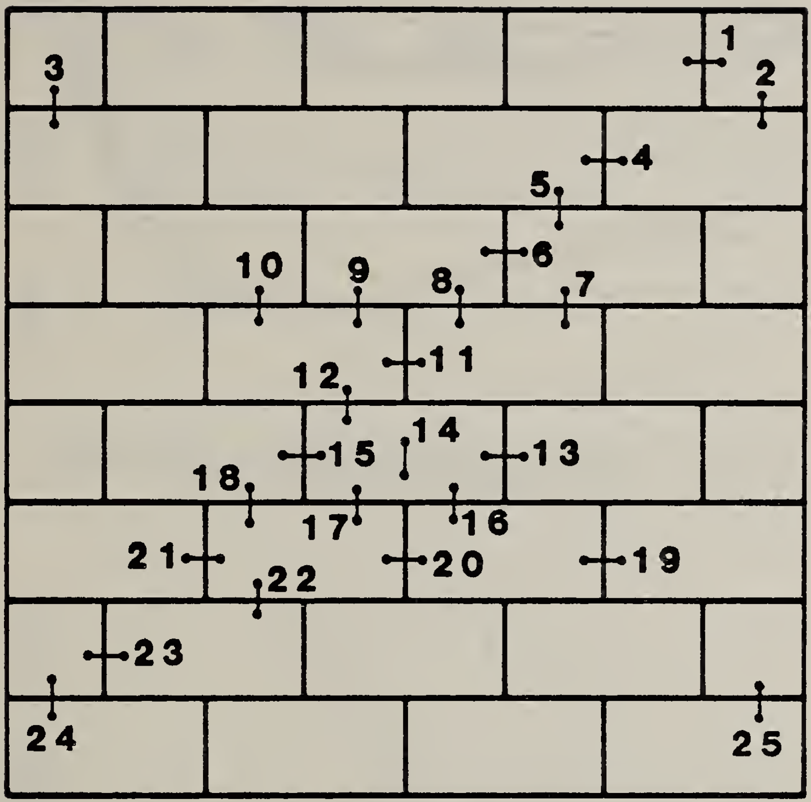

Looking to the north.

Figure 6.28. Strain measuring locations for wall P8

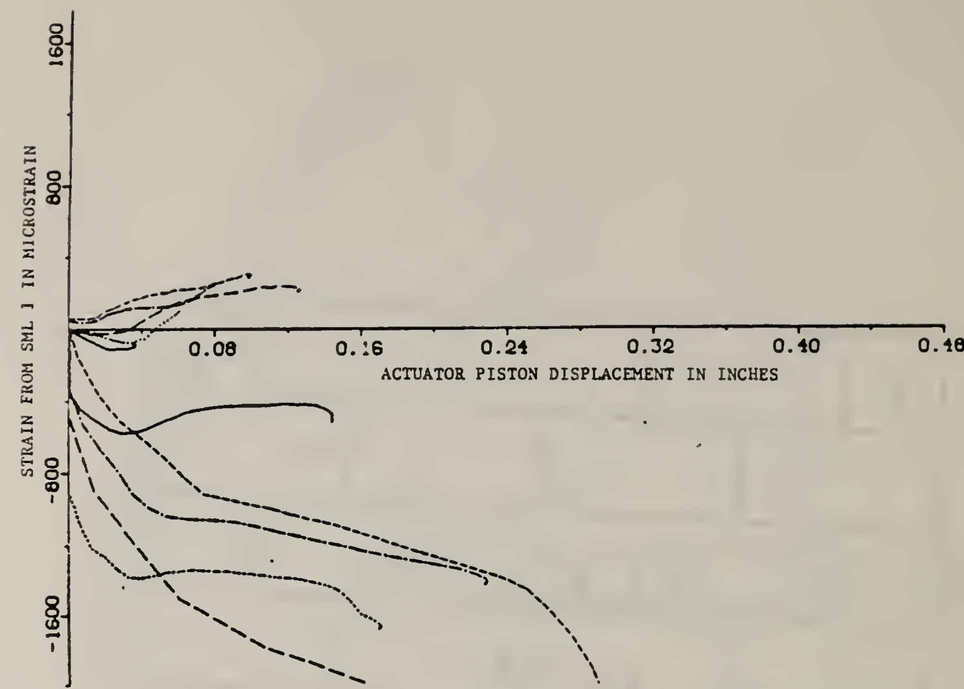

Figure 6.29. Strain history of SML 1 for wall P8

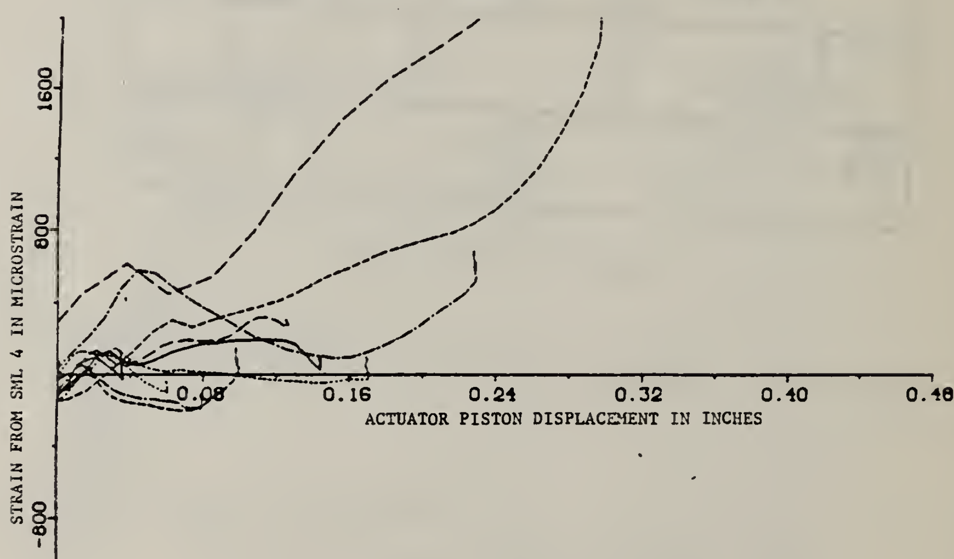

Figure 6.30. Strain history of SML 4 for wall P8

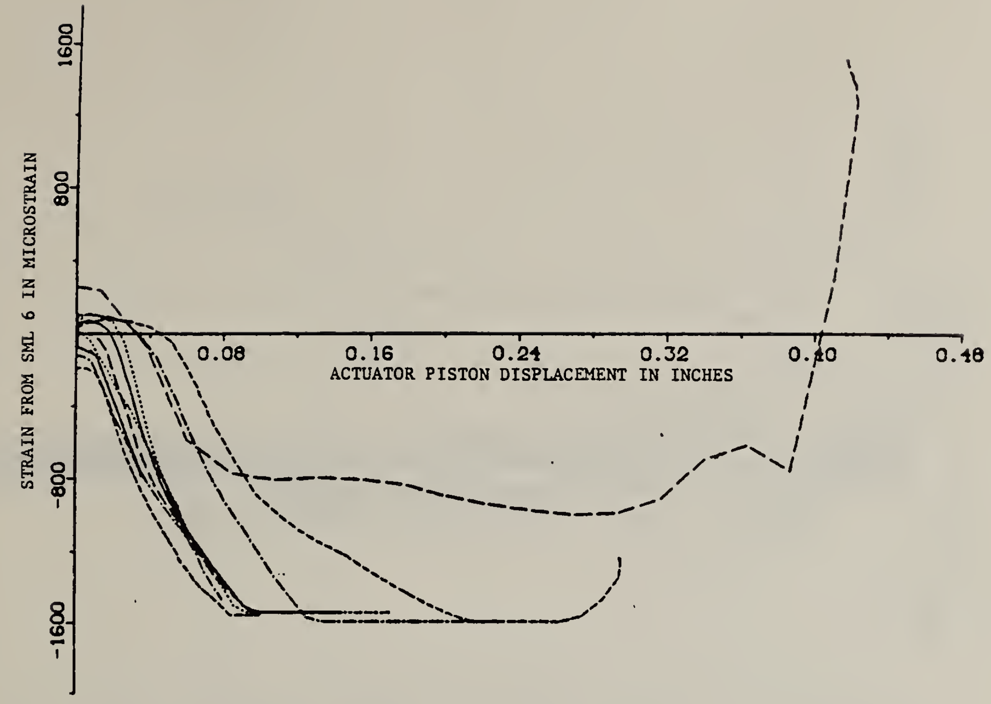

Figure 6.31. Strain history of SML 6 for wall P8

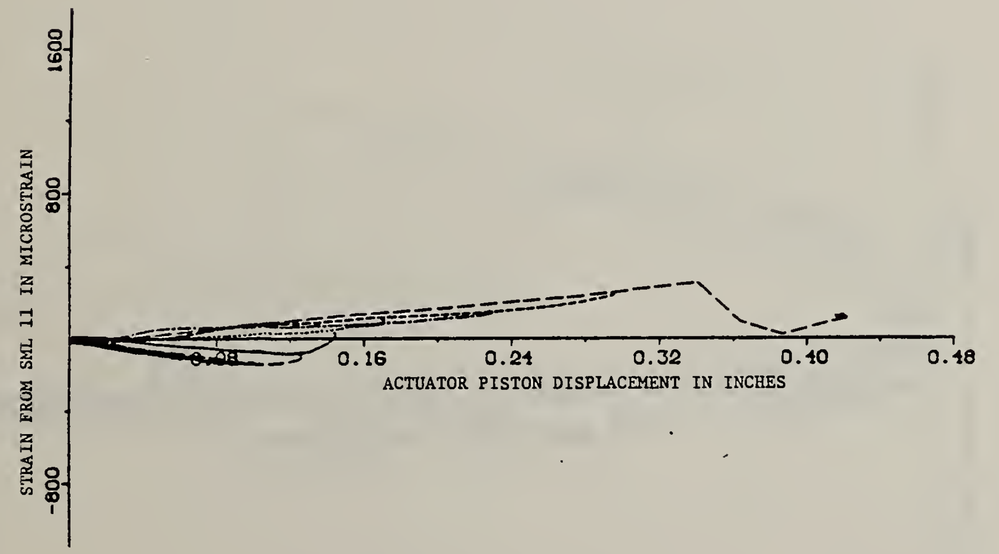

Figure 6.32. Strain history of SML 11 for wall P8

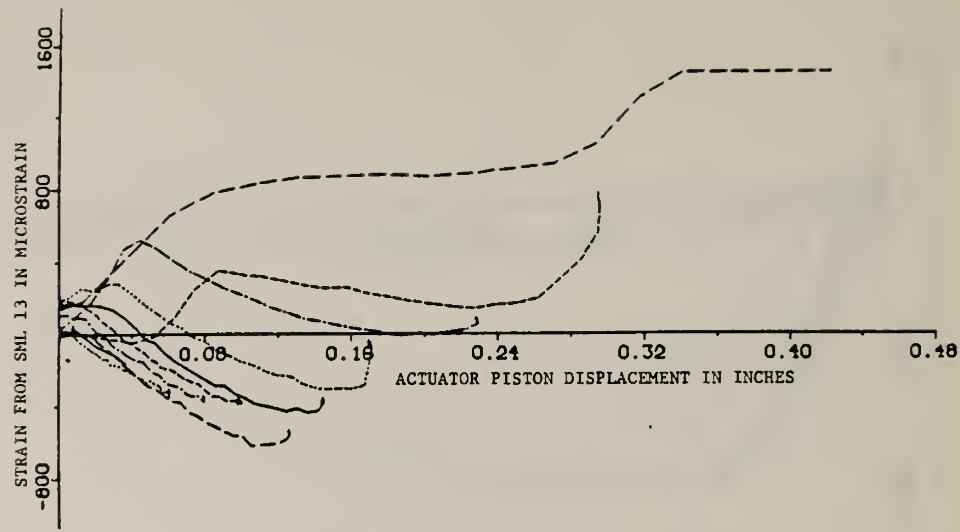

Figure 6.33. Strain history of SML 13 for wall P8

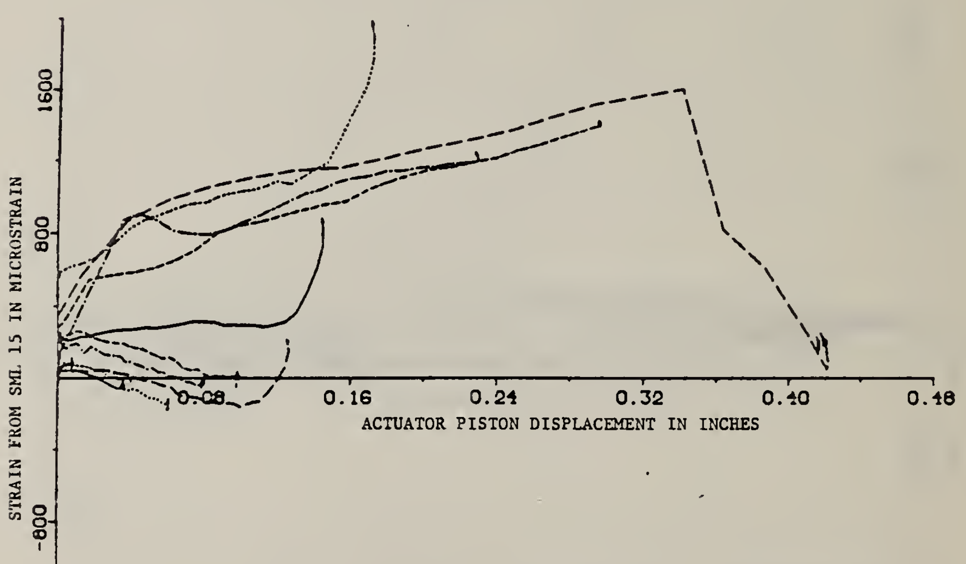

Figure 6.34. Strain history of SML 15 for wall P8

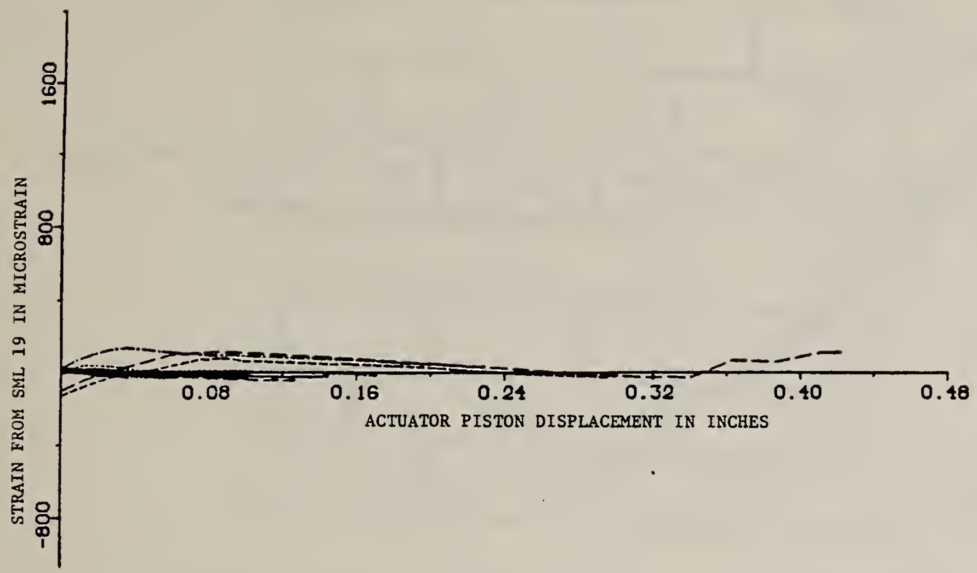

Figure 6.35. Strain history of SML 19 for wall P8

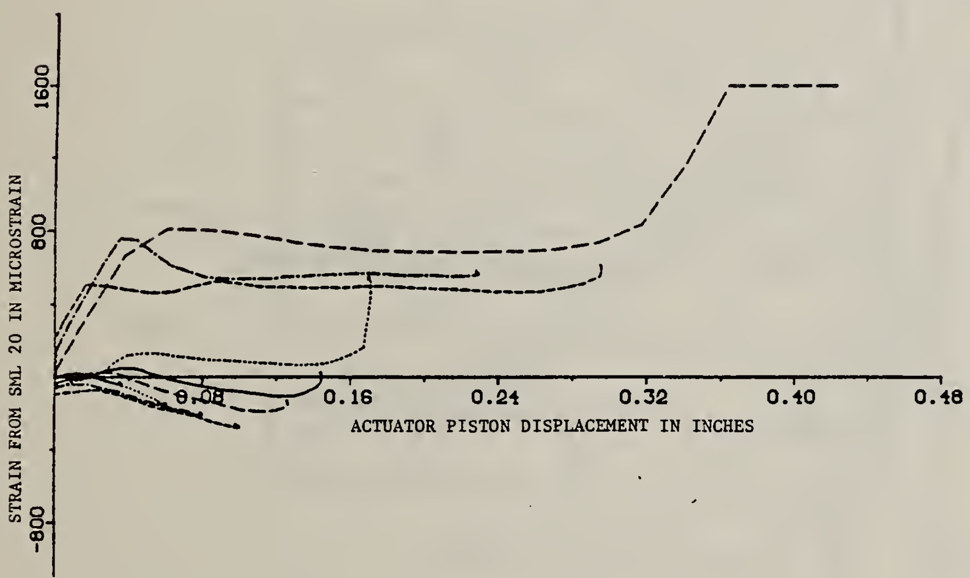

Figure 6.36. Strain history of SML 20 for wall P8

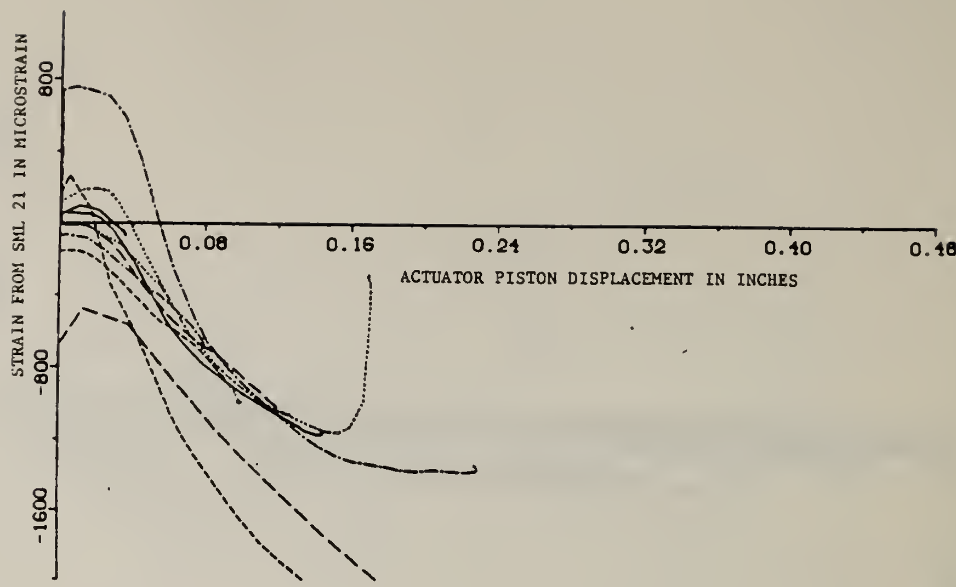

Figure 6.37. Strain history of SML 21 for wall P8

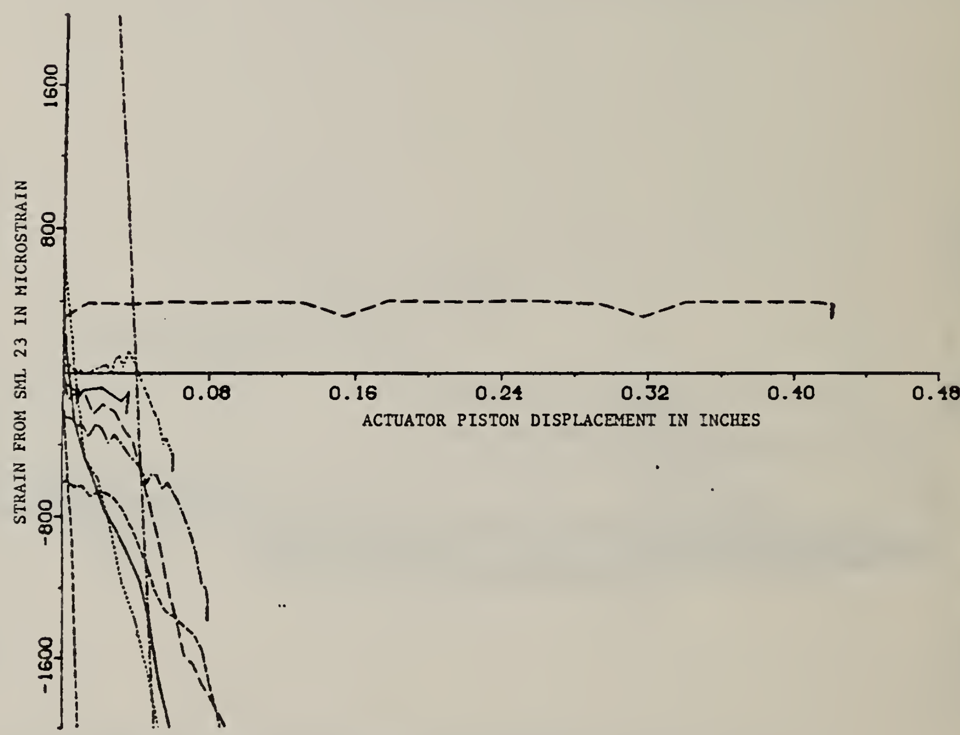

Figure 6.38. Strain history of SML 23 for wall P8

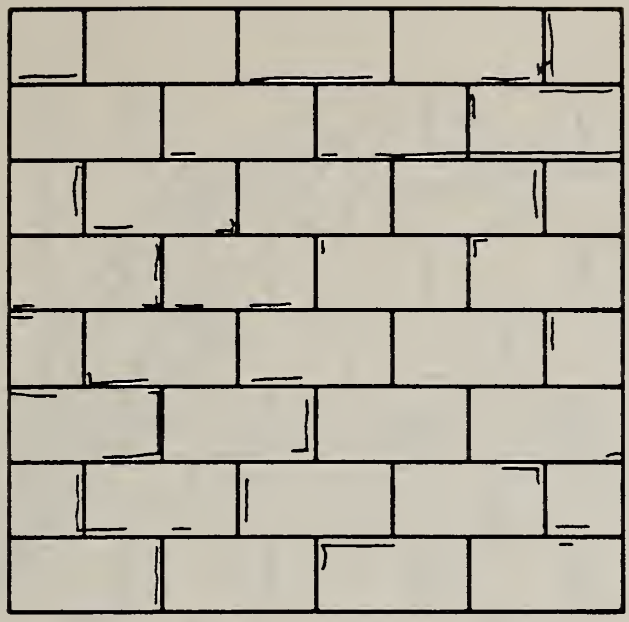

Figure 6.39. Pre-test crack observations for wall P8

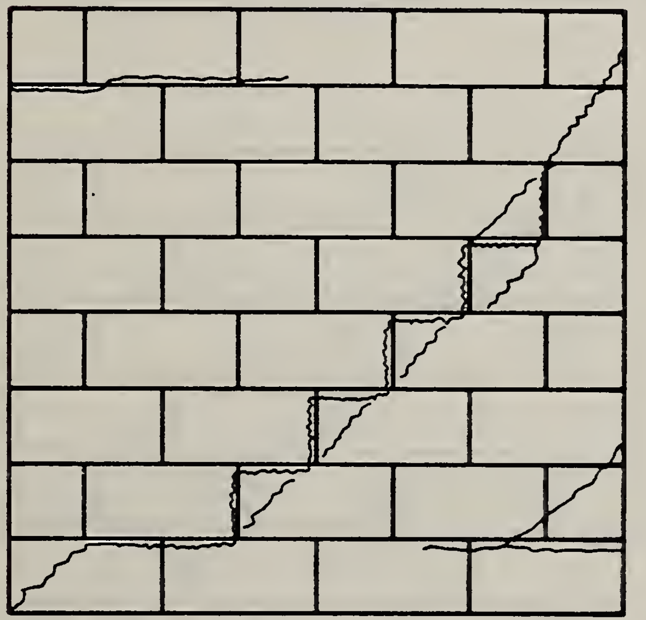

Looking to the north.

Figure 6.40. Post-test crack observations for wall P8

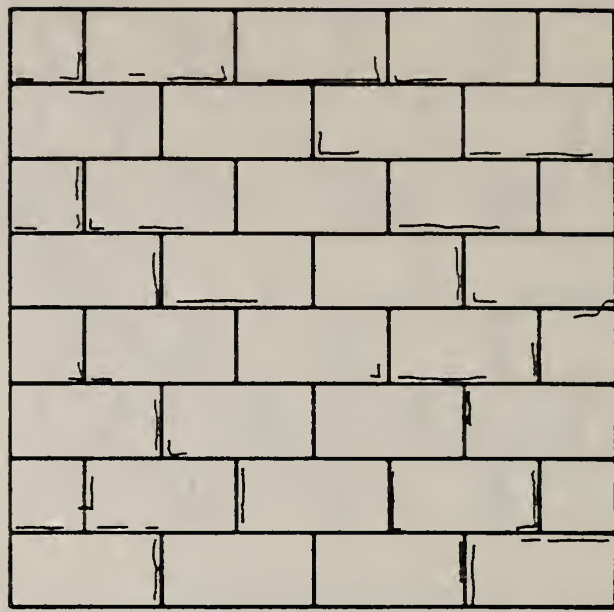

Figure 6.41. Pre-test crack observations for wall P4

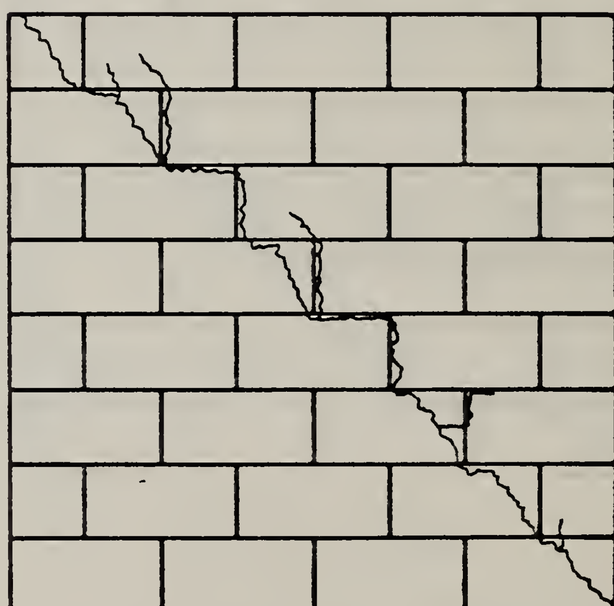

Looking to the south.

Figure 6.42. Post-test crack observations for wall P4

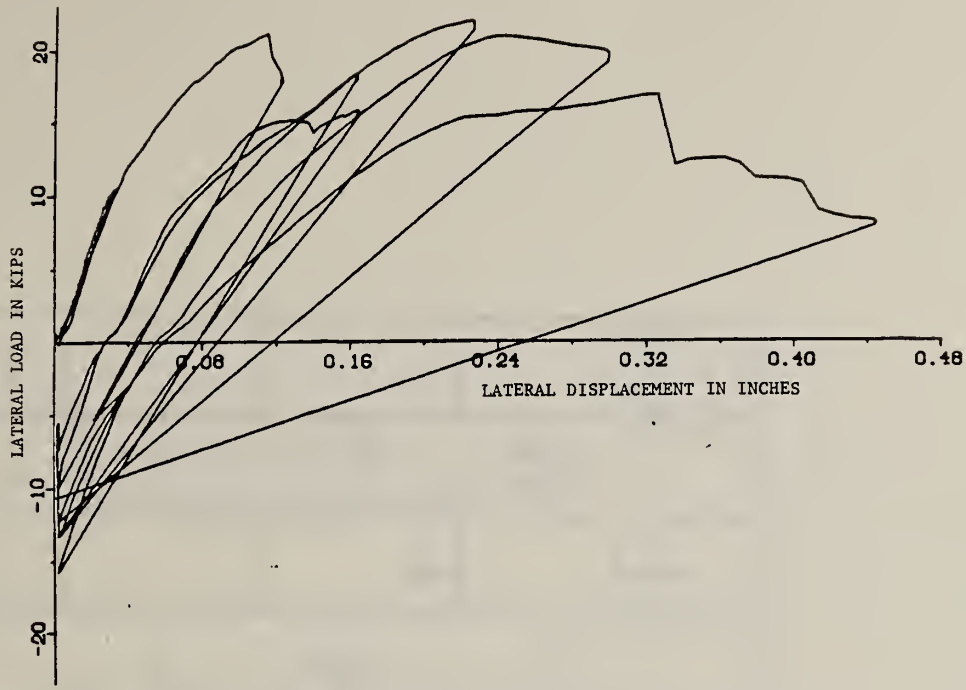

Figure 6.43. Lateral load versus piston displacement for wall P2

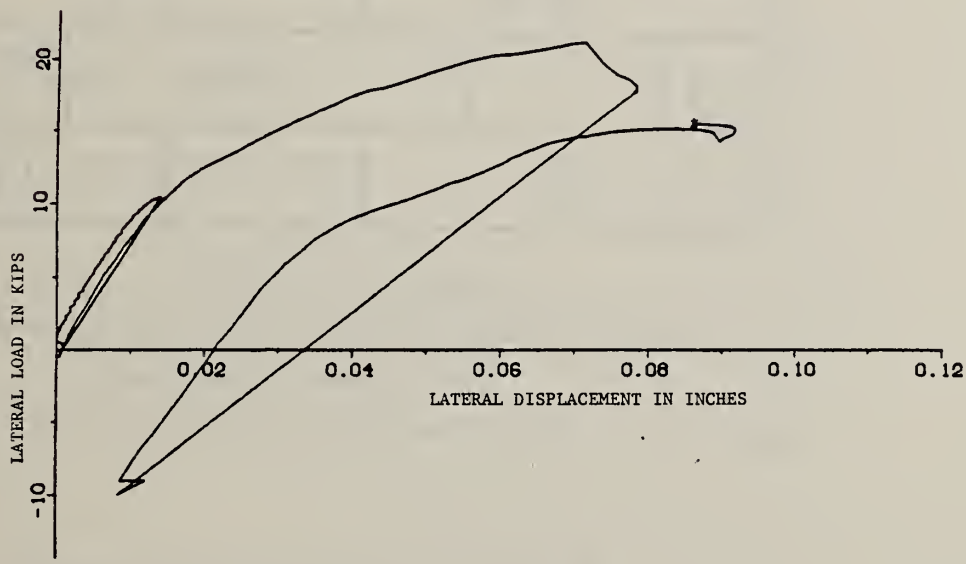

Figure 6.44. Lateral load versus wall displacement for wall P2

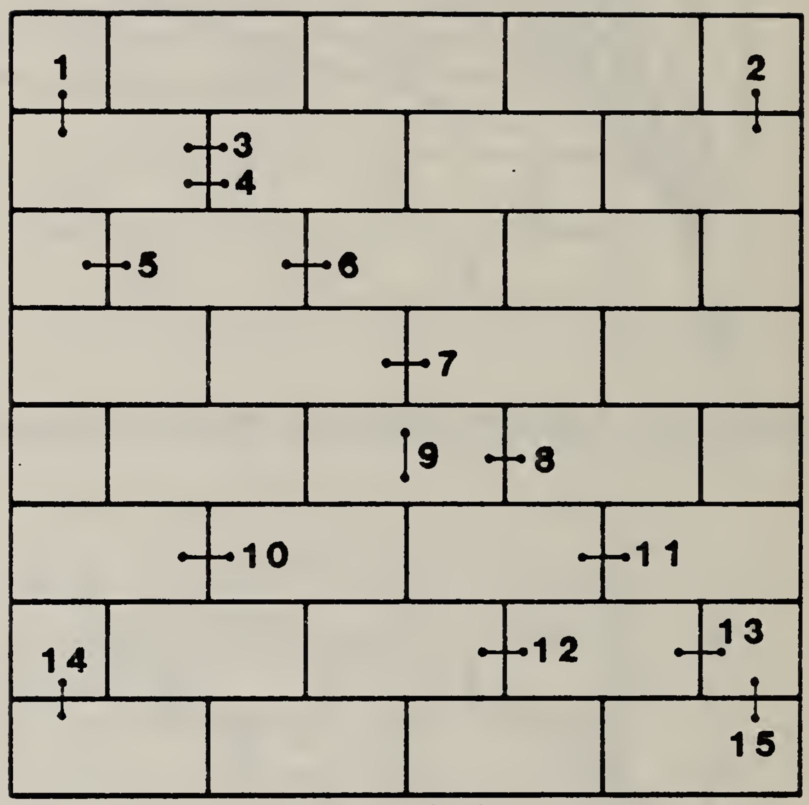

Looking to the south.

Figure 6.45. Strain measuring locations for wall P2

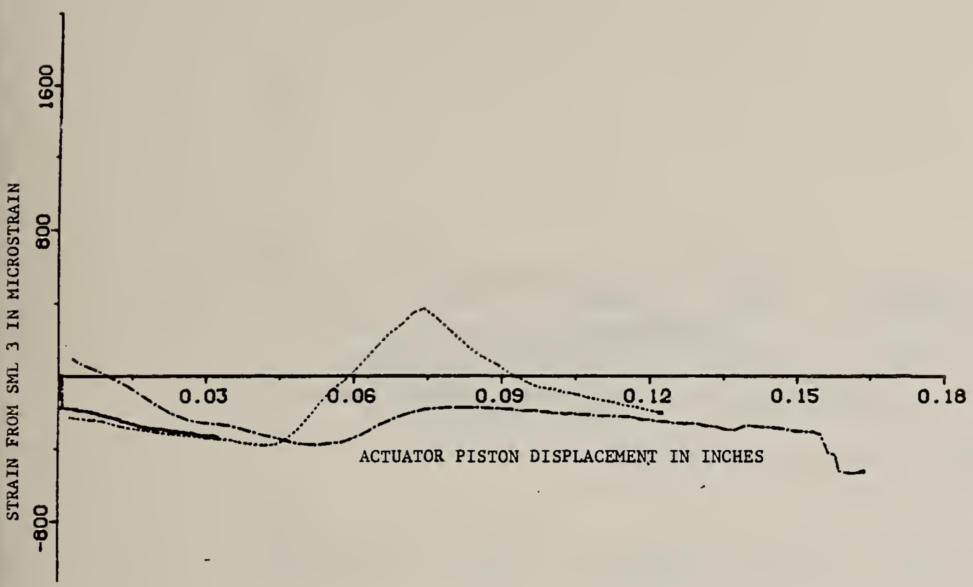

Figure 6.46. Strain history of SML 3 for wall P2

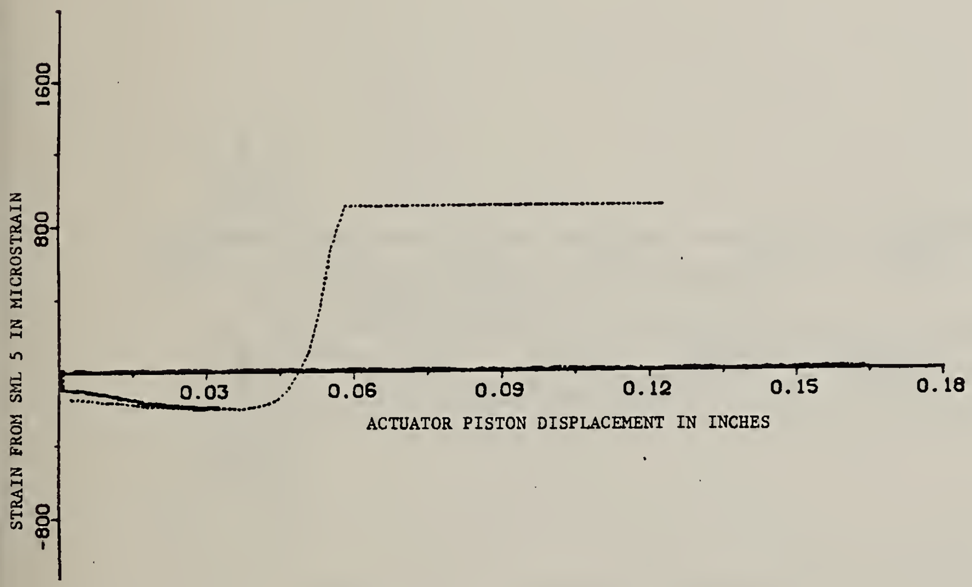

Figure 6.47. Strain history of SML 5 for wall P2

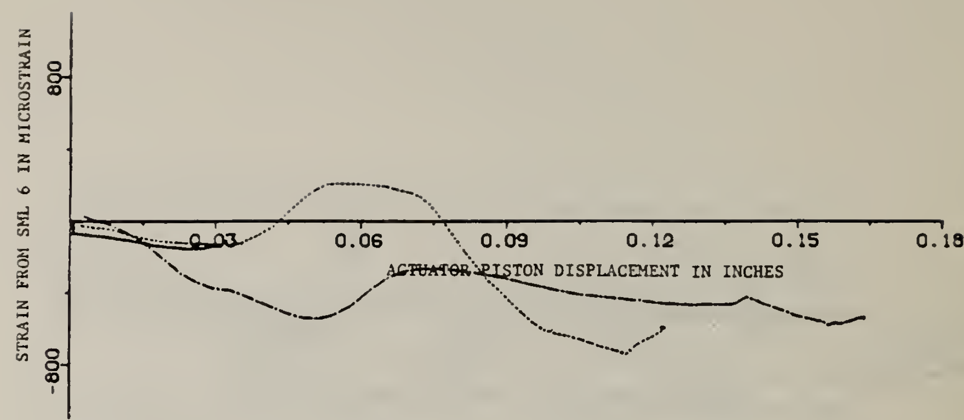

Figure 6.48. Strain history of SML 6 for wall P2

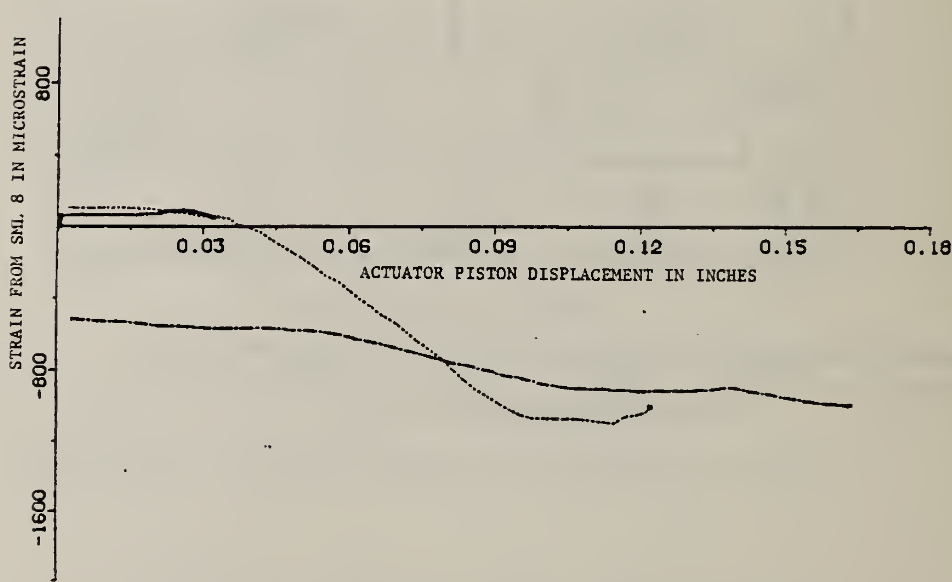

Figure 6.49. Strain history of SML 8 for wall P2

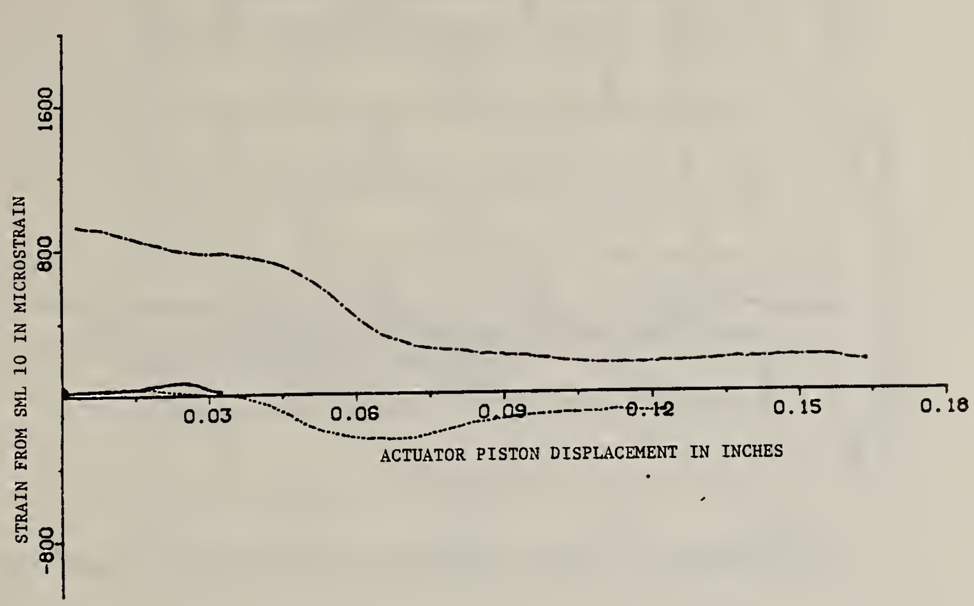

Figure 6.50. Strain history of SML 10 for wall P2

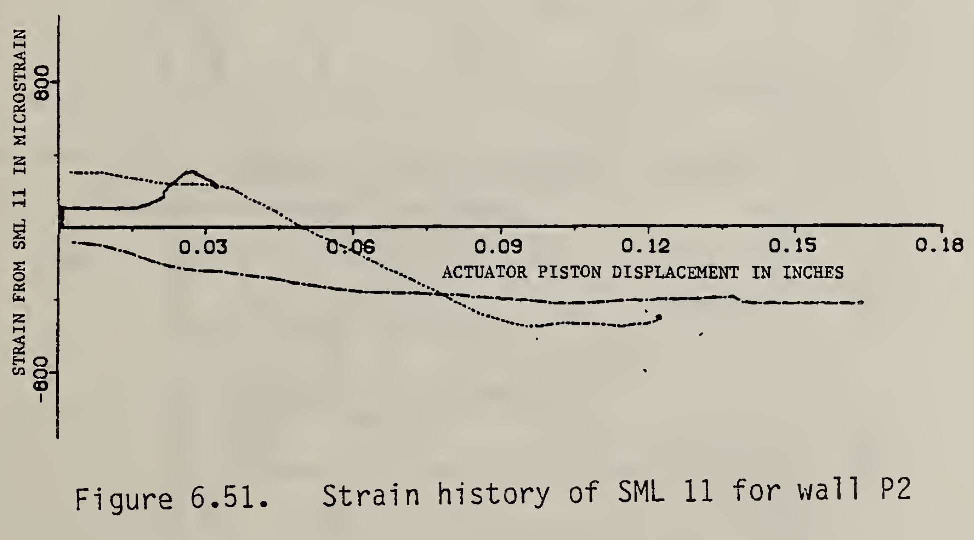

Figure 6.51. Strain history of SML 11 for wall P2

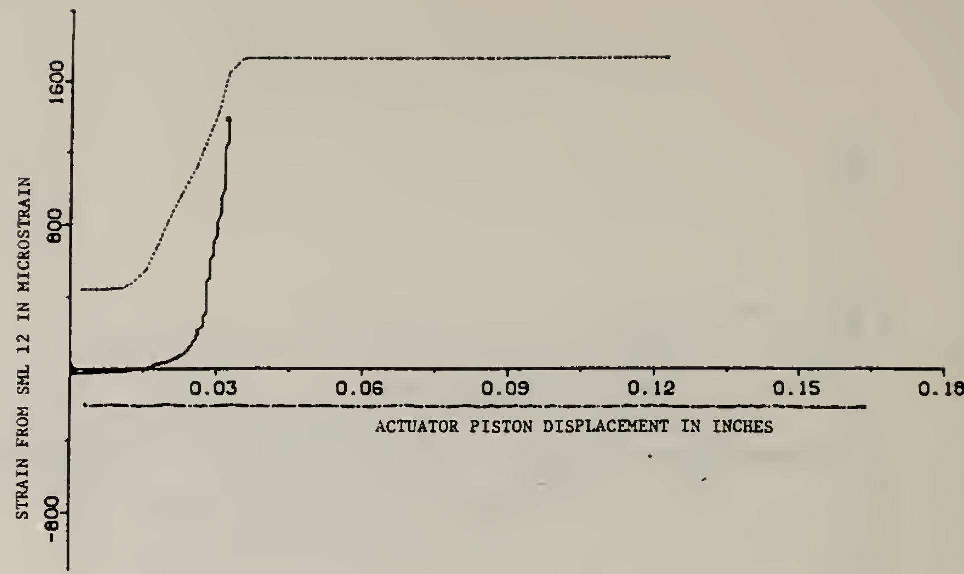

Figure 6.52. Strain history of SML 12 for wall P2

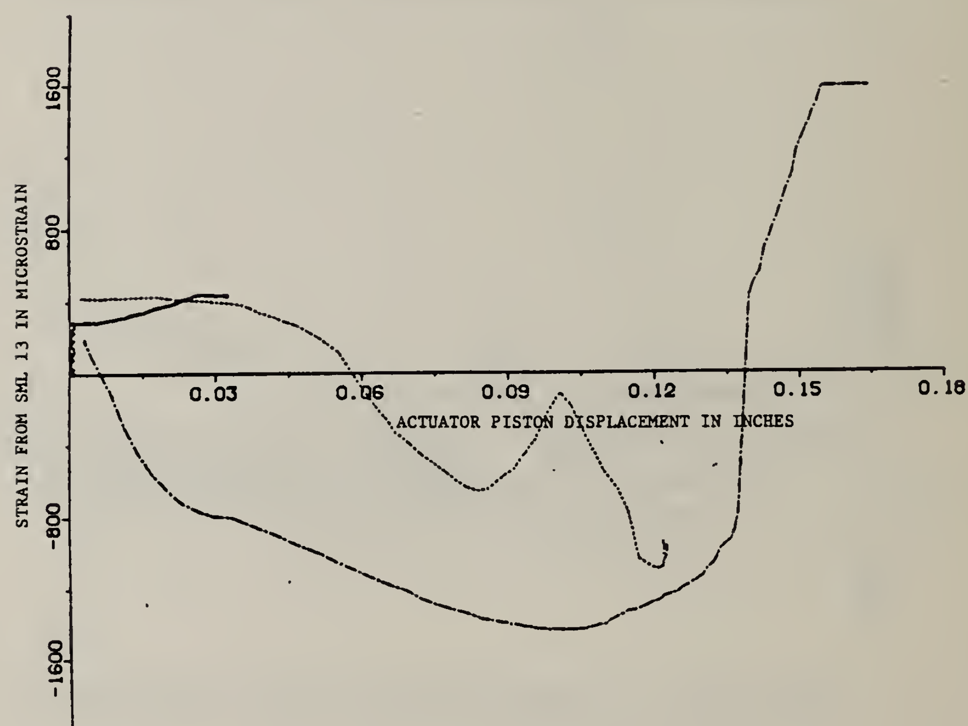

Figure 6.53. Strain history of SML 13 for wall P2

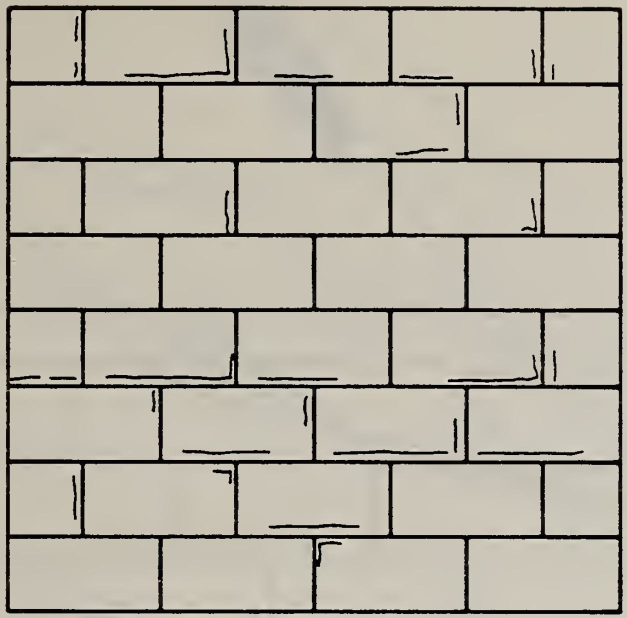

Figure 6.54. Pre-test crack observations for wall P2

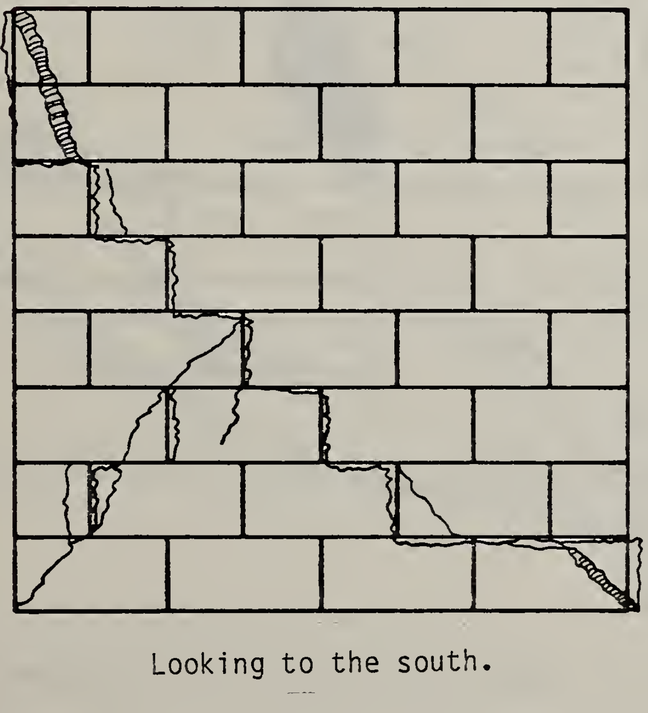

Looking to the south.

Figure 6.55. Post-test crack observations for wall P2

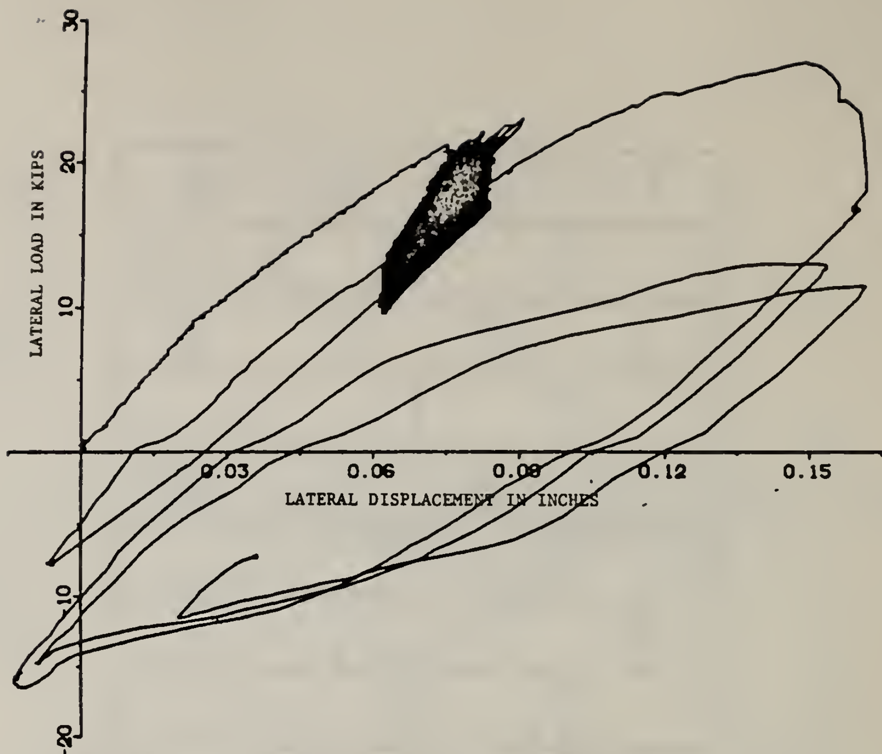

Figure 6.56. Lateral load versus piston displacement for wall P5

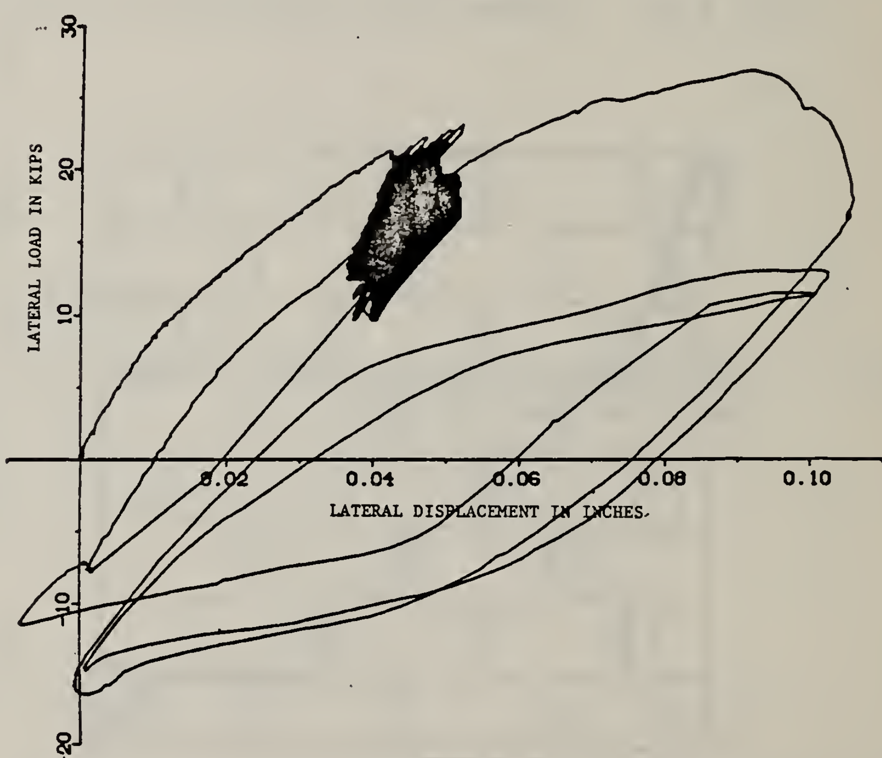

Figure 6.57. Lateral load versus wall displacement for wall P5

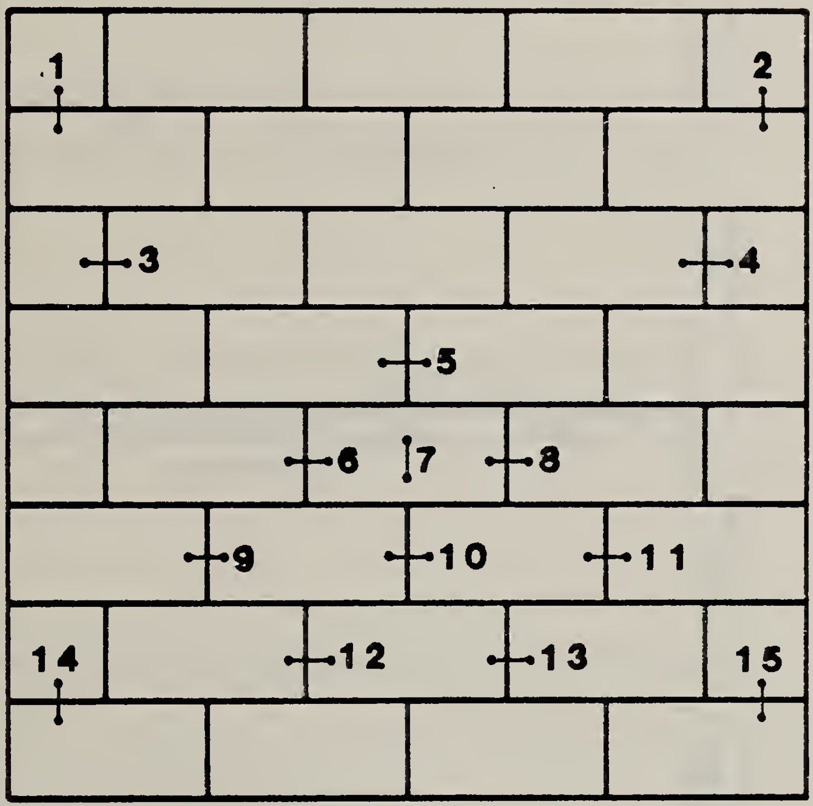

Looking to the south.

Figure 6.58. Strain measuring locations for wall P5

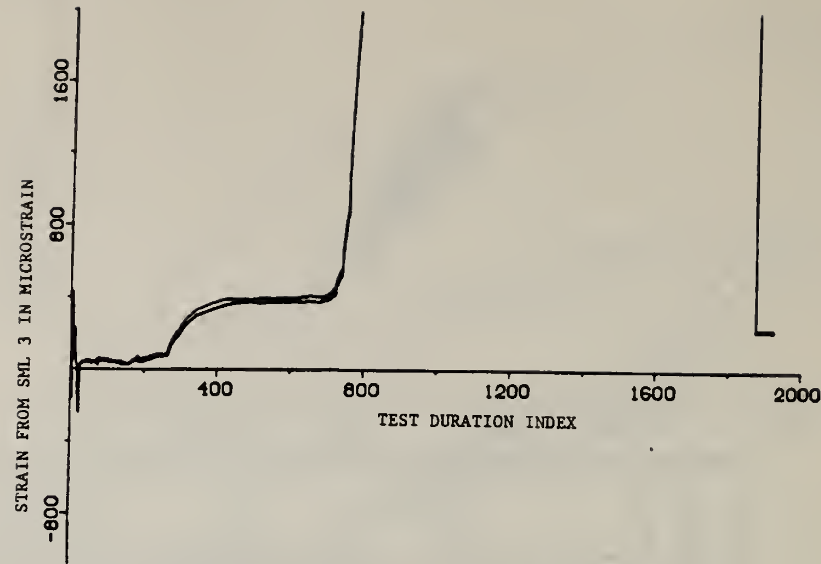

Figure 6.59. Strain history of SML 3 for wall P5

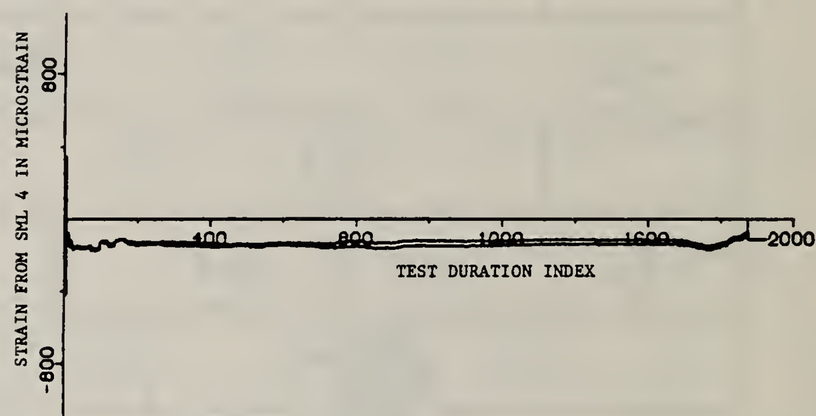

Figure 6.60. Strain history of SML 4 for wall P5

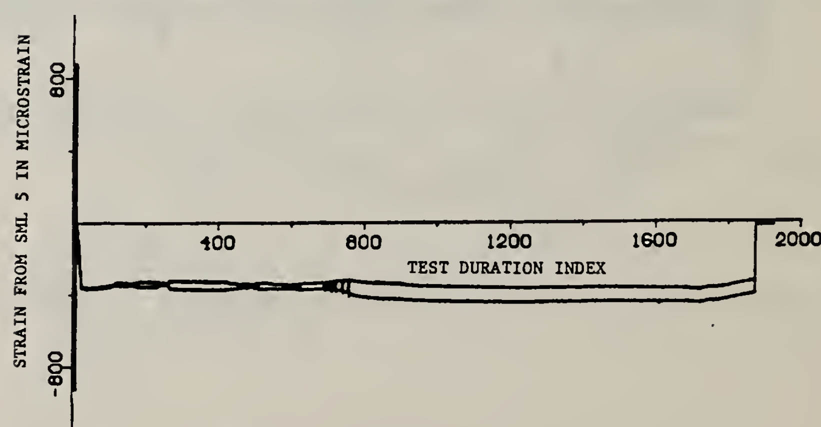

Figure 6.61. Strain history of SML 5 for wall P5

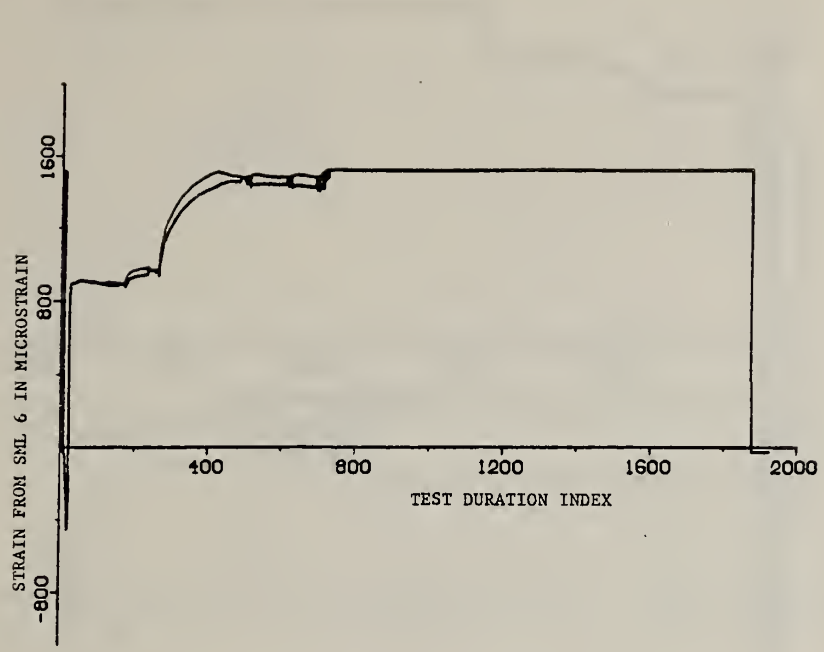

Figure 6.62. Strain history of SML 6 for wall P5

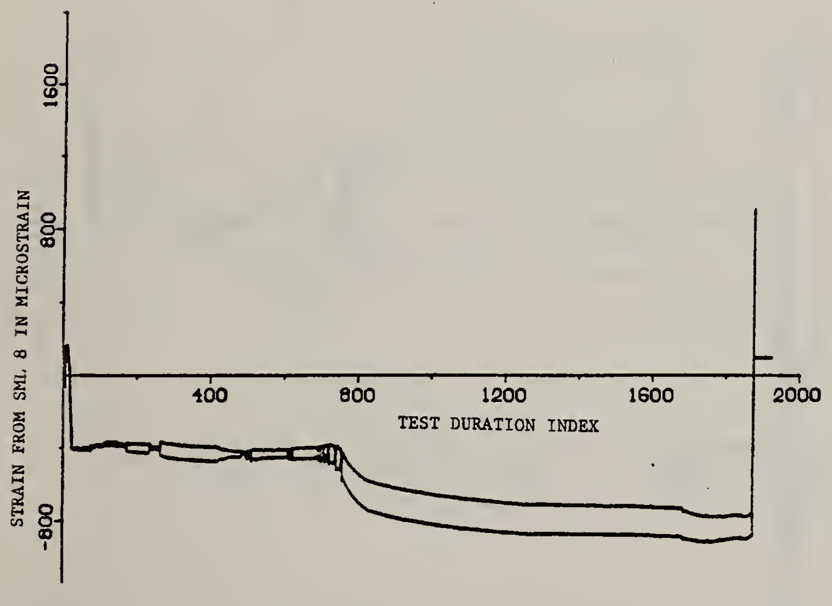

Figure 6.63. Strain history of SML 8 for wall P5

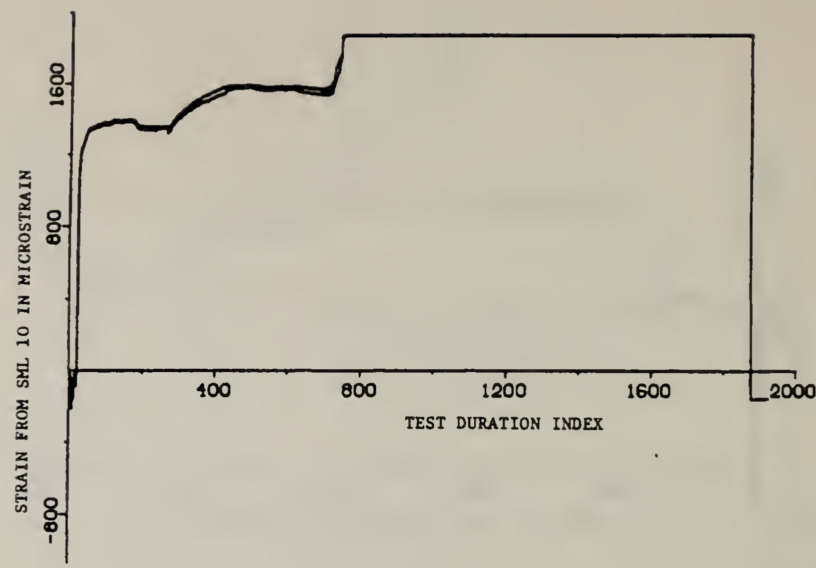

Figure 6.64. Strain history of SML 10 for wall P5

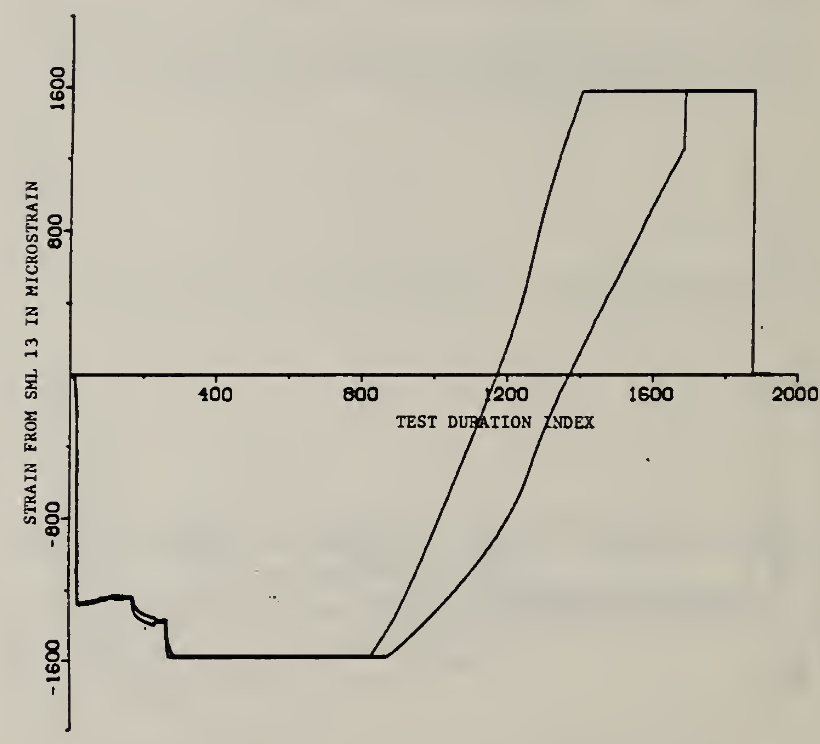

Figure 6.65. Strain history of SML 13 for wall P5

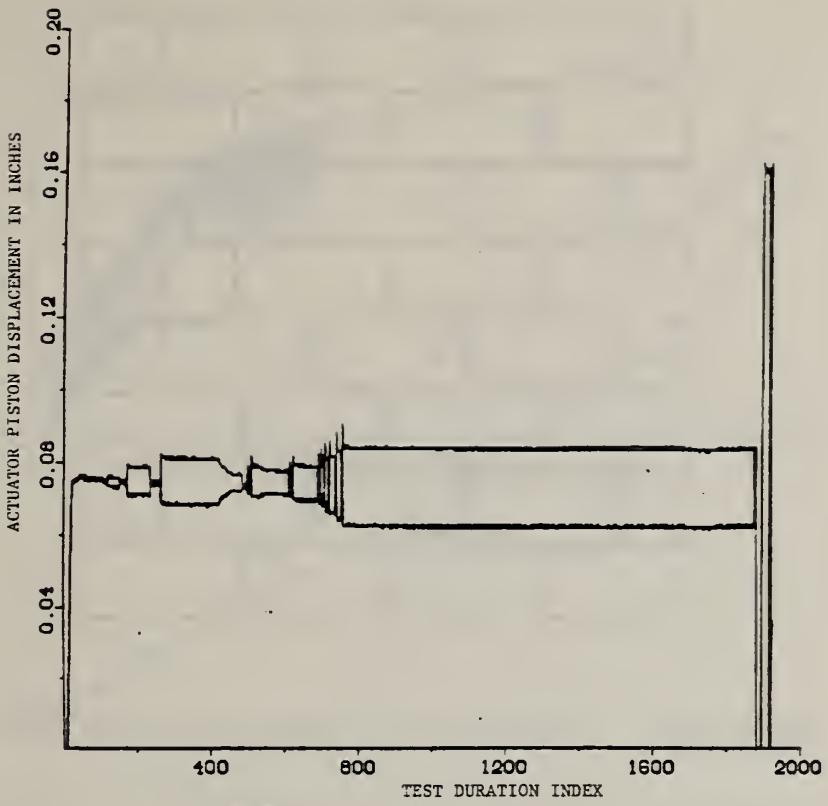

Figure 6.66. Piston displacement history for wall P5

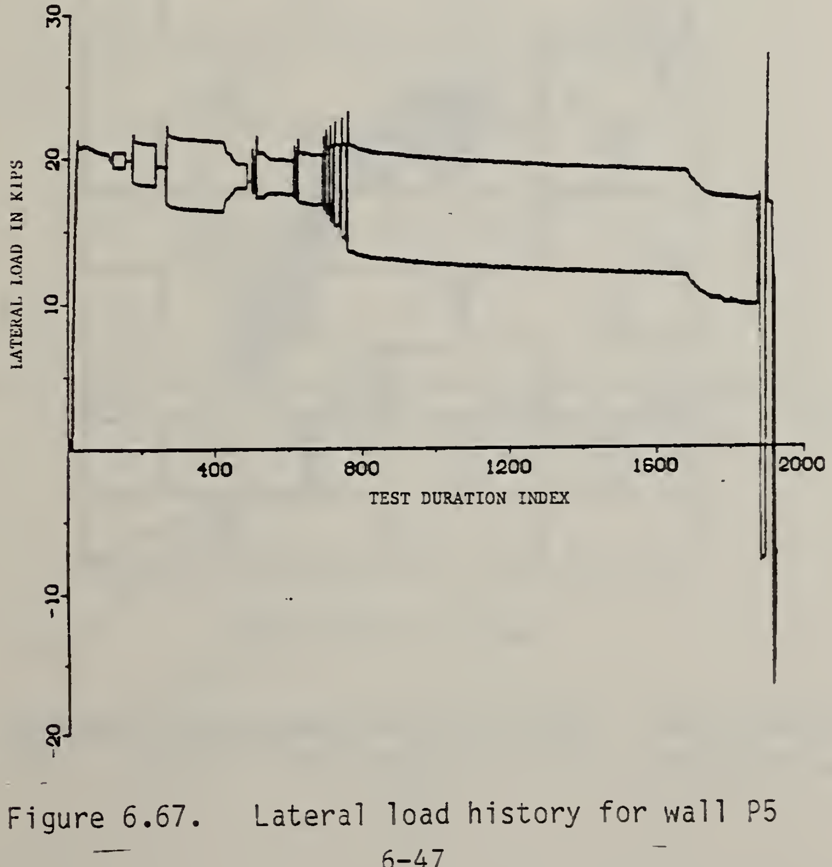

Figure 6.67. Lateral load history for wall P5

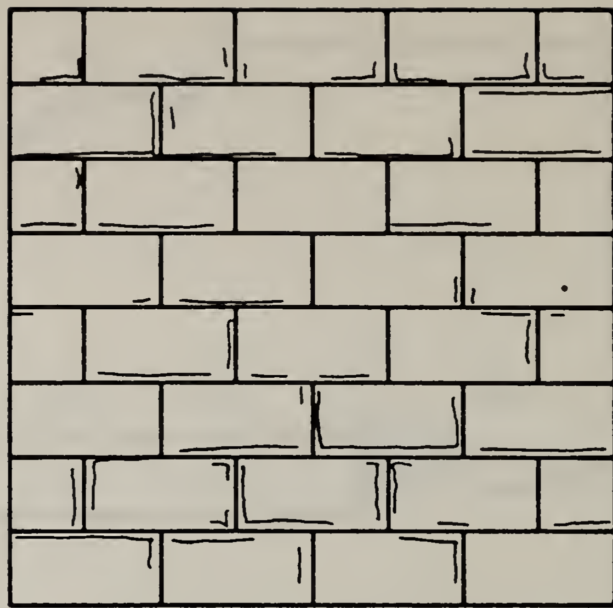

Figure 6.68. Pre-test crack observations for wall P5

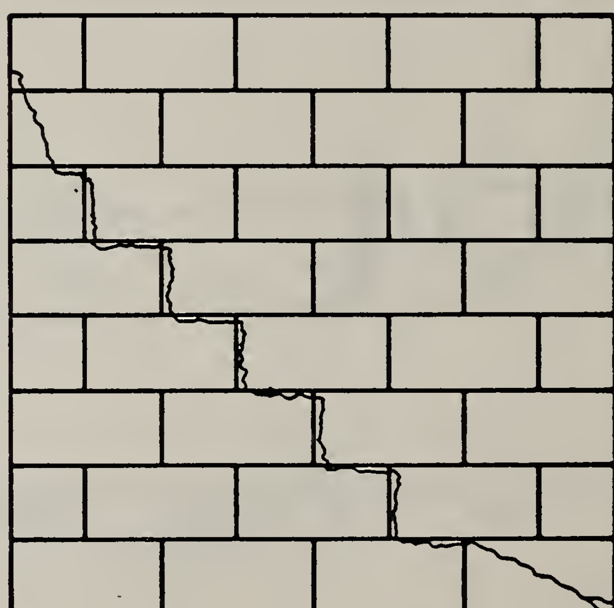

Looking to the south.

Figure 6.69. Post-test crack observations for wall P5

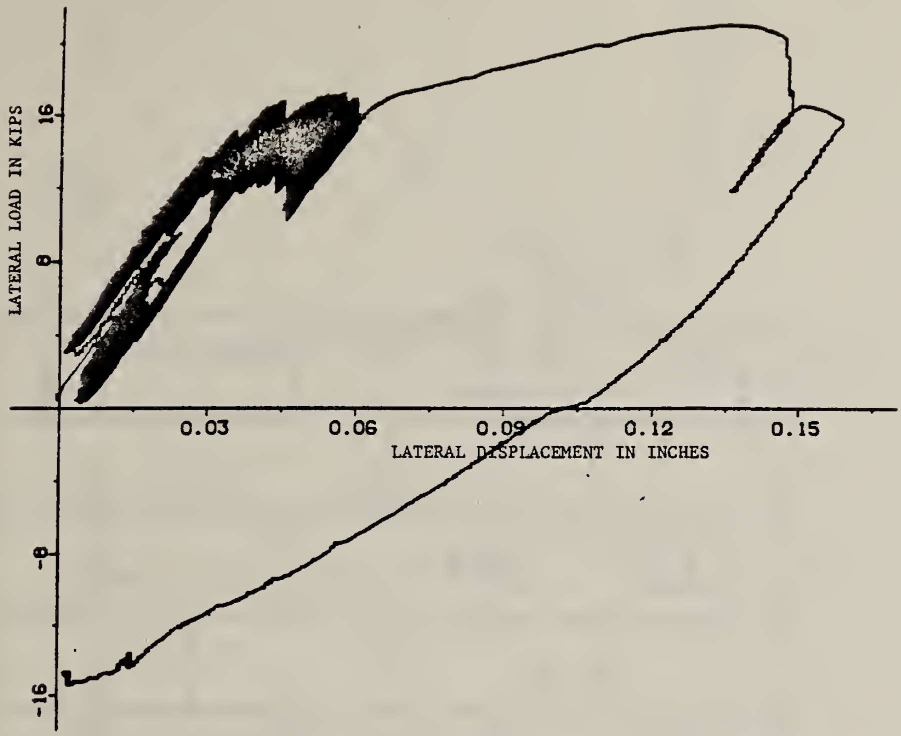

Figure 6.70. Lateral load versus piston displacement for wall P3

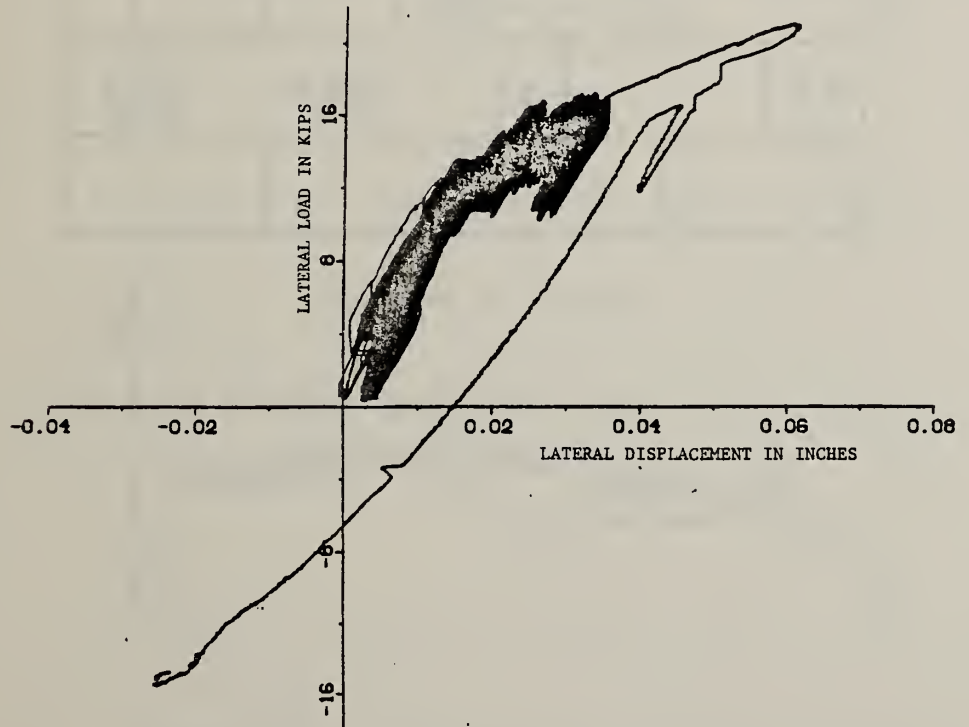

Figure 6.71. Lateral load versus wall displacement for wall P3

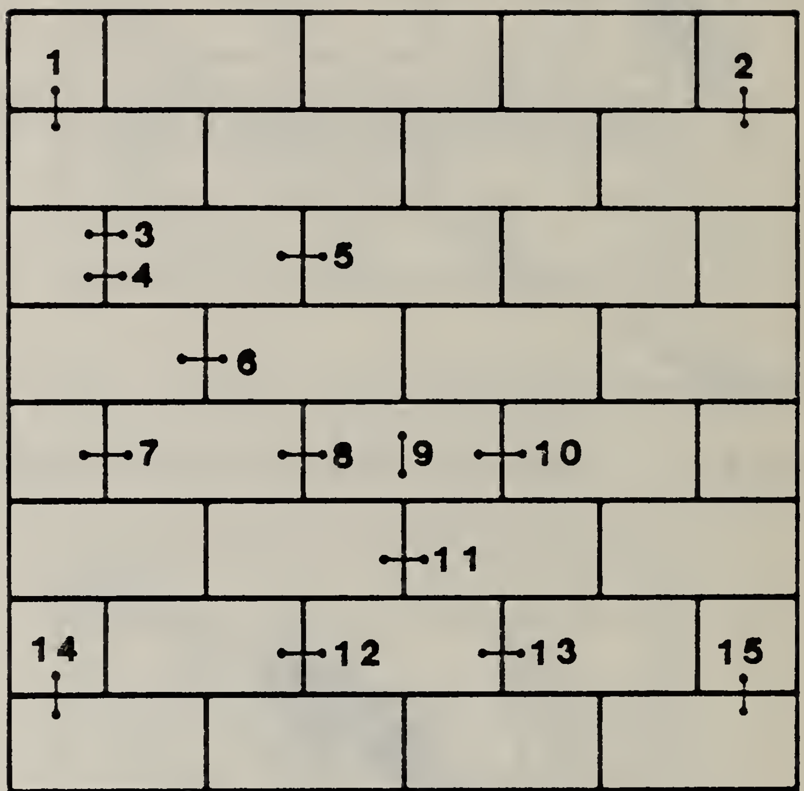

Looking to the south.

Figure 6.72. Strain measuring locations for wall P3

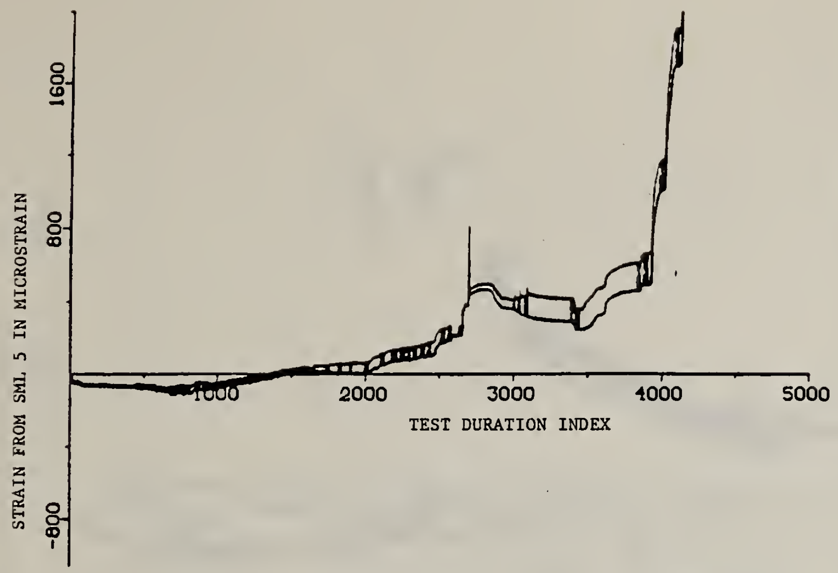

Figure 6.73. Strain history of SML 5 for wall P3

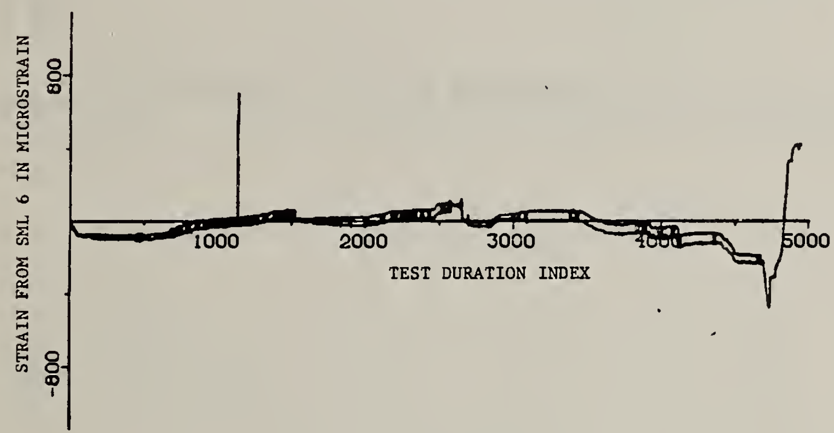

Figure 6.74. Strain history of SML 6 for wall P3

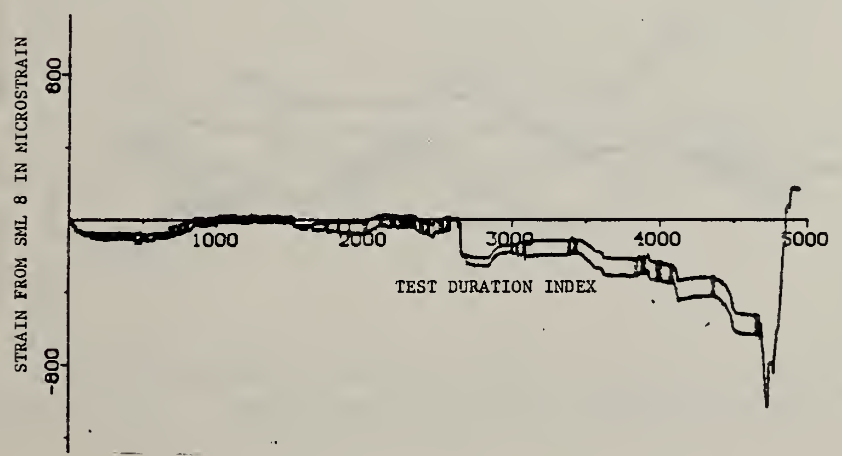

Figure 6.75. Strain history of SML 8 for wall P3

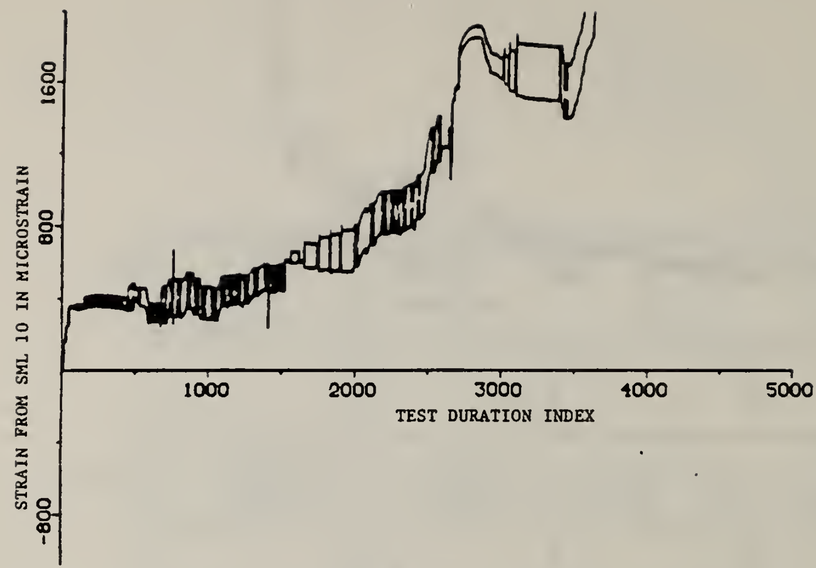

Figure 6.76. Strain history of SML 10 for wall P3

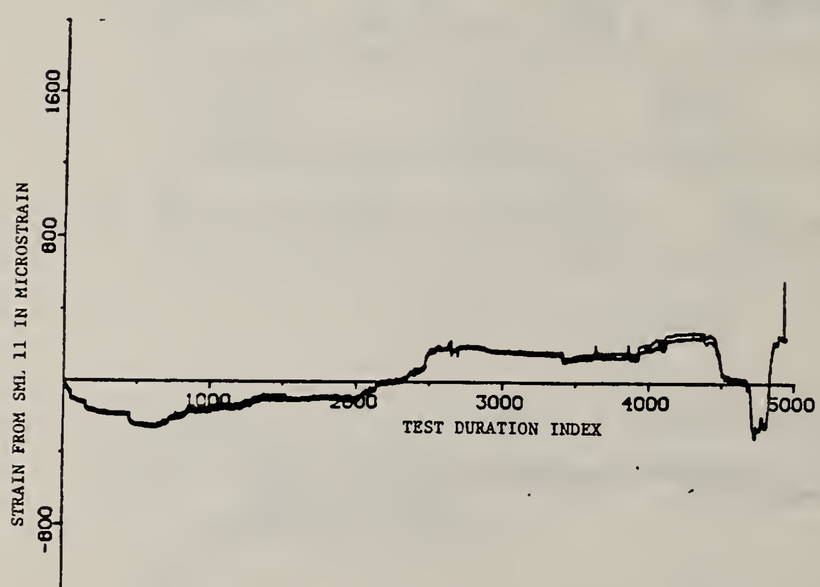

Figure 6.77. Strain history of SML 11 for wall P3

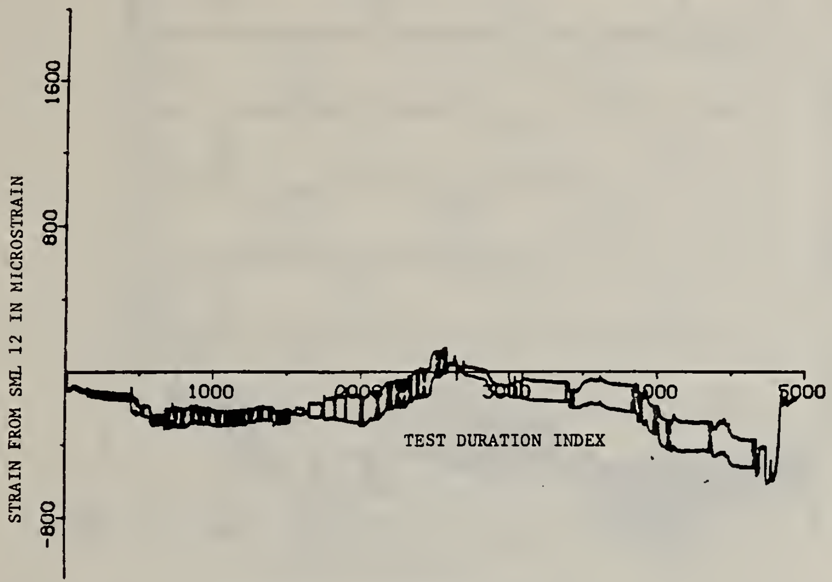

Figure 6.78. Strain history of SML 12 for wall P3

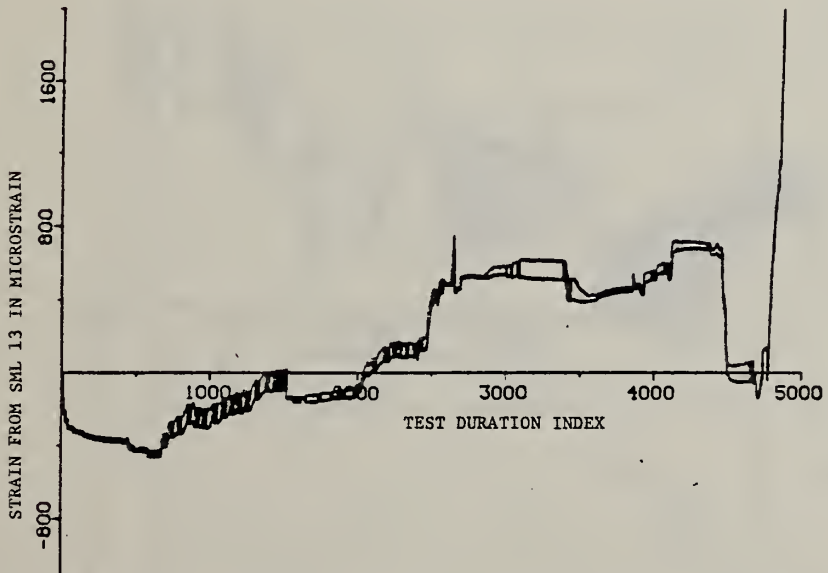

Figure 6.79. Strain history of SML 13 for wall P3

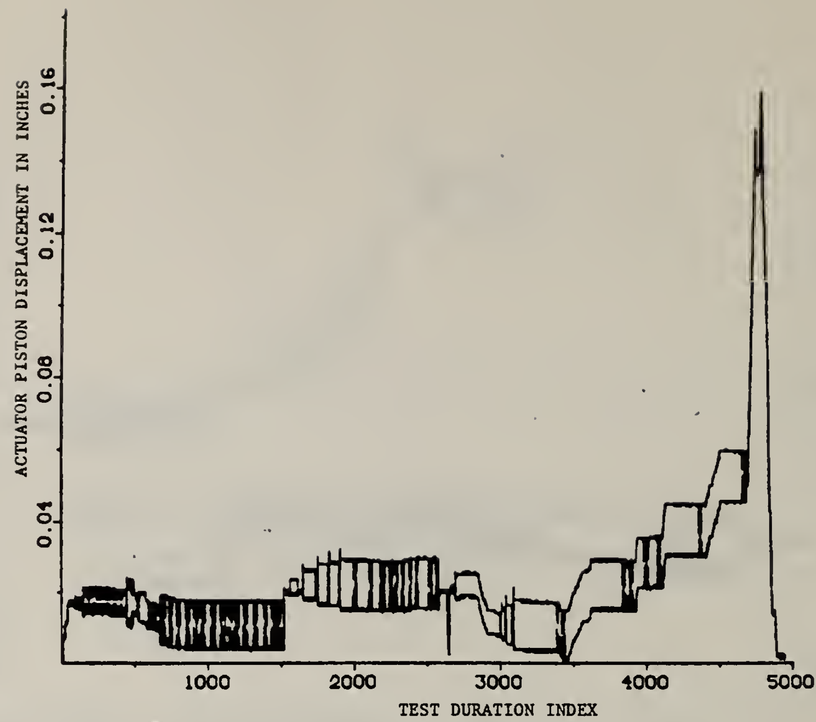

Figure 6.80. Piston displacement history for wall P3

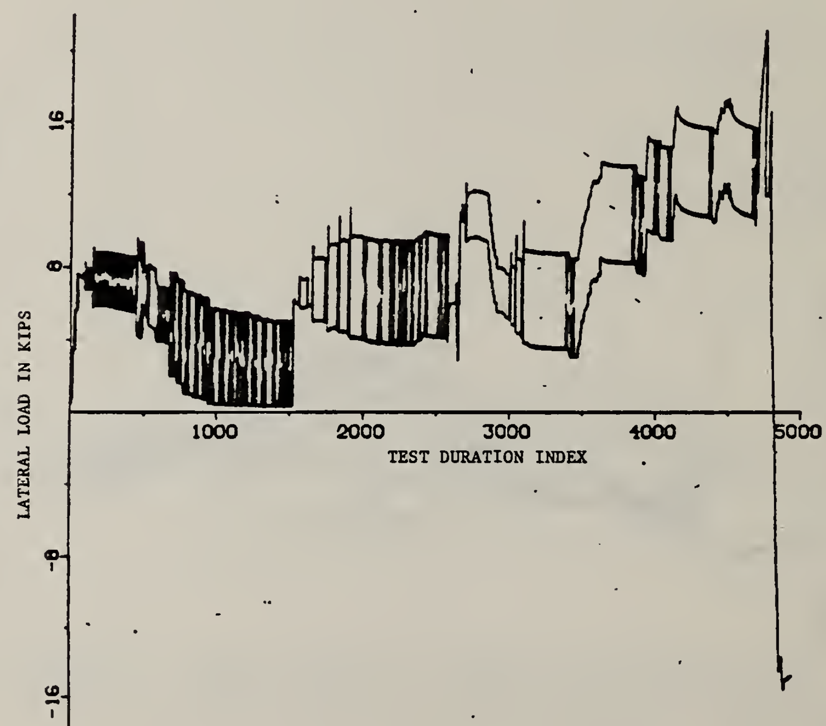

Figure 6.81. Lateral load history for wall P3

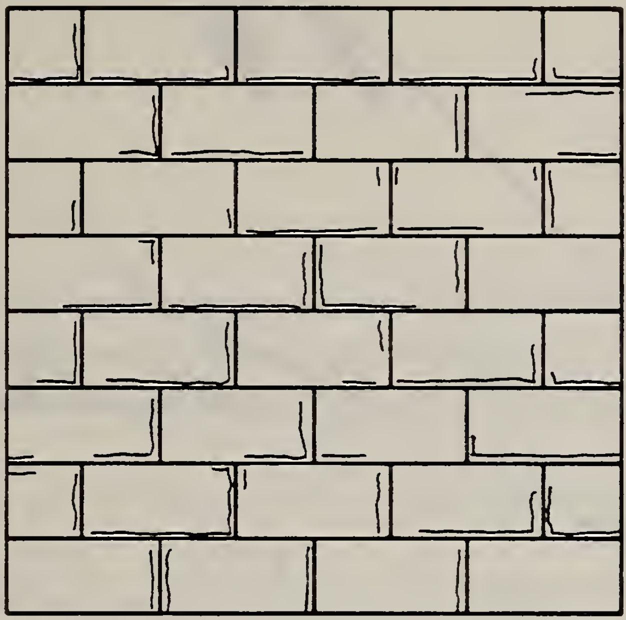

Figure 6.82. Pre-test crack observations for wall P3

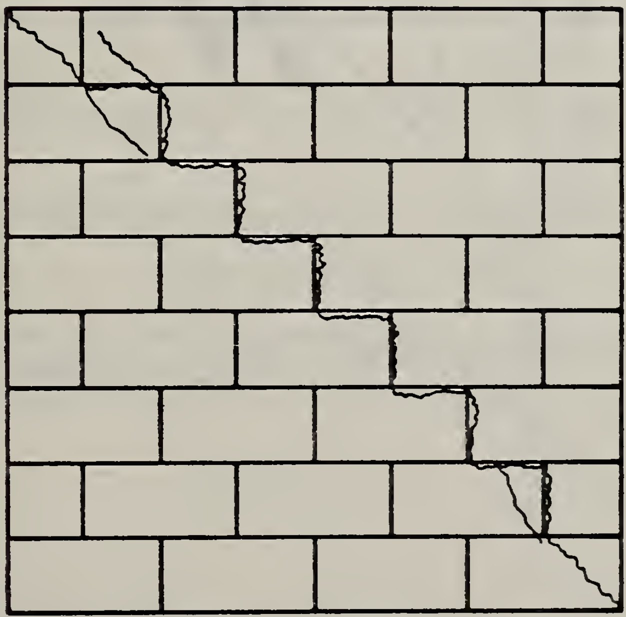

Looking to the south.

Figure 6.83. Post-test crack observations for wall P3

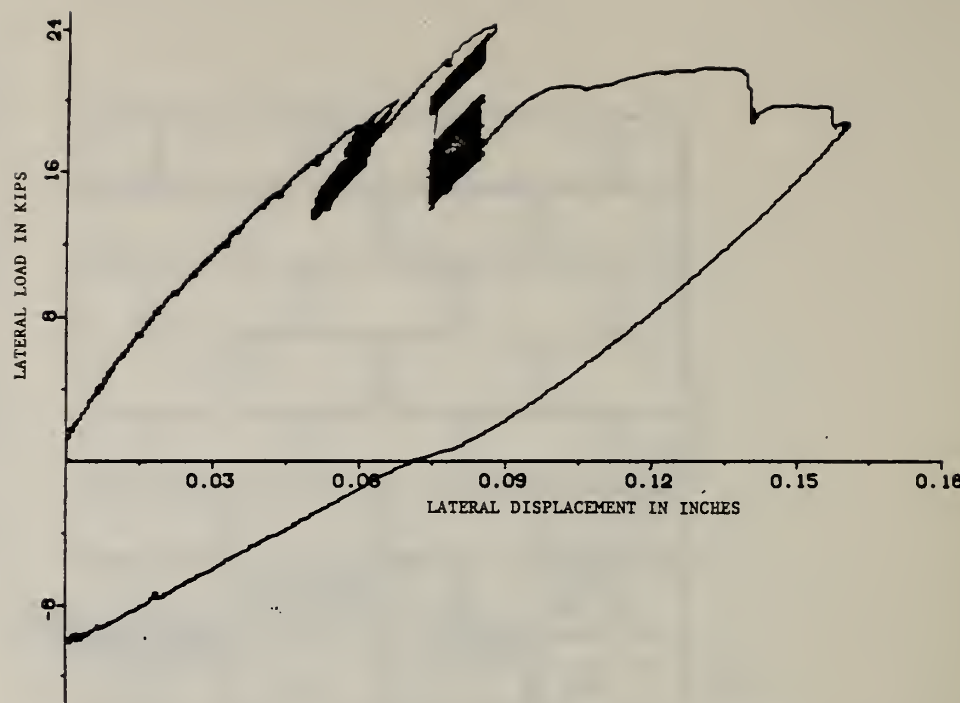

Figure 6.84. Lateral load versus piston displacement for wall P1

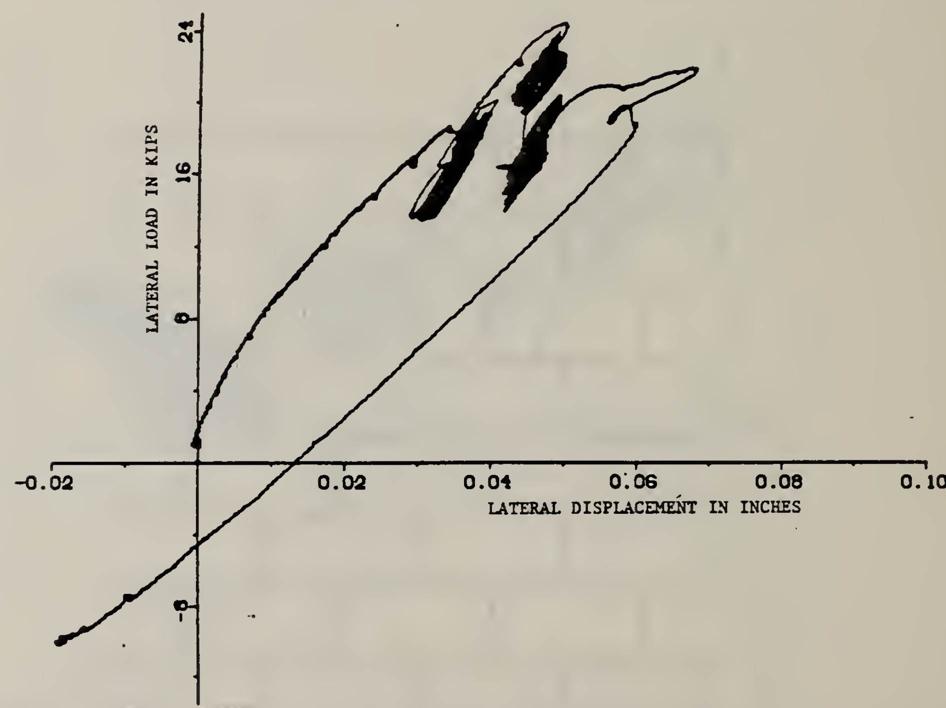

Figure 6.85. Lateral load versus wall displacement for wall P1

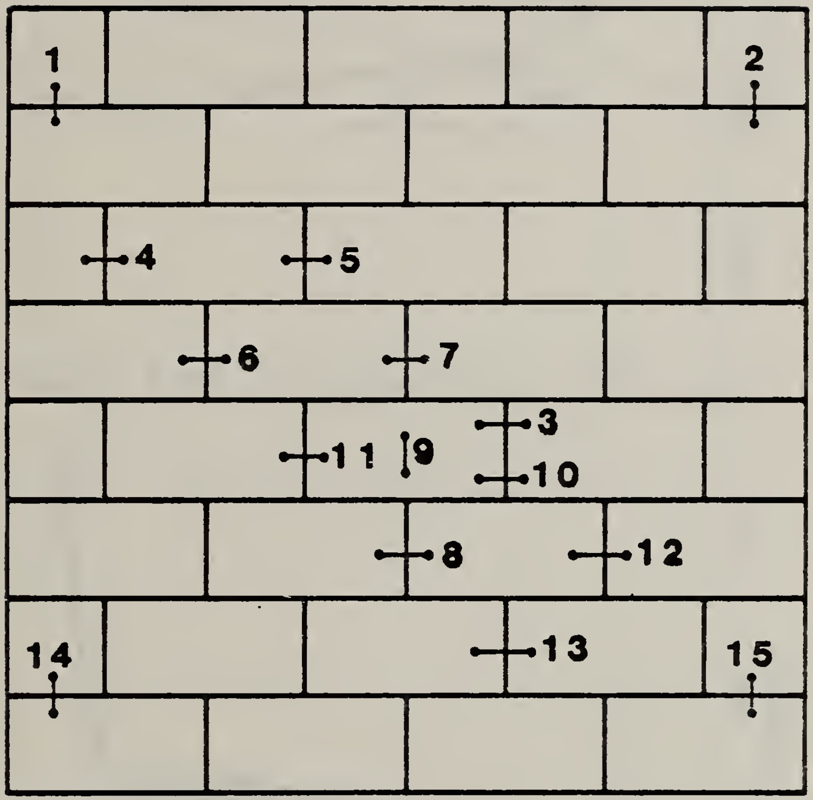

Looking to the south.

Figure 6.86. Strain measuring locations for wall P1

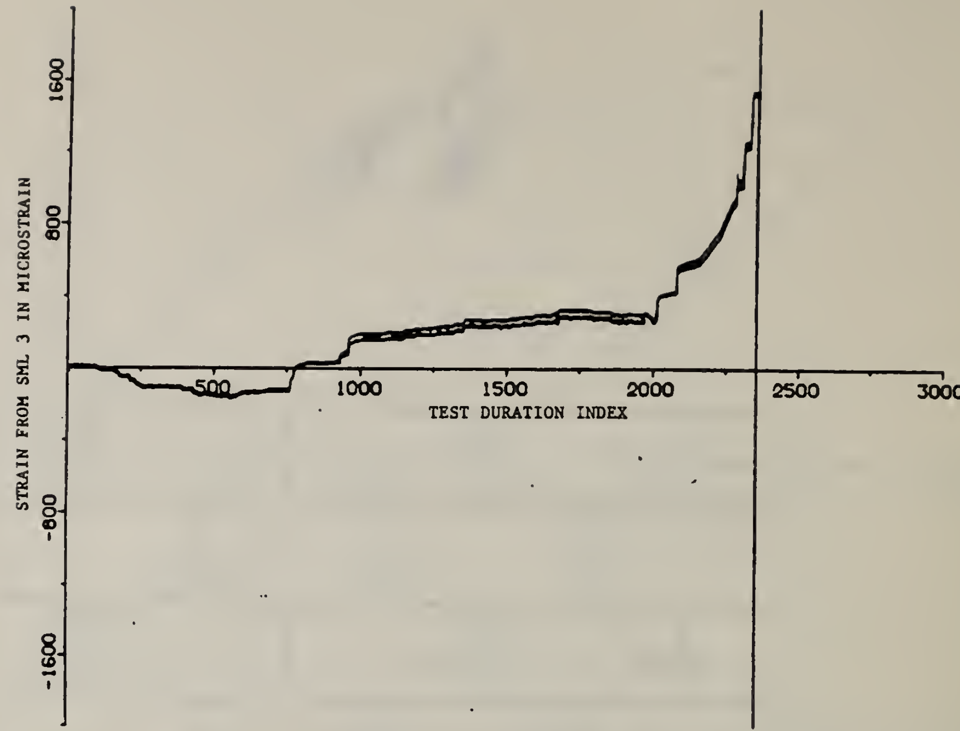

Figure 6.87. Strain history of SML 3 for wall P1

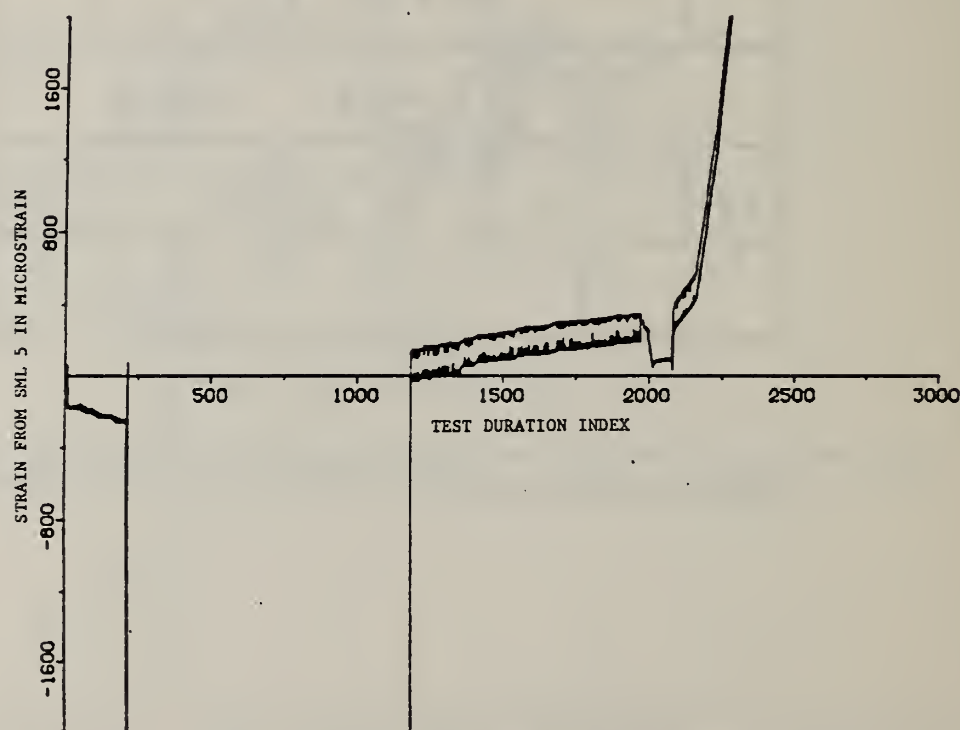

Figure 6.88. Strain history of SML 5 for wall P1

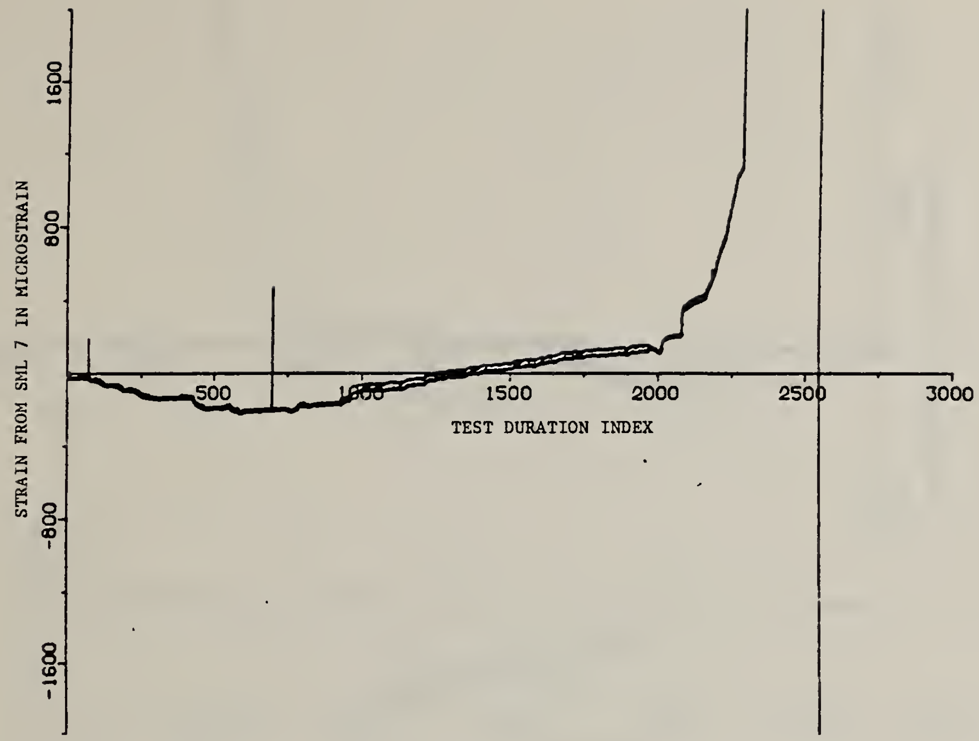

Figure 6.89. Strain history of SML 7 for wall P1

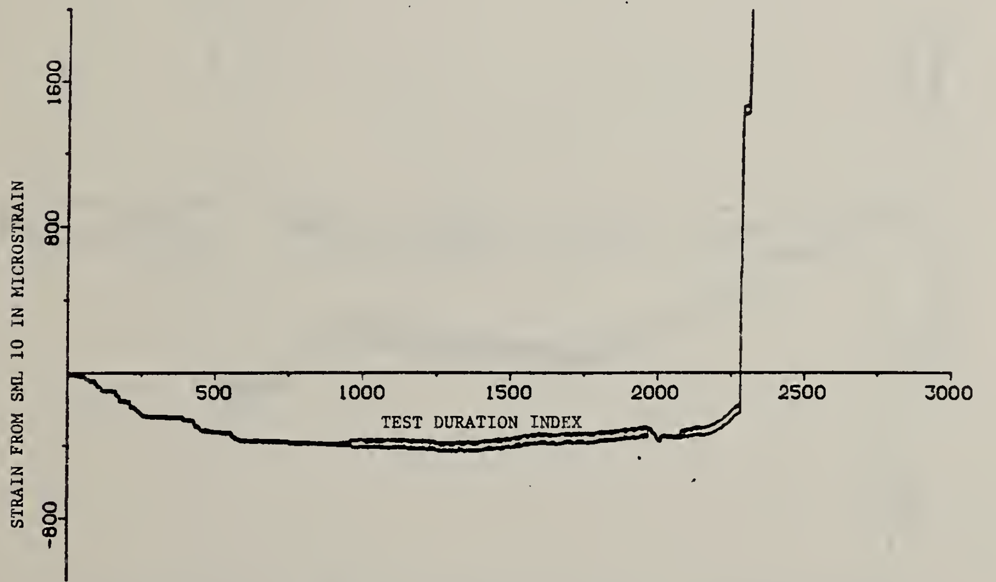

Figure 6.90. Strain history of SML 10 for wall P1

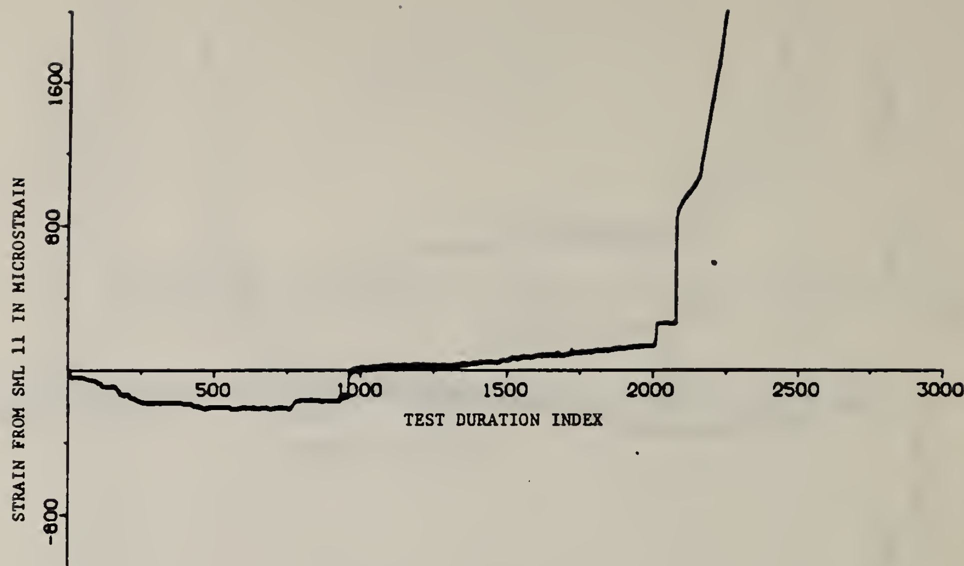

Figure 6.91. Strain history of SML 11 for wall P1

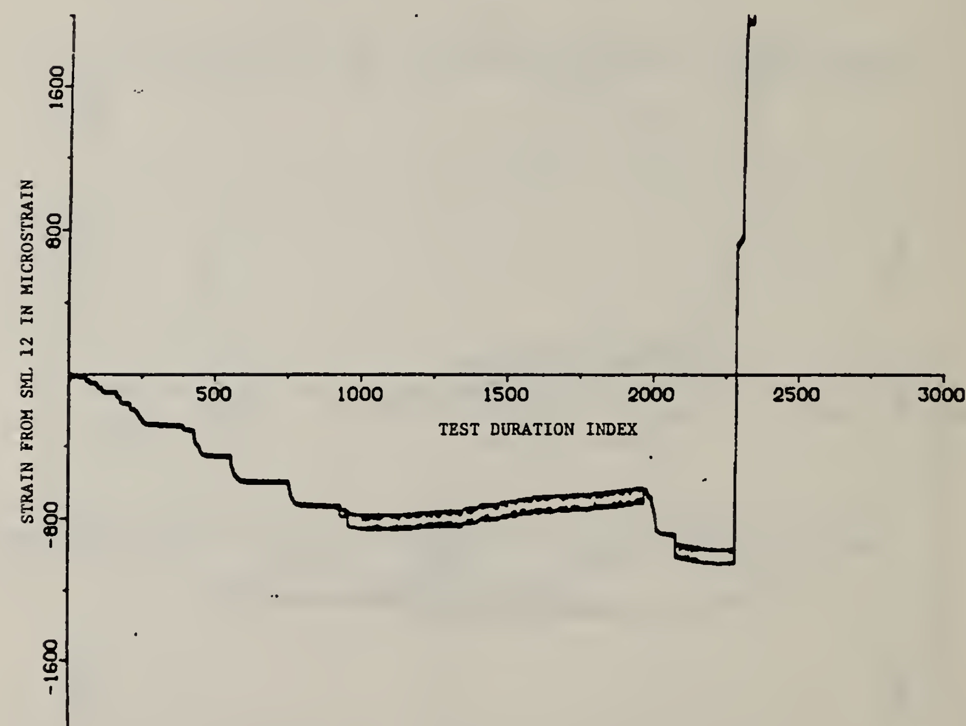

Figure 6.92. Strain history of SML 12 for wall P1

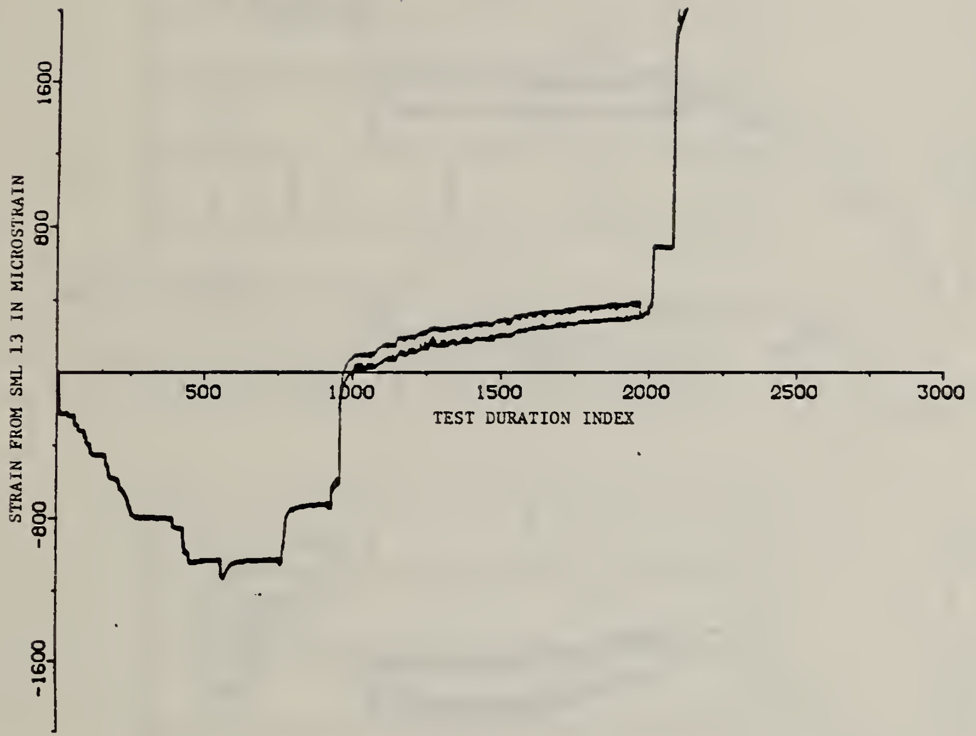

Figure 6.93. Strain history of SML 13 for wall P1

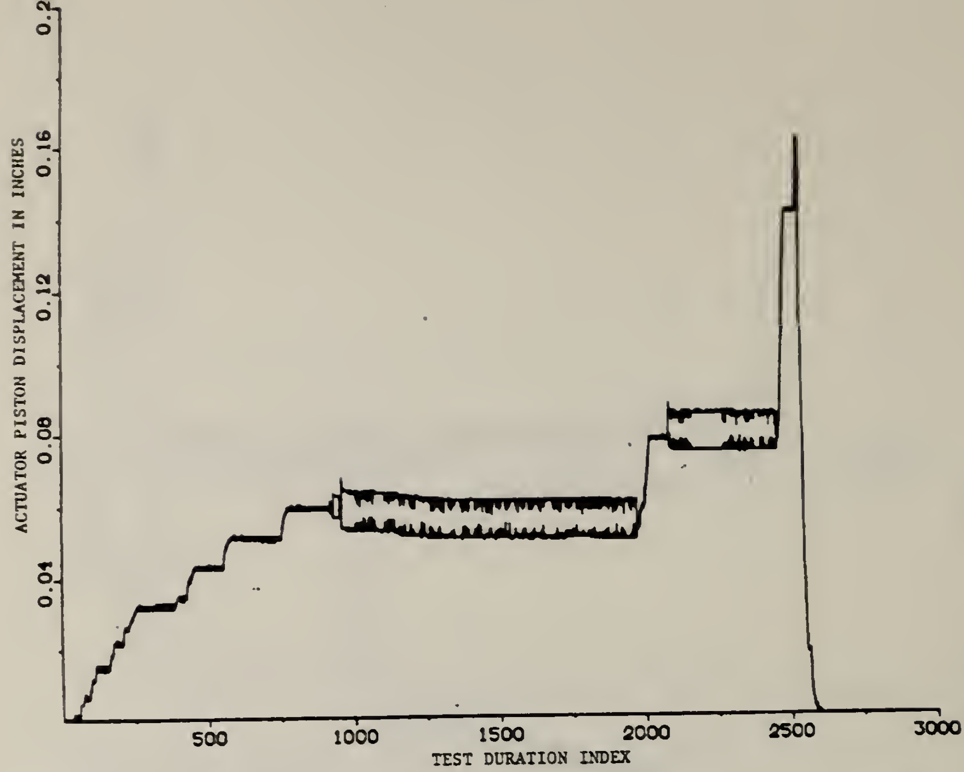

Figure 6.94. Piston displacement history for wall P1

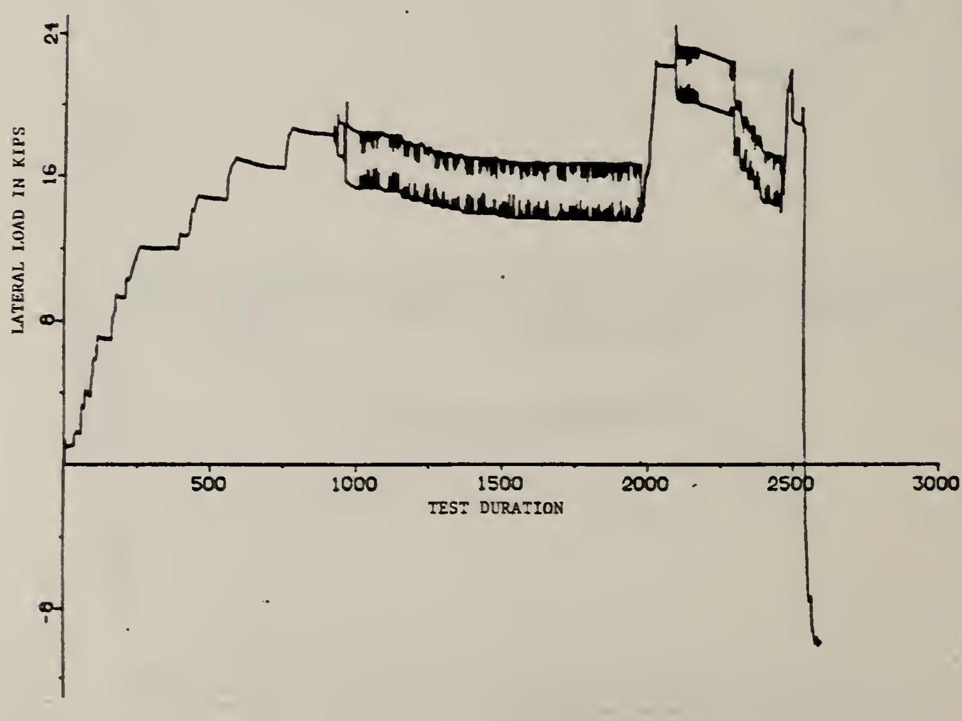

Figure 6.95. Lateral load history for wall P1

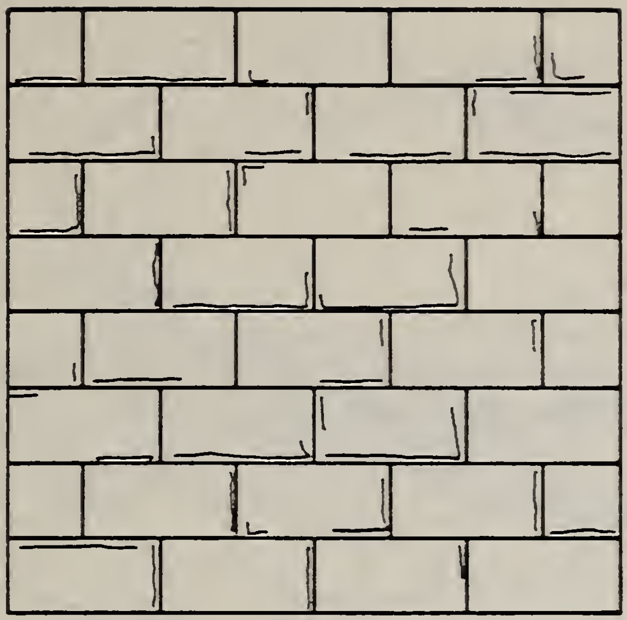

Figure 6.96. Pre-test crack observations for wall P1

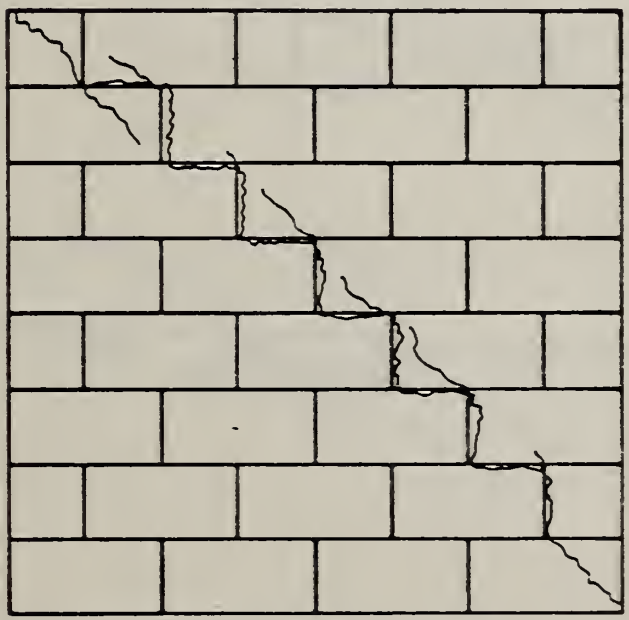

Looking to the south.

Figure 6.97. Post-test crack observations for wall P1

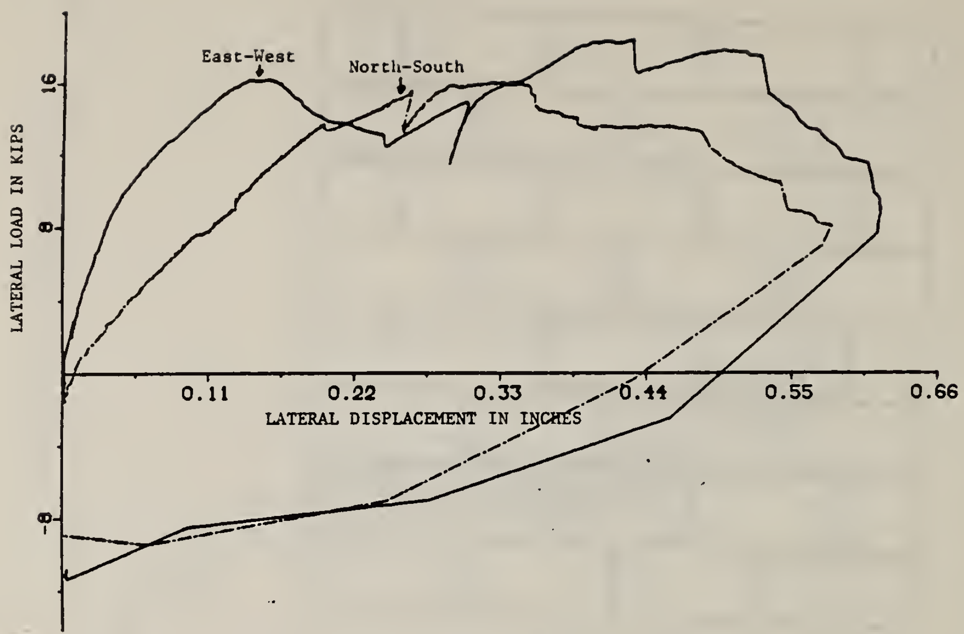

Figure 6.98. Lateral load versus piston displacement for wall C5

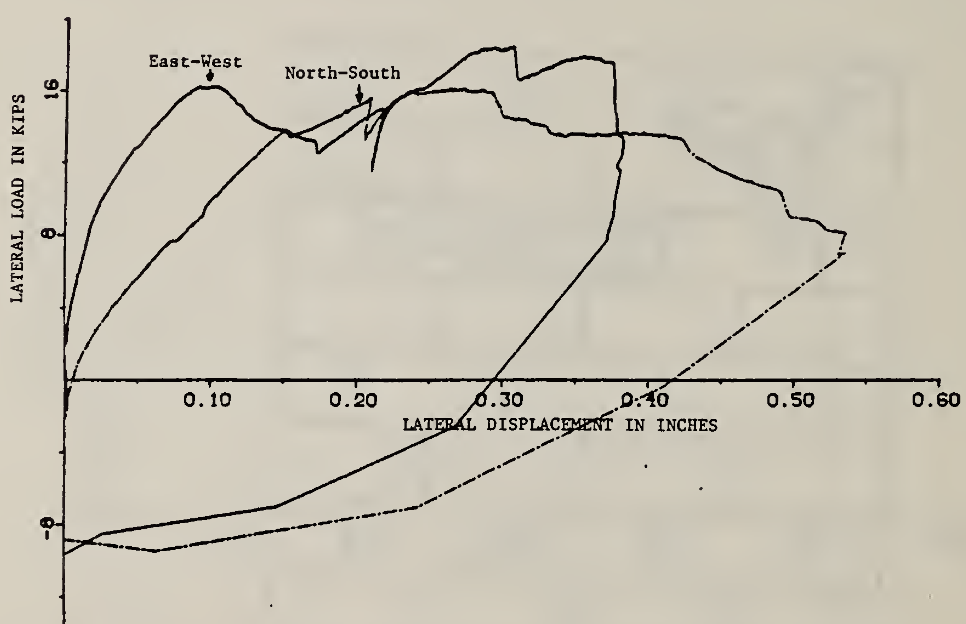

Figure 6.99. Lateral load versus wall displacement for wall C5

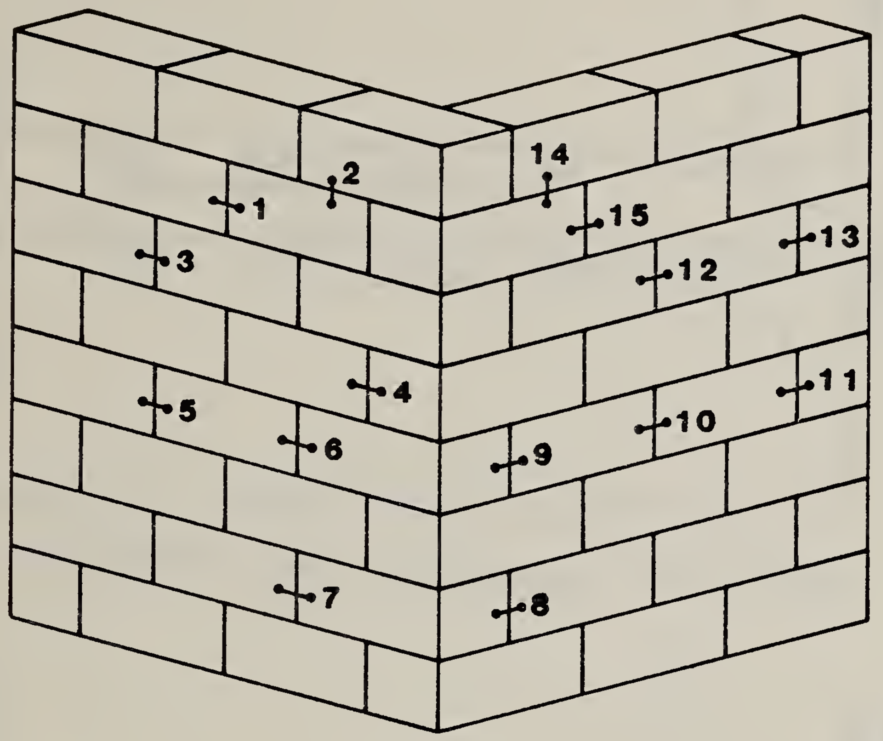

Figure 6.100. Strain measuring locations for wall C5

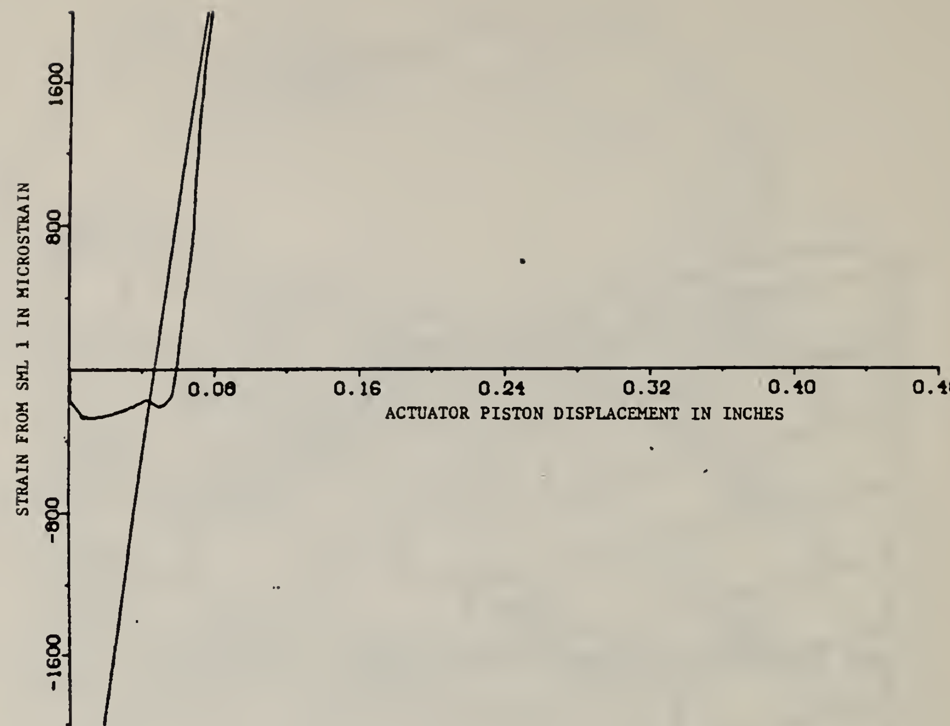

Figure 6.101. Strain history of SML 1 for wall C5

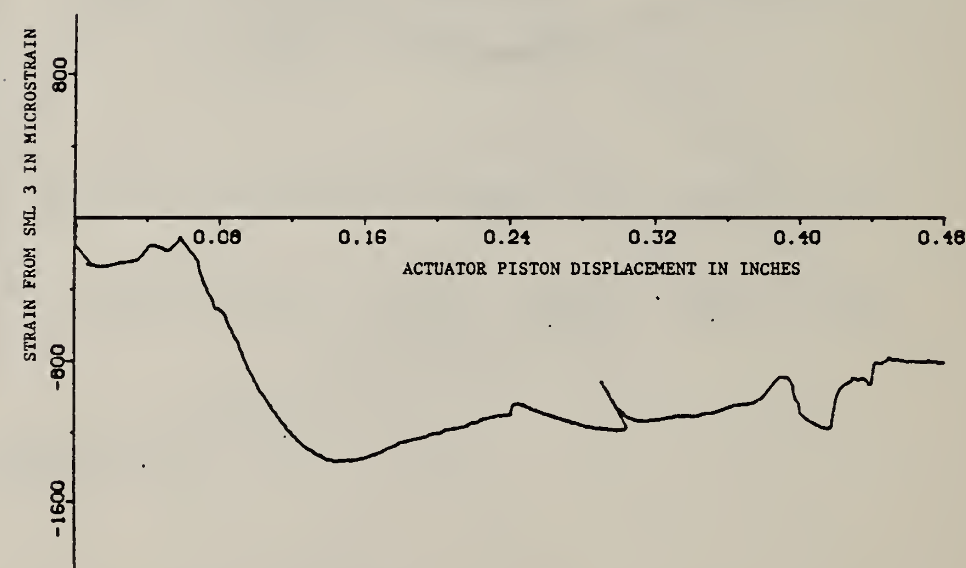

Figure 6.102. Strain history of SML 3 for wall C5

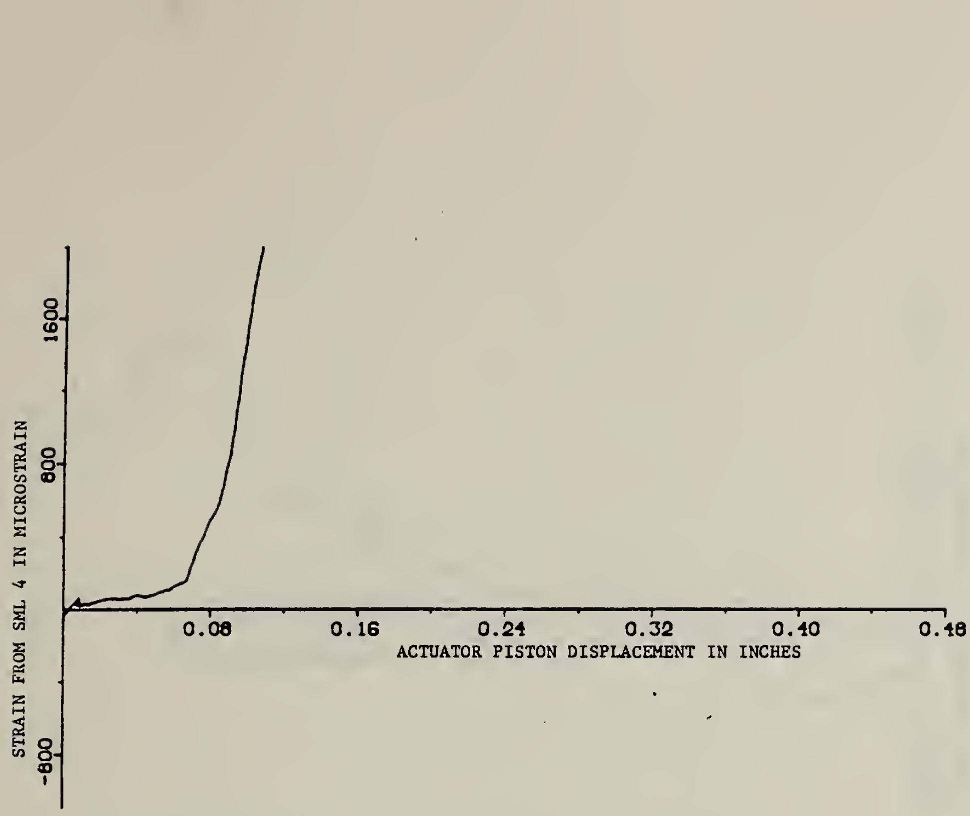

Figure 6.103. Strain history of SML 4 for wall C5

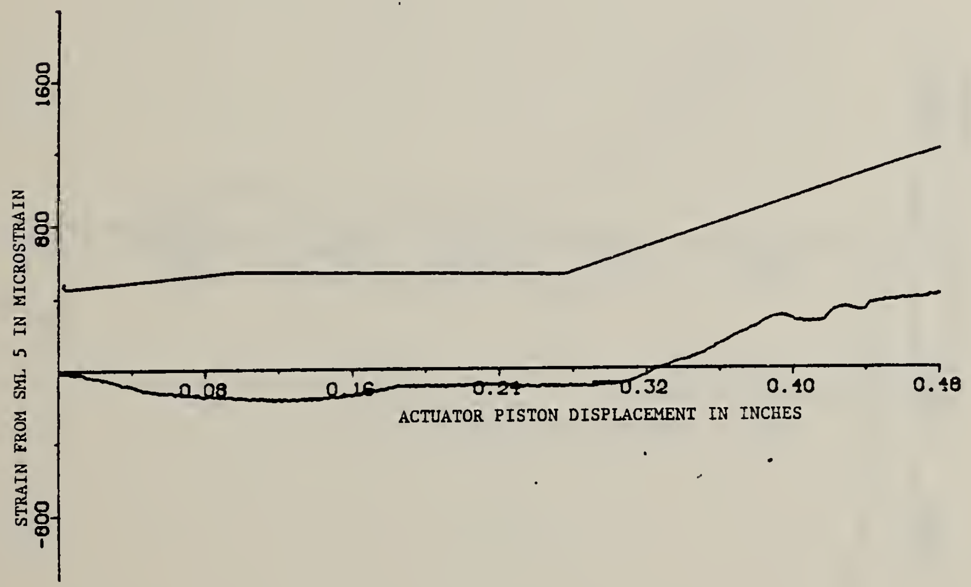

Figure 6.104. Strain history of SML 5 for wall C5

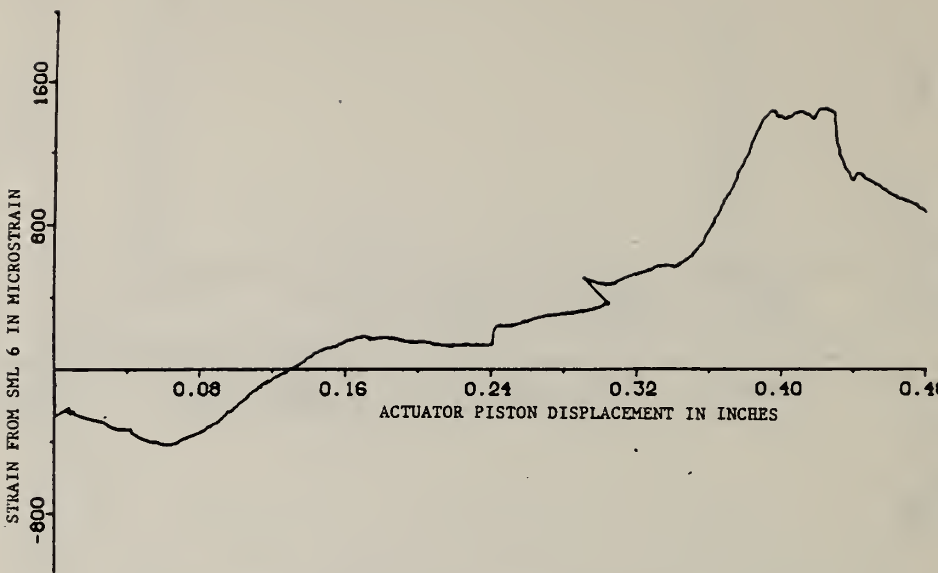

Figure 6.105. Strain history of SML 6 for wall C5

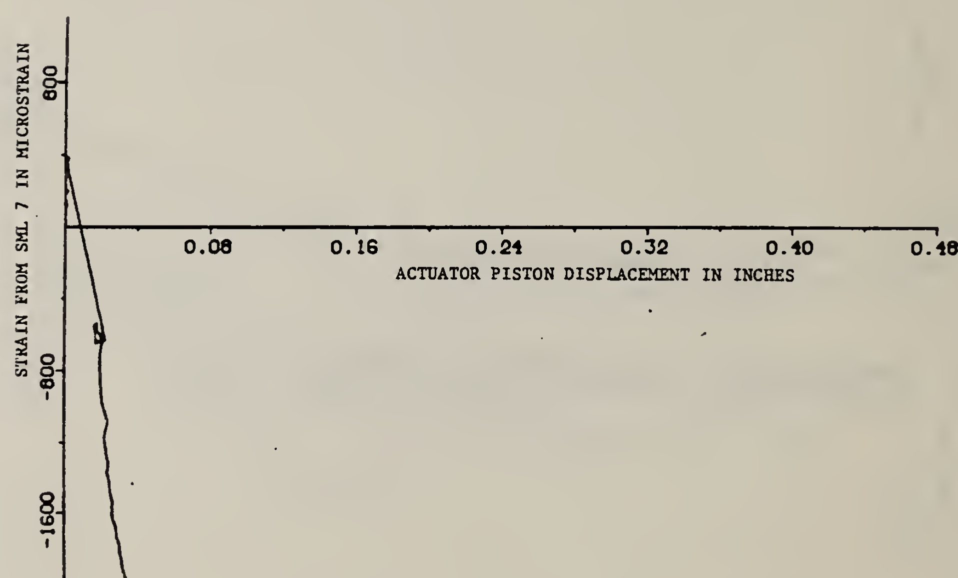

Figure 6.106. Strain history of SML 7 for wall C5

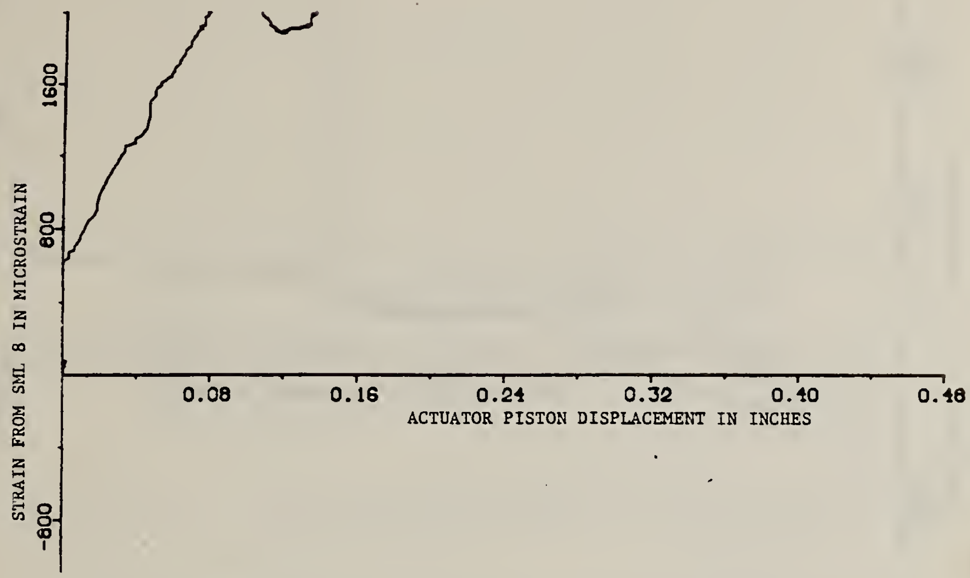

Figure 6.107. Strain history of SML 8 for wall C5

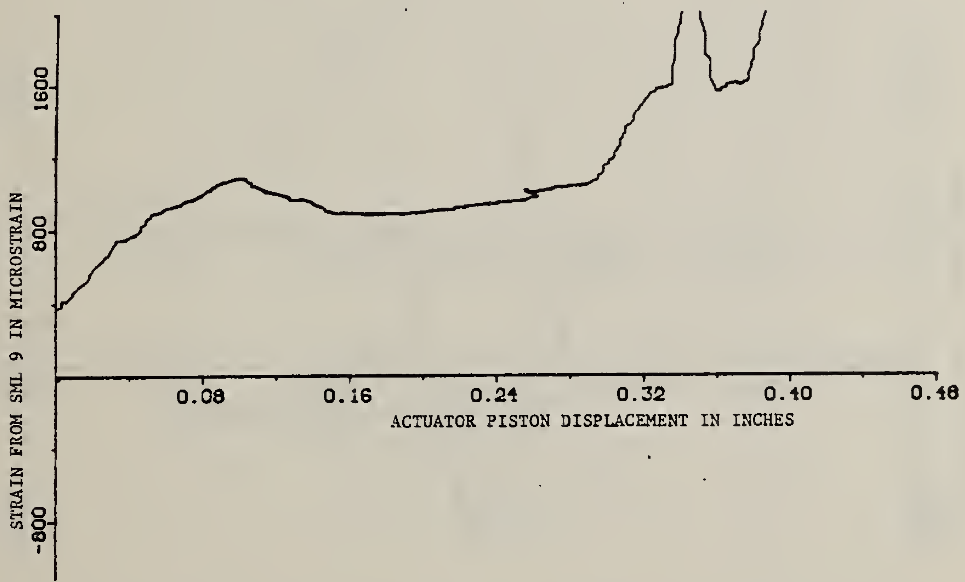

Figure 6.108. Strain history of SML 9 for wall C5

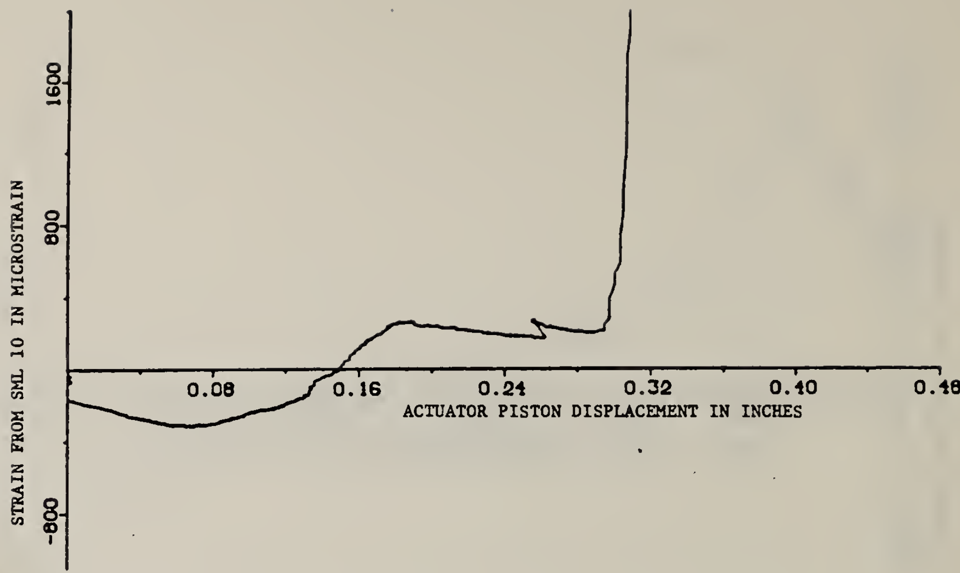

Figure 6.109. Strain history of SML 10 for wall C5

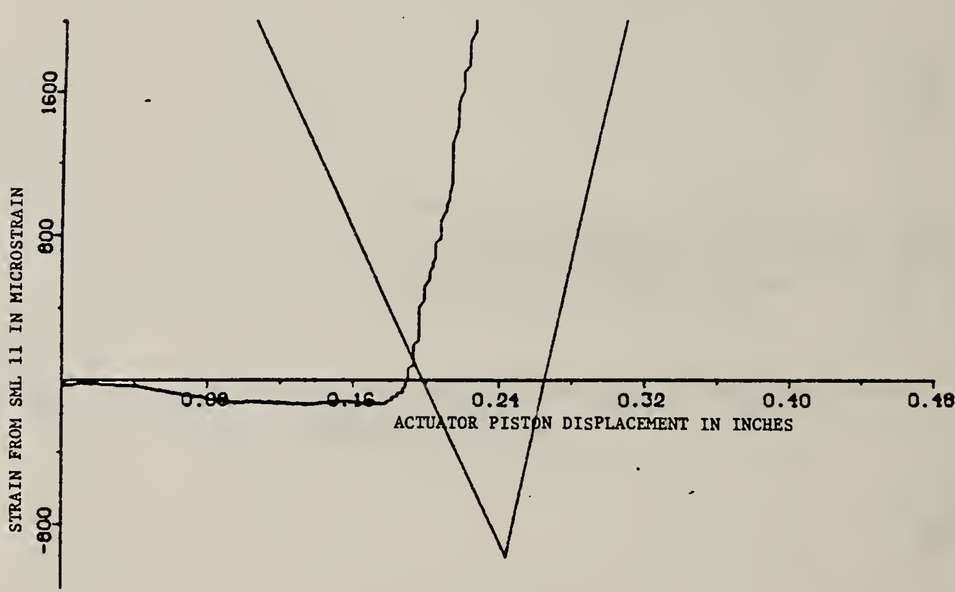

Figure 6.110. Strain history of SML 11 for wall C5

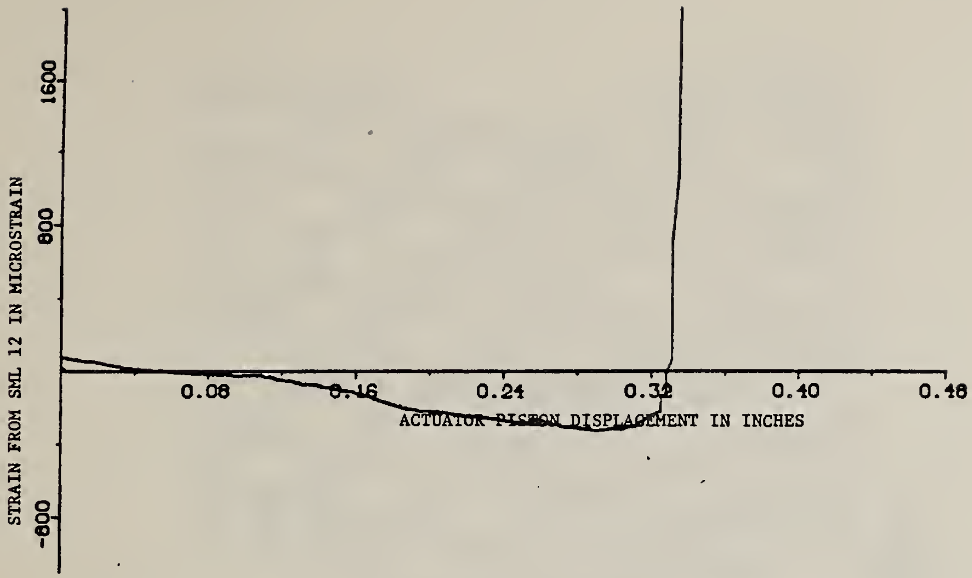

Figure 6.111. Strain history of SML 12 for wall C5

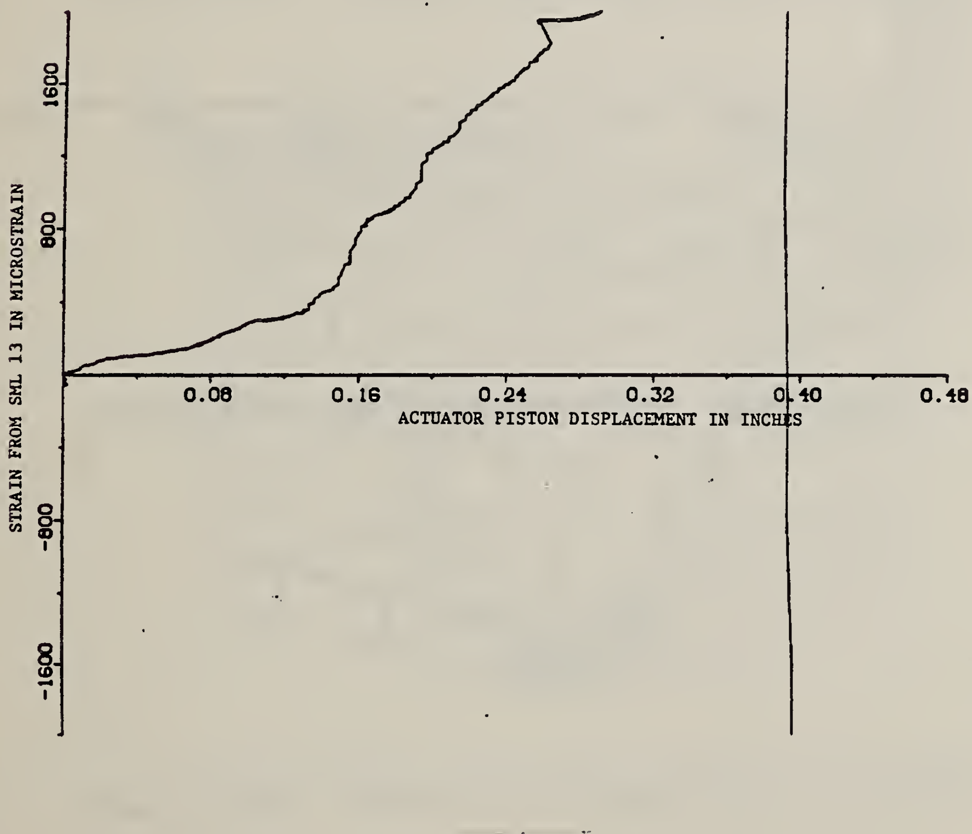

Figure 6.112. Strain history of SML 13 for wall C5

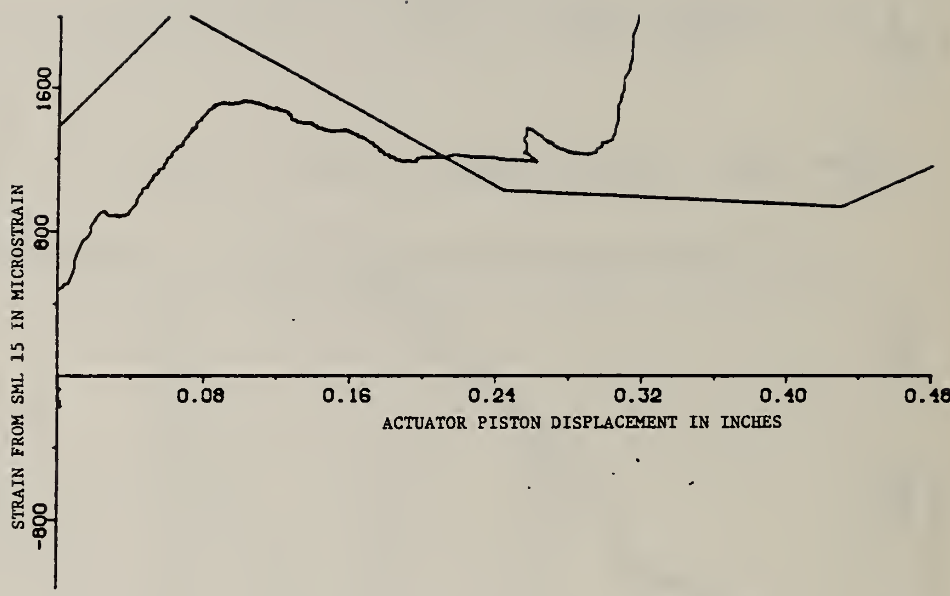

Figure 6.113. Strain history of SML 15 for wall C5

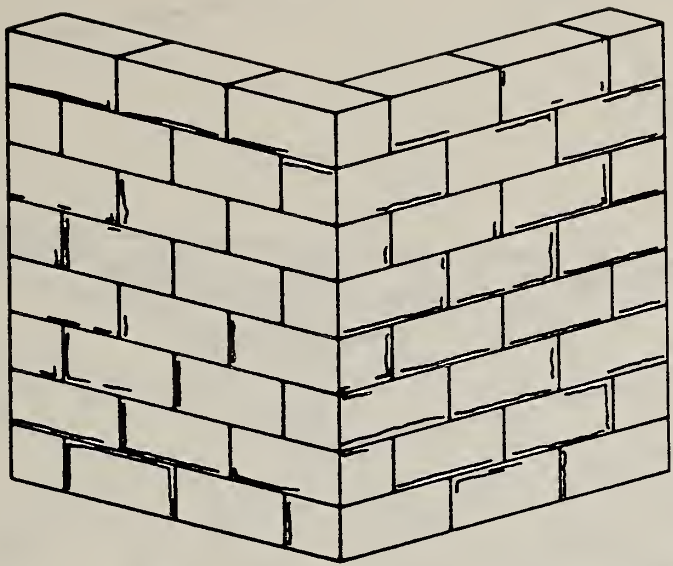

Figure 6.114. Pre-test crack observations for wall C5

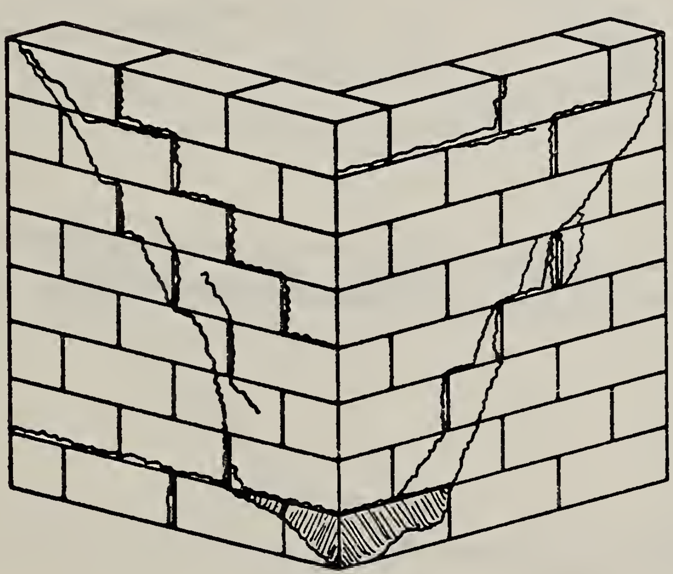

Figure 6.115. Post-test crack observations for wall C5

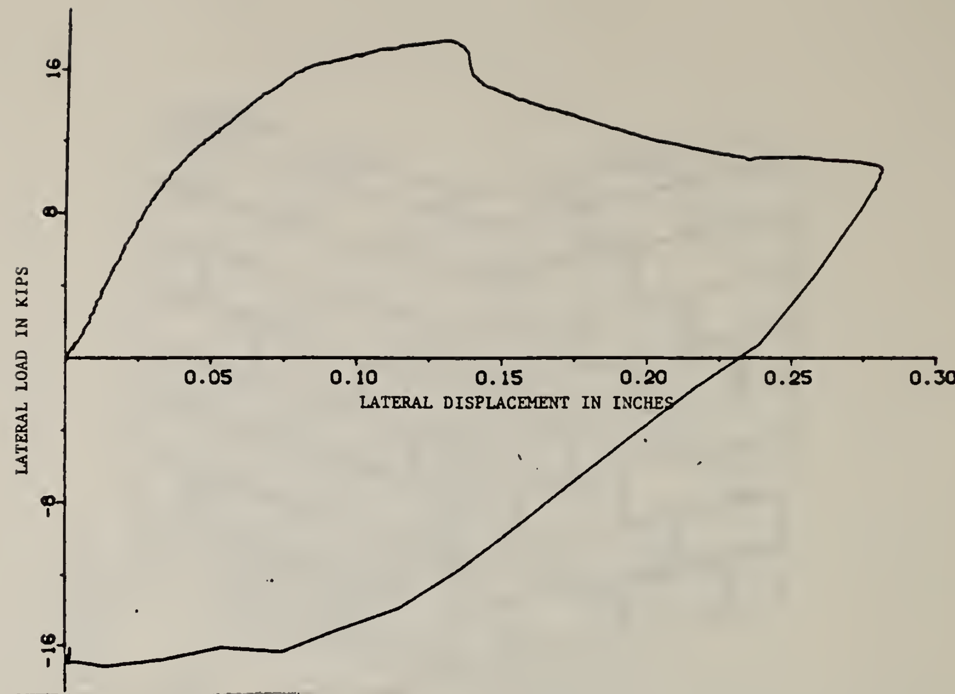

Figure 6.116. Lateral load versus piston displacement for wall C4

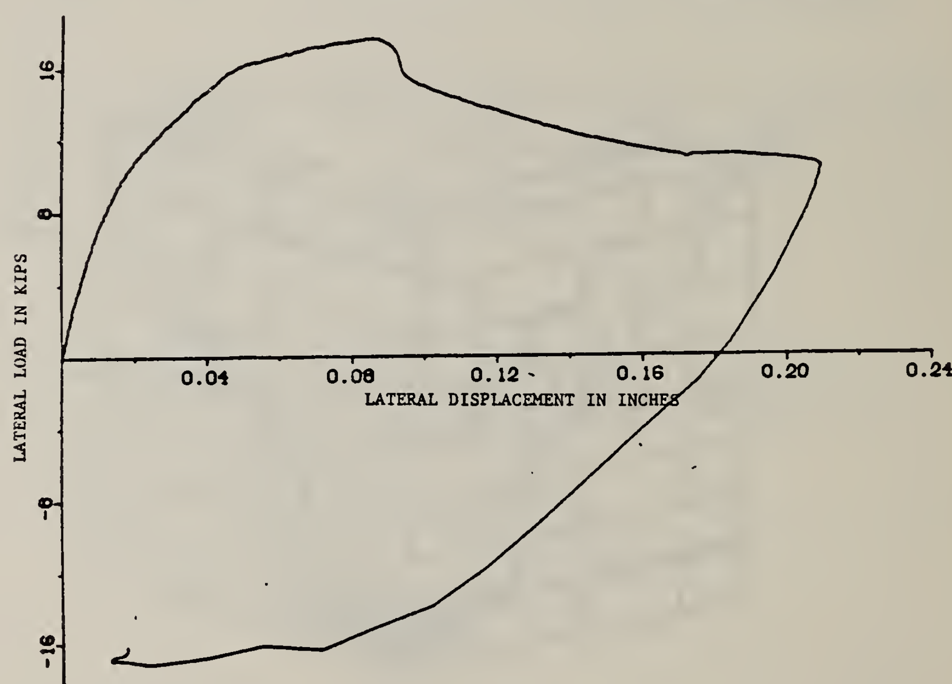

Figure 6.117. Lateral load versus wall displacement for wall C4

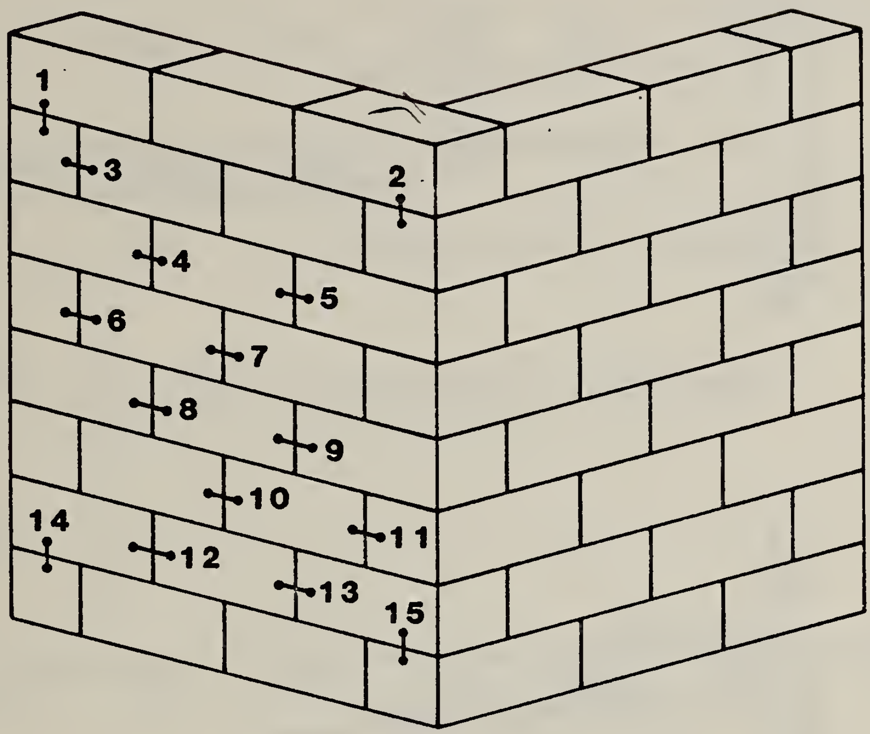

Figure 6.118. Strain measuring locations for wall C4

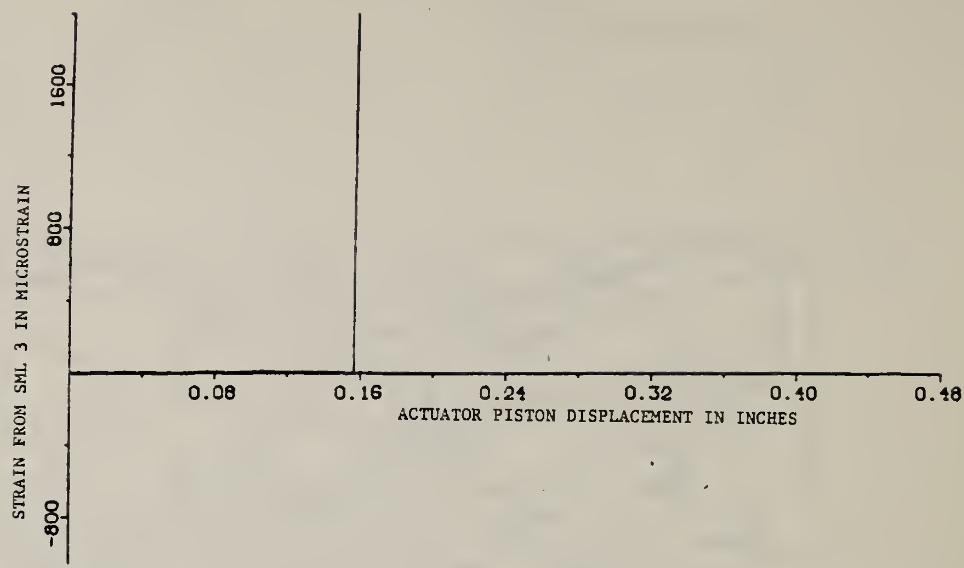

Figure 6.119. Strain history of SML 3 for wall C4

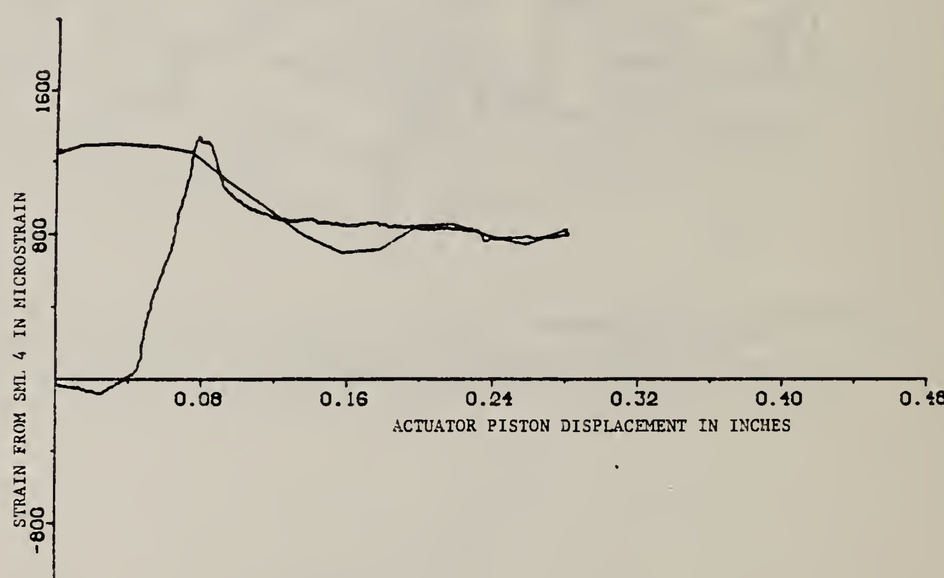

Figure 6.120. Strain history of SML 4 for wall C4

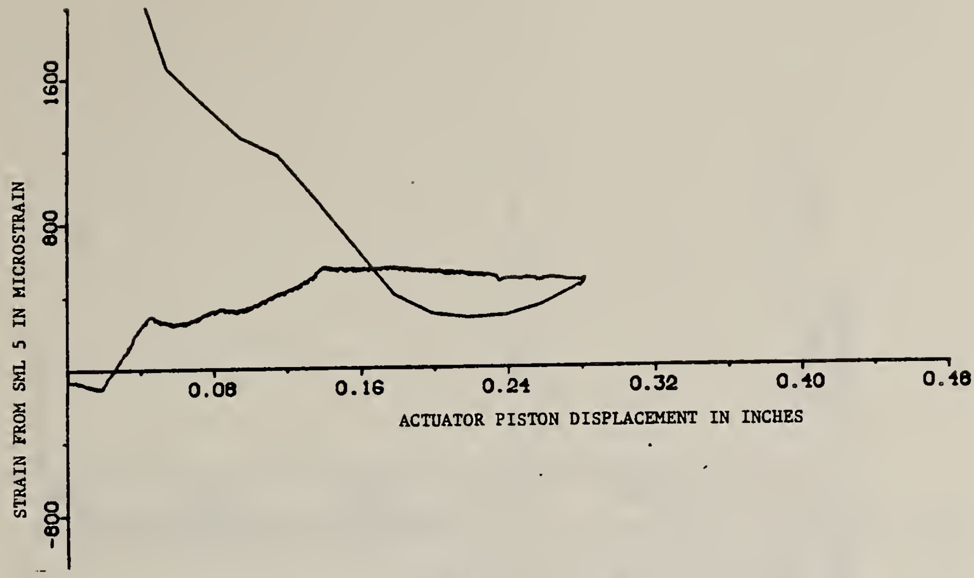

Figure 6.121. Strain history of SML 5 for wall C4

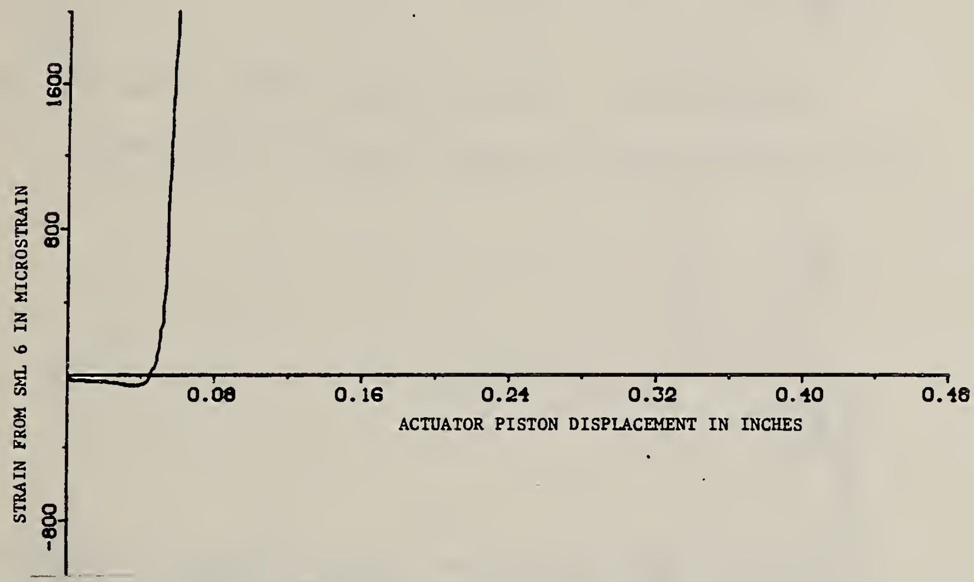

Figure 6.122. Strain history of SML 6 for wall C4

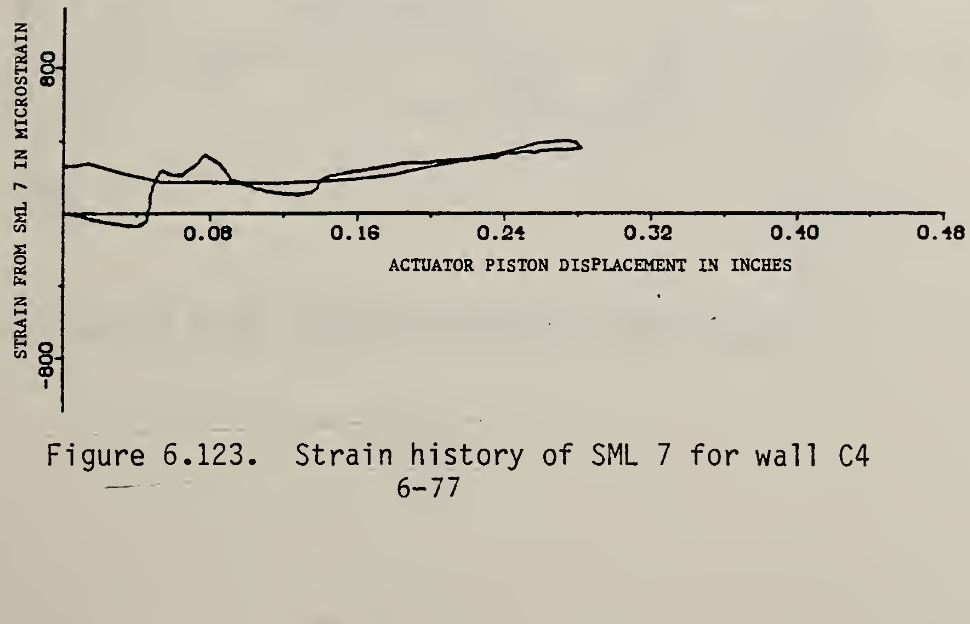

Figure 6.123. Strain history of SML 7 for wall C4

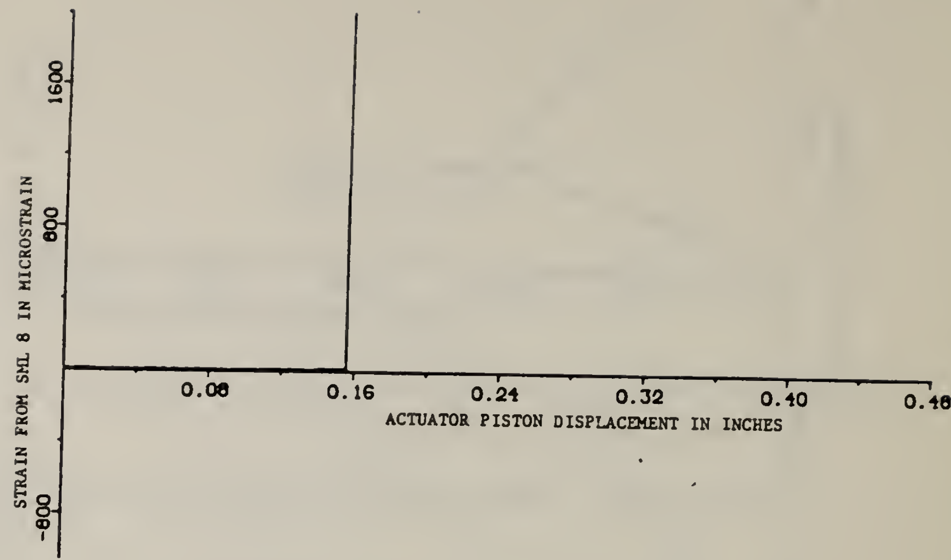

Figure 6.124. Strain history of SML 8 for wall C4

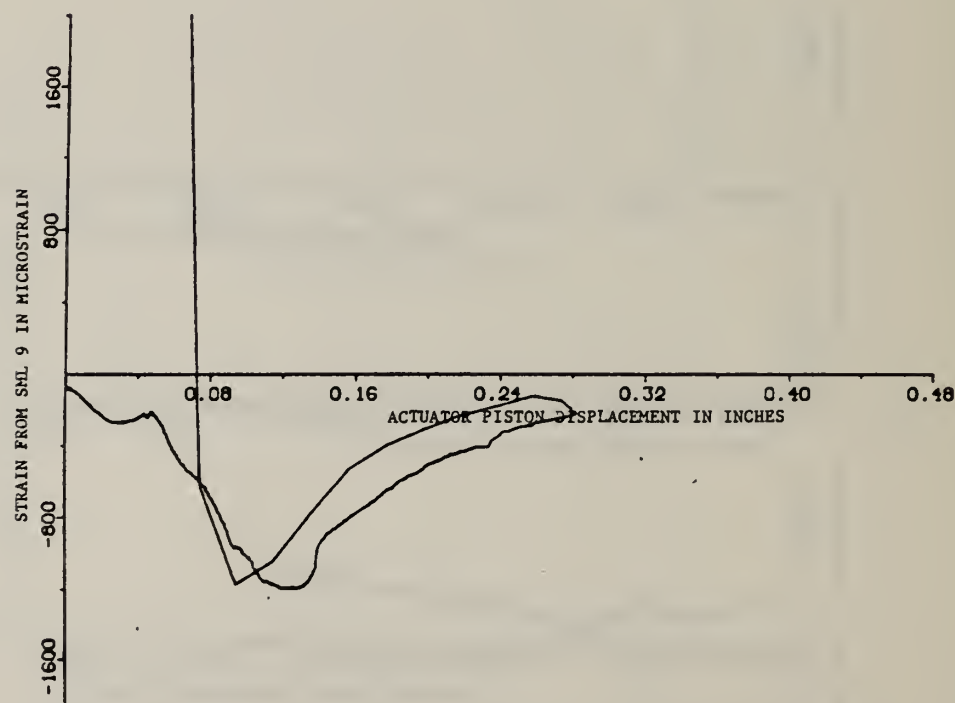

Figure 6.125. Strain history of SML 9 for wall C4

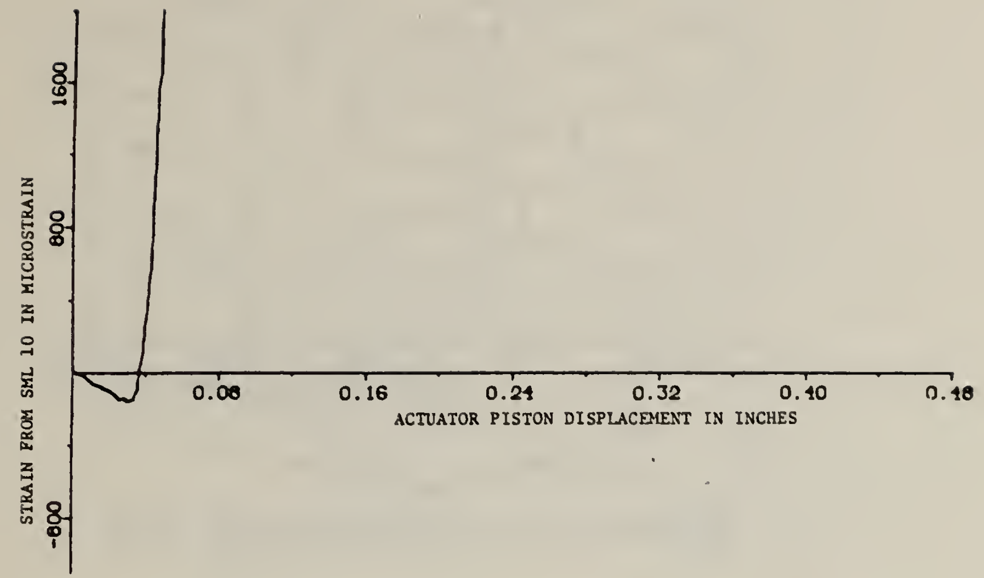

Figure 6.126. Strain history of SML 10 for wall C4

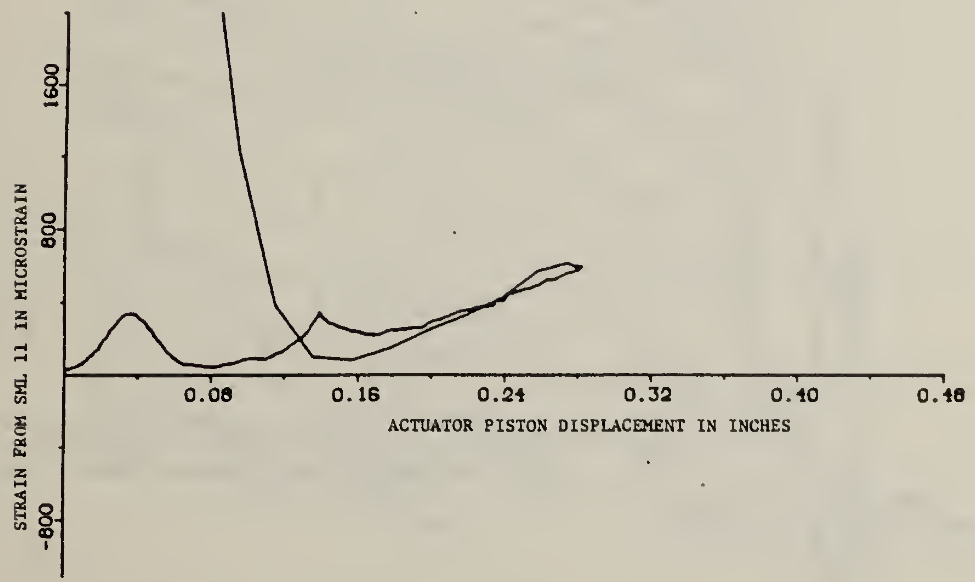

Figure 6.127. Strain history of SML 11 for wall C4

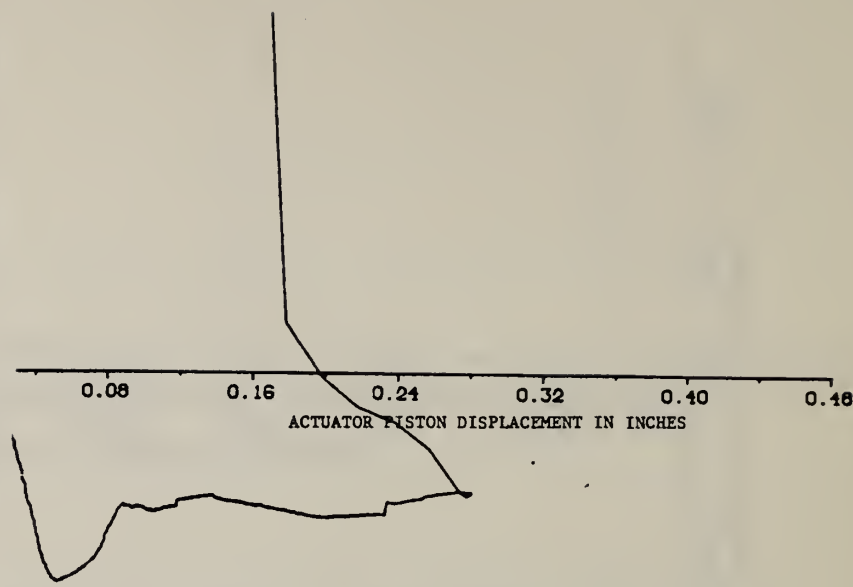

Figure 6.128. Strain history of SML 12 for wall C4

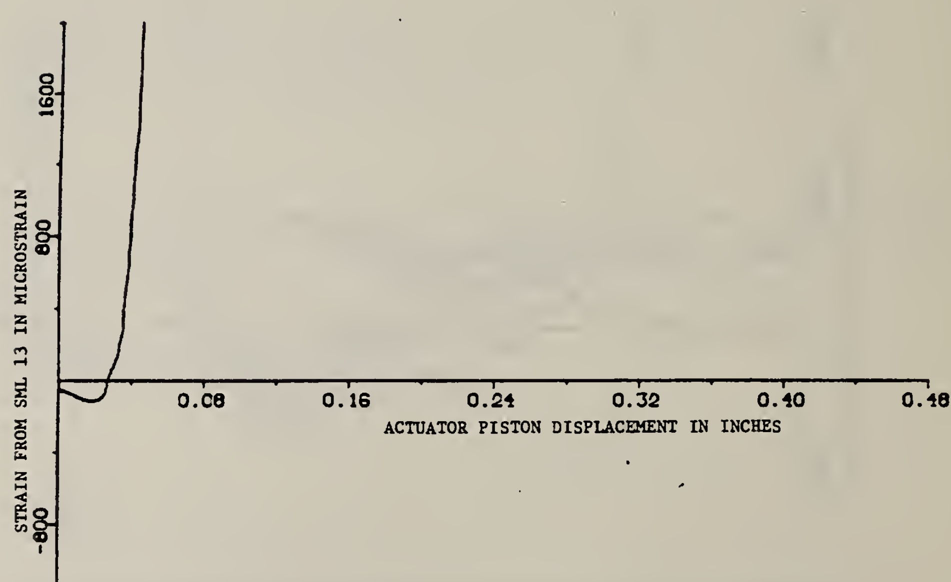

Figure 6.129. Strain history of SML 13 for wall C4

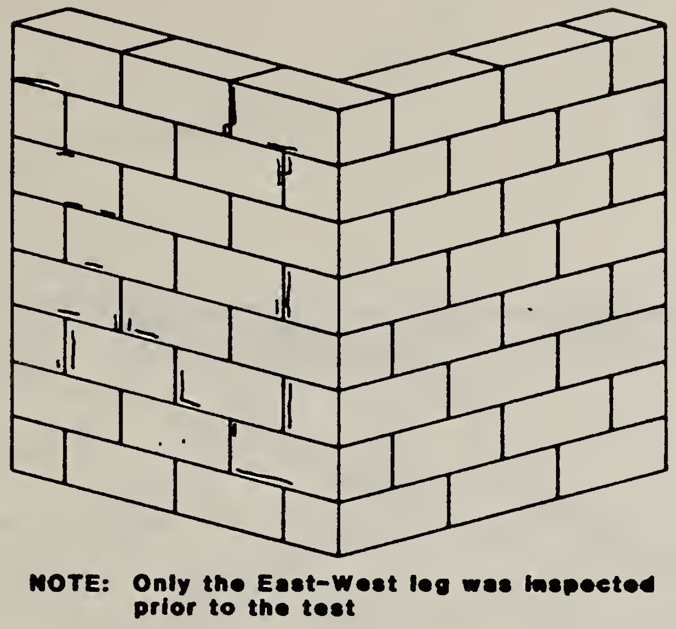

Figure 6.130. Pre-test crack observations for wall C4

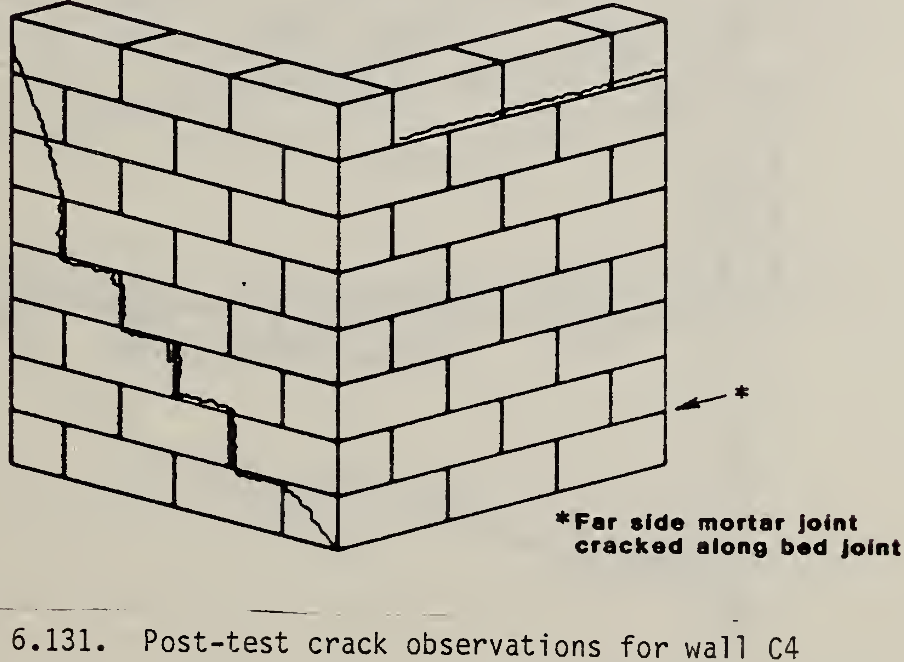

Figure 6.131. Post-test crack observations for wall C4

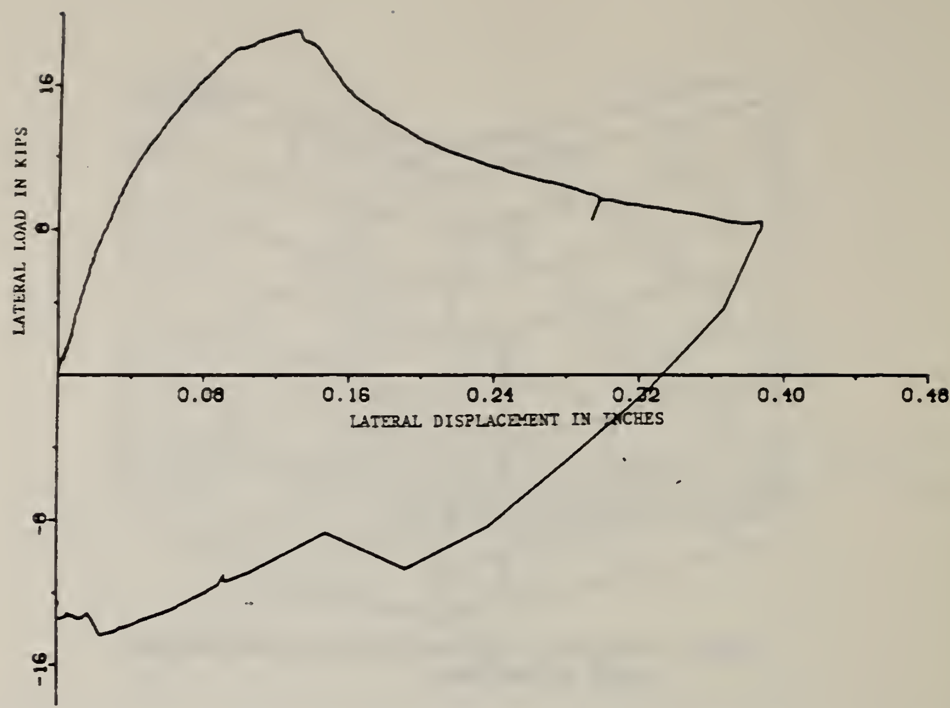

Figure 6.132. Lateral load versus piston displacement for wall C3

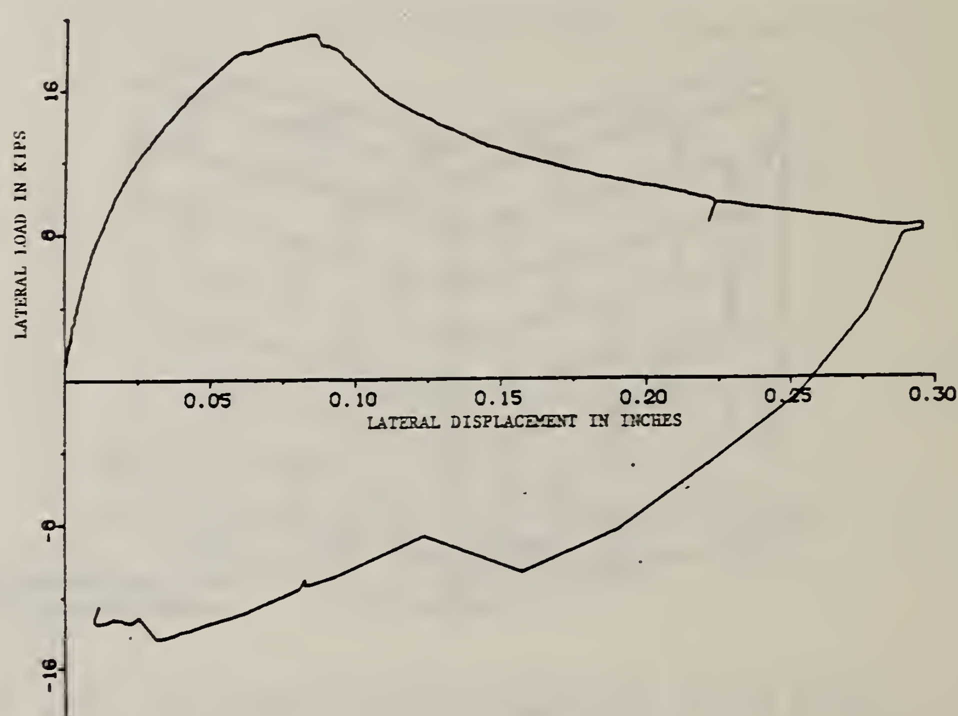

Figure 6.133. Lateral load versus wall displacement for wall C3

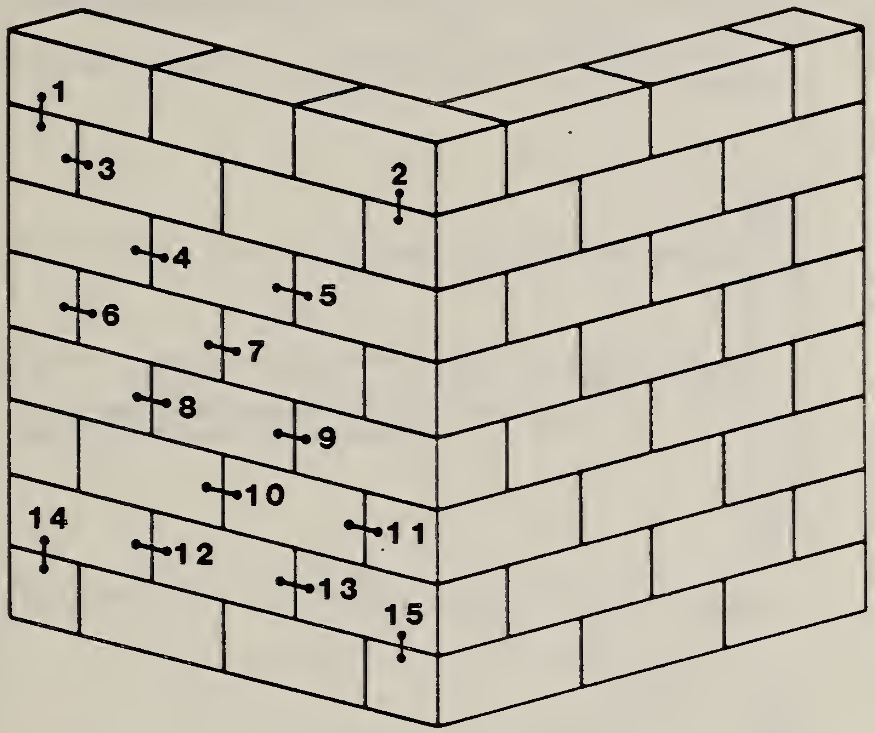

Figure 6.134. Strain measuring locations for wall C3

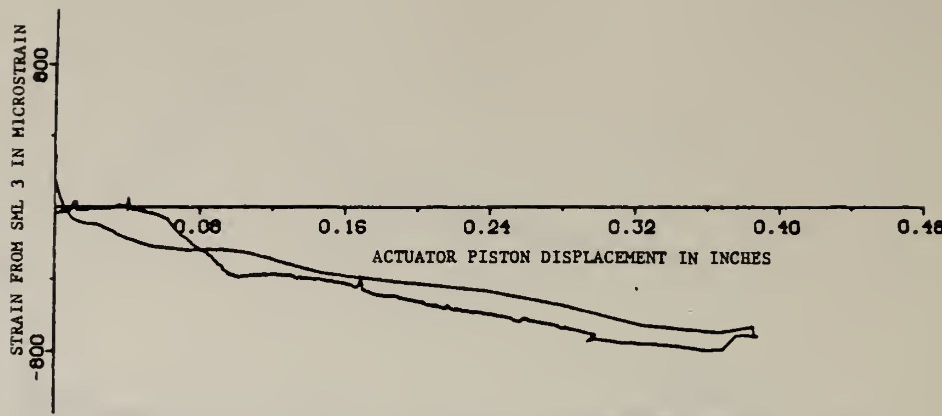

Figure 6.135. Strain history of SML 3 for wall C3

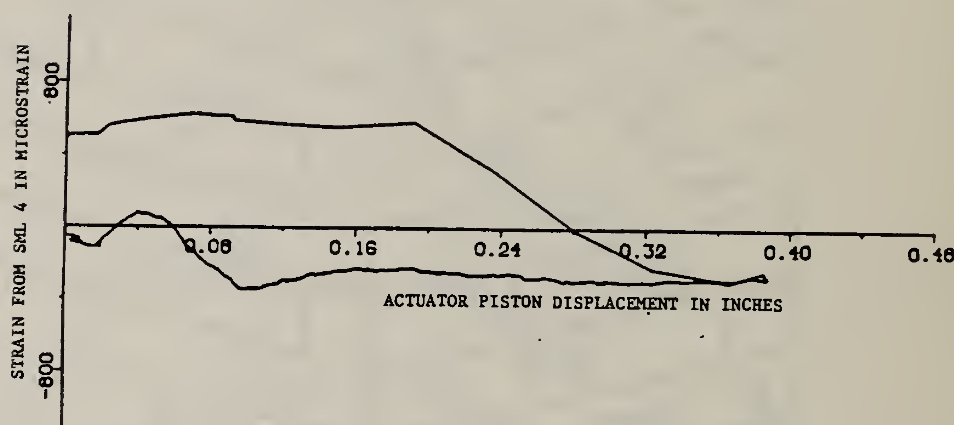

Figure 6.136. Strain history of SML 4 for wall C3

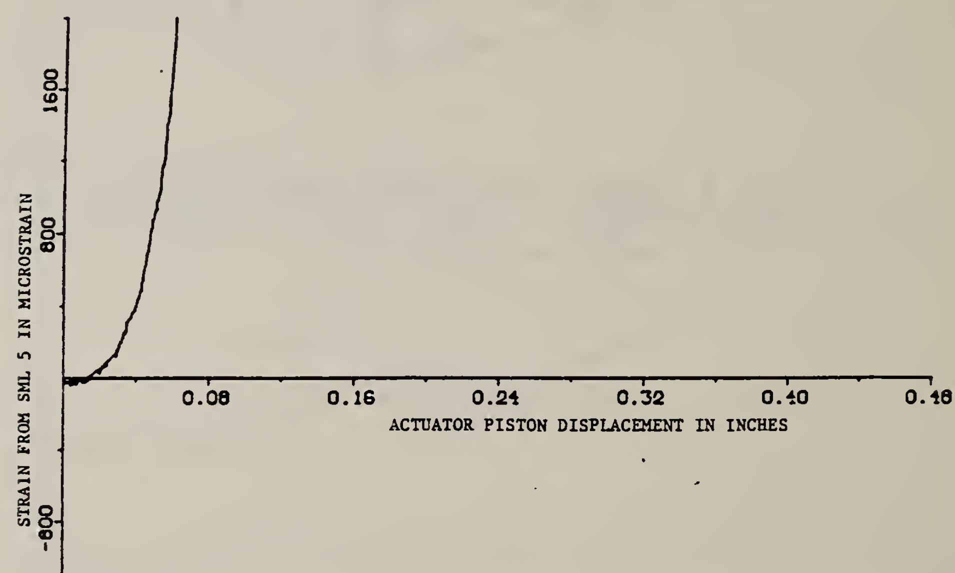

Figure 6.137. Strain history of SML 5 for wall C3

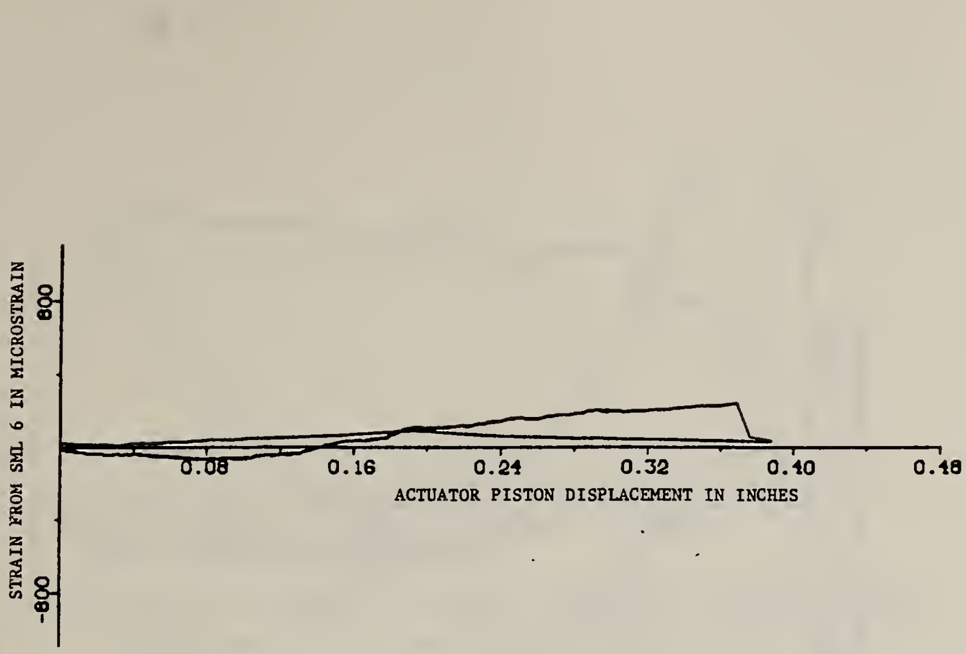

Figure 6.138. Strain history of SML 6 for wall C3

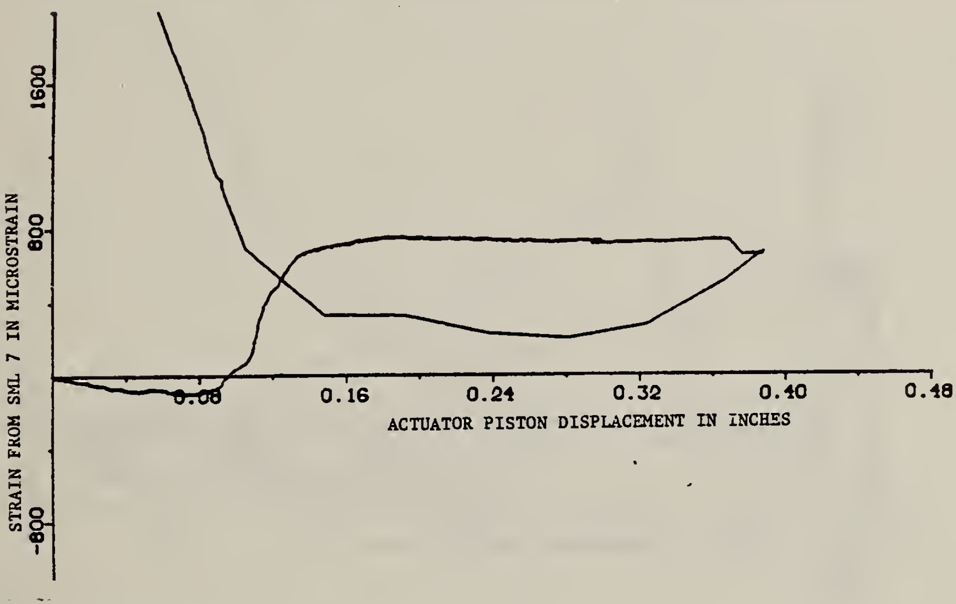

Figure 6.139. Strain history of SML 7 for wall C3

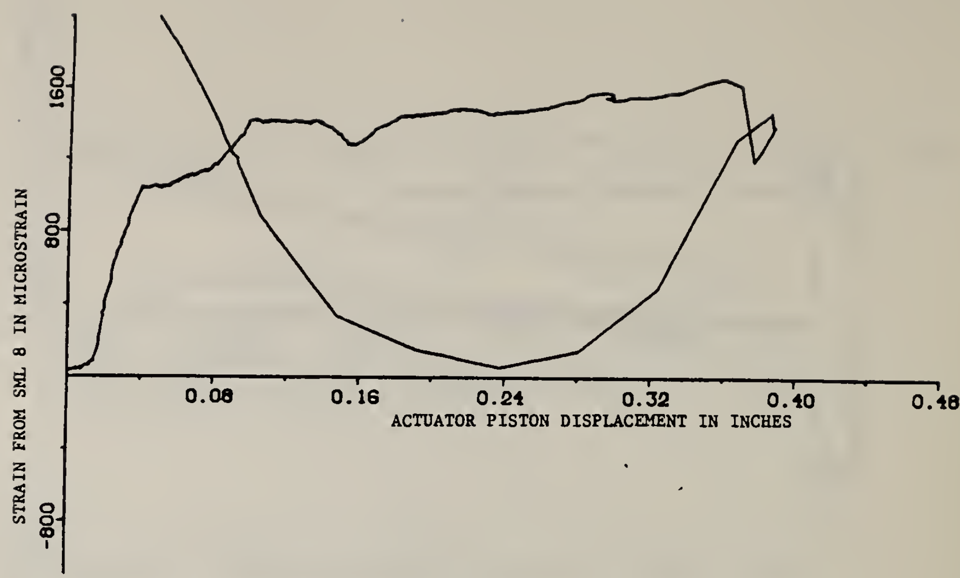

Figure 6.140. Strain history of SML 8 for wall C3

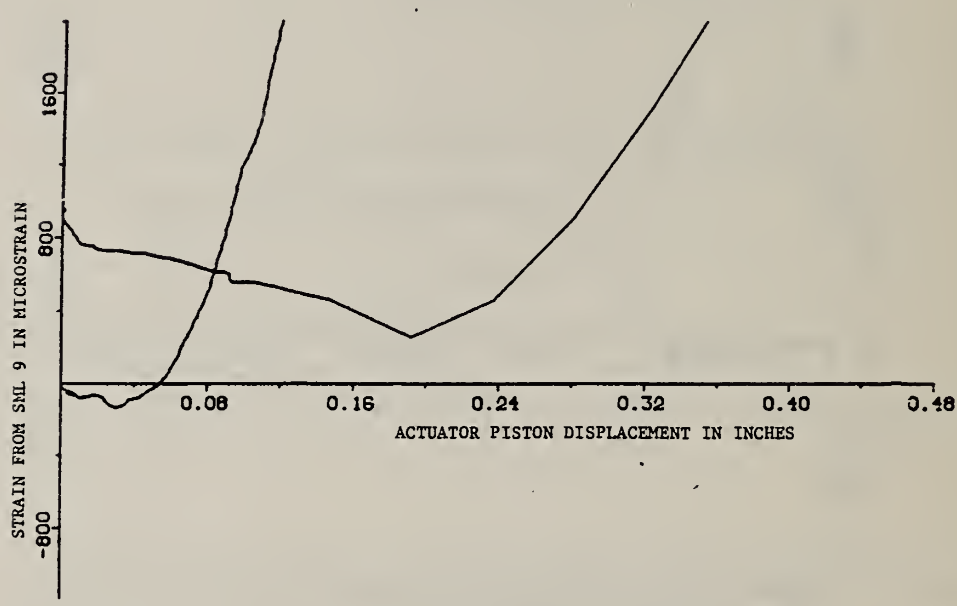

Figure 6.141. Strain history of SML 9 for wall C3

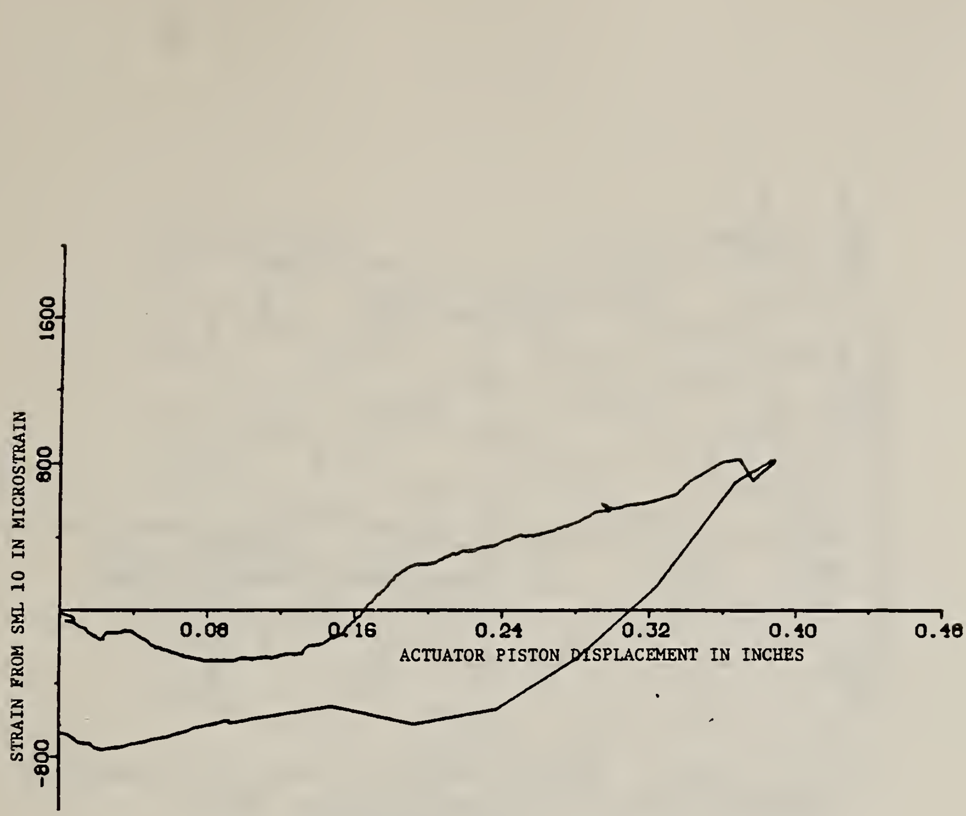

Figure 6.142. Strain history of SML 10 for wall C3

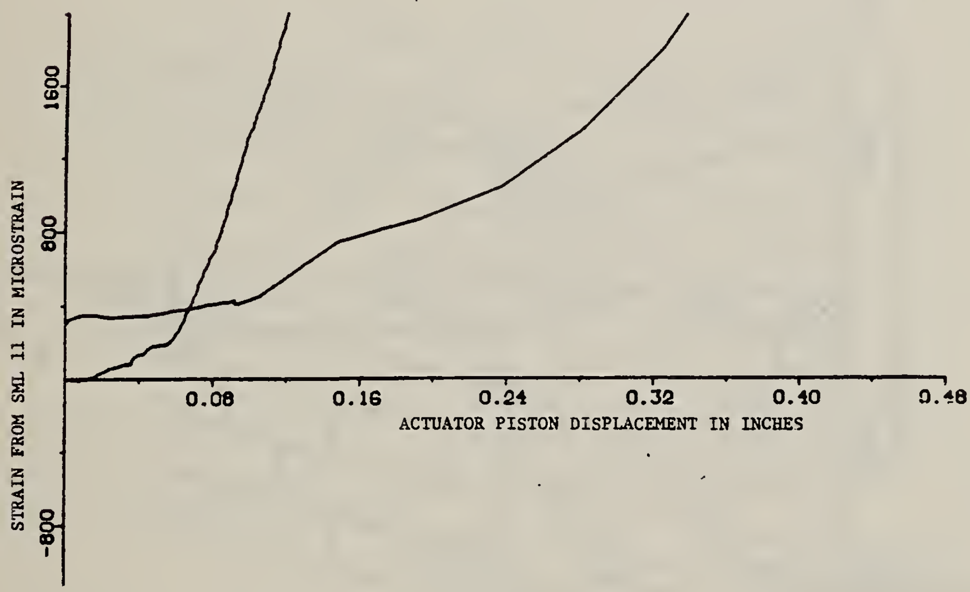

Figure 6.143. Strain history of SML 11 for wall C3

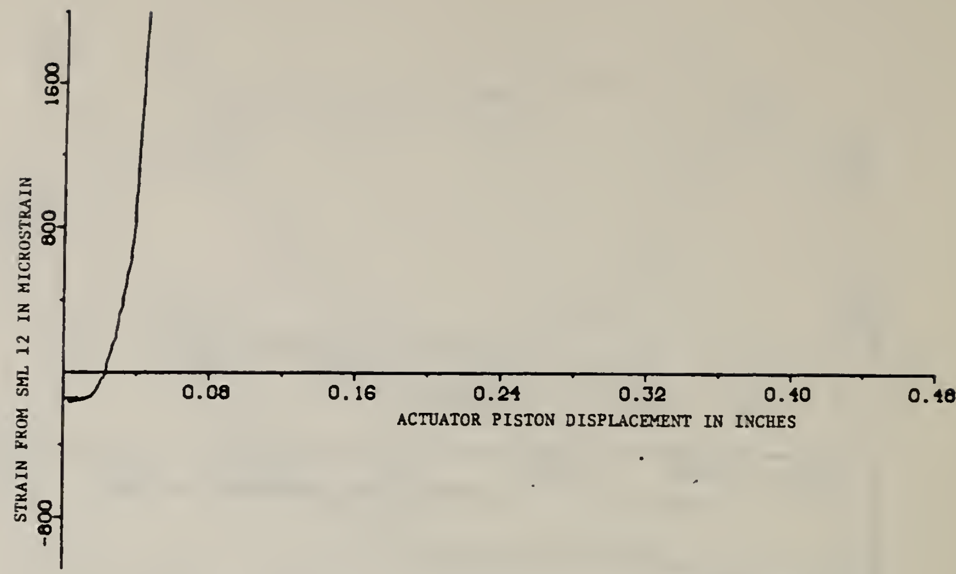

Figure 6.144. Strain history of SML 12 for wall C3

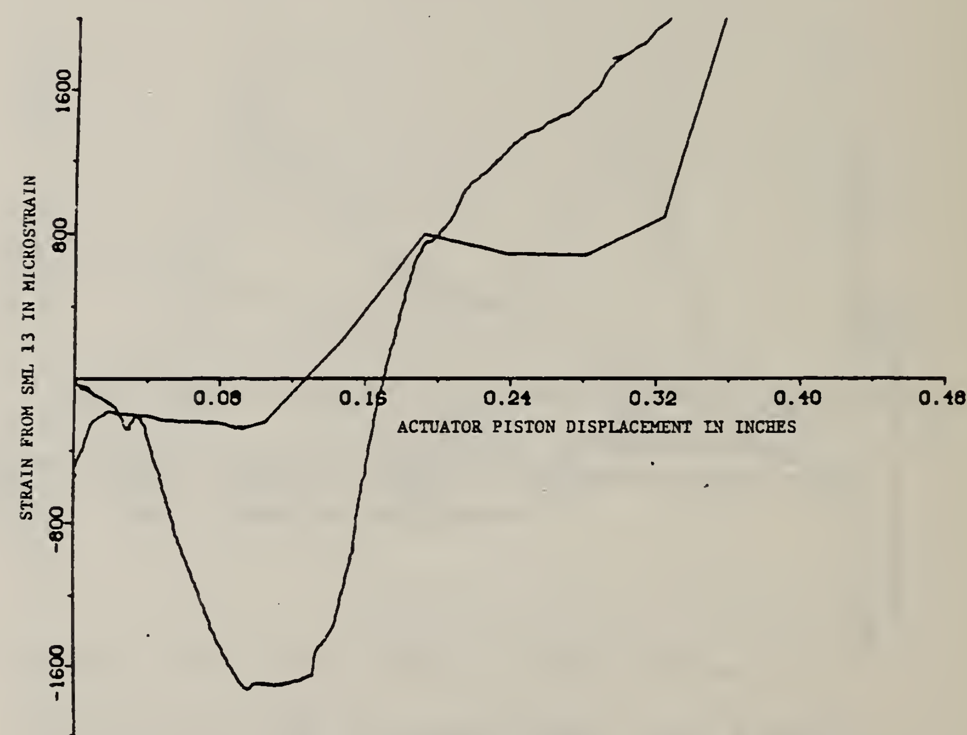

Figure 6.145. Strain history of SML 13 for wall C3

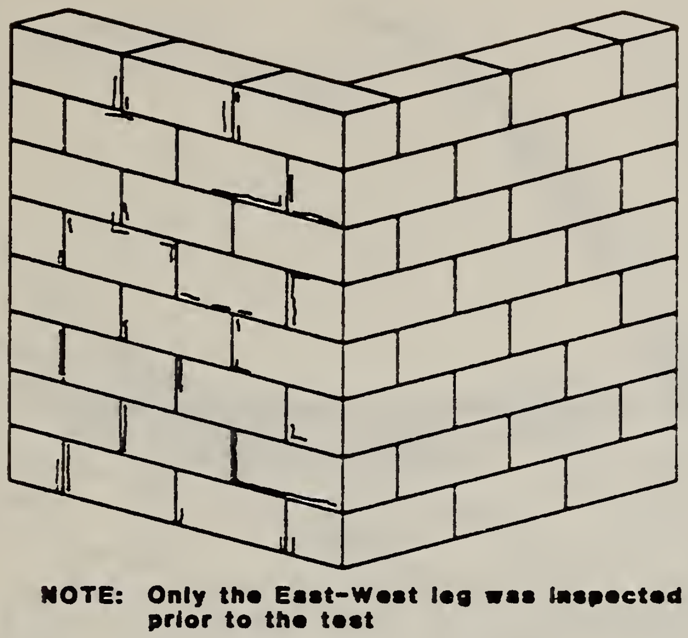

Figure 6.146. Pre-test crack observations for wall C3

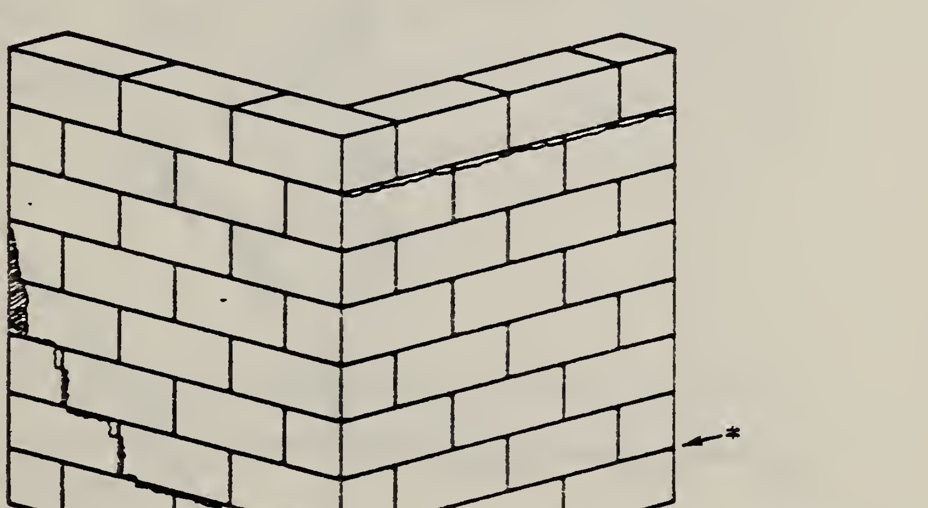

Figure 6.147. Post-test crack observations for wall C3

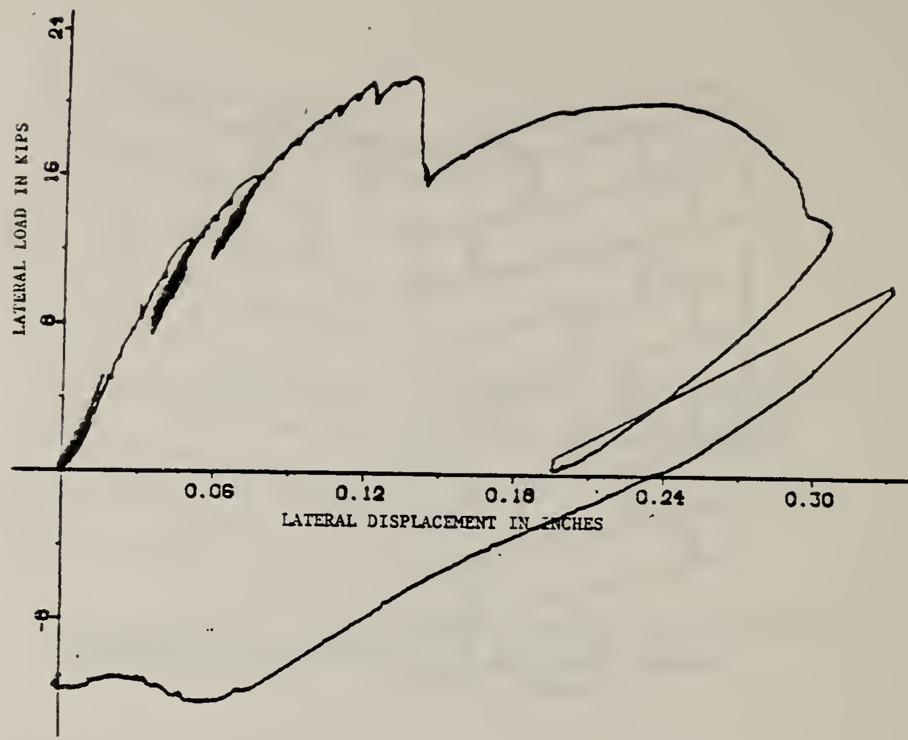

Figure 6.148. Lateral load versus piston displacement for wall C2

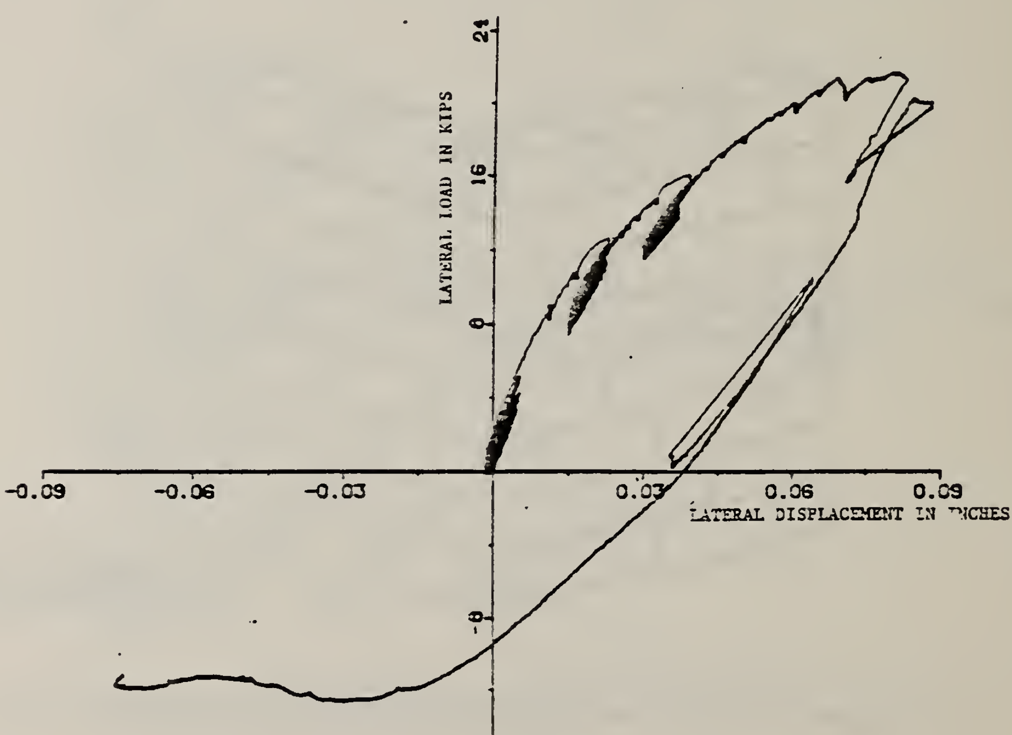

Figure 6.149. Lateral load versus wall displacement for wall C2

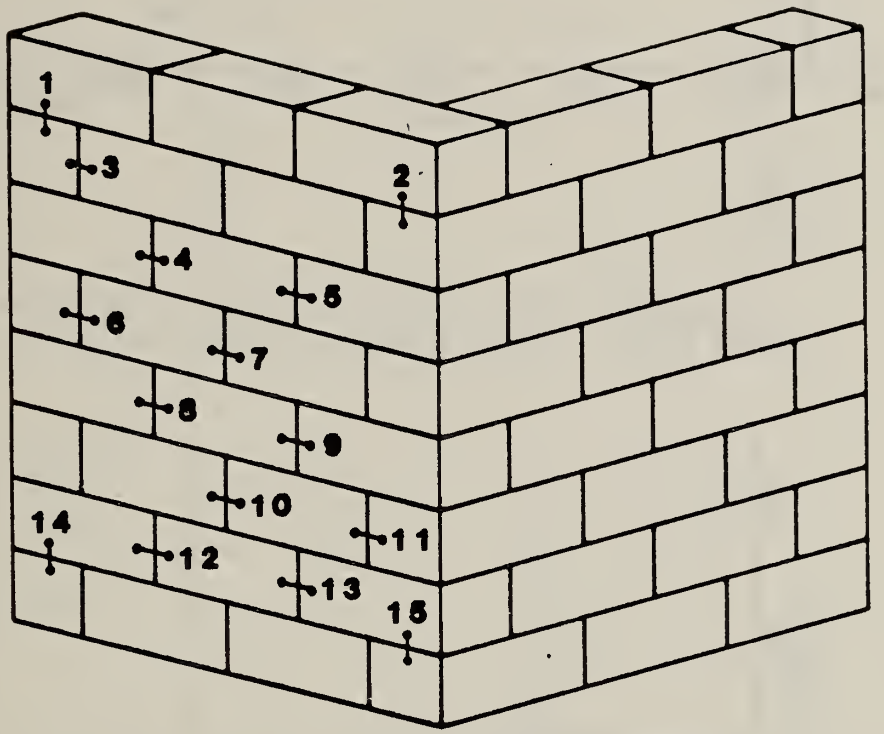

Figure 6.150. Strain measuring locations for wall C2

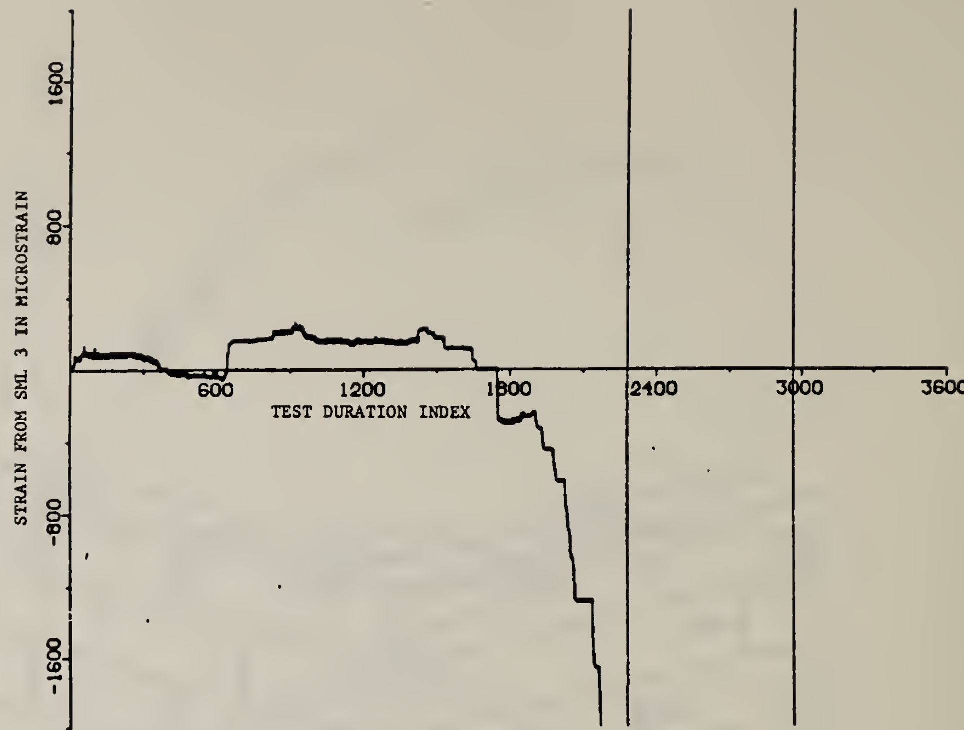

Figure 6.151. Strain history of SML 3 for wall C2

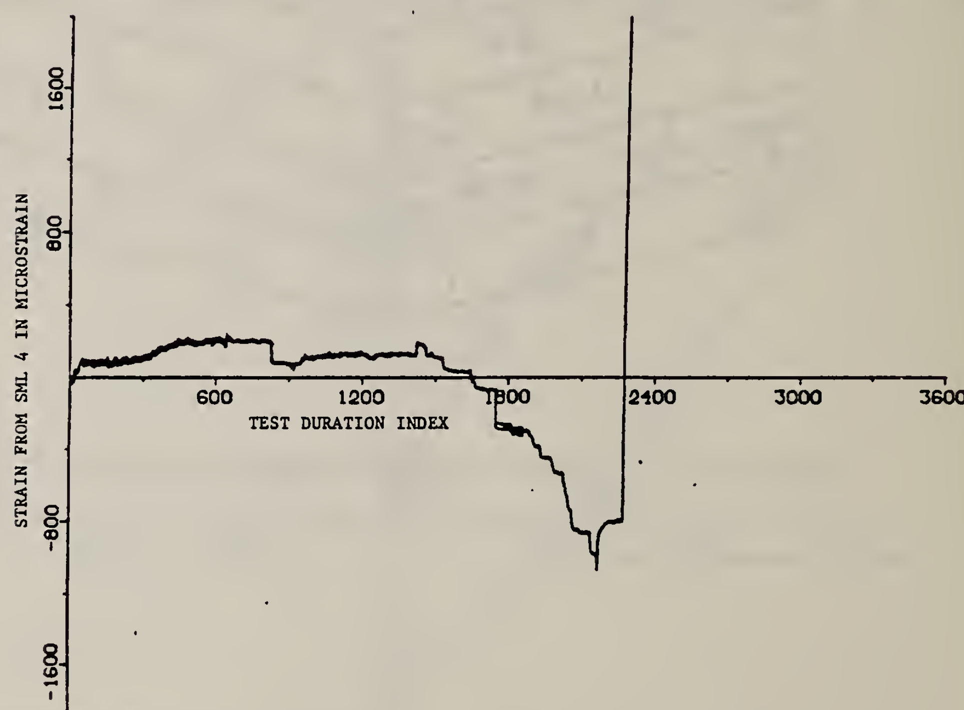

Figure 6.152. Strain history of SML 4 for wall C2

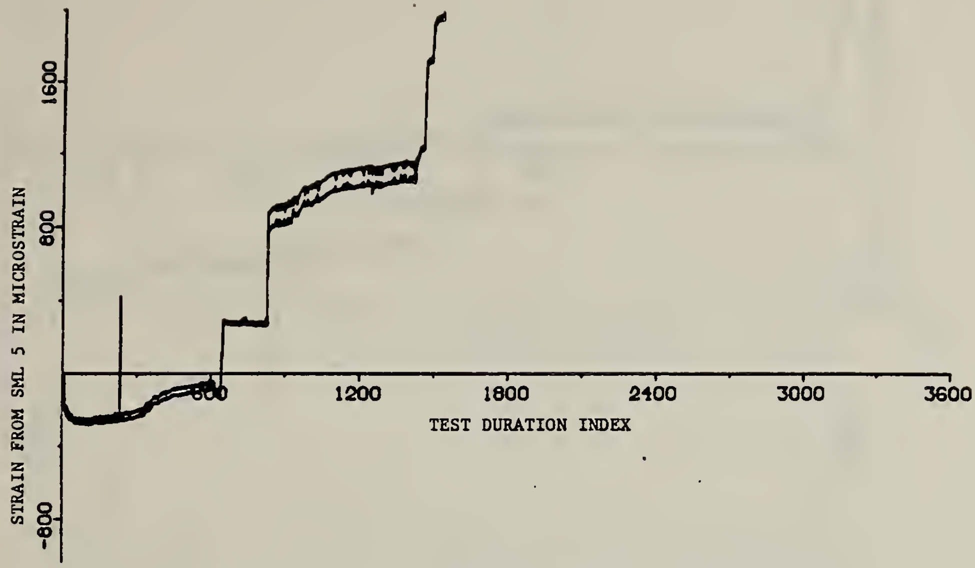

Figure 6.153. Strain history of SML 5 for wall C2

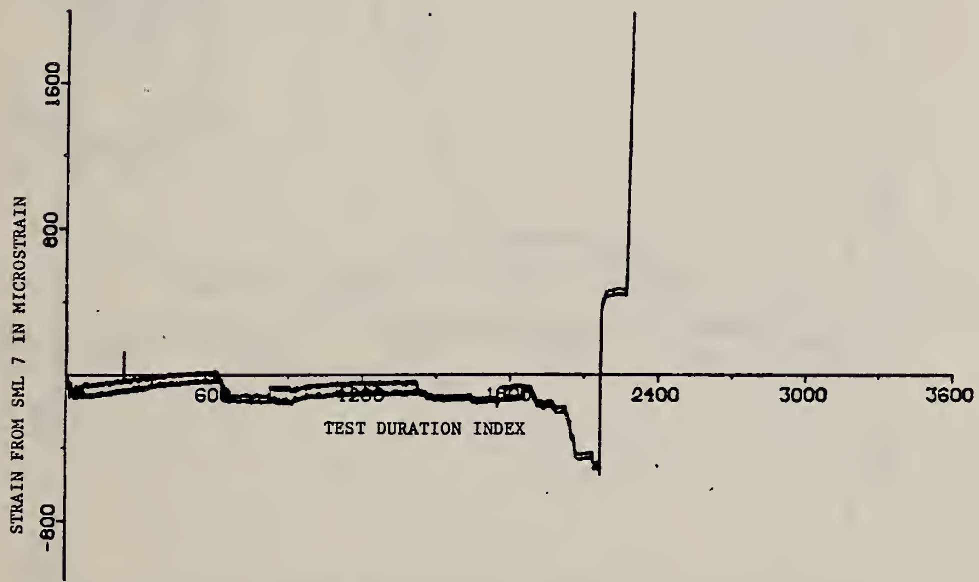

Figure 6.154. Strain history of SML 7 for wall C2

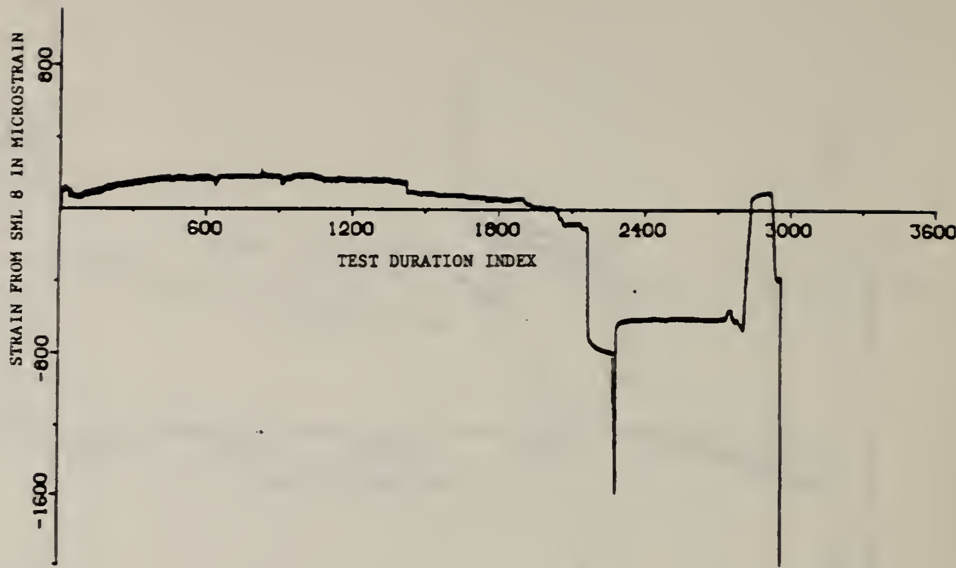

Figure 6.155. Strain history of SML 8 for wall C2

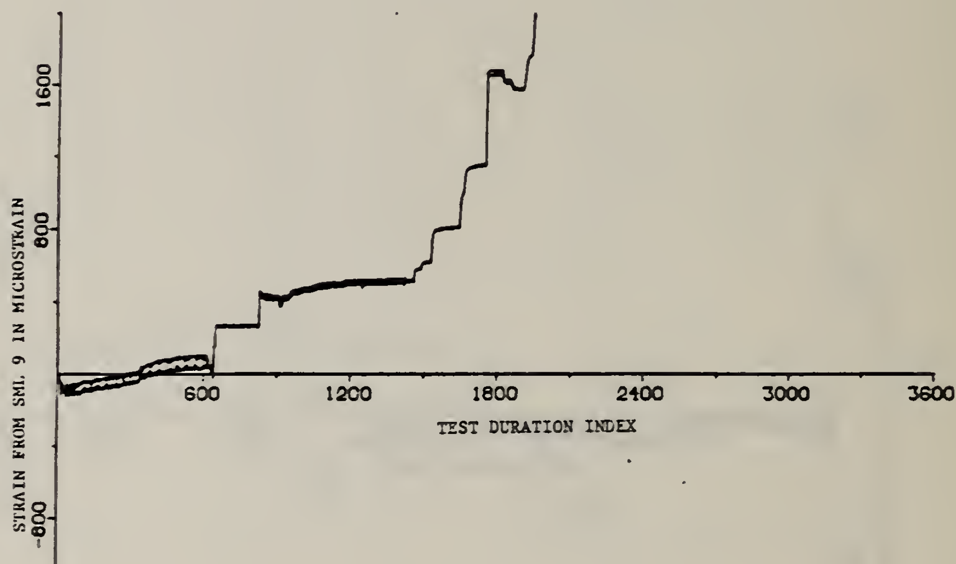

Figure 6.156. Strain history of SML 9 for wall C2

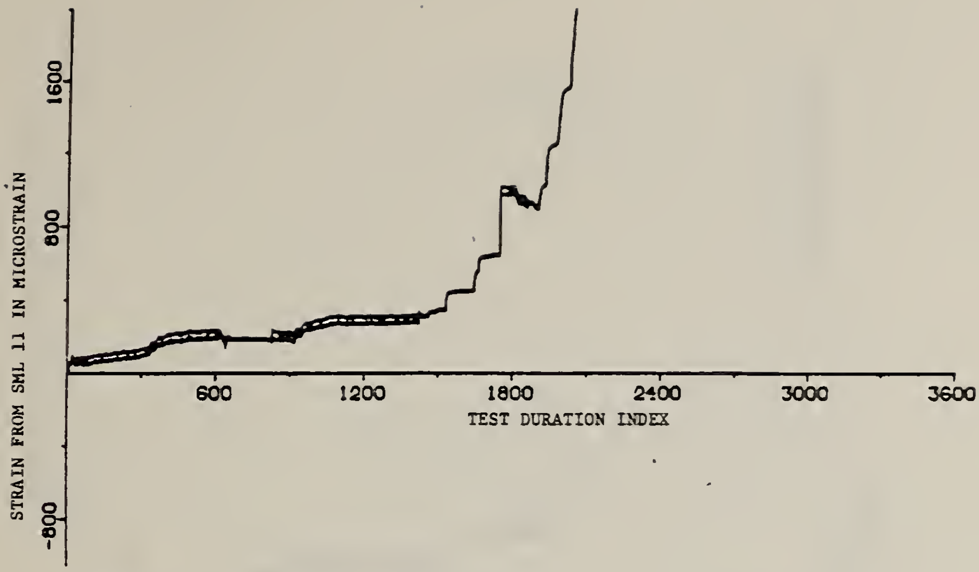

Figure 6.157. Strain history of SML 11 for wall C2

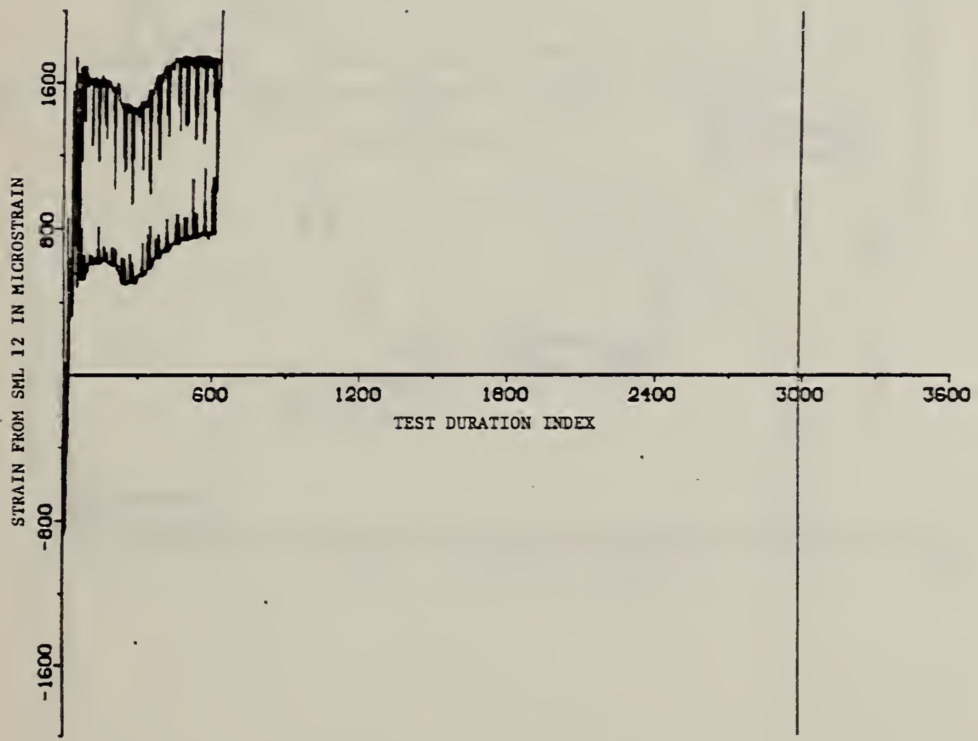

Figure 6.158. Strain history of SML 12 for wall C2

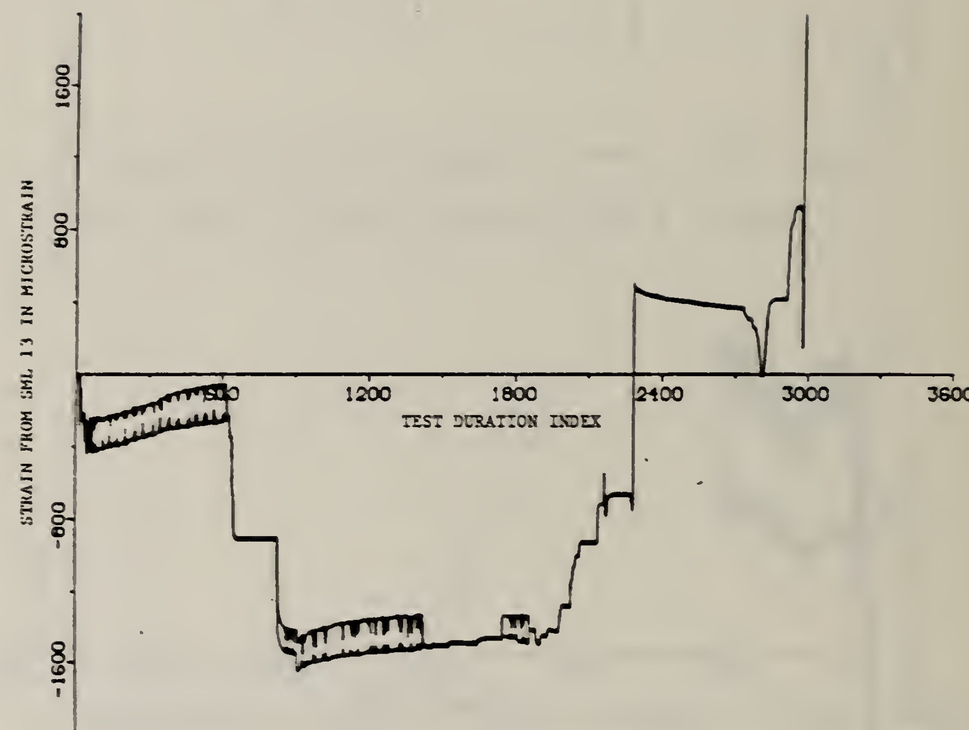

Figure 6.159. Strain history of SML 13 for wall C2

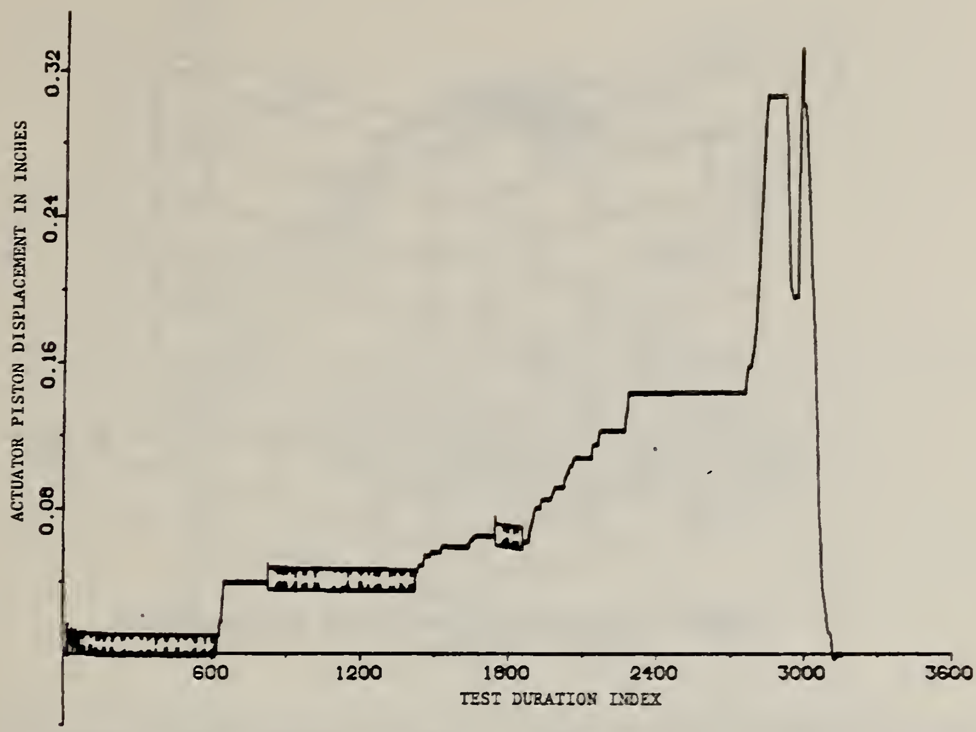

Figure 6.160. Piston displacement history for wall C2

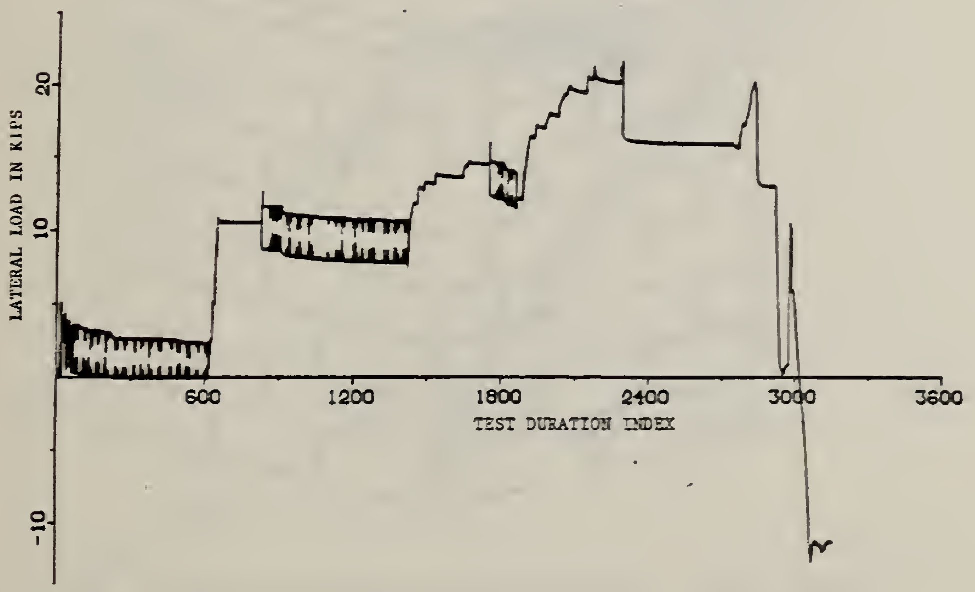

Figure 6.161. Lateral load history for wall C2

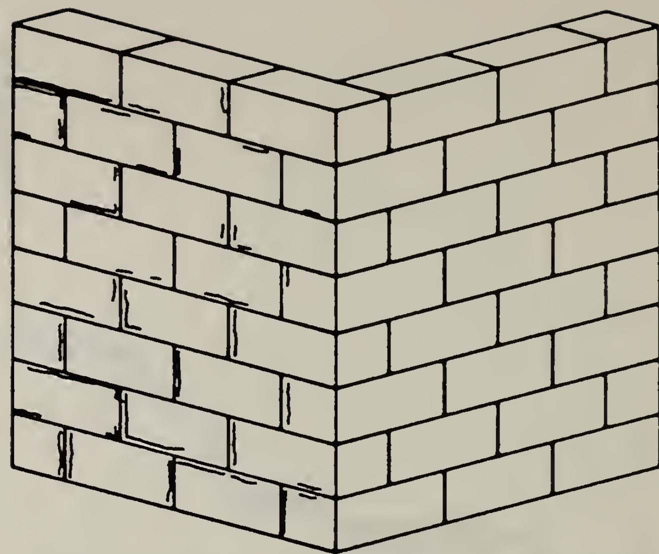

Figure 6.162. Pre-test crack observations for wall C2

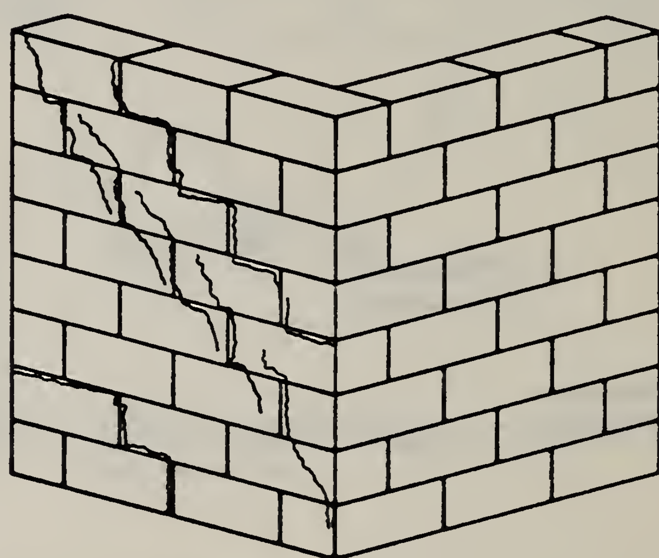

Figure 6.163. Post-test crack observations for wall C2

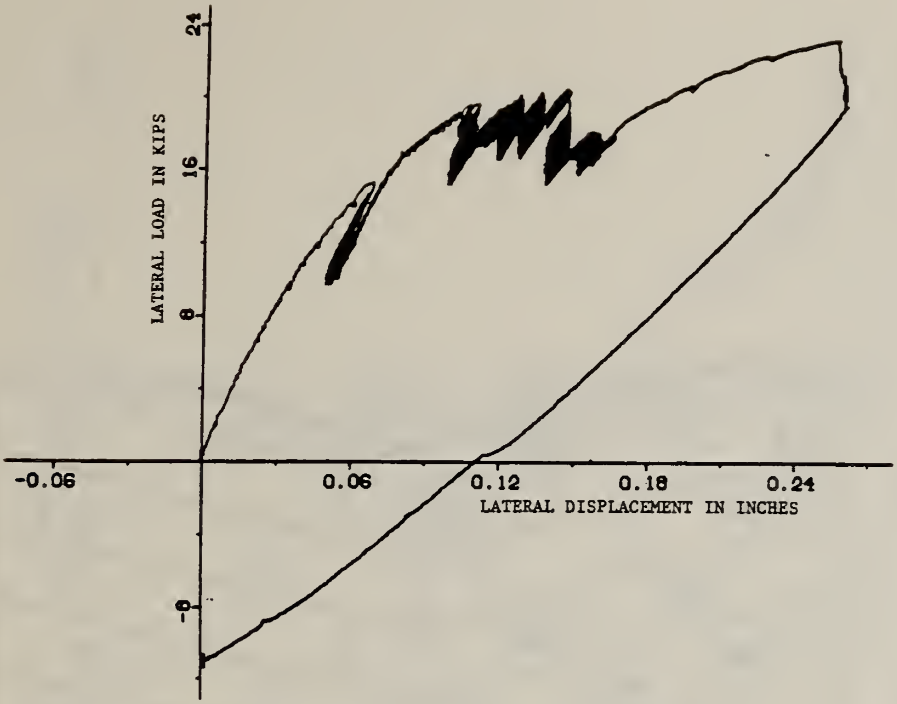

Figure 6.164. Lateral load versus piston displacement for wall C1

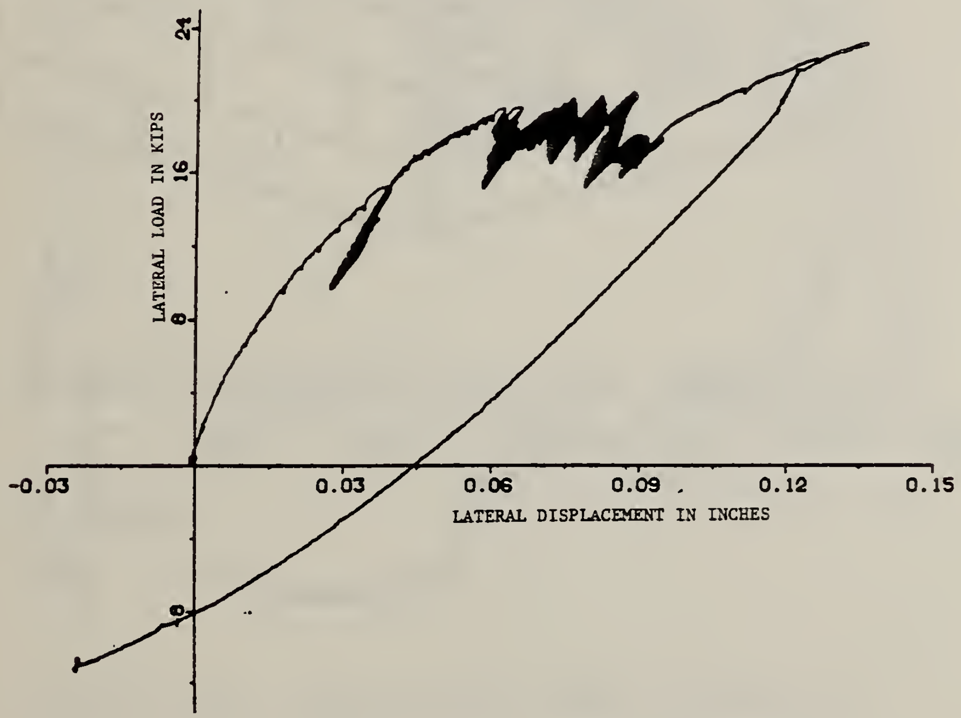

Figure 6.165. Lateral load versus wall displacement for wall C1

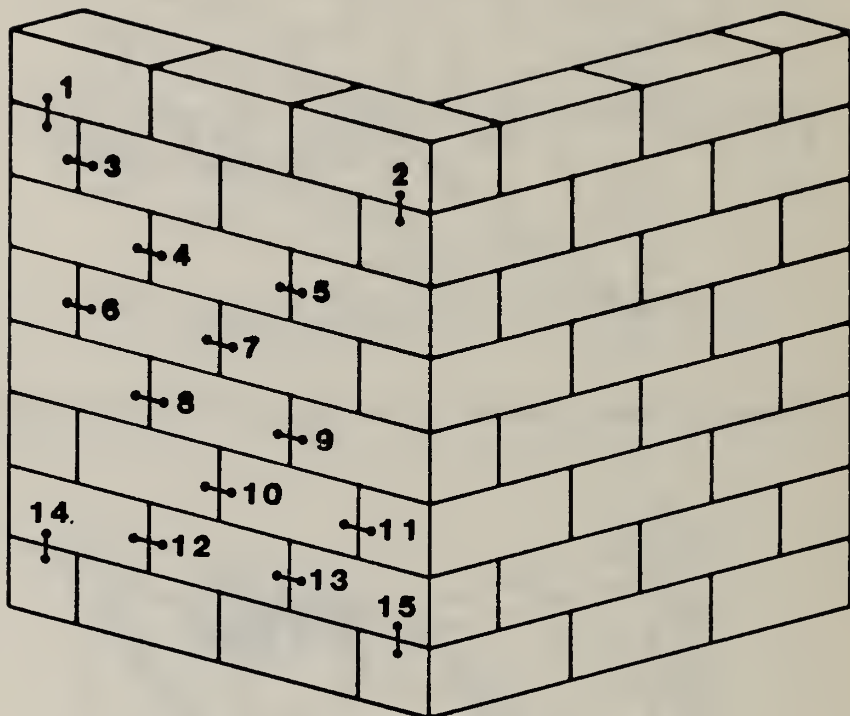

Figure 6.166. Strain measuring locations for wall C1

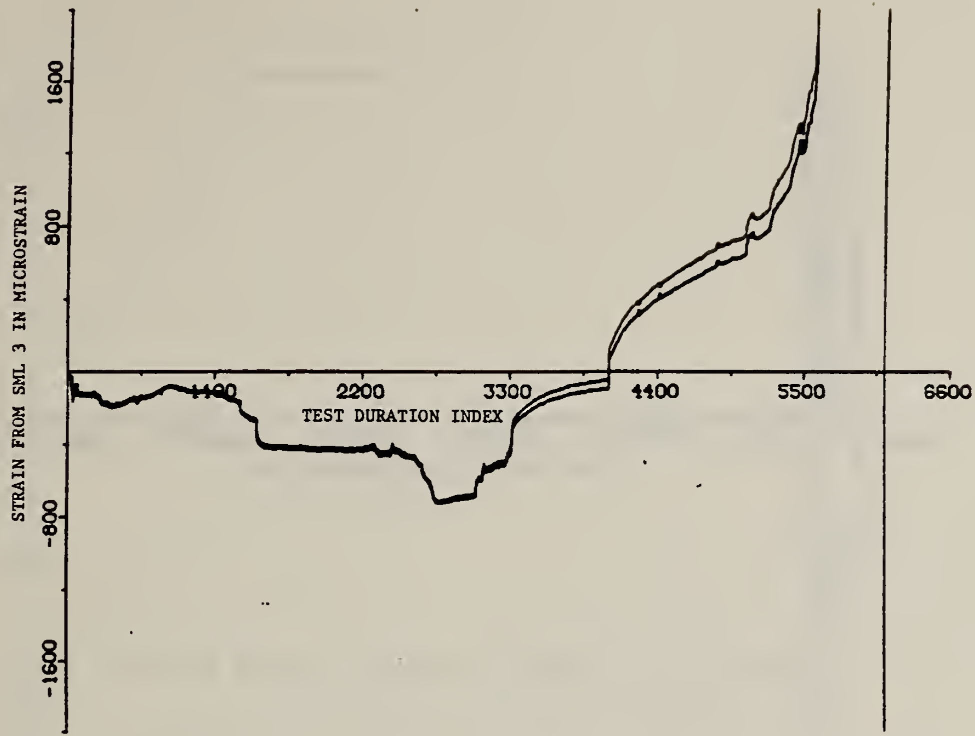

Figure 6.167. Strain history of SML 3 for wall C1

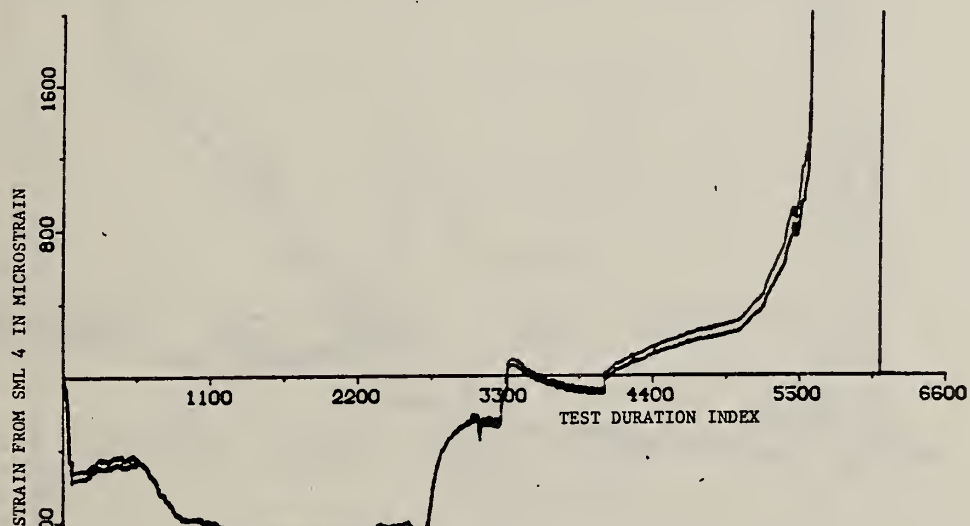

Figure 6.168. Strain history of SML 4 for wall C1

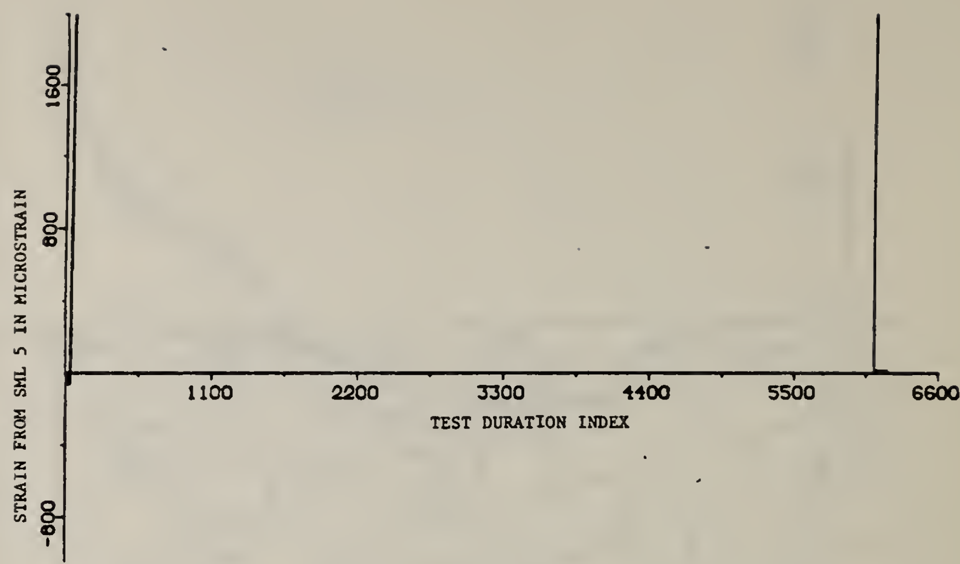

Figure 6.169. Strain history of SML 5 for wall C1

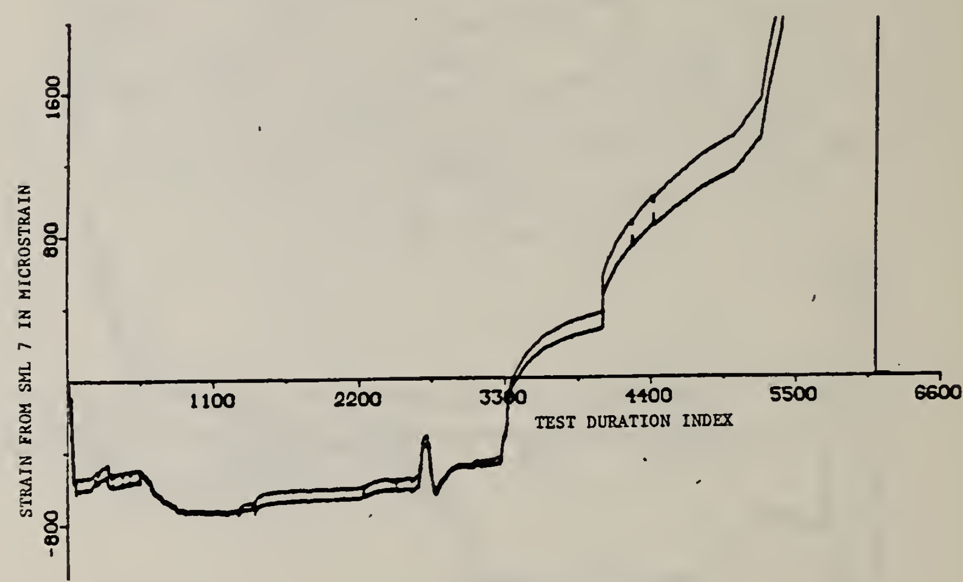

Figure 6.170. Strain history of SML 7 for wall C1

Figure 6.171. Strain history of SML 9 for wall C1

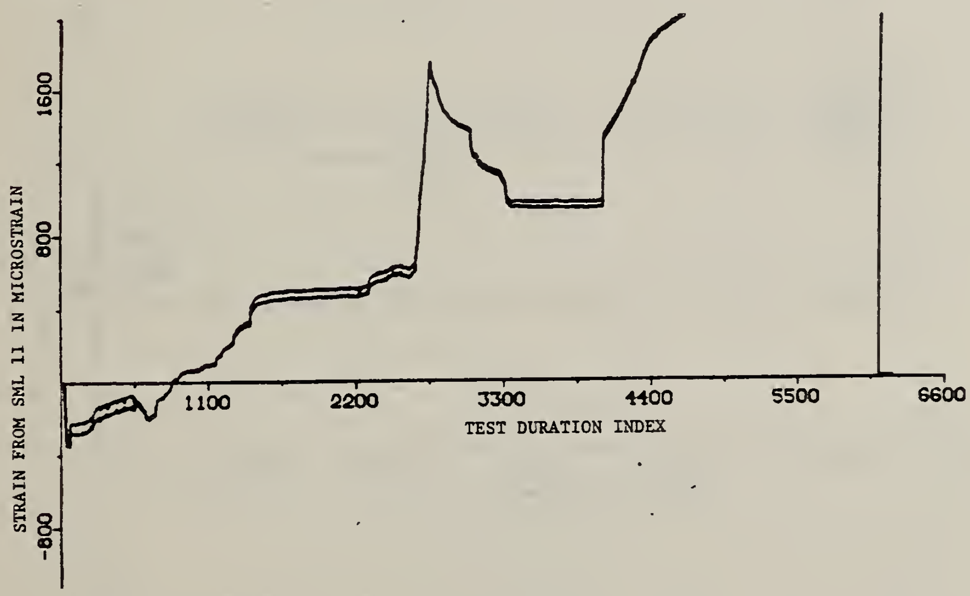

Figure 6.172. Strain history of SML 11 for wall C1

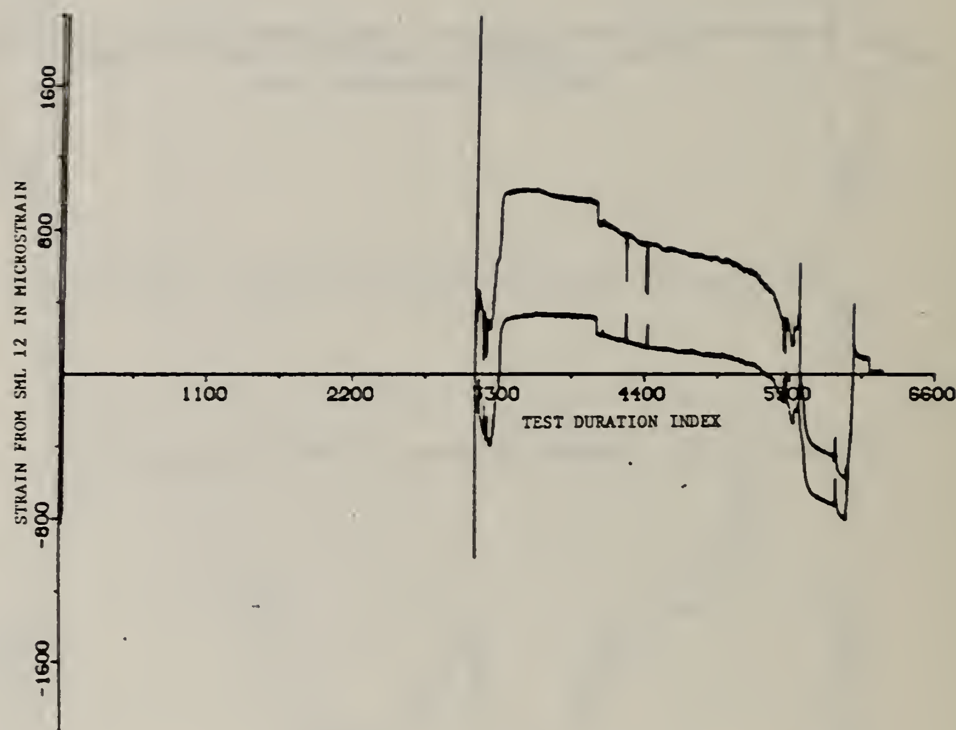

Figure 6.173. Strain history of SML 12 for wall C1

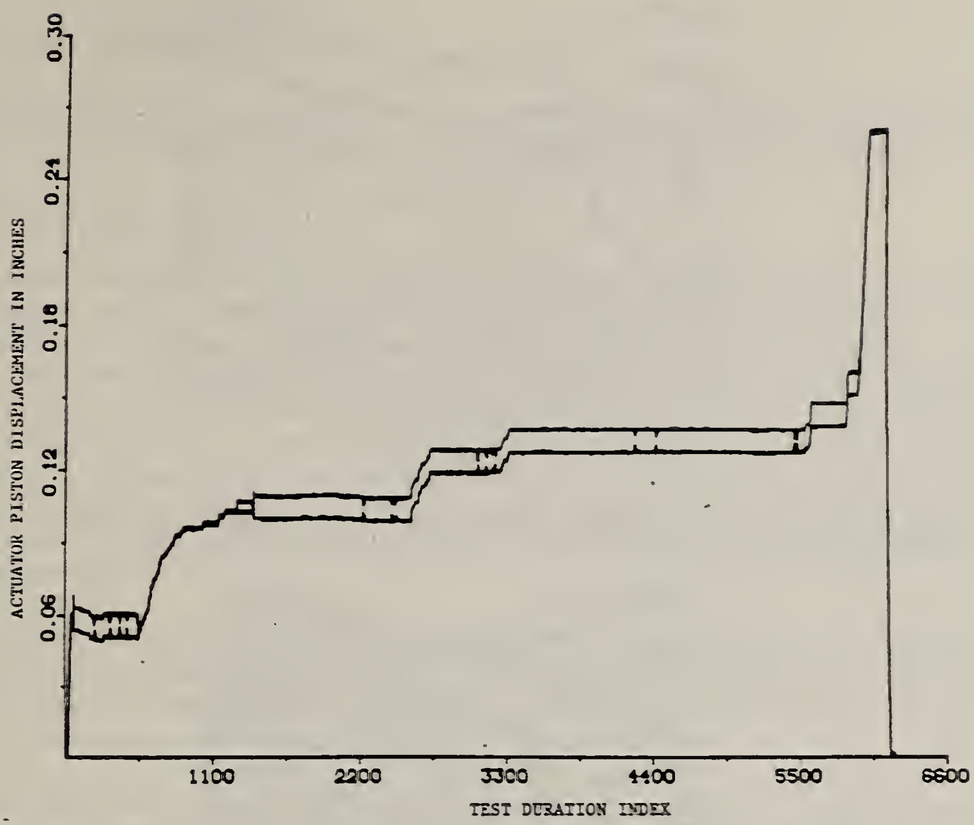

Figure 6.174. Piston displacement history for wall C1

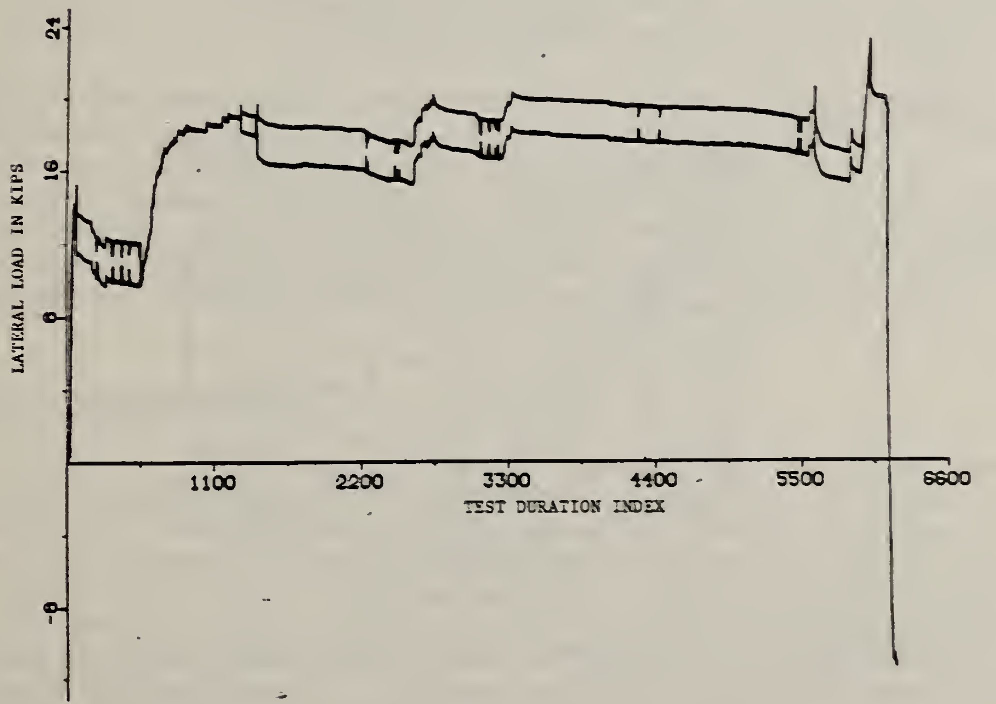

Figure 6.175. Lateral load history for wall C1

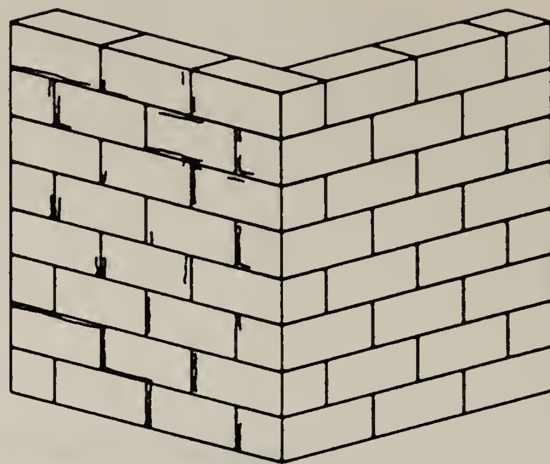

Figure 6.176. Pre-test crack observations for wall C1

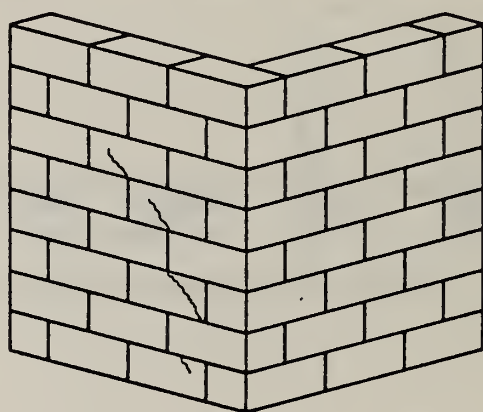

Figure 6.177. Initial diagonal crack observation for wall C1

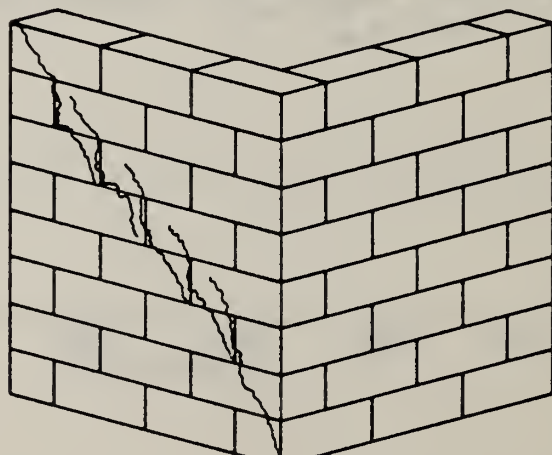

Figure 6.178. Post-test crack observations for wall C1

7. ANALYSIS AND INTERPRETATION

In this chapter the data and observations presented in chapter 6 as well as supplemental information are evaluated and interpretations presented.

7.1 FAILURE MODE AND CRACKING

The failure mode associated with the load capacity failure point was of the diagonal tension form. The diagonal cracking which formed near the failure load/displacement ran from compression corner to compression corner (figure 7.1) and stair-stepped through the joints in most cases. Extensions of the mortar joint cracks did extend into the block but did not connect to form a continuous crack. A good example of such cracking is found in test P8 (figure 6.40). In some tests, a diagonal crack formed just prior to failure, but at failure another diagonal crack formed separate from the first. The first crack then became barely visible and all subsequent crack opening occurred in the second crack.

An interesting observation was that the diagonal cracking first formed near the center of the wall. The wall was still capable of resisting more load at this stage of crack development. However, coincident with load capacity failure the corner blocks split to complete the diagonal crack.

Local cracking around various mortar joints occurred prior to formation of the diagonal crack. Such cracking in some cases confused the interpretation of the strain data. In all probability such cracking occurred at joints already weakened by shrinkage cracking or at joints with little bond capacity simply due to construction. In any event, the local cracking not on the diagonal did not cause shifting of the crack pattern or affect the expected failure crack.

In discussing failure and cracking up to now no mention has been made of flexure. Flexural tension cracks did occur, but the final failure at the maximum load capacity was not a flexural failure, as is discussed in section 7.7. The flexural failure of the wall occurred early in the test, but because an alternate load resisting mechanism was available, namely diagonal compression, additional load resistance was available. Since the flexure failure mode was not critical in these tests it has been omitted from discussion.

7.2 EFFECT OF LOADING HISTORY

The effect of loading history on overall wall behavior is best illustrated using load displacement curves. The in-plane load versus in-plane ram piston-displacement curves (hereafter simply referred to as load-displacement curves) were presented in chapter 6, but for convenience only the significant part of each curve is shown in figures 7.2 through 7.13. Only the quadrant of the plot which includes the load capacity failure point is shown to enhance clarity. The load capacity failure point is defined for purposes of this report to be that point at which load capacity decreases with increasing displacement. Also noted on each of the figures (7.2 through 7.13) is the displacement at which diagonal cracking was observed. As an aid to comparison, the envelope curves are plotted on the same axis for the planar walls (figure 7.14) and corner walls (figure 7.15). An envelope curve is simply a curve which describes the outline of the extreme perimeter of a multi-cycle curve. The major test parameters for each wall are presented in table 7.1.

Loading history can have a pronounced effect on the overall wall behavior as demonstrated by the envelope curves of both the planar and corner walls (figures 7.14 and 7.15). However, it appears that the effect is only significant past a certain load-displacement level. The test P1 (figure 7.8) illustrates this behavior very clearly in that 100,000 cycles were performed at a load-displacement level with no apparent effect on the stiffness and load capacity of the wall. However, the next sequence of cycling at a larger load-displacement level caused a significant drop in load capacity and the formation of a diagonal crack. The same behavior was exhibited by walls C2 and C1, figures 7.11 and 7.12, respectively.

The three tests P1, C2, and C1 used only a small cyclic displacement amplitude and some question as to the effect of larger cyclic displacement test amplitudes is raised, but test P6 (figure 7.4) which was a fully reversed cyclic test exhibited the same general behavior. The test results suggest, then, that loading history can significantly affect the overall response of the wall, but only if some threshold value of load/displacement is exceeded. With the test results available it is not possible to define the actual threshold value for susceptibility, but it is clear that in general terms the load threshold is a sizable proportion of the walls actual load capacity failure level. For general design considerations such a high threshold would generally imply that normal service condition loadings would not produce any cyclic effects.

The actual effect that loading history has on the overall wall behavior when the susceptibility threshold is reached can not be fully described with the limited data available. It does not appear that stiffness within the small cyclic displacement range, is noticeably affected but the load capacity corresponding to a particular displacement level can be dramatically reduced. The magnitude of the effect on stiffness may be dependent on some particular parameter in the general loading history because while tests P1 and P5 (figures 7.9 and 7.7) exhibited almost no stiffness reduction in the range of cyclic displacements, tests P8 and P3 (figures 7.5 and 7.8) exhibited noticeable stiffness reduction. The difference in behavior between the two sets of tests may be due to a significant difference in cyclic displacement range. While the stiffness of the walls measured between small changes in displacement does not seem particularly affected by cycling, it is clear the cycling reduces the in-plane stiffness of the wall as measured from the zero displacement position to the achieved displacement. Cycling in the susceptible range causes the displacements associated with a certain load to increase, reduced stiffness. Higher load resistance may only be achieved at the expense of larger displacements. A good example of this behavior is test C1 (figure 7.13) in which the load capacity lost due to cycling was recovered but only by a significant increase in lateral displacement.

The discussion up to now has focused on behavior prior to the load capacity failure point. It is clearly evident that post-failure behavior is extremely poor with large reductions in load capacity, a negative stiffness. The effect of repeated excursions into the failure zone is much more pronounced than excursions in the susceptibility range. Test P5 (figure 7.7) shows quite graphically the kind of severe degradation which comes about by cycling to displacements greater than the failure displacement.

The effect of loading history on the overall wall behavior has been described in terms of global parameters, applied load, and displacement. The general observation was that there was no effect until a definite threshold value of load-displacement was reached. The effect of loading history on the measured local strains was masked by the general variability of the local strains. It would seem, however, that the effect is much the same on the strains as it was for the overall behavior, but not nearly so pronounced. During cycling between constant displacement levels some local strains showed a tendency to increase in an absolute sense, but the cyclic strain amplitude did not significantly change. This observation is not true, of course, for the strains measured across the diagonal cracks after the load capacity failure point. In this case, the strains in some cases grew both absolutely and in terms of the cyclic amplitude. In summary, the value of local strains was most dependent on the displacement level itself and not on the repetitions of achieving the displacement level.

Included in loading history is rate effect. The cyclic tests were all run at between 2 and 6 Hz with most at 6 Hz. This frequency was considered high enough that the dynamics of vibration loading was at least represented. For information purposes, however test P9 was used to examine the likely effect of strain rate. Two half cycle loadings to about half of the expected maximum load capacity at two very different loading rates (section 6.4.3) indicated that the rate did not affect the wall response. This can be seen by the load-displacement curve (figure 7.3) and the strain histories (figures 6.9 and 6.10). However, the third loading to load capacity failure at a high rate suggests that such a conclusion is not true for the entire loading history. It is seen in figure 7.14 that a comparison shows that test P9 maintained its initial stiffness to a higher maximum load capacity compared to the other tests. There is insufficient information at present to positively determine the effect of rate because of the changing parameters between the walls tested. For example, test P9 had a higher initial precompression compared to the others and it is not possible at this time to separate the effect of precompression.

7.3 CORNER WALL VERSUS PLANAR WALL BEHAVIOR

The following discussion excludes the corner wall displaced along its z-axis which is discussed separately.

There did not seem to be any reason to differentiate the behavior of planar walls from corner walls. The effect of the outstanding leg in the corner walls was negligible on the cracking pattern and general wall behavior. Comparing the envelope curves in figures 7.14 and 7.15 shows the corner walls have a slightly smaller stiffness and a uniformly lower maximum load capacity. These reductions can be attributed to the smaller size of the in-plane leg of the corner wall (48 x 64 in) as compared to the planar wall (64 x 64 in). The diagonal cracking of the corner walls did not include any portion of the outstanding leg and as in the planar walls extended essentially from compression corner to compression corner along the diagonal in a stair-step fashion.

7.4 EFFECT OF Z-AXIS DISPLACEMENT

The final failure mode of the z-axis displaced corner wall was a diagonal crack in both legs from the compression corners at the upper surface of the wall to the compression corner at the wall intersection on the bottom surface (figure 6.115). It is evident that each leg contributed to the total lateral load resistance. It would also seem that the total load resistance was roughly equally divided between the two legs as indicated in figure 6.98. The actual loading history imposed on the wall as shown in figure 6.98 shows that the imposed displacement in the north-south direction lagged behind the displacement in the east-west direction. This may have influenced the total wall behavior since the east-west leg may have failed before the north-south leg causing a major redistribution of the additional imposed load onto the north-south leg. The resultant load-displacement diagram, plotted to the same scale as the curves in figure 7.15 is presented in figure 7.16. It is clear that the stiffness of the z-axis loaded wall suffered a major reduction in stiffness at a fairly low level of displacement. The first load plateau on the curve is at a level which is comparable to the total load capacity of the other corner walls. However, the wall continued accepting load at substantially higher displacements as shown in figure 7.17 which presents the complete resultant curve. An interesting fact from the complete curve is that the maximum resultant lateral load capacity was approximately equal to the value obtained by taking the average maximum load value of walls C3 and C4 (also, both montonic tests) and multiplying by $\sqrt{2}$. It would seem that the total (resultant) capacity of a corner wall can be computed by finding the resultant of the component resistances.

7.5 LOCALLY MEASURED STRAINS

An important component of the instrumentation was strain measuring devices mounted across mortar joints on one wall surface. Similar instrumentation had been used in the field studies and it was expected that the information gathered in the different studies could be correlated. The devices themselves worked well, but their usefulness was limited. The strain measuring devices were to serve several purposes: 1) provide information on the relationship between measured strain and visible cracking; 2) serve as a benchmark between field studies and the tests reported herein; and 3) indicate the level of damage or distress in a wall.

It appears that as used in the research reported herein, the strain measuring devices did not produce strain values which correlated with the onset of visible cracking. This is not surprising considering the difficulty of observing small cracks on a very disjointed and textured surface typical of a concrete block wall. There are many surface disruptions at joints which appear as cracks. In some cases strains of over 1000 microstrain were measured with no cracking visible even with magnification. In other cases cracks were visible at locations where as litle as 500 microstrain was measured.

The usefulness of locally measured strains as benchmarks between tests is also extremely limited. The strains measured at single points in a matrix material were unduly affected by local irregularities and flaws. It was apparent that in early stages of a test the strain values reflected the general variability of the materials. A joint crossed by a strain measuring device and having unusually weak tensile bond due to shrinkage cracking, for example, could show large strains during the test and not be part of the final diagonal cracking. The local strains reflected the general breakdown of the matrix bond between the blocks and are a result of many things, including just a gradual breakdown as a result of repeated movements. It is clear that no single local strain value provided reliable information as to the state of damage in the wall.

So far the impression has been negative as to the usefulness of the local strains. However, as a general measure of wall behavior the strains do serve a very useful function to the researcher. Taken as a whole rather than individually the strains can provide clues as to the proximity to failure. For example, one strain gage could be measuring a very high local tension strain, but if other gages along the probable diagonal crack path indicated only small tensile strains or compression strains then it would be clear that total failure was not imminent. However, a great deal of judgment is obviously required since a diagonal crack can form quite suddenly.

7.6 DAMAGE THRESHOLD

As indicated in an earlier section, the tests indicate that there is a load-displacement threshold above which the walls are subject to damage due to cycling. What constitutes damage is, of course, somewhat arbitrary. If visible cracking is the criteria then the threshold value becomes vague since some visible cracking of the local nature can occur at almost any time. If damage is taken to mean that a loss in load capacity occurs with repeated excursions to a particular displacement level then it is easier to establish a threshold value. The clearest illustration of the existance of a threshold comes from the corner wall tests. The envelope curves shown in figure 7.15 clearly show a consistent break in the curves at a definite displacement value though not load. This consistency can be taken as evidence that it is displacement (strain) which is the critical parameter for defining the threshold. The planar walls show the same general trend (figure 7.14), but the curves are harder to compare because of the changing test parameters not found in the corner wall tests. From previous discussions it is clear that it would be extremely difficult to relate the global displacement threshold to a local strain value as measured by the strain devices. However, a global strain approach may lead to a more reliable and uniform relationship.

7.7 APPLICABILITY OF TEST RESULTS

The failure of the walls is best described as a diagonal tension failure with the accompanying diagonal cracking. This mode of failure was expected, and, in fact, desired since the observed crack pattern in the field studies was along diagonals of the walls. However, the supplementary requirements that proved to be necessary to produce the diagonal tension failure for in-plane shear make it doubtful that the diagonal cracking of typical concrete block masonry walls in residential dwellings is due solely or even primarily to in-plane shear forces.

In table 7.1 there is reference to the axial load applied to the wall at the time the maximum load capacity is reached. The values are considerably higher than the precompression axial loads which are also listed. This apparent discrepancy points to the manner in which the load resisting mechanism of the walls change during the test. Normally, a resistance is determined by the weakest resistance mechanism. For the simple case of an unreinforced wall subjected to a lateral (in-plane) load the most likely weak link is flexure. Using an incremental summing technique and assuming a representative stress-strain curve for concrete block masonry the ultimate flexural capacities of the walls were computed. The resulting capacities (table 7.2) indicate that at best (assuming a 100 psi tension capacity) the equivalent ultimate lateral load is about 9 kips. A value of 9 kips is approximately one-half of even the minimum lateral load capacities measured in the test. Flexural tension cracks were observed in the test so the flexure mechanism was active during at least part of the test. Clearly, flexure was not the only mechanism present.

The second mechanism which permitted the increased lateral resistance was the formation of a compression strut (figure 7.1). However, the compression strut could only become active as a result of the boundary conditions imposed on the wall. A flexural failure, if it were to occur in these walls, would lead to overturning of the wall-almost as a rigid block rotating about the lower compression corner (figure 7.18). Such overturning would be accompanied by an upward movement of part of the wall. However, the test setup intentionally restrained vertical displacement to prevent rotation of the upper wall surface. The result is a reaction point which resists overturning which then increases the apparent lateral load resistance. The restraint reaction increases or adds to the axial load intentionally applied to the wall.

In the end the reaction force can only increase to the level where the combination of axial load and lateral load acting principally at opposite corners cause a diagonal tension failure.

The fact that the compression strut mechanism comes into play only after exceeding the flexural capacity of the wall can be shown by the plots of total applied axial load versus measured restraining moment in the tests. For clarity, only results from the monotonic tests are shown in figure 7.19 the tests P2, C3, and C4 have comparable levels of axial precompression stress. It is clear that the applied axial load only begins to increase past the precompresion at a definite applied moment which agrees well with the computed flexural capacities of the walls accounting for the actual precompression stress (table 7.2). In addition to the increase in axial load it was found that the location of axial thrust varied as the compression strut mechanism came into play. At the time of failure the axial thrust had moved to the extreme compression end of the wall leading to an applied force distribution as shown in figure 7.1.

The implications of the preceding discussions do not invalidate the tests. Rather, the information illustrates the applicability of the test behavior to actual design situations. Because of the requirement for vertical restraint it is clear that to apply the wall behavior from these tests to single family residential construction would be unwise. The tests are more applicable to components in high-rise load bearing construction where it is more likely that sufficient vertical restraint is present.

Table 7.1. Wall Test Parameters

			At Point of Maximum In-Plane Load			
Wall	Precompression Axial Load (kips)	Loading History Type	In-plane Load (kips)	Axial Load (kips)	In-plane Ram Displacement (in.)	In-plane Wall Displacement (in.)
P1	14	Cyclic/Prestrain	24.4	28.8	0.087	0.050
P2	14	Monotonic/Ramps	22.2	29.6	0.226	0.073
P3	14	Cyclic/Prestrain	21.2	36.6	0.135	0.061
P5	14	Cyclic/Prestrain	27.0	35.9	0.162	0.106
P6	4	Cyclic/Reversed	17.5	16.9	0.082	0.053
P8	5	Monotonic/Ramps	27.3	33.0	0.167	0.129
P9	18	Cyclic/Prestrain	30.0	37.2	0.131	0.087
P10	13	Cyclic/Reversed	19.4	21.8	0.093	0.063
C1	16	Cyclic/Prestrain	23.2	54.1	0.256	0.136
C2	16	Cyclic/Prestrain	21.7	35.5	0.138	0.080
C3	16	Monotonic	19.1	31.7	0.129	0.084
C4	16	Monotonic	17.6	30.6	0.129	0.084

Table 7.2. Axial Load - Moment Interaction Values

Planar Walls

Axial Load (kips)	Moment (kip-inches)
40	1129
30	887
20	615
14	438
10	315
5	158
3	96

Corner Walls

Axial Load (kip)	Moment (kips-inches)
40	1156
30	907
20	629
16	509
10	322
5	162
3	98

Notes: The values are based on an ultimate compressive strength of 1400 psi.

Net bedded area section properties were assumed.

The stress-strain history was assumed to follow Hognestad's curve.

The corner wall values are for the outstanding leg in tension.

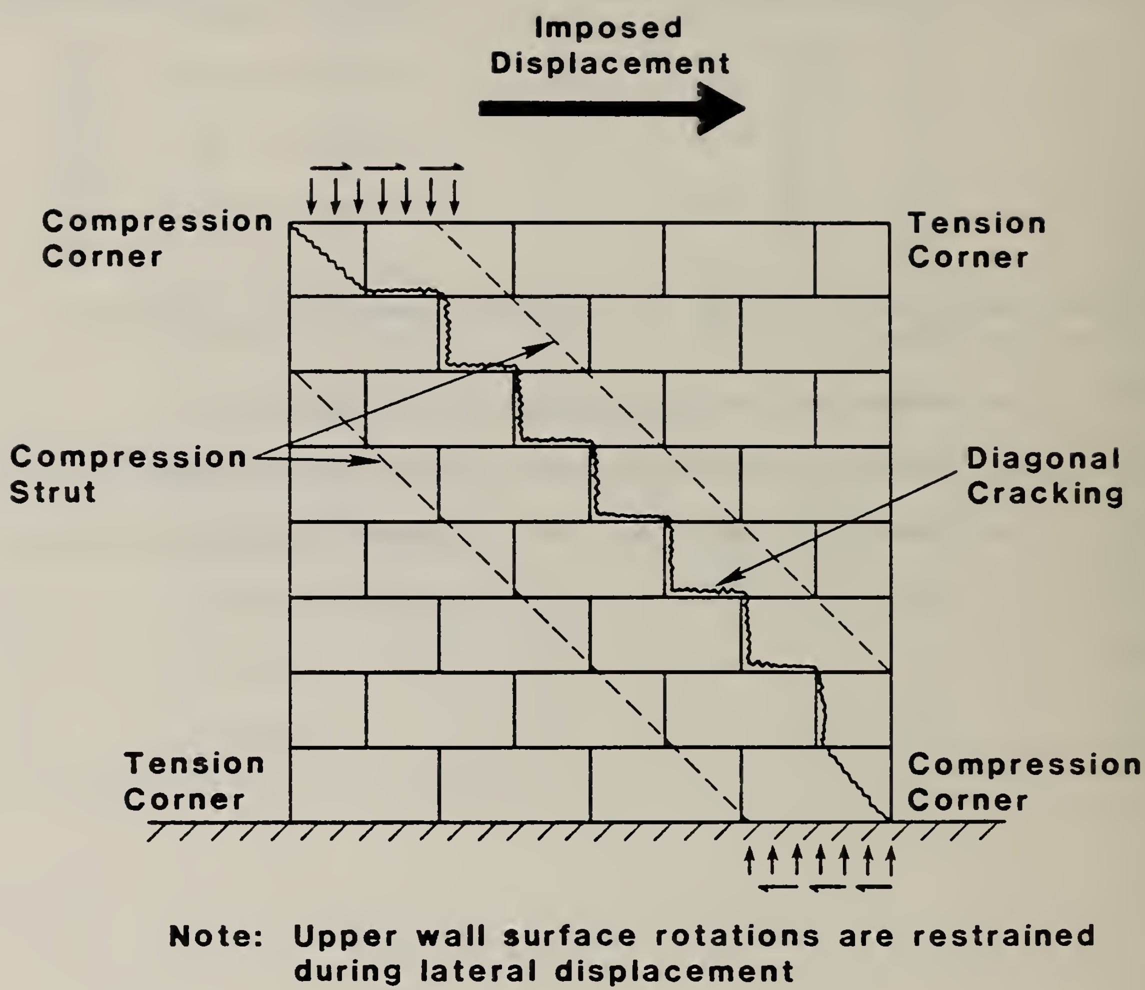

Figure 7.1. Diagonal tension failure

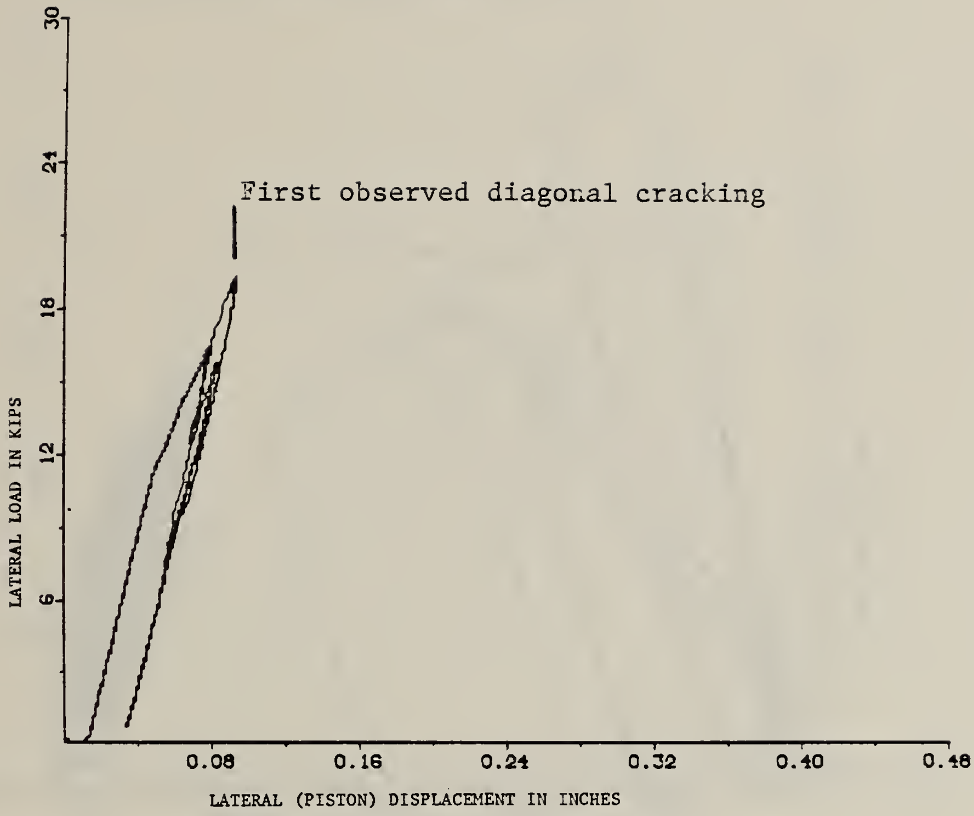

Figure 7.2. Load displacement curve for test P10

First observed diagonal cracking

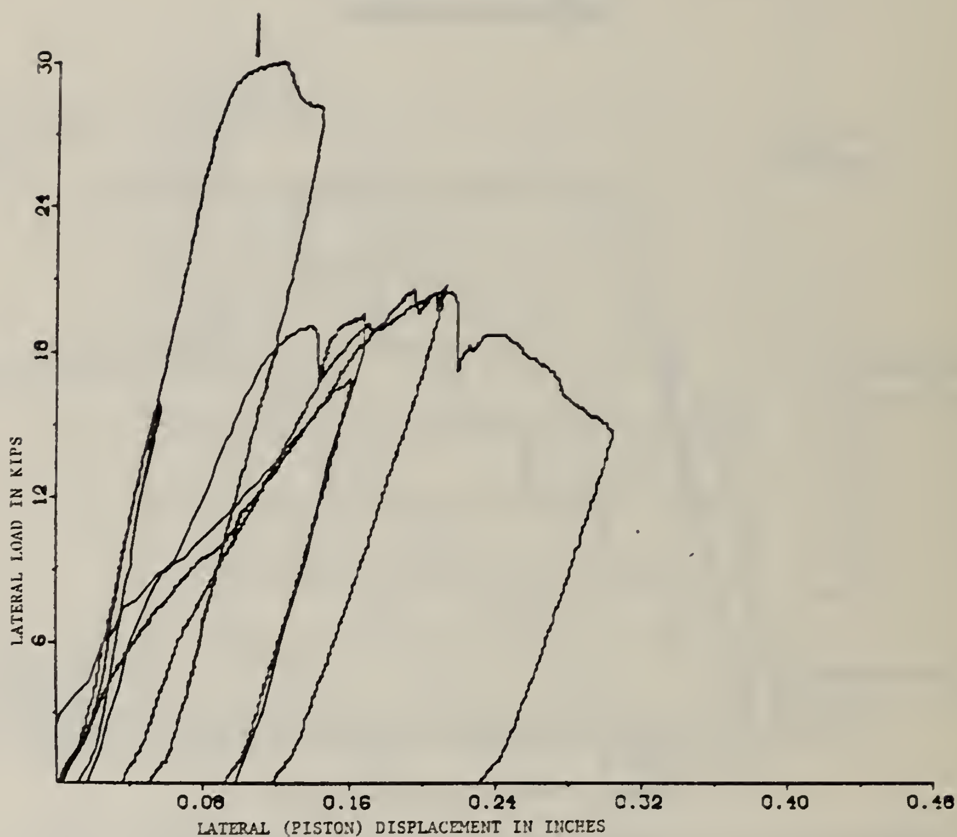

Figure 7.3. Load displacement curve for test P9

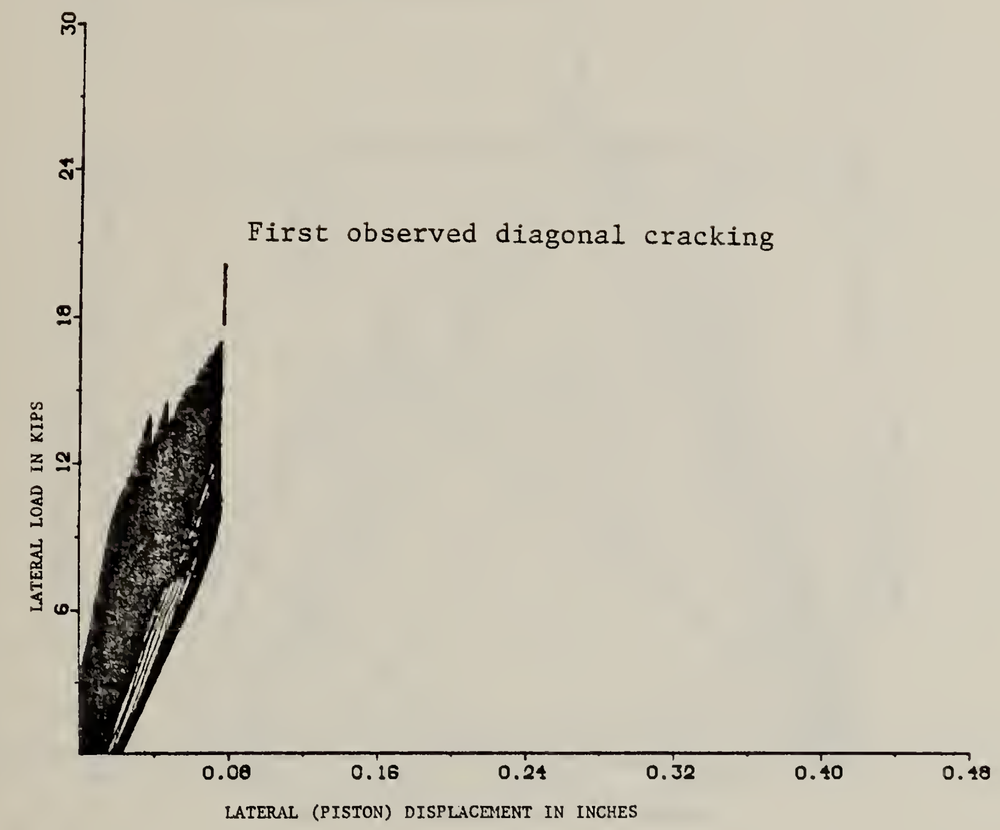

Figure 7.4. Load displacement curve for test P6

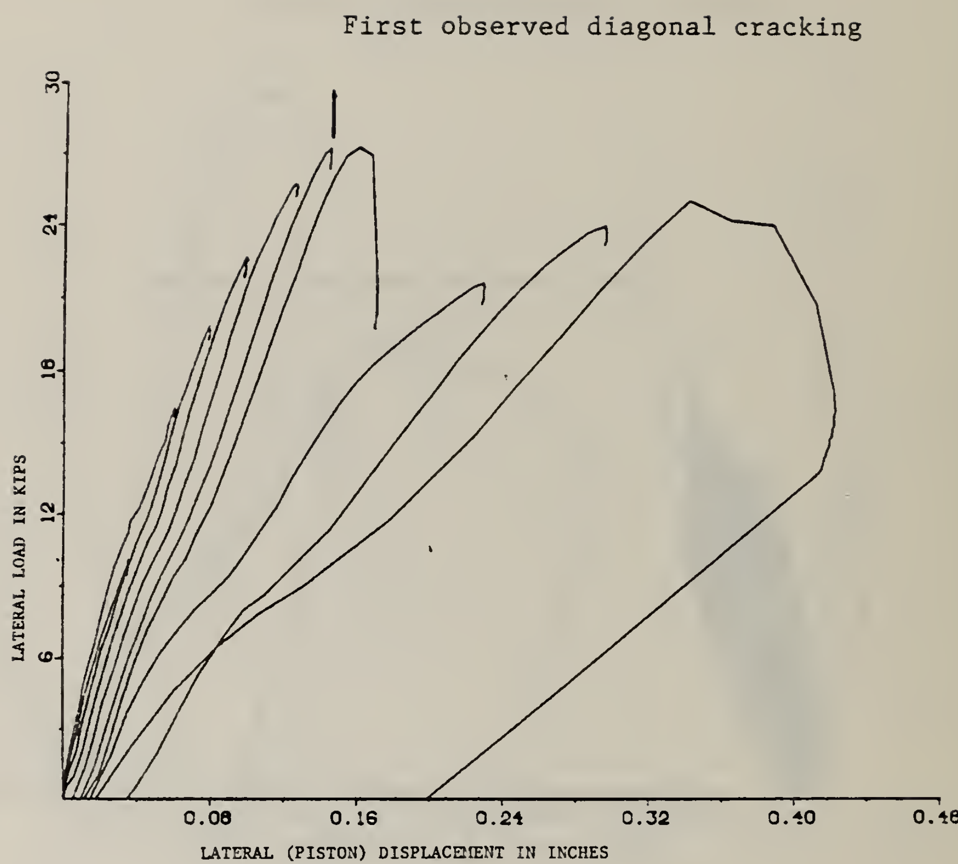

Figure 7.5. Load displacement curve for test P8

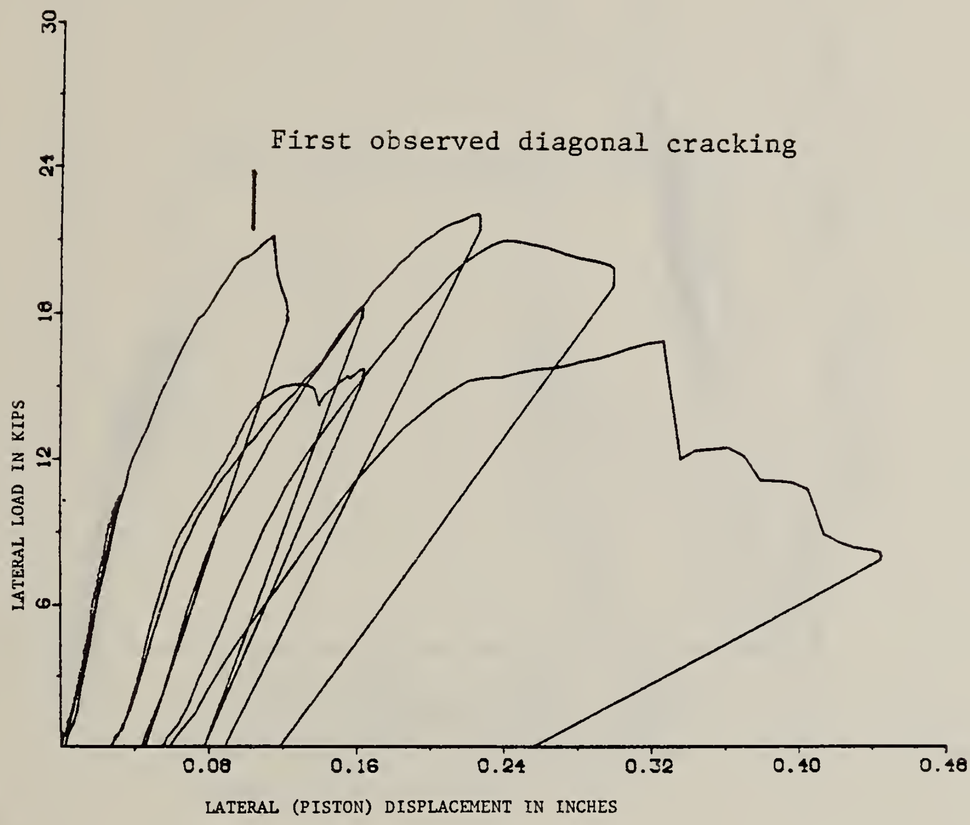

Figure 7.6. Load displacement curve for test P2

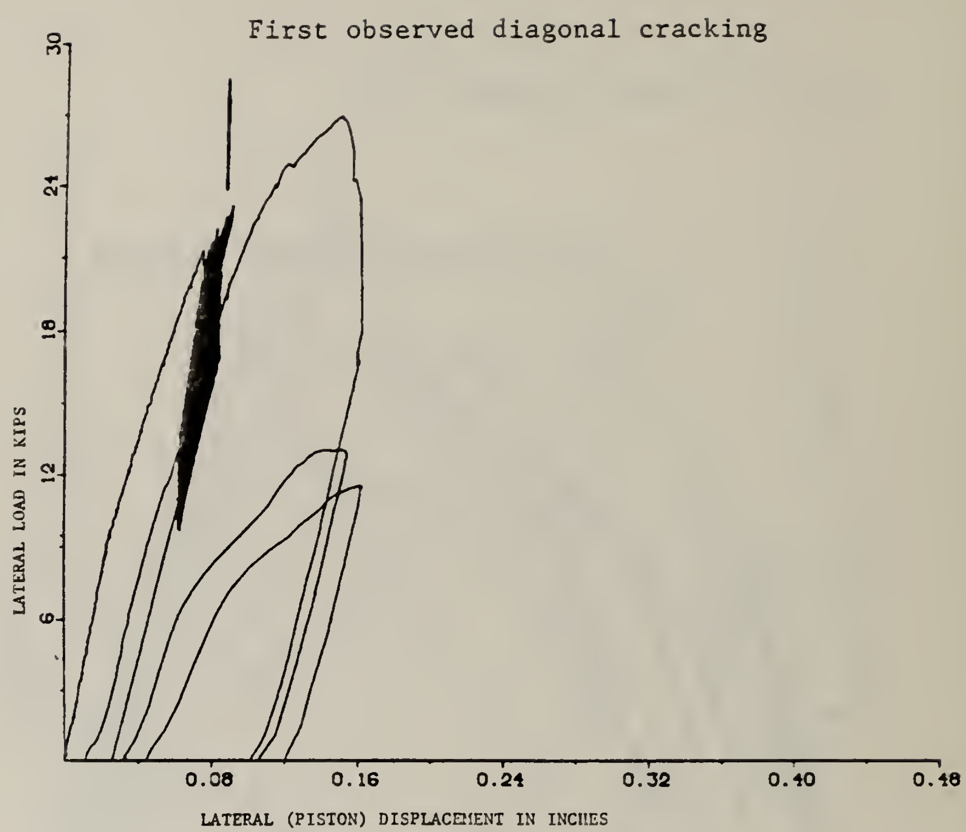

Figure 7.7. Load displacement curve for test P5

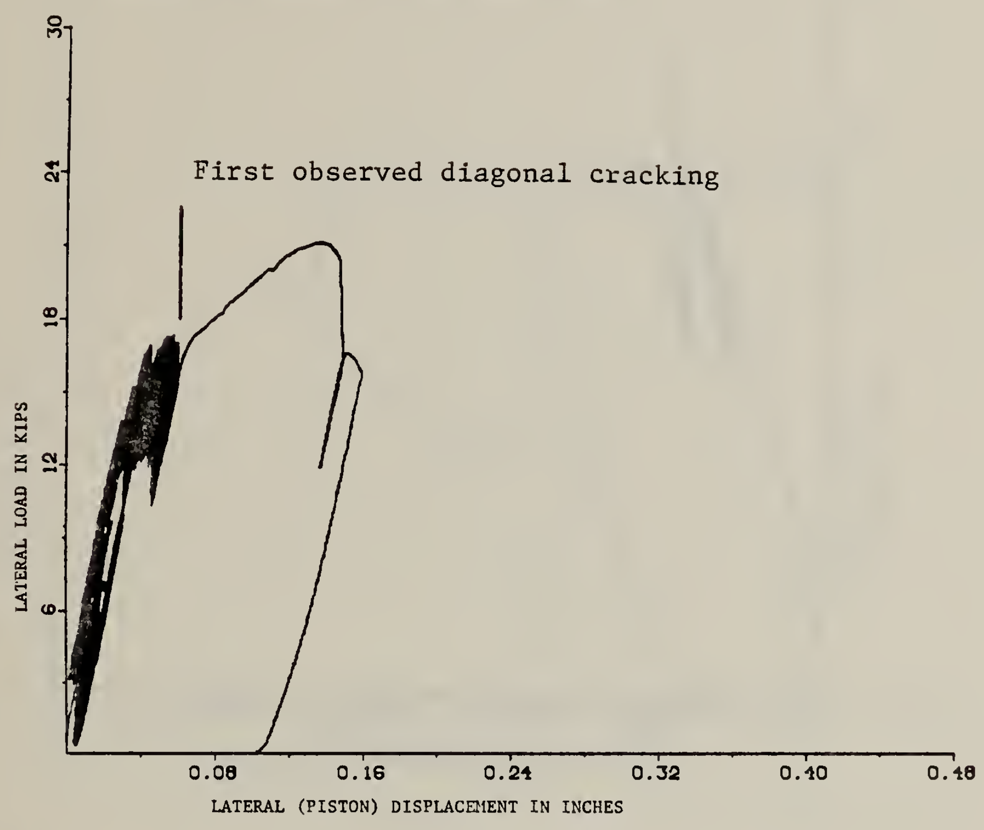

Figure 7.8. Load displacement curve for test P3

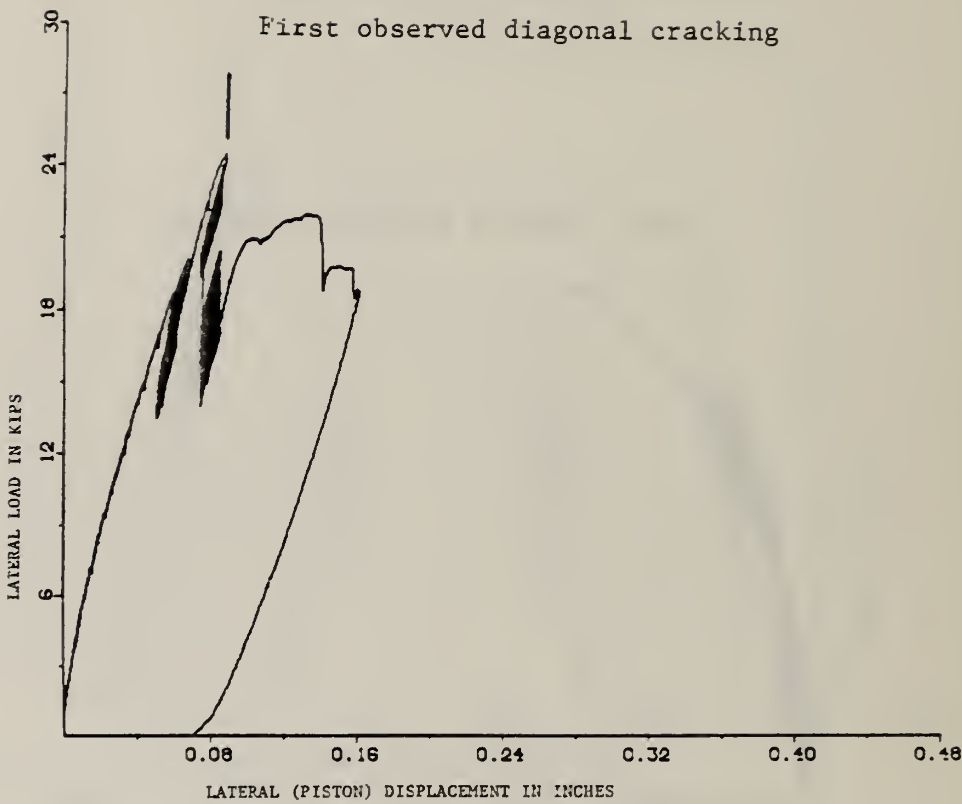

Figure 7.9. Load displacement curve for test P1

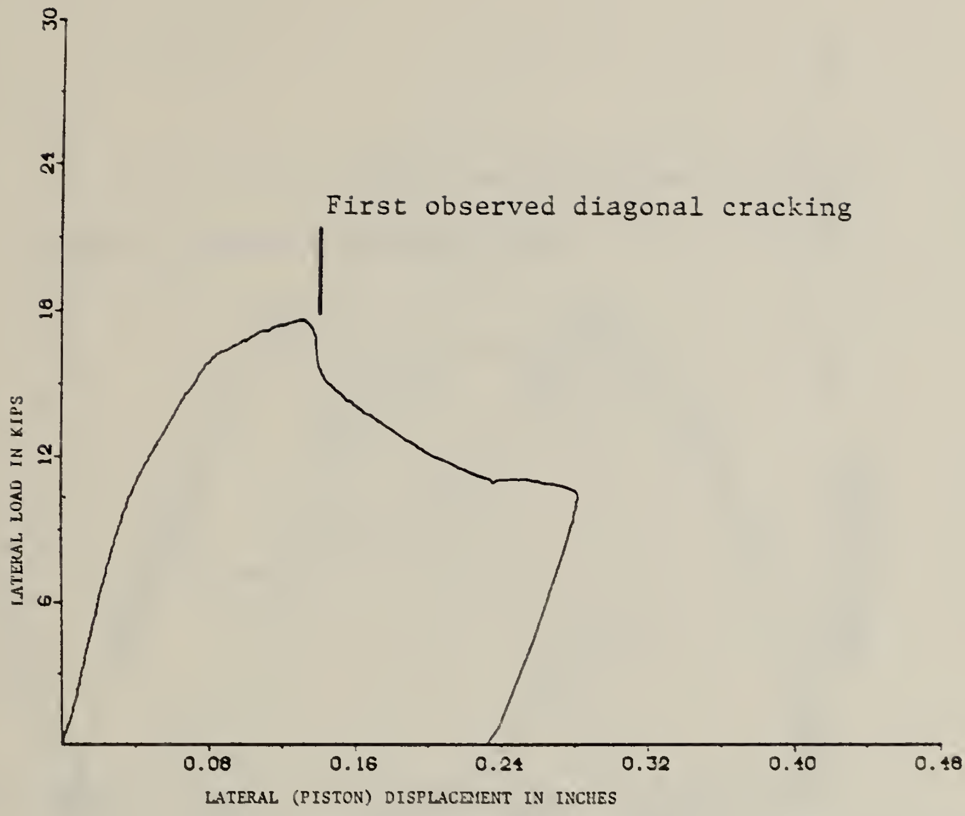

Figure 7.10. Load displacement curve for test C4

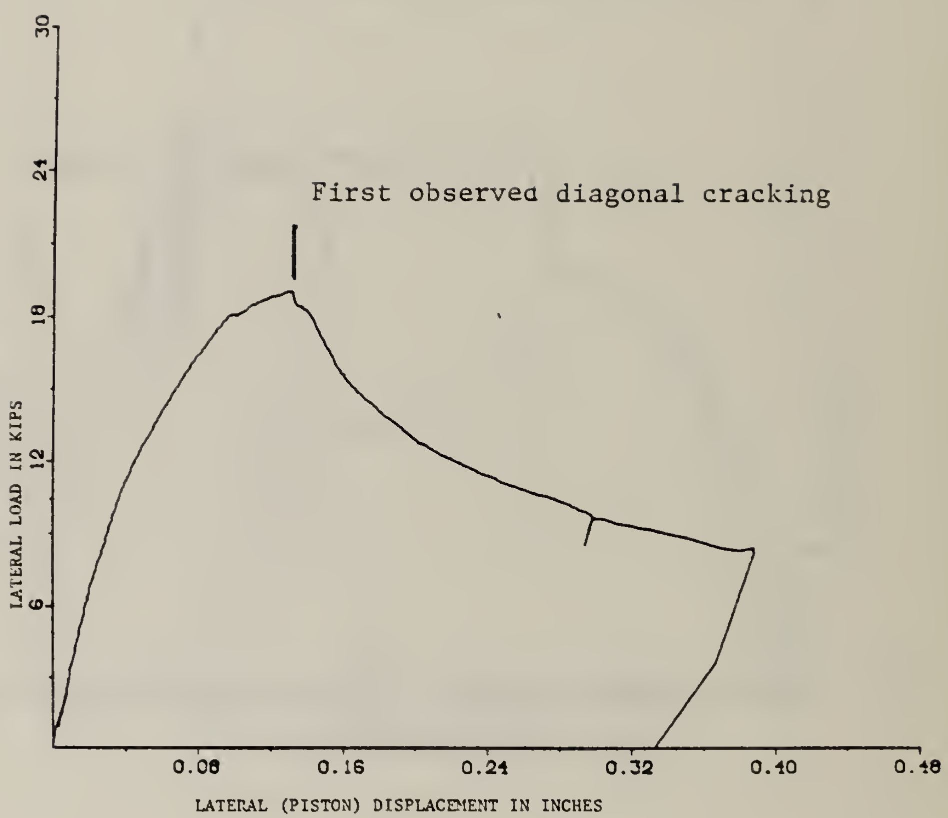

Figure 7.11. Load displacement curve for test C3

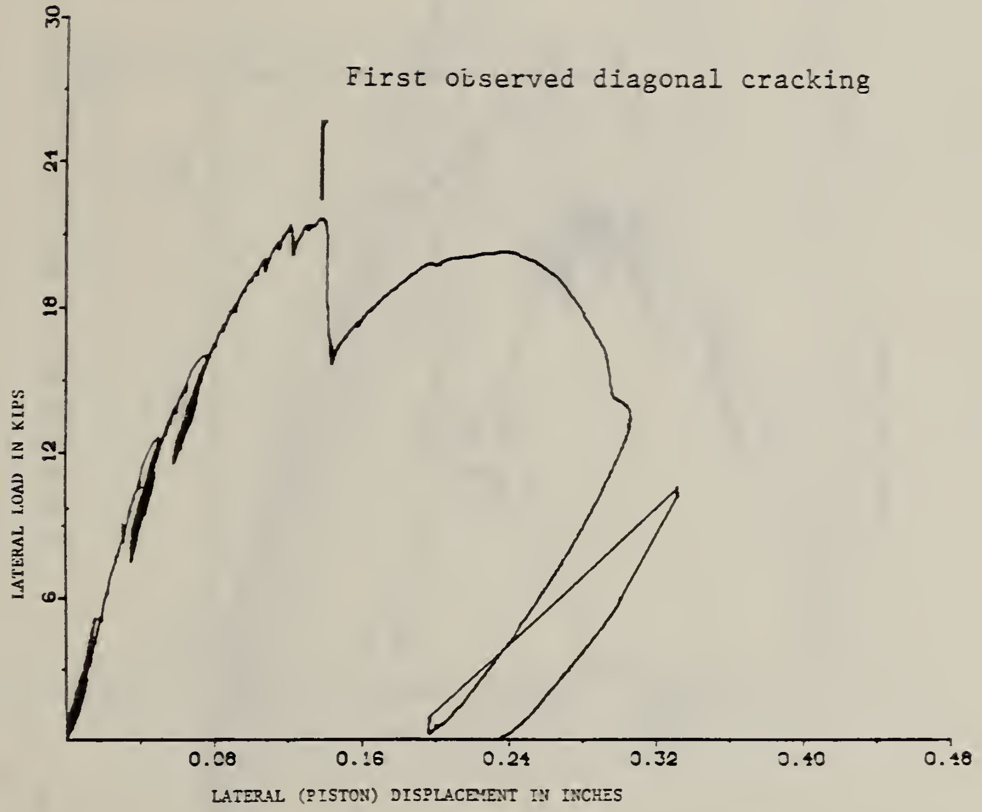

Figure 7.12. Load displacement curve for test C2

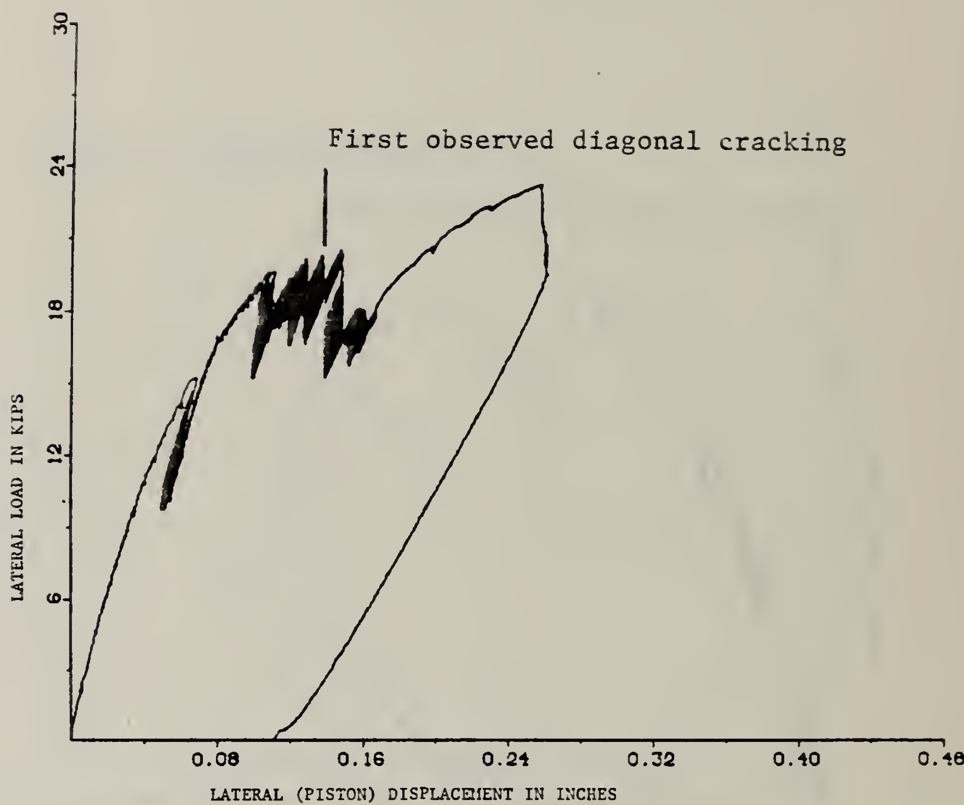

Figure 7.13. Load displacement curve for test C1

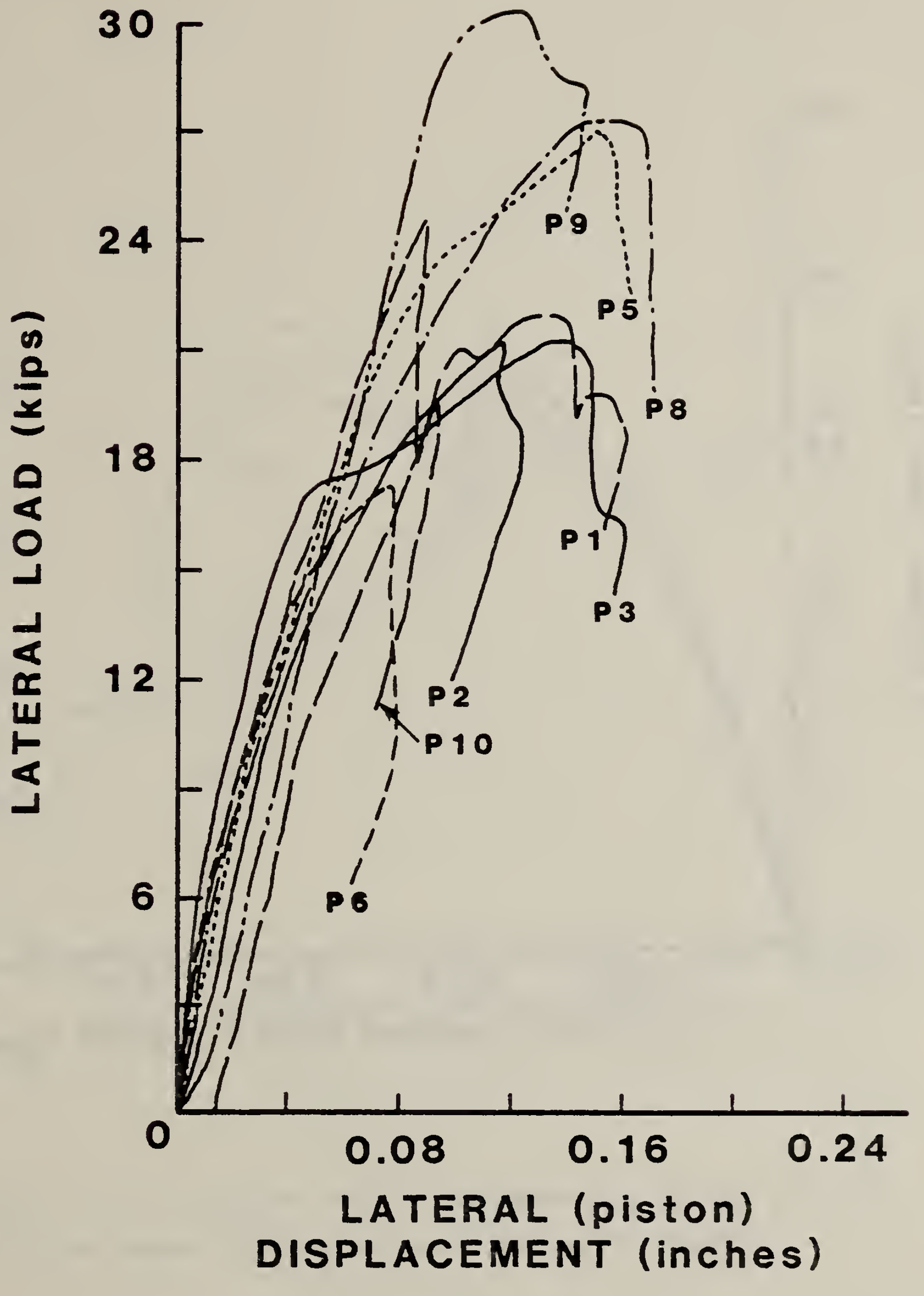

Figure 7.14. Envelope curves for planar wall tests

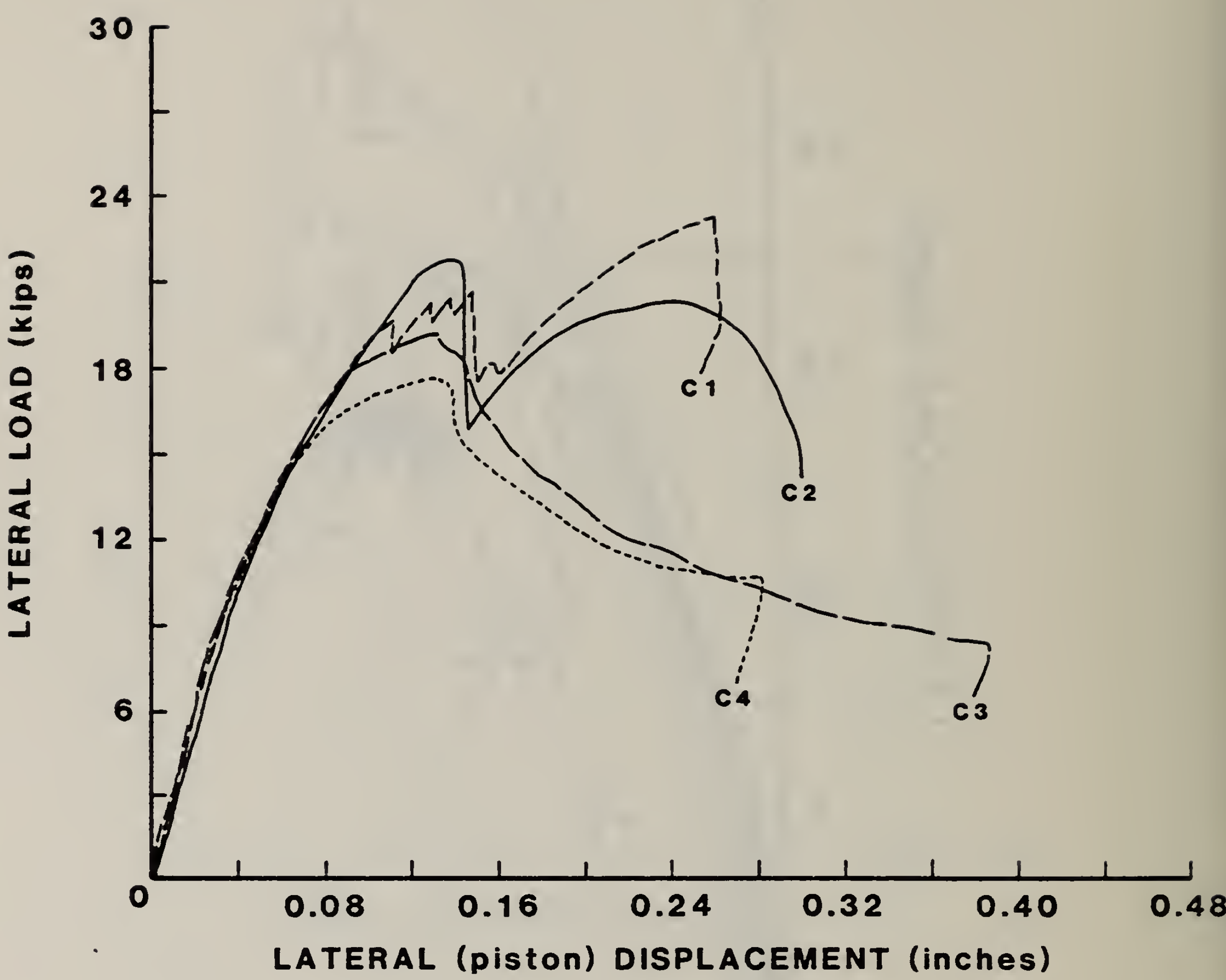

Figure 7.15. Envelope curves for corner wall tests

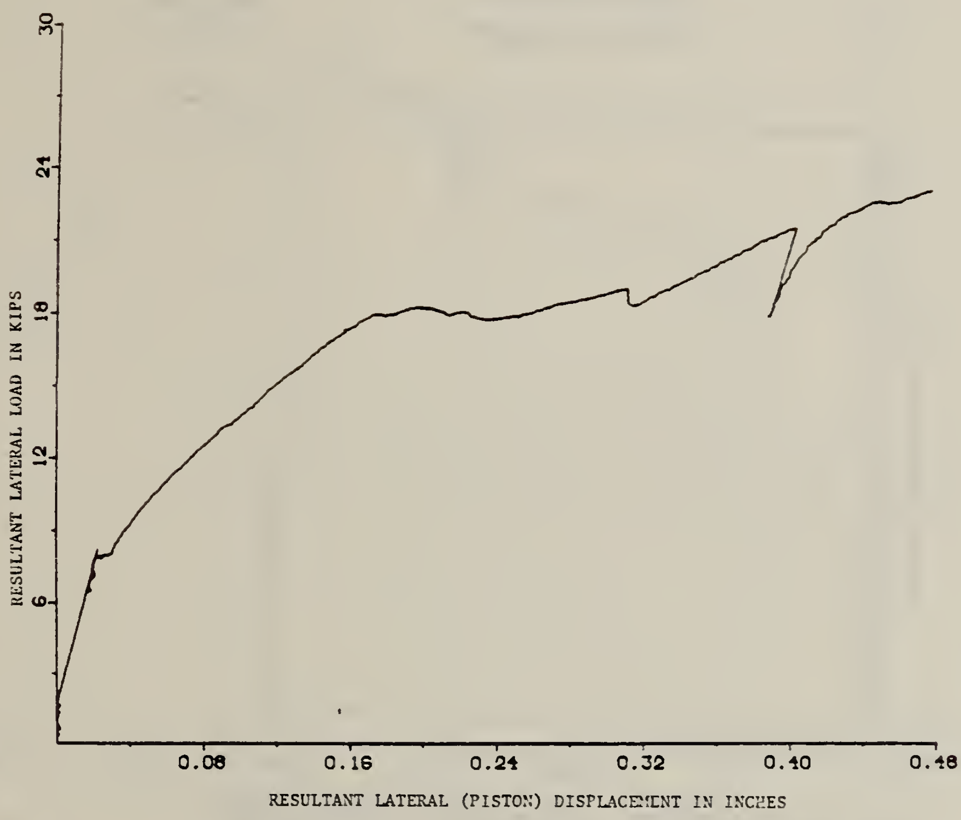

Figure 7.16. Resultant load-displacement curve for test C5

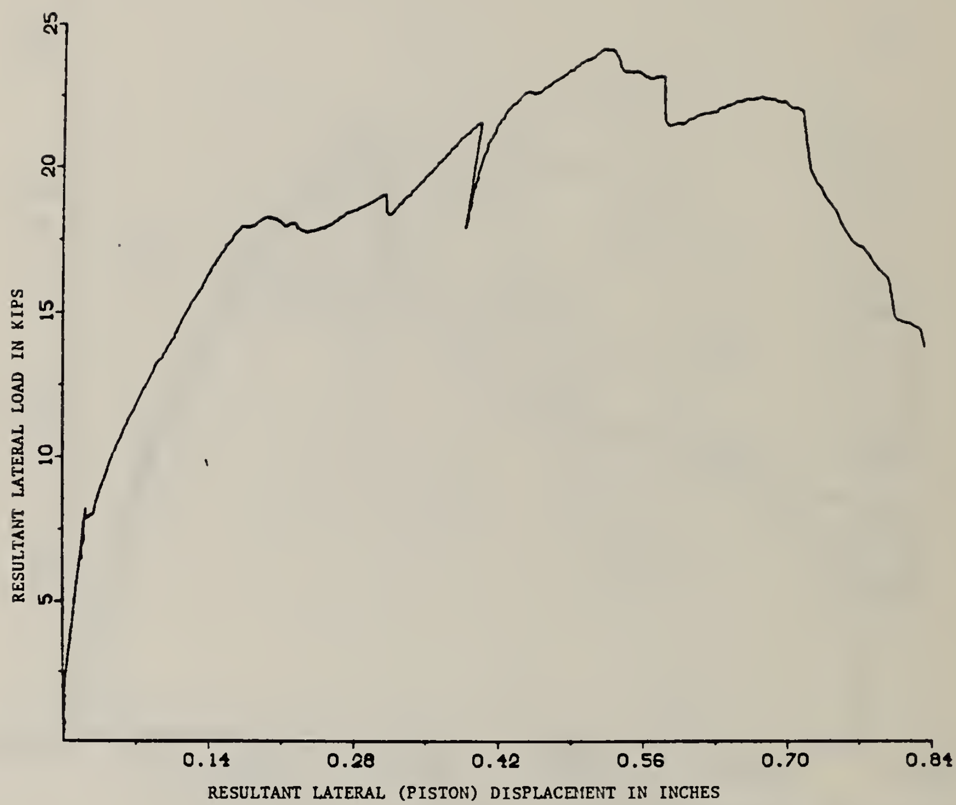

Figure 7.17. Resultant load displacement curve for test C5

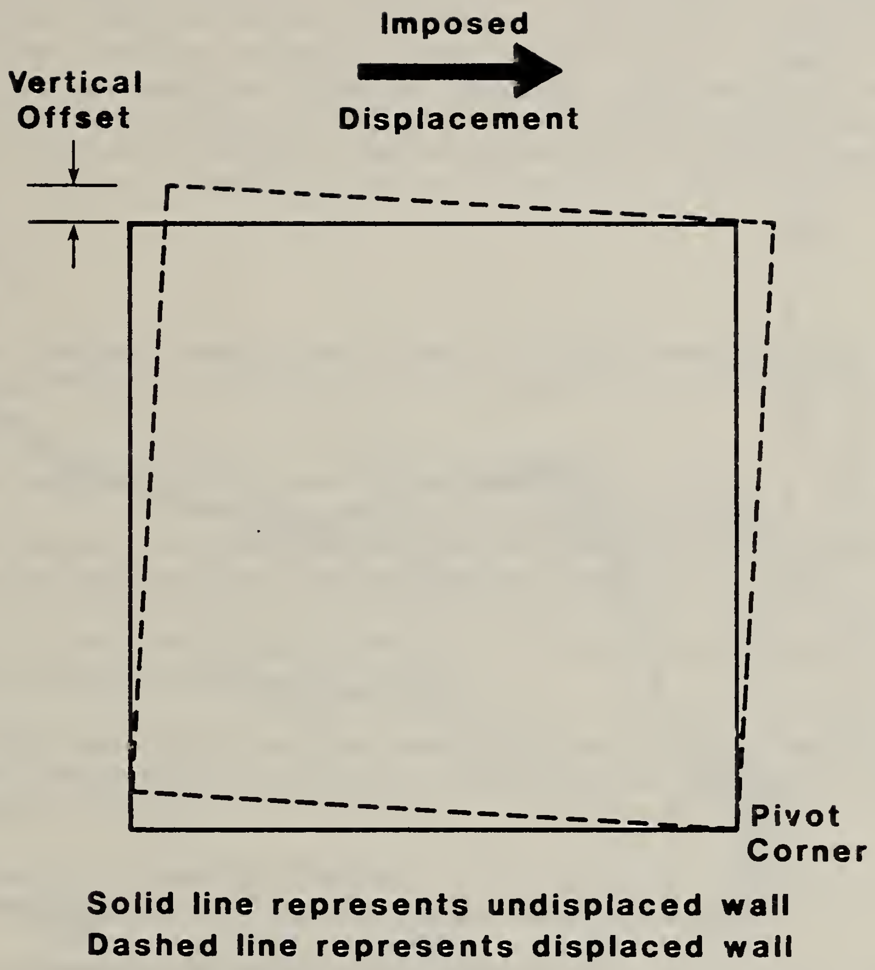

Figure 7.18. Overturning

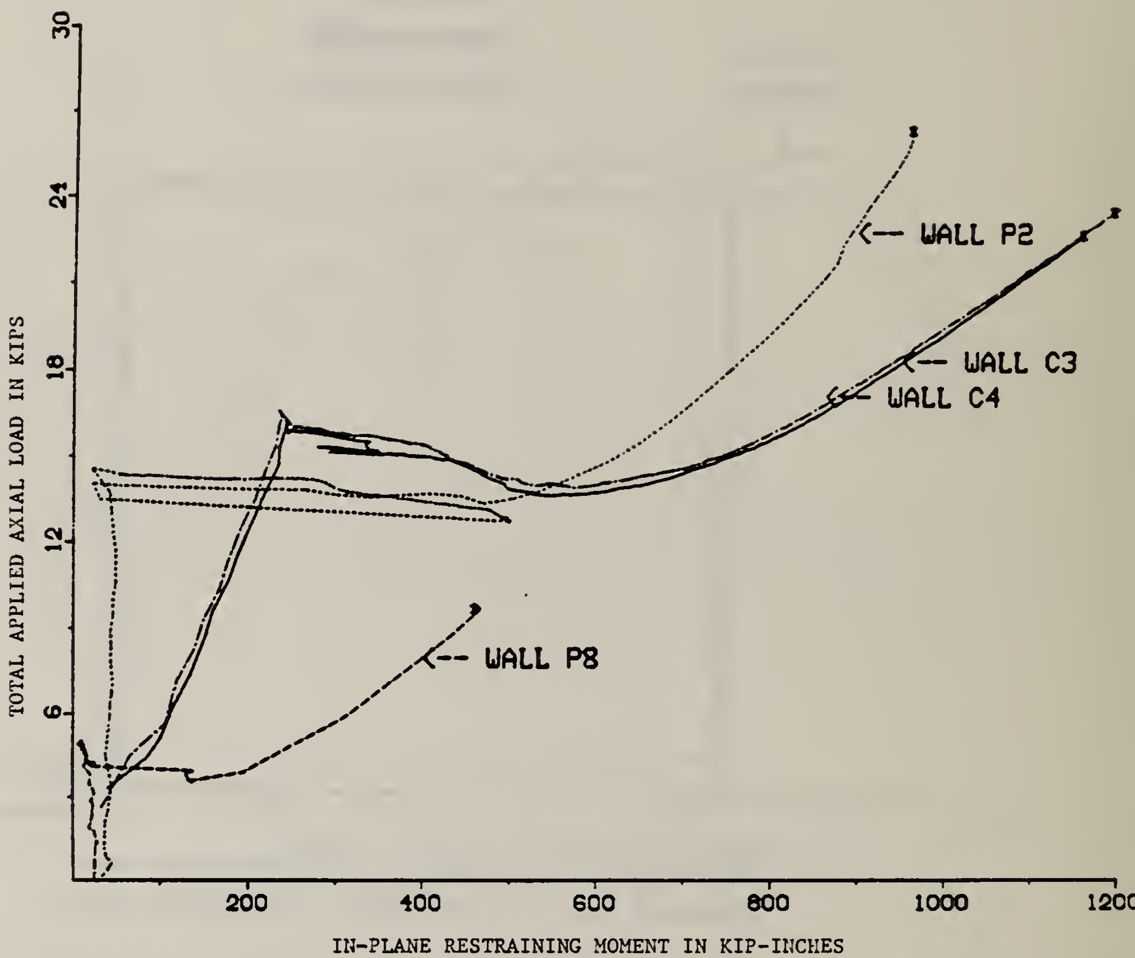

Figure 7.19. Axial load versus restraining moment

8. SUMMARY AND CONCLUSIONS

8.1 SUMMARY

An experimental research project investigating the susceptibility to cracking of unreinforced, ungrouted, concrete block masonry walls due to cyclic loading was undertaken. Ten planar and five corner walls were tested. All of the walls with the exception of one corner wall were subjected to in-plane lateral displacements. A single corner wall was subjected to bidirectional displacements such that the wall was displaced along its z-axis. The loading history was the principal variable with the objective being to determine if visible cracking could be produced through numerous cycles of changing displacements. The parameters most varied were number of cycles and the initial displacement imposed on the walls prior to cycling. The acquired data included displacements, loads, and locally measured strains at various locations on the surface of the walls.

8.2 CONCLUSIONS

A number of conclusions were reached as a result of this investigation. All of the conclusions are qualitative and bear on the method of testing and general wall behavior.

- The observed mode of failure was diagonal tension failure of the wall.

- The mode of failure was achieved only by restraining the vertical movement of the wall so that overturning was prevented.

- The results of the investigation may not be directly applicable to walls lightly loaded axially.

- In-plane shear capacity is not the most probable limiting load resistance criteria for unreinforced, ungrounted walls with low levels of applied axial compressive load.

- The appearance of a complete diagonal crack indicates the onset of load capacity failure.

- There is a threshold in-plane lateral displacement below which loading history does not affect observed wall behavior. The threshold is sufficiently large that for the normal design range of loads there is no effect of repeated loadings. Repeated imposed displacements greater than the threshold displacement cause both stiffness and load capacity reductions.

- The effect of repeated excursions to displacements past the displacement corresponding to the maximum lateral load capacity cause very large stiffness and load capacity reductions.

- Local strain readings by themselves are unreliable indicators of crack severity or wall distress. However, the readings from a number of different locations taken together do provide an indication of the degree of distress in the wall.

- The outstanding leg of a corner wall has a negligible effect on wall capacity, behavior, and failure mode when displacement is imposed along the axis of the in-plane leg.
- Corner walls displaced along their diagonal (or z) axis have maximum resistances equal to the resultant of the in-plane resistance of each leg.

NBS-114A (REV. 2-80)

U.S. DEPT. OF COMM. BIBLIOGRAPHIC DATA SHEET (See instructions)	1. PUBLICATION OR REPORT NO. NBSIR 83-2780	2. Performing Organ. Report No.	3. Publication Date October 1983

4. TITLE AND SUBTITLE

Behavior of Concrete Block Masonry Walls Subjected to Repeated Cyclic Displacements

5. AUTHOR(S)

Kyle Woodward and Frank Rankin

6. PERFORMING ORGANIZATION (If joint or other than NBS, see instructions)

NATIONAL BUREAU OF STANDARDS
DEPARTMENT OF COMMERCE
WASHINGTON, D.C. 20234

7. Contract/Grant No.

8. Type of Report & Period Covered

9. SPONSORING ORGANIZATION NAME AND COMPLETE ADDRESS (Street, City, State, ZIP)

Bureau of Mines
Department of the Interior
Washington, DC 20241

10. SUPPLEMENTARY NOTES

☐ Document describes a computer program; SF-185, FIPS Software Summary, is attached.

11. ABSTRACT (A 200-word or less factual summary of most significant information. If document includes a significant bibliography or literature survey, mention it here)

An experimental investigation into the behavior of unreinforced, ungrouted concrete block masonry walls subjected to repeated in-plane cyclic displacements was undertaken. A total of 15 walls were tested of which 10 were 64 in. x 64 in. planar walls and 5 were 64 in. higher corner walls having equal leg lengths of 48 in. The primary parameter varied in the investigation was loading history. Monotonic tests at both slow and rapid strain rates were done. The cyclic tests included fully reversed displacement patterns and reversed displacement patterns superimposed on static displacement offsets. The cyclic tests included at least 100,000 repetitions. The test results indicated a pronounced effect of loading history on the wall performance, but only at load/displacements nearing the load capacity failure point.

12. KEY WORDS (Six to twelve entries; alphabetical order; capitalize only proper names; and separate key words by semicolons)

Cracking; cyclic; fatigue; masonry; shear; strain rate; walls

13. AVAILABILITY

☒ Unlimited
☐ For Official Distribution. Do Not Release to NTIS
☐ Order From Superintendent of Documents, U.S. Government Printing Office, Washington, D.C. 20402.
☒ Order From National Technical Information Service (NTIS), Springfield, VA. 22161

14. NO. OF PRINTED PAGES

178

15. Price

$17.50

USCOMM-DC 6043-P80